6-14-2021

Epigenetic Mechanisms as Drivers of Environmental Responses in Stony Corals

Javier A. Rodriguez Casariego
javirodr@fiu.edu

FLORIDA INTERNATIONAL UNIVERSITY

Miami, Florida

EPIGENETIC MECHANISMS AS DRIVERS OF ENVIRONMENTAL RESPONSES IN STONY CORALS

A dissertation submitted in partial fulfillment of

the requirements for the degree of

DOCTOR OF PHILOSOPHY

in

BIOLOGY

by

Javier A. Rodriguez Casariego

2021

To: Dean Michael R. Heithaus
College of Arts, Sciences and Education

This dissertation, written by Javier A. Rodriguez Casariego, and entitled Epigenetic Mechanisms as Drivers of Environmental Responses in Stony Corals, having been approved in respect to style and intellectual content, is referred to you for judgment.

We have read this dissertation and recommend that it be approved.

_____
James Fourqurean

_____
Mauricio Rodriguez-Lanetty

_____
Gary Rand

_____
Deron Burkepile

_____
Jose M. Eirin-Lopez, Major Professor

Date of Defense: June 14, 2021

The dissertation of Javier A. Rodriguez Casariego is approved.

_____
Dean Michael R. Heithaus
College of Arts, Sciences and Education

_____
Andrés G. Gil
Vice President for Research and Economic Development
and Dean of the University Graduate School

Florida International University, 2021

Chapters II and III were published in peer-reviewed journals. Journals where both articles were published, “Ecology and Evolution” and “Frontiers of Marine Science”, are Open Access and can be used without permission with adequate citation.

DEDICATION

A mamá

ACKNOWLEDGMENTS

Academic and personal growth require individual constancy and dedication, yet no success story occurs without the contribution of many people carving a path for it and shaping you along the way. This dissertation and the experience that came with it would not be possible without the direct and indirect contribution of so many who have inspired, educated, supported, and even criticized me, forging an improved version of my work and myself. For that, I want to thank you all.

First, I want to thank my major advisor Dr. Jose M. Eirin-Lopez (Chema). I really appreciate the unique opportunity he gave me, and the great support and guidance provided through these years. I could have never asked for a better mentor.

Thanks to the members of my academic committee for their exceptional support and advice. In particular, thanks to Dr. Gary Rand for taking the risk of giving me my first research job in the US and keep-up with me for the last 7 years. It all started with that opportunity.

I am very grateful to Dr. Todd Crowl and Dr. Rita Teutonico. Their support throughout these years goes way beyond the academic environment, making me feel like family. I owe them more than they can imagine.

Thanks to my lab mates and undergrads both in Ecotox and EELab. I have learned a great deal from all of you. In particular, many thanks to Dr. Smith (Abe) for the friendship and the trust when even I was doubting, and to Dr. Gonzalez-Romero (Rodri) and Dr. Suarez-Ulloa (Vicky) for all the training and mentoring.

Many thanks to my collaborators, most especially to Chris Lopes, Dr. Mercado-Molina (Alejandrito) and Dr. Garcia-Souto (Dani), my partners in (scientific) crime.

I am very grateful of all the organizations that funded my work during these years, especially NSF-CREST CAChE, instrumental for my success as student and researcher. My work was also supported by the Graduate Assistantship and Tropics Fellowship from Florida International University, the AMLC Grants in Aid, the NSF-RAPID program, and the exceptional support of the Sociedad Ambiente Marino (SAM-PR).

Special thanks go to my Family. They have been my eternal source of inspiration, unconditional support, and love. Even while scattered across the globe, I have always felt them very close. This little “cabezon” have always looked up to all of you.

Last but definitely not least (the complete opposite), I want to thank my wife Yaimet. Without her I would not be who I am today. Her love, trust and care have given me the strength to overcome many obstacles in the way to reach this milestone. I hope we can keep carrying each other to better and brighter things.

ABSTRACT OF THE DISSERTATION

EPIGENETIC MECHANISMS AS DRIVERS OF ENVIRONMENTAL RESPONSES IN STONY CORALS

by

Javier A. Rodriguez Casariego

Florida International University, 2021

Miami, Florida

Professor Jose M. Eirin-Lopez, Major Professor

The current pace of anthropogenic global change is imposing unprecedented conditions to biological systems. Coral reef ecosystems are particularly sensitive to the rapid increase in thermal anomalies and the changes in water chemistry caused by global change. However, although their decline has been documented worldwide, there are signs suggesting that stony corals harbor greater phenotypic plasticity than previously expected, sparking the interest in the study acquired non-genetic modifications (e.g., epigenome, microbiome) potentially increasing their resilience to global change, and constituting one of the main targets for intervention.

Epigenetics constitutes an exciting frontier to understand how the environment influences the regulation of the expression of genetic information and modulates phenotypic variation. This has the potential to change the way we understand short-term acclimation and adaptation to a changing environment, aiding to improve predictive models of ecosystemic persistence under current and future climatic scenarios. However, while there is evidence supporting the idea of epigenetic mechanisms participating in rapid-response acclimatization, specific details about how this process is influenced by

specific environmental conditions are lacking. In non-model organisms, we often lack information about the presence and functionality of some of these mechanisms, limiting the application of epigenetics in the study of ecosystem resilience in response to global change.

This dissertation aims to elucidate how epigenetic mechanisms contribute to coral phenotypic responses to the effects of global change in the oceans. For that purpose, hypotheses about the presence and responsiveness of different epigenetic mechanisms in corals, its interaction with the genome and microbial communities, as well as its role modulating gene expression and phenotypic responses to diverse stressors were explored. Histone repertoires and/or full methylomes were characterized for the first time in the corals *Acropora cervicornis* and *Montastraea cavernosa*. The participation of these epigenetic mechanisms modulating responses to nutrient contamination, seasonal environmental change, thermal stress, and acidification was demonstrated, providing evidence supporting its participation in intragenerational plasticity. A conserved seasonal methylation program was observed in *A. cervicornis*. This together with the strong influence of the genome over DNA methylation evidence its heritability and its potential to participate in intergenerational plasticity

TABLE OF CONTENTS

CHAPTER PAGE

LIST OF TABLES

TABLE PAGE

LIST OF FIGURES

FIGURE PAGE

ABBREVIATIONS AND ACRONYMS

IGR: Inherited Gene Regulation

IGP: IntraGenerational Plasticity

ItGP: InterGenerational Plasticity

TGP: TransGenerational Plasticity

ROS: Reactive Oxygen Species

DIN: Dissolved Inorganic Nitrogen

SRP: Soluble Reactive Phosphorus

C: Carbon (element)

P: Phosphorus (element)

N: Nitrogen (element)

PAR: Photosynthetically Active Radiation

DO: Dissolved Oxygen

MSAP: Methylation-Sensitive Amplification Polymorphism

MBD-BS: Methyl-Binding Domain Bisulfite Sequencing

WGBS: Whole Genome Bisulfite Sequencing

MSL: Methylation-Susceptible Loci

NML: Loci Not Susceptible to Methylation

NMT: Non-Methylated Target

ICM: Internal Cytosine Methylation in Target

HMM: HemiMethylated Target

HPM: HyperMethylated Target

PTMs: Post-translational modifications

5-mC: A cytosine methylated in the carbon 5

gbM: Gene-body methylation

CpG: Genomic context where a cytosine is followed by a guanine nucleotide.

CHG: Genomic context where a nucleotide other than a guanine is between a cytosine and a guanine.

CHH: Genomic context where a cytosine is followed by two nucleotides other than guanine

DMG: Differentially Methylated Gene

DMR: Differentially Methylated Region

TagSeq: 3' biased transcriptome sequencing

DEG: Differentially Expressed Gene

CDS: Coding Sequence (corresponds with exons in *M. cavernosa* genome annotation)

LTRs: Long Terminal Repeats

UTR: Untranslated Region

GO: Gene ontology

KOG: Eukaryotic orthologous group

ITS2: Internal Transcribed Spacer 2 region of nuclear ribosomal DNA

ChE: Cholesterol esters

FA: Fatty Acids

MG: monoacylgrycerols

MGDG: monogalactosyldiacylgylcerols

PC: phosphatidylcholines

PE: phosphatidylethanolamines

TG: triglycerides

WE: Wax esters

CHAPTER I.

GENERAL INTRODUCTION

Human-driven global change is now an unquestionable phenomenon supported by abundant evidence (Pörtner et al. 2019; The Royal Society and The National Academy of Sciences 2020). The accumulation of greenhouse gas emissions are causing the continuous increase in the average ocean-surface temperature (Pörtner et al. 2019), and in the magnitude and frequency of thermal anomalies [i.e. marine heatwaves (Frölicher, Fischer, and Gruber 2018; Oliver et al. 2021)]. In addition, the modifications in the chemical balance of the ocean, caused by CO_2 accumulation (i.e., acidification) and pollution, and the overexploitation of marine resources, have caused dire effects on the physiology of marine organisms (Somero 2010; Bennett et al. 2019), affecting their spatial distribution and demographic traits (Poloczanska et al. 2013, 2016; Roberts 2019). Environmental stressor (including changes in abiotic parameters and pollutants) effects are evident at different levels within individual organisms, from early genetic responses triggered by the action of the stressor (Hoffmann and Willi 2008; Hansen et al. 2012; Lajoie and Vellend 2018), to whole-individual physiological and behavioral responses (Boyd et al. 2014; Beever et al. 2017; Williams et al. 2021). These changes often equate to disruptions in population dynamics and interspecific interactions [e.g. trophic pathways, (Van der Putten, Macel, and Visser 2010; Kwiatkowski, Aumont, and Bopp 2019)], instrumental for spreading the effect of climate change bidirectionally (bottom-up and top-down) through the ecosystem (Doney et al. 2012). This is particularly evident in key organisms (critical for the functioning and the physical structure of an ecosystem such as the case of reef-building corals), where their collapse results in the disappearance of complete ecosystems.

Organism functioning, in the broadest sense, ultimately depends on the instructions stored in the genome that become active (or inactive) in response to environmental fluctuations, defining the phenotype during development and mediating its plasticity during adulthood. Thus, the limits to the phenotypic plasticity of an organism are ultimately determined by the genetic information stored in the DNA (Li et al. 2018). However, within those limits, epigenetics — molecules and mechanisms able to regulate gene expression through the generation of alternative gene activity states in the context of the same DNA sequence (Cavalli and Heard 2019) — contribute to modulate the phenome (set of all phenotypes expressed by a cell, tissue or organ) in response to environmental conditions, leading in some cases to drastic differences in the resulting phenotypes (Biémont 2010; Waddington 2012).

Epigenetics constitutes an exciting frontier to understand how the environment influences gene expression regulation and modulate phenotypic variation (Bollati and Baccarelli 2010; Cortessis et al. 2012; Beal et al. 2018; Eirin-Lopez and Putnam 2019). Moreover, these environmentally modified transcriptional states may be inherited by the offspring [Inherited Gene Regulation, IGR (Adrian-Kalchhauser et al. 2020)], producing diverse outcomes from a single genome and accelerating ecological and evolutionary change (Eirin-Lopez and Putnam 2018; Ryu et al. 2018). While there is evidence of intergenerational inheritance of acclimatized phenotypes (Vignet et al. 2015; Marsh and Pasqualone 2014; Greco et al. 2013; Navarro-Martín et al. 2011; Vandegehuchte et al. 2009), and epigenetic marks (Liew et al. 2020; Schunter et al. 2018; Bernal et al. 2018), it is not clear how the regulation and inheritance of gene expression states are mediated by a combination of interdependent non-genetic mechanisms during responses to both

developmental and environmental signals, especially in ecologically relevant non-model organisms (Eirin-Lopez and Putnam 2019). In contrast to the stable and irreversible variation in the genome (driven by mutation), the epigenome has been shown to be very dynamic, reversible, and non-deterministic (Braun et al. 2017; Adrian-Kalchhauser et al. 2020). Observed crosstalk between epigenetic mechanisms (Zhao et al. 2021; Choi et al. 2020; Li et al. 2018; Wendte and Pikaard 2017) and non-linear relationships of individual mechanisms with gene expression make it extremely complex to study and interpret in the context of a specific response to an environmental driver. In addition, epigenetic mechanisms, like most cellular functions, depend on the cellular energetic conditions (Wallace and Fan 2010; Donohoe and Bultman 2012). Consequently, changes in energetic balances induced by environmental conditions can limit the availability of cofactors and other compounds necessary for the onset of epigenetic marks, resulting in the impairment of gene regulation mechanisms and disease (Wallace and Fan 2010). This complex scenario added to the fact that we even lack information about the presence and functionality of some of these mechanisms in many non-model organisms, constitutes the main factors limiting the broad application of epigenetic analyses to the much-needed modeling of ecosystem-level capacity for resilience and adaptability in response to the challenges posed by global change.

Environmental epigenetics: broadening epigenetic analyses to non-model organisms.

Multiple mechanisms have been proposed to encode epigenetic information including methylation of DNA and RNA (Bird 2002; Fu et al. 2014), histone variants [replacement of canonical histones with a set encompassing specialized functions in chromatin metabolism (Henikoff and Smith 2015; Talbert and Henikoff 2021)] and their

post-translational modifications (PTMs) (Ng and Cheung 2016; Taylor and Young 2021), non-coding RNAs (Wei et al. 2017; Dhanoa et al. 2018), and transcription factor regulatory networks (Davidson 2010). In each one's specific way, all these mechanisms provide the genome with the capacity to produce multiple phenotypes from the same genetic material, while influenced by developmental differentiation signals (Waddington 2012) and/or environmental factors (Cavalli and Heard 2019). Such link between environment and gene expression has opened a new field to the study of the epigenetic mechanisms mediating exposure-response relationships (Bollati and Baccarelli 2010; Vandegehuchte and Janssen 2011; Eirin-Lopez and Putnam 2019), providing information about how different environmental factors influence phenotypic variation and starting to incorporate this and other non-genetic modulators of the phenome into eco-evo-devo theory (Skúlason et al. 2019; Putnam 2021).

DNA methylation is the best studied epigenetic mechanism, with a growing number of studies focused on non-model organisms, including many marine invertebrates (Eirin-Lopez and Putnam 2019). In eukaryotes, DNA methylation generally involves the transfer of a methyl group (-CH_3) from S-adenosyl-L-methionine to a cytosine residue, commonly in a CpG (cytosine followed by a guanine) context. This chemical modification (5-mC) can physically limit the access transcriptional machinery to gene regions and/or serve as signals to other factors binding the DNA, regulating expression, generating alternative splicing of expressed genes, or modulating other aspects of genomic functioning (Luo, Hajkova, and Ecker 2018). However, major differences between the widely studied mammal model and other taxa, make the study of the methylome structure and function in non-model organisms very challenging. Mammals

display highly methylated genomes with accumulation of 5-mC marks in CpG islands associated with gene promoters (Smith and Meissner 2013). Functionally, methylation of these CpG islands produce gene silencing by blocking the access to the transcriptional machinery, therefore serving as on-off switches for gene expression. In invertebrates, conversely, DNA methylation is more sparse through the genome (with as low as 1% of the genome being methylated), and occurs predominantly across gene bodies (Sarda et al. 2012; Gavery and Roberts 2013; Dixon et al. 2018). This overlapping of DNA methylation signals and the gene, poses the challenge of balancing methylation-induced mutation and the selective preservation of the coding region (Dixon, Bay, and Matz 2016). Opposite to the mammalian model, highly methylated genes in invertebrates tend to be highly expressed, potentially by the reduction of spurious transcription through the blocking of intragenomic initiation positions (Roberts and Gavery 2012; Dixon et al. 2018; Li et al. 2018). Other authors have proposed the hypothesis that gene body methylation in invertebrates is involved in differential splicing (Flores et al. 2012). Consequently, the function of DNA methylation in invertebrates and its involvement in modulating phenotypic plasticity still requires substantial investigation.

Another key epigenetic mechanism is the modification of the chromatin accessibility by the replacement of canonical histones with specialized variants and their post translational modifications (PTMs). By regulating the access of different cellular components to DNA, these modifications to the chromatin can regulate transcription, replication, recombination, and repair (Zink and Hake 2016; Bannister and Kouzarides 2011). Accordingly, histones not only constitute the basis for the physical structure of the chromatin but are also determinants of its functionality (Allis et al. 2007). The

interaction between two units of each core histones (H2A, H2B, H3 and H4 families) forms an octameric structure around which the DNA wraps. This nucleoprotein complex (the nucleosome core particle) is highly dynamic (Zlatanova et al. 2009). The replacement of canonical histones by specialized variants (Zink and Hake 2016; Talbert and Henikoff 2021) and/or the occurrence of PTMs of their amino-terminal tails [e.g. acetylation, ubiquitination, phosphorylation, methylation (Zhou et al. 2014; Ng and Cheung 2016; Taylor and Young 2021)] produce changes in the nucleosome compaction, allowing or restricting access to the DNA, or serve as signals for effector proteins and transcription factors [e.g. H3.3K36me3 as signal for tumor suppressor (Lan and Shi 2015)]. Despite its incredible appeal, studies addressing the epigenetic role of chromatin structural components (e.g., histone variants and their modifications) are very scarce in non-model organisms. This is mostly because of the lack of knowledge about their specific chromatin structure and dynamic, as well as by the absence of specific antibodies enabling the dynamic study of these proteins genome-wide. During the last decade, however, several studies have advanced in the description of chromatin in bivalve molluscs [reviewed in (González-Romero, Rivera-Casas, Fernández-Tajes, et al. 2012; Suárez-Ulloa et al. 2013)]. The presence of very conserved histone variants widely studied in model vertebrates including H2A.X, H2A.Z was evidenced in invertebrates (González-Romero, Rivera-Casas, Frehlick, et al. 2012; Rivera-Casas, González-Romero, et al. 2016; Cheema et al. 2020), including its description in corals as a result of this dissertation (Rodriguez-Casariego et al. 2018). More recently, H3.3 and macroH2A (Rivera-Casas, Gonzalez-Romero, et al. 2016) were also added to the chromatin components repertoire in bivalves. Histone repertoires have been described at the gene

level in other marine invertebrates (Lee et al. 2020; Arenas-Mena, Wong, and Arandi-Foroshani 2007), but characterizations at the protein level are very scarce with very few examples [marine diatom (Veluchamy et al. 2015)]. Overall, the study of epigenetic mechanisms (e.g., DNA methylation and histone modification) within the context of marine organisms' responses to global change will be critical for the assessment and prediction of the effects global change will have on marine ecosystems.

Corals as model systems for environmental epigenetics.

Coral reefs represent the ocean's most diverse ecosystems (Knowlton et al. 2010) providing critical services and goods for human society [e.g. fisheries and aquaculture production, shoreline protection, and recreation (Woodhead et al. 2019)]. Hermatypic (i.e., reef-building) corals are key foundational organisms for these ecosystems and are particularly affected by global change stressors (Hoegh-Guldberg et al. 2017; Vercelloni et al. 2020), with documented declines in coral populations worldwide. Among them, thermal anomalies surpassing the summer mean are particularly important by disrupting coral's obligatory symbiosis with dinoflagellates of the family Symbiodinaceae in a stress response known as "bleaching" (Weis 2008; Baker and Cunning 2015). This process is the main cause of coral population declines given that often results in mortality or increased susceptibility to diseases. Additional reduction of calcification rates and skeletal density (Enzor et al. 2018; Putnam, Davidson, and Gates 2016), and decreased reproduction success (Putnam et al. 2013) are other effects attributed to global change stressors. Consequently, there is an urgency for studying coral responses to global change, including ocean acidification, ocean warming and pollution, integrating

physiological, ecological, and molecular approaches to determine their capacity for rapid acclimatization and adaptation under predicted conditions (Putnam 2021).

Corals have very complex life cycles and are sessile most of their long lives, increasing their vulnerability in a rapidly changing environment, but also supporting the idea that their success so far must be driven by mechanisms maximizing phenotypic plasticity. Enhanced acclimatization mechanisms have allowed corals to colonize highly heterogeneous environments (Todd 2008) and survive drastic environmental changes during their evolutionary history (Jackson 2008). Such plasticity could ultimately determine the survival of tropical reefs under the predicted future climatic scenario (Hoegh-Guldberg et al. 2007; Putnam 2021), making corals remarkable candidates to the study of acquired non-genetic modifications (e.g., epigenome and microbiome dynamic) potentially increasing their resilience to global change in a relevant time-frame (van Oppen et al. 2015; 2017). Accordingly, recent works have highlighted the role of microbial communities (Leal et al. 2015; Silverstein, Cunning, and Baker 2015; Peixoto et al. 2017; Morrow, Muller, and Lesser 2018), and changes in the epigenome [DNA methylation (Putnam, Davidson, and Gates 2016; Liew et al. 2018, 2020; Eirin-Lopez and Putnam 2019; Dimond and Roberts 2020), histone variants (Rodriguez-Casariego et al. 2018; Li et al. 2018), non-coding RNA (Gajigan and Conaco 2017)] mediating responses to different drivers of global change. This has further advanced the idea of incorporating epigenetic and microbiome manipulations into "assisted evolution" intervention strategies aimed at reverting coral population trajectories (National Academies of Sciences, Engineering, and Medicine et al. 2019). However, the current understanding of such mechanisms is insufficient to make informed decisions about its

feasibility and safety as intervention strategies, requiring additional basic research as has been developed in this dissertation.

Final remarks

The identification and selection of individuals displaying a better ability to respond to environmental stressors or the induction of "preconditioned" or "hardened" phenotype, is becoming one of the pillars of the new intervention paradigm in coral reef management (van Oppen et al. 2017). The manipulation of non-genetic processes with the potential to accelerate the rate of phenotypic change (Fig. 1) can result in enhanced resilience of coral recruits, with several studies [previously mentioned and reviewed in (Eirin-Lopez and Putnam 2019; Putnam 2021)] providing incipient support for the role of epigenetic mechanisms and the microbiome, promoting such "preconditioned" phenotypes. Accordingly, lab-based experiments have increased thermal tolerance of corals through controlled heat-stress exposures, mainly promoting shifts to more thermally tolerant symbionts (Silverstein, Cunning, and Baker 2015; Cunning and Baker 2020). In addition, the presence gene expression plasticity and frontloading of stress-response genes (Barshis et al. 2013; Bay and Palumbi 2015; Kenkel and Matz 2016) resulting from coral acclimation to stressful conditions hint the intercorrelation of mechanisms, including epigenetics (Liew et al. 2018), in the modulation of such responses and its memory. However, further efforts are still required to elucidate the functionality and responsiveness of epigenetic mechanisms in corals, study the interaction between genome, epigenome, transcriptome, and microbiome in holobiont physiological responses to realistic environmental conditions, and evaluate the role of non-genetic mechanisms in coral acclimatization (including interaction with symbiotic

and other microbial manipulations). Consequently, these constitute the specific aims pursued in this dissertation and divided in four experimental chapters:

Chapter II. Coral epigenetic responses to nutrient stress: histone H2A.X phosphorylation dynamics and DNA methylation in the staghorn coral *Acropora cervicornis.*

Chapter III. Genome-Wide DNA Methylation Analysis Reveals a Conserved Epigenetic Response to Seasonal Environmental Variation in the Staghorn Coral *Acropora cervicornis*

Chapter IV. Symbiont shuffling induces differential DNA methylation responses to thermal stress in the coral *Montastraea cavernosa*.

Chapter V. Multi-omic analysis reveals marked phenotypic plasticity in coral clones outplanted to divergent environments.

References

Adrian-Kalchhauser, Irene, Sonia E. Sultan, Lisa N. S. Shama, Helen Spence-Jones, Stefano Tiso, Claudia Isabelle Keller Valsecchi, and Franz J. Weissing. 2020. "Understanding'Non-genetic'Inheritance: Insights from Molecular-Evolutionary Crosstalk." *Trends in Ecology & Evolution*. https://www.sciencedirect.com/science/article/pii/S0169534720302263.

Arenas-Mena, César, Kimberly Suk-Ying Wong, and Navid R. Arandi-Foroshani. 2007. "Histone H2A.Z Expression in Two Indirectly Developing Marine Invertebrates Correlates with Undifferentiated and Multipotent Cells." *Evolution & Development* 9 (3): 231–43.

Baker, Andrew C., and Ross Cunning. 2015. "Coral 'bleaching' as a Generalized Stress Response to Environmental Disturbance." *Diseases of Coral*, 396–409.

Bannister, Andrew J., and Tony Kouzarides. 2011. "Regulation of Chromatin by Histone Modifications." *Cell Research* 21 (3): 381–95.

Barshis, Daniel J., Jason T. Ladner, Thomas A. Oliver, François O. Seneca, Nikki Traylor-Knowles, and Stephen R. Palumbi. 2013. "Genomic Basis for Coral Resilience to Climate Change." *Proceedings of the National Academy of Sciences*. https://doi.org/10.1073/pnas.1210224110.

Bay, Rachael A., and Stephen R. Palumbi. 2015. "Rapid Acclimation Ability Mediated by Transcriptome Changes in Reef-Building Corals." *Genome Biology and Evolution* 7 (6): 1602–12.

Beal, Andria, Javier Rodriguez-Casariego, Ciro Rivera-Casas, Victoria Suarez-Ulloa, and Jose M. Eirin-Lopez. 2018. "Environmental Epigenomics and Its Applications in Marine Organisms." *Population Genomics*. https://doi.org/10.1007/13836_2018_28.

Beever, Erik A., L. Embere Hall, Johanna Varner, Anne E. Loosen, Jason B. Dunham, Megan K. Gahl, Felisa A. Smith, and Joshua J. Lawler. 2017. "Behavioral Flexibility as a Mechanism for Coping with Climate Change." *Frontiers in Ecology and the Environment* 15 (6): 299–308.

Bennett, Scott, Carlos M. Duarte, Núria Marbà, and Thomas Wernberg. 2019. "Integrating within-Species Variation in Thermal Physiology into Climate Change Ecology." *Philosophical Transactions of the Royal Society of London. Series B, Biological Sciences* 374 (1778): 20180550.

Bernal, Moisés A., Jennifer M. Donelson, Heather D. Veilleux, Taewoo Ryu, Philip L. Munday, and Timothy Ravasi. 2018. "Phenotypic and Molecular Consequences of Stepwise Temperature Increase across Generations in a Coral Reef Fish." *Molecular Ecology* 27 (22): 4516–28.

Biémont, C. 2010. "From Genotype to Phenotype. What Do Epigenetics and Epigenomics Tell Us?" *Heredity* 105 (1): 1–3.

Bird, A. 2002. "DNA Methylation Patterns and Epigenetic Memory." *Genes & Development*. https://doi.org/10.1101/gad.947102.

Bollati, V., and A. Baccarelli. 2010. "Environmental Epigenetics." *Heredity*. https://doi.org/10.1038/hdy.2010.2.

Boyd, Philip W., Sinikka T. Lennartz, David M. Glover, and Scott C. Doney. 2014. "Biological Ramifications of Climate-Change-Mediated Oceanic Multi-Stressors." *Nature Climate Change* 5 (December): 71.

Braun, Simon M. G., Jacob G. Kirkland, Emma J. Chory, Dylan Husmann, Joseph P. Calarco, and Gerald R. Crabtree. 2017. "Rapid and Reversible Epigenome Editing by Endogenous Chromatin Regulators." *Nature Communications* 8 (1): 560.

Cavalli, Giacomo, and Edith Heard. 2019. "Advances in Epigenetics Link Genetics to the Environment and Disease." *Nature* 571 (7766): 489–99.

Cheema, Manjinder S., Katrina V. Good, Bohyun Kim, Heddy Soufari, Connor O'Sullivan, Melissa E. Freeman, Gilda Stefanelli, et al. 2020. "Deciphering the Enigma of the Histone H2A.Z-1/H2A.Z-2 Isoforms: Novel Insights and Remaining Questions." *Cells* 9 (5). https://doi.org/10.3390/cells9051167.

Choi, Jaemyung, David B. Lyons, M. Yvonne Kim, Jonathan D. Moore, and Daniel Zilberman. 2020. "DNA Methylation and Histone H1 Jointly Repress Transposable Elements and Aberrant Intragenic Transcripts." *Molecular Cell* 77 (2): 310–23.e7.

Cortessis, Victoria K., Duncan C. Thomas, A. Joan Levine, Carrie V. Breton, Thomas M. Mack, Kimberly D. Siegmund, Robert W. Haile, and Peter W. Laird. 2012. "Environmental Epigenetics: Prospects for Studying Epigenetic Mediation of Exposure–response Relationships." *Human Genetics* 131 (10): 1565–89.

Cunning, Ross, and Andrew C. Baker. 2020. "Thermotolerant Coral Symbionts Modulate Heat Stress-responsive Genes in Their Hosts." *Molecular Ecology*. https://doi.org/10.1111/mec.15526.

David Allis, C., Thomas Jenuwein, Danny Reinberg, and Marie-Laure Caparros. 2007. *Epigenetics*. CSHL Press.

Davidson, Eric H. 2010. *The Regulatory Genome: Gene Regulatory Networks In Development And Evolution*. Elsevier.

Dhanoa, Jasdeep Kaur, Ram Saran Sethi, Ramneek Verma, Jaspreet Singh Arora, and Chandra Sekhar Mukhopadhyay. 2018. "Long Non-Coding RNA: Its Evolutionary Relics and Biological Implications in Mammals: A Review." *Hanguk Tongmul Chawon Kwahakhoe Chi = Journal of Animal Science and Technology* 60 (October): 25.

Dimond, James L., and Steven B. Roberts. 2020. "Convergence of DNA Methylation Profiles of the Reef Coral Porites Astreoides in a Novel Environment." *Frontiers in Marine Science* 6: 792.

Dixon, Groves B., Line K. Bay, and Mikhail V. Matz. 2016. "Evolutionary Consequences of DNA Methylation in a Basal Metazoan." *Molecular Biology and Evolution* 33 (9): 2285–93.

Dixon, Groves, Yi Liao, Line K. Bay, and Mikhail V. Matz. 2018. "Role of Gene Body Methylation in Acclimatization and Adaptation in a Basal Metazoan." *Proceedings of the National Academy of Sciences of the United States of America* 115 (52): 13342–46.

Doney, Scott C., Mary Ruckelshaus, J. Emmett Duffy, James P. Barry, Francis Chan, Chad A. English, Heather M. Galindo, et al. 2012. "Climate Change Impacts on Marine Ecosystems." *Annual Review of Marine Science* 4: 11–37.

Donohoe, Dallas R., and Scott J. Bultman. 2012. "Metaboloepigenetics: Interrelationships between Energy Metabolism and Epigenetic Control of Gene Expression." *Journal of Cellular Physiology* 227 (9): 3169–77.

Eirin-Lopez, Jose M., and Hollie M. Putnam. 2019. "Marine Environmental Epigenetics." *Annual Review of Marine Science*. https://doi.org/10.1146/annurev-marine-010318-095114.

Eirin-Lopez, Jose, and Hollie Putnam. 2018. "Marine Environmental Epigenetics." *Annual Review of Marine Science* in press.

Enzor, Laura A., Cheryl Hankins, Deborah N. Vivian, William S. Fisher, and Mace G. Barron. 2018. "Calcification in Caribbean Reef-Building Corals at High pCO2 Levels in a Recirculating Ocean Acidification Exposure System." *Journal of Experimental Marine Biology and Ecology* 499 (February): 9–16.

Flores, Kevin, Florian Wolschin, Jason J. Corneveaux, April N. Allen, Matthew J. Huentelman, and Gro V. Amdam. 2012. "Genome-Wide Association between DNA Methylation and Alternative Splicing in an Invertebrate." *BMC Genomics* 13 (September): 480.

Frölicher, Thomas L., Erich M. Fischer, and Nicolas Gruber. 2018. "Marine Heatwaves under Global Warming." *Nature* 560 (7718): 360–64.

Fu, Ye, Dan Dominissini, Gideon Rechavi, and Chuan He. 2014. "Gene Expression Regulation Mediated through Reversible m^6A RNA Methylation." *Nature Reviews. Genetics* 15 (5): 293–306.

Gajigan, Andrian P., and Cecilia Conaco. 2017. "A microRNA Regulates the Response of Corals to Thermal Stress." *Molecular Ecology* 26 (13): 3472–83.

Gavery, Mackenzie R., and Steven B. Roberts. 2013. "Predominant Intragenic Methylation Is Associated with Gene Expression Characteristics in a Bivalve Mollusc." *PeerJ* 1 (November): e215.

González-Romero, Rodrigo, Ciro Rivera-Casas, Juan Fernández-Tajes, Juan Ausió, Josefina Méndez, and José M. Eirín-López. 2012. "Chromatin Specialization in Bivalve Molluscs: A Leap Forward for the Evaluation of Okadaic Acid Genotoxicity in the Marine Environment." *Comparative Biochemistry and Physiology. Toxicology & Pharmacology: CBP* 155 (2): 175–81.

González-Romero, Rodrigo, Ciro Rivera-Casas, Lindsay J. Frehlick, Josefina Méndez, Juan Ausió, and José M. Eirín-López. 2012. "Histone H2A (H2A.X and H2A.Z) Variants in Molluscs: Molecular Characterization and Potential Implications for Chromatin Dynamics." *PloS One* 7 (1): e30006.

Greco, M., A. Chiappetta, L. Bruno, and M. B. Bitonti. 2013. "Effects of Light Deficiency on Genome Methylation in Posidonia Oceanica." *Marine Ecology Progress Series* 473 (January): 103–14.

Hansen, Michael M., Isabelle Olivieri, Donald M. Waller, Einar E. Nielsen, and GeM Working Group. 2012. "Monitoring Adaptive Genetic Responses to Environmental Change." *Molecular Ecology* 21 (6): 1311–29.

Henikoff, Steven, and M. Mitchell Smith. 2015. "Histone Variants and Epigenetics." *Cold Spring Harbor Perspectives in Biology* 7 (1): a019364.

Hoegh-Guldberg, O., P. J. Mumby, A. J. Hooten, R. S. Steneck, P. Greenfield, E. Gomez, C. D. Harvell, et al. 2007. "Coral Reefs under Rapid Climate Change and Ocean Acidification." *Science* 318 (5857): 1737–42.

Hoegh-Guldberg, Ove, Elvira S. Poloczanska, William Skirving, and Sophie Dove. 2017. "Coral Reef Ecosystems under Climate Change and Ocean Acidification." *Frontiers in Marine Science* 4 (May): 321.

Hoffmann, Ary A., and Yvonne Willi. 2008. "Detecting Genetic Responses to Environmental Change." *Nature Reviews. Genetics* 9 (6): 421–32.

Jackson, Jeremy B. C. 2008. "Ecological Extinction and Evolution in the Brave New Ocean." *Proceedings of the National Academy of Sciences of the United States of America* 105 (Supplement 1): 11458–65.

Kenkel, Carly D., and Mikhail V. Matz. 2016. "Gene Expression Plasticity as a Mechanism of Coral Adaptation to a Variable Environment." *Nature Ecology & Evolution* 1 (1): 14.

Knowlton, Nancy, Russell E. Brainard, Rebecca Fisher, Megan Moews, Laetitia Plaisance, and M. Julian Caley. 2010. "Coral Reef Biodiversity." *Life in the World's Oceans: Diversity Distribution and Abundance*, 65–74.

Kwiatkowski, Lester, Olivier Aumont, and Laurent Bopp. 2019. "Consistent Trophic Amplification of Marine Biomass Declines under Climate Change." *Global Change Biology*. https://doi.org/10.1111/gcb.14468.

Lajoie, Geneviève, and Mark Vellend. 2018. "Characterizing the Contribution of Plasticity and Genetic Differentiation to Community-Level Trait Responses to Environmental Change." *Ecology and Evolution* 8 (8): 3895–3907.

Lan, Fei, and Yang Shi. 2015. "Histone H3.3 and Cancer: A Potential Reader Connection." *Proceedings of the National Academy of Sciences*. https://doi.org/10.1073/pnas.1418996111.

Leal, M. C., K. Hoadley, D. T. Pettay, A. Grajales, R. Calado, and M. E. Warner. 2015. "Symbiont Type Influences Trophic Plasticity of a Model Cnidarian-

Dinoflagellate Symbiosis." *Journal of Experimental Biology*. https://doi.org/10.1242/jeb.115519.

Lee, Young Hwan, Min-Sub Kim, Haksoo Jeong, Atsushi Hagiwara, and Jae-Seong Lee. 2020. "Genome-Wide Identification and Transcriptional Modulation of Histone Variants and Modification Related Genes in the Low pH-Exposed Marine Rotifer Brachionus Koreanus." *Comparative Biochemistry and Physiology. Part D, Genomics & Proteomics* 36 (December): 100748.

Liew, Yi Jin, Emily J. Howells, Xin Wang, Craig T. Michell, John A. Burt, Youssef Idaghdour, and Manuel Aranda. 2020. "Intergenerational Epigenetic Inheritance in Reef-Building Corals." *Nature Climate Change* 10 (3): 254–59.

Liew, Yi Jin, Didier Zoccola, Yong Li, Eric Tambutté, Alexander A. Venn, Craig T. Michell, Guoxin Cui, et al. 2018. "Epigenome-Associated Phenotypic Acclimatization to Ocean Acidification in a Reef-Building Coral." *Science Advances* 4 (6): eaar8028.

Li, Xin, Tingting Guo, Qi Mu, Xianran Li, and Jianming Yu. 2018. "Genomic and Environmental Determinants and Their Interplay Underlying Phenotypic Plasticity." *Proceedings of the National Academy of Sciences of the United States of America* 115 (26): 6679–84.

Li, Yong, Yi Jin Liew, Guoxin Cui, Maha J. Cziesielski, Noura Zahran, Craig T. Michell, Christian R. Voolstra, and Manuel Aranda. 2018. "DNA Methylation Regulates Transcriptional Homeostasis of Algal Endosymbiosis in the Coral Model Aiptasia." *Science Advances* 4 (8): eaat2142.

Luo, Chongyuan, Petra Hajkova, and Joseph R. Ecker. 2018. "Dynamic DNA Methylation: In the Right Place at the Right Time." *Science* 361 (6409): 1336–40.

Marsh, Adam G., and Annamarie A. Pasqualone. 2014. "DNA Methylation and Temperature Stress in an Antarctic Polychaete, Spiophanes Tcherniai." *Frontiers in Physiology* 5 (May): 173.

Morrow, K. M., E. Muller, and M. P. Lesser. 2018. "How Does the Coral Microbiome Cause, Respond To, or Modulate the Bleaching Process?" In *Coral Bleaching: Patterns, Processes, Causes and Consequences*, edited by Madeleine J. H. van Oppen and Janice M. Lough, 153–88. Cham: Springer International Publishing.

Navarro-Martín, Laia, Jordi Viñas, Laia Ribas, Noelia Díaz, Arantxa Gutiérrez, Luciano Di Croce, and Francesc Piferrer. 2011. "DNA Methylation of the Gonadal Aromatase (cyp19a) Promoter Is Involved in Temperature-Dependent Sex Ratio Shifts in the European Sea Bass." *PLoS Genetics* 7 (12): e1002447.

Ng, Marlee K., and Peter Cheung. 2016. "A Brief Histone in Time: Understanding the Combinatorial Functions of Histone PTMs in the Nucleosome Context." *Biochemistry and Cell Biology = Biochimie et Biologie Cellulaire* 94 (1): 33–42.

Oliver, Eric C. J., Jessica A. Benthuysen, Sofia Darmaraki, Markus G. Donat, Alistair J. Hobday, Neil J. Holbrook, Robert W. Schlegel, and Alex Sen Gupta. 2021. "Marine Heatwaves." *Annual Review of Marine Science* 13 (January): 313–42.

Oppen, Madeleine J. H., Ruth D. Gates, Linda L. Blackall, Neal Cantin, Leela J. Chakravarti, Wing Y. Chan, Craig Cormick, et al. 2017. "Shifting Paradigms in Restoration of the World's Coral Reefs." *Global Change Biology* 23 (9): 3437–48.

Oppen, Madeleine J. H. van, James K. Oliver, Hollie M. Putnam, and Ruth D. Gates. 2015. "Building Coral Reef Resilience through Assisted Evolution." *Proceedings of the National Academy of Sciences*. https://doi.org/10.1073/pnas.1422301112.

Peixoto, Raquel S., Phillipe M. Rosado, Deborah Catharine de Assis Leite, Alexandre S. Rosado, and David G. Bourne. 2017. "Beneficial Microorganisms for Corals (BMC): Proposed Mechanisms for Coral Health and Resilience." *Frontiers in Microbiology* 8 (March): 341.

Poloczanska, Elvira S., Christopher J. Brown, William J. Sydeman, Wolfgang Kiessling, David S. Schoeman, Pippa J. Moore, Keith Brander, et al. 2013. "Global Imprint of Climate Change on Marine Life." *Nature Climate Change* 3 (10): 919–25.

Poloczanska, Elvira S., Michael T. Burrows, Christopher J. Brown, Jorge García Molinos, Benjamin S. Halpern, Ove Hoegh-Guldberg, Carrie V. Kappel, et al. 2016. "Responses of Marine Organisms to Climate Change across Oceans." *Frontiers in Marine Science* 3: 62.

Pörtner, Hans-Otto, Debra C. Roberts, Valérie Masson-Delmotte, Panmao Zhai, Melinda Tignor, Elvira Poloczanska, Katja Mintenbeck, et al. 2019. "IPCC Special Report on the Ocean and Cryosphere in a Changing Climate." *IPCC Intergovernmental Panel on Climate Change: Geneva, Switzerland* 1 (3).

Putnam, H. M., A. B. Mayfield, T. Y. Fan, C. S. Chen, and R. D. Gates. 2013. "The Physiological and Molecular Responses of Larvae from the Reef-Building Coral Pocillopora Damicornis Exposed to near-Future Increases in Temperature and pCO2." *Marine Biology* 160 (8): 2157–73.

Putnam, Hollie M. 2021. "Avenues of Reef-Building Coral Acclimatization in Response to Rapid Environmental Change." *The Journal of Experimental Biology* 224 (Pt Suppl 1). https://doi.org/10.1242/jeb.239319.

Putnam, Hollie M., Jennifer M. Davidson, and Ruth D. Gates. 2016. "Ocean Acidification Influences Host DNA Methylation and Phenotypic Plasticity in Environmentally Susceptible Corals." *Evolutionary Applications*. https://doi.org/10.1111/eva.12408.

Rivera-Casas, Ciro, Rodrigo Gonzalez-Romero, Manjinder S. Cheema, Juan Ausió, and José M. Eirín-López. 2016. "The Characterization of macroH2A beyond

Vertebrates Supports an Ancestral Origin and Conserved Role for Histone Variants in Chromatin." *Epigenetics: Official Journal of the DNA Methylation Society* 11 (6): 415–25.

Rivera-Casas, Ciro, Rodrigo González-Romero, Ángel Vizoso-Vazquez, Manjinder S. Cheema, M. Esperanza Cerdán, Josefina Méndez, Juan Ausió, and Jose M. Eirin-Lopez. 2016. "Characterization of Mussel H2A.Z.2: A New H2A.Z Variant Preferentially Expressed in Germinal Tissues from Mytilus." *Biochemistry and Cell Biology = Biochimie et Biologie Cellulaire* 94 (5): 480–90.

Roberts, Sarah M. 2019. "The Role of Cyclical Climate Oscillations in Species Distribution Shifts under Climate Change." *Predicting Future Oceans*. https://doi.org/10.1016/b978-0-12-817945-1.00011-3.

Roberts, Steven B., and Mackenzie R. Gavery. 2012. "Is There a Relationship between DNA Methylation and Phenotypic Plasticity in Invertebrates?" *Frontiers in Physiology* 2. https://doi.org/10.3389/fphys.2011.00116.

Rodriguez-Casariego, Javier A., Mark C. Ladd, Andrew A. Shantz, Christian Lopes, Manjinder S. Cheema, Bohyun Kim, Steven B. Roberts, et al. 2018. "Coral Epigenetic Responses to Nutrient Stress: Histone H2A.X Phosphorylation Dynamics and DNA Methylation in the Staghorn Coral Acropora Cervicornis." *Ecology and Evolution* 8 (23): 12193–207.

Ryu, Taewoo, Heather D. Veilleux, Jennifer M. Donelson, Philip L. Munday, and Timothy Ravasi. 2018. "The Epigenetic Landscape of Transgenerational Acclimation to Ocean Warming." *Nature Climate Change*. https://doi.org/10.1038/s41558-018-0159-0.

Sarda, Shrutii, Jia Zeng, Brendan G. Hunt, and Soojin V. Yi. 2012. "The Evolution of Invertebrate Gene Body Methylation." *Molecular Biology and Evolution* 29 (8): 1907–16.

Schunter, Celia, Megan J. Welch, Göran E. Nilsson, Jodie L. Rummer, Philip L. Munday, and Timothy Ravasi. 2018. "An Interplay between Plasticity and Parental Phenotype Determines Impacts of Ocean Acidification on a Reef Fish." *Nature Ecology & Evolution* 2 (2): 334–42.

Silverstein, Rachel N., Ross Cunning, and Andrew C. Baker. 2015. "Change in Algal Symbiont Communities after Bleaching, Not Prior Heat Exposure, Increases Heat Tolerance of Reef Corals." *Global Change Biology*. https://doi.org/10.1111/gcb.12706.

Skúlason, Skúli, Kevin J. Parsons, Richard Svanbäck, Katja Räsänen, Moira M. Ferguson, Colin E. Adams, Per-Arne Amundsen, et al. 2019. "A Way Forward with Eco Evo Devo: An Extended Theory of Resource Polymorphism with Postglacial Fishes as Model Systems." *Biological Reviews of the Cambridge Philosophical Society* 94 (5): 1786–1808.

Smith, Zachary D., and Alexander Meissner. 2013. “DNA Methylation: Roles in Mammalian Development.” *Nature Reviews. Genetics* 14 (3): 204–20.

Somero, G. N. 2010. “The Physiology of Climate Change: How Potentials for Acclimatization and Genetic Adaptation Will Determine ‘Winners’ and ‘Losers’. *The Journal of Experimental Biology* 213 (6): 912–20.

Suárez-Ulloa, Victoria, Juan Fernández-Tajes, Chiara Manfrin, Marco Gerdol, Paola Venier, and José M. Eirín-López. 2013. “Bivalve Omics: State of the Art and Potential Applications for the Biomonitoring of Harmful Marine Compounds.” *Marine Drugs* 11 (11): 4370–89.

Talbert, Paul B., and Steven Henikoff. 2021. “Histone Variants at a Glance.” *Journal of Cell Science* 134 (6). https://doi.org/10.1242/jcs.244749.

Taylor, Bethany C., and Nicolas L. Young. 2021. “Combinations of Histone Post-Translational Modifications.” *Biochemical Journal* 478 (3): 511–32.

The Royal Society, and The National Academy of Sciences. 2020. *Climate Change: Evidence and Causes: Update 2020*. National Academies Press.

Todd, Peter A. 2008. “Morphological Plasticity in Scleractinian Corals.” *Biological Reviews of the Cambridge Philosophical Society* 83 (3): 315–37.

Vandegehuchte, Michiel B., and Colin R. Janssen. 2011. “Epigenetics and Its Implications for Ecotoxicology.” *Ecotoxicology* 20 (3): 607–24.

Vandegehuchte, Michiel B., Tina Kyndt, Bartel Vanholme, Annelies Haegeman, Godelieve Gheysen, and Colin R. Janssen. 2009. “Occurrence of DNA Methylation in Daphnia Magna and Influence of Multigeneration Cd Exposure.” *Environment International* 35 (4): 700–706.

Van der Putten, Wim H., Mirka Macel, and Marcel E. Visser. 2010. “Predicting Species Distribution and Abundance Responses to Climate Change: Why It Is Essential to Include Biotic Interactions across Trophic Levels.” *Philosophical Transactions of the Royal Society of London. Series B, Biological Sciences* 365 (1549): 2025–34.

Veluchamy, Alaguraj, Achal Rastogi, Xin Lin, Bérangère Lombard, Omer Murik, Yann Thomas, Florent Dingli, et al. 2015. “An Integrative Analysis of Post-Translational Histone Modifications in the Marine Diatom Phaeodactylum Tricornutum.” *Genome Biology* 16 (May): 102.

Vercelloni, Julie, Benoit Liquet, Emma V. Kennedy, Manuel González-Rivero, M. Julian Caley, Erin E. Peterson, Marji Puotinen, Ove Hoegh-Guldberg, and Kerrie Mengersen. 2020. “Forecasting Intensifying Disturbance Effects on Coral Reefs.” *Global Change Biology* 26 (5): 2785–97.

Vignet, Caroline, Lucette Joassard, Laura Lyphout, Tiphaine Guionnet, Manon Goubeau, Karyn Le Menach, François Brion, et al. 2015. "Exposures of Zebrafish through Diet to Three Environmentally Relevant Mixtures of PAHs Produce Behavioral Disruptions in Unexposed F1 and F2 Descendant." *Environmental Science and Pollution Research International* 22 (21): 16371–83.

Waddington, C. H. 2012. "The Epigenotype." *International Journal of Epidemiology* 41 (1): 10–13.

Wallace, Douglas C., and Weiwei Fan. 2010. "Energetics, Epigenetics, Mitochondrial Genetics." *Mitochondrion* 10 (1): 12–31.

Wei, Jian-Wei, Kai Huang, Chao Yang, and Chun-Sheng Kang. 2017. "Non-Coding RNAs as Regulators in Epigenetics (Review)." *Oncology Reports* 37 (1): 3–9.

Weis, Virginia M. 2008. "Cellular Mechanisms of Cnidarian Bleaching: Stress Causes the Collapse of Symbiosis." *The Journal of Experimental Biology* 211 (Pt 19): 3059–66.

Wendte, Jered M., and Craig S. Pikaard. 2017. "The RNAs of RNA-Directed DNA Methylation." *Biochimica et Biophysica Acta, Gene Regulatory Mechanisms* 1860 (1): 140–48.

Williams, Amanda, Eric N. Chiles, Dennis Conetta, Jananan S. Pathmanathan, Phillip A. Cleves, Hollie M. Putnam, Xiaoyang Su, and Debashish Bhattacharya. 2021. "Metabolomic Shifts Associated with Heat Stress in Coral Holobionts." *Science Advances* 7 (1). https://doi.org/10.1126/sciadv.abd4210.

Woodhead, Anna J., Christina C. Hicks, Albert V. Norström, Gareth J. Williams, and Nicholas A. J. Graham. 2019. "Coral Reef Ecosystem Services in the Anthropocene." *Functional Ecology*, no. 1365-2435.13331 (March). https://doi.org/10.1111/1365-2435.13331.

Zhao, Yanchun, Yunhao Chen, Mei Jin, and Jin Wang. 2021. "The Crosstalk between m6A RNA Methylation and Other Epigenetic Regulators: A Novel Perspective in Epigenetic Remodeling." *Theranostics* 11 (9): 4549–66.

Zhou, P., E. Wu, H. B. Alam, and Y. Li. 2014. "Histone Cleavage as a Mechanism for Epigenetic Regulation: Current Insights and Perspectives." *Current Molecular Medicine* 14 (9): 1164–72.

Zink, Lisa-Maria, and Sandra B. Hake. 2016. "Histone Variants: Nuclear Function and Disease." *Current Opinion in Genetics & Development* 37 (April): 82–89.

Zlatanova, Jordanka, Thomas C. Bishop, Jean-Marc Victor, Vaughn Jackson, and Ken van Holde. 2009. "The Nucleosome Family: Dynamic and Growing." *Structure* 17 (2): 160–71.

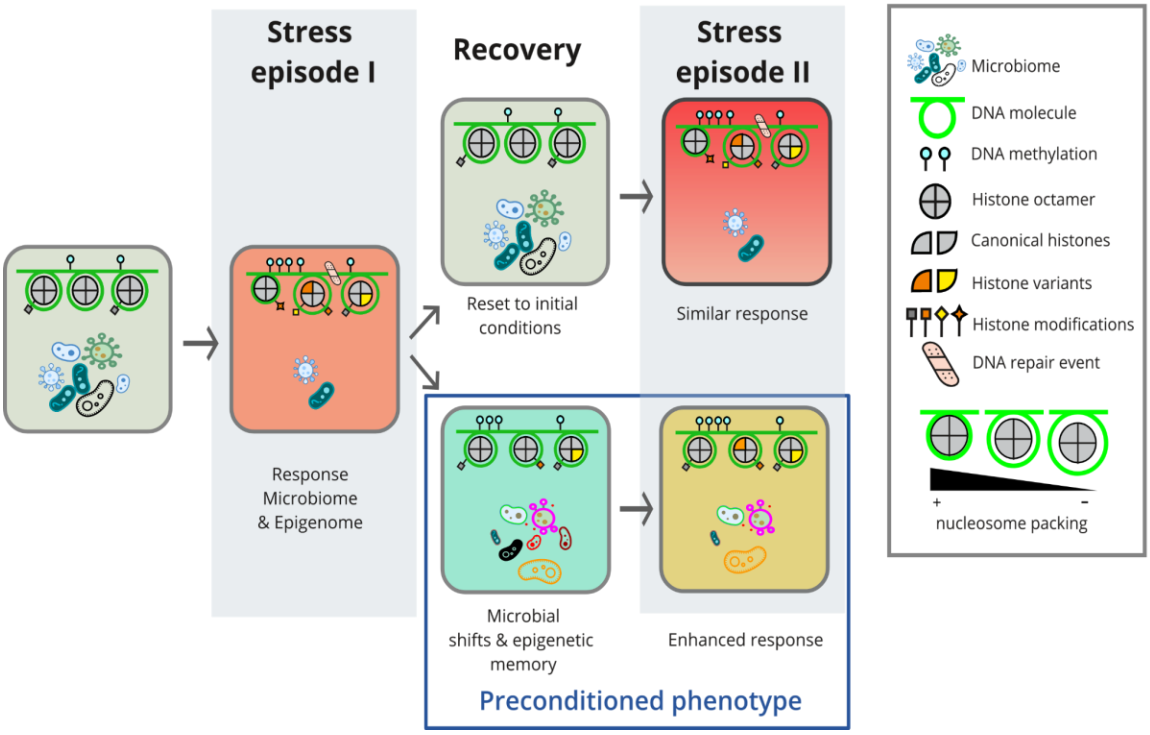

Fig. 1. Hypothesized model for environmental preconditioning through non-genetic mechanisms in the stony coral holobiont. Both epigenetic memory and microbiome shifts have the potential to respond to environmental change providing or modulating phenotypic plasticity. Such plastic responses could be reverted to initial conditions or result in preconditioned phenotypes in the absence of the stress. Preconditioned phenotypes will display enhanced responses to repetitive episodes of the same or similar stress. Figure from Beal et al. (2018).

CHAPTER II.

CORAL EPIGENETIC RESPONSES TO NUTRIENT STRESS: HISTONE H2A.X PHOSPHORYLATION DYNAMICS AND DNA METHYLATION IN THE STAGHORN CORAL *ACROPORA CERVICORNIS*.

This manuscript was published in Ecology and Evolution 2018, 8 (23), 12193-12207, and formatted according to the publisher's requirements.

Abstract

Nutrient pollution and thermal stress constitute two of the main drivers of global change in the coastal oceans. While different studies have addressed the physiological effects and ecological consequences of these stressors in corals, the role of acquired modifications in the coral epigenome during acclimatory and adaptive responses remains unknown. The present work aims to address that gap by monitoring two types of epigenetic mechanisms, namely histone modifications and DNA methylation, during a seven week-long experiment in which staghorn coral fragments (*Acropora cervicornis*) were exposed to nutrient stress (nitrogen, nitrogen + phosphorus) in the presence of thermal stress. The major conclusion of this experiment can be summarized by two main results: First, coral holobiont responses to the combined effects of nutrient enrichment and thermal stress involve the post-translational phosphorylation of the histone variant H2A.X (involved in responses to DNA damage), as well as non-significant modifications in DNA methylation trends. Second, the reduction in H2A.X phosphorylation (and the subsequent potential impairment of DNA repair mechanisms) observed after prolonged coral exposure to nitrogen enrichment and thermal stress is consistent with the symbiont-driven phosphorus limitation previously observed in corals subject to nitrogen enrichment. The alteration of this epigenetic mechanism could help to explain the synergistic effects of nutrient imbalance and thermal stress on coral fitness (i.e., increased bleaching and mortality) while supporting the positive effect of phosphorus addition to improving coral resilience to thermal stress. Overall, this work provides new insights into

the role of epigenetic mechanisms during coral responses to global change, discussing future research directions and the potential benefits for improving restoration, management, and conservation of coral reef ecosystems worldwide.

Introduction

Hermatypic (i.e., reef-building, stony) corals constitute the structural basis of reef ecosystems, providing the foundation for over 25% of marine and coastal biodiversity. Unfortunately, during the last decades, coral reefs have experienced dramatic declines worldwide, caused by local and global anthropogenic stressors (Pandolfi et al., 2003). The sessile lifestyle and long lifespan of corals increase their vulnerability to a rapidly changing environment (Cunning & Baker, 2012; Nesa & Hidaka, 2009), but also support the idea that their evolutionary success relies on a remarkable level of phenotypic plasticity (Barshis et al., 2013; Bruno & Edmunds, 1997; Dimond & Roberts, 2016; Dixon, Bay, & Matz, 2014). Although a high degree of genotypic diversity can be found in some coral species (Ayre & Hughes, 2000, 2004; Souter, 2010), it is becoming increasingly clear that the plasticity provided by this mechanism will not be enough to keep up with the rapid progression to a warmer, more polluted, more acidic, and carbonate-limited ocean (Hoegh-Guldberg et al., 2007; Hughes et al., 2017). Such a dark perspective has sparked the interest for the study of environmentally acquired nongenetic modifications (i.e., microbiome and epigenome dynamics) in these organisms, given their intrinsic potential to increase coral acclimatization and adaptation rates under rapidly changing environments (Palumbi, Barshis, Taylor-Knowles Nikki, & Bay, 2014; van Oppen, Oliver, Putnam, & Gates, 2015). For instance, recent reports have revealed that

specific symbiont strains can provide corals with higher tolerances to thermal stress (Leal et al., 2015; Silverstein, Cunning, & Baker, 2015, 2017), and that coral responses to different drivers of global climate change do in fact involve changes in the epigenome (i.e., DNA methylation) (Beal, Rodriguez-Casariego, Rivera-Casas, Suarez-Ulloa, & Eirín-López, 2018; Eirin-Lopez & Putnam, 2019; Liew et al., 2018; Putnam, Davidson, & Gates, 2016).

Organismal responses to environmental changes involve the activation of different mechanisms operating at diverse levels, from early genetic responses (Hoffmann & Willi, 2008) to whole-individual physiological responses (Boyd et al., 2015; Shultz et al., 2014). While different, all these mechanisms invariably require the modulation of the expression of specific sets of genes, promoting dynamic and sometimes reversible responses facilitating the onset of acclimatized phenotypes (Stillman & Armstrong, 2015). Epigenetic modifications, defined as phenomena and mechanisms that cause heritable (both mitotically and/or meiotically) chromosome-bound changes to gene expression, not involving changes to DNA sequence (sensu Deans & Maggert, 2015), are at the center of this regulatory process (Eirin-Lopez & Putnam, 2019). Among the different epigenetic mechanisms known so far, DNA methylation is the most studied in all types of organisms (Schübeler, 2015), including corals where recent studies have characterized DNA methylation levels in the germline and evidenced the involvement of this mechanism in responses to ocean acidification (Dimond & Roberts, 2016; Dixon et al., 2014; Liew et al., 2018; Marsh, Hoadley, & Warner, 2016; Putnam et al., 2016). Yet, studies elucidating the links between DNA methylation and gene expression, the interaction among different types of epigenetic mechanisms, as well

as their precise involvement in responses to different drivers of global climate change in ecologically and environmentally relevant organisms, are still lacking (Beal et al., 2018).

Among the multiple threats posed by global change, anthropogenic nutrient pollution constitutes one of the major drivers of coral decline (Fabricius, 2005; Wagner, Kramer, & van Woesik, 2010; Wooldridge, 2009). Their potential effects include increased coral bleaching (Cunning & Baker, 2012; Vega Thurber et al., 2014; Wooldridge, 2009), disease (Zaneveld, McMinds, & Thurber, 2017), reduced growth rates (Dunn, Sammarco, & LaFleur, 2012; Shantz & Burkepile, 2014) and impaired reproduction (Loya, Lubinevsky, Rosenfeld, & Kramarsky-Winter, 2004). A possible mechanism underlying these deleterious effects is the rapid proliferation of symbiont populations triggered by the disruption of the nitrogen (N)-limited environment maintained by the coral host inside the symbiosome (Downs et al., 2002; Nesa, Baird, Harii, Yakovleva, & Hidaka, 2012). The resulting phosphorus (P) starvation damages the photosynthetic machinery and alters the ionic balance in the symbiont thylakoid membranes (Pogoreutz et al., 2017; Wiedenmann et al., 2012), subsequently increasing the export of reactive oxygen species (ROS) to the intracellular space while intensifying oxidative and DNA damage in both the host and the symbiont (Baruch, Avishai, & Rabinowitz, 2005; Ezzat, Maguer, Grover, & Ferrier-Pagès, 2016; McGinty, Pieczonka, & Mydlarz, 2012; Nesa et al., 2012; Saragosti, Tchernov, Katsir, & Shaked, 2010; Wiedenmann et al., 2012). Overall, the effects of nutrient pollution will work synergistically with other stressors (particularly thermal stress) increasing bleaching at a mechanistic level (Pogoreutz et al., 2017) and coral mortality (Nesa & Hidaka, 2009; Yakovleva et al., 2009).

Although the potential ways in which nutrient and thermal stress can affect corals are well studied (Brown,1997; D'Angelo & Wiedenmann, 2014; Nielsen, Petrou, & Gates, 2018), the identity and the precise role of the epigenetic mechanisms linked to acclimatory and adaptive responses to these stressors remains unknown. In order to fill that gap, the present work conducted a field experiment consisting of two different types of coral nutrient enrichments (treatment 1, nitrogen only; treatment 2, nitrogen + phosphorus) using the staghorn coral *Acropora cervicornis* as model organism. Given that a thermal stress event was observed in the study at the same time that this experiment was taking place, the obtained results provide a unique opportunity to analyze the synergies between both types of stress mediating epigenetic responses in field conditions. Two types of epigenetic mechanisms were studied for that purpose, including histone modifications [histone H2A.X phosphorylation also known as gamma-H2A.X, a histone modification involved in DNA repair and a universal marker of DNA damage (González-Romero et al., 2012; Maré Chal & Zou, 2013)] and DNA methylation. It is hypothesized that nutrient enrichment will accelerate the growth of the symbiont population within the holobiont, resulting in a higher production of ROS which will in turn cause DNA damage, triggering an increase in gamma-H2A.X (associated to DNA repair activation) and changes in DNA methylation. It is also hypothesized that gamma-H2A.X formation will be impaired in corals exposed only to N enrichment (treatment 1), due to the P limitation caused by proliferation of symbionts in the absence of a P supply. Consequently, corals subject to N enrichment (treatment 1) would be expected to experience lower levels of DNA repair, encompassing deleterious phenotypic effects.

Methods

Study Site, Experimental and Sampling Design

Nutrient exposures were conducted using a common garden experiment in a large sand flat located near Pickles Reef in the Upper Florida Keys, Key Largo, FL (Fig. 1A) (25° 00′ 05″ N, 80° 24′ 55″ W) in approximately 5 - 7 m depth of water. Ambient nutrient conditions are relatively oligotrophic at this site (dissolved inorganic nitrogen (DIN) < 1.2 μM, soluble reactive phosphorus (SRP) < 0.04 μM; Zaneveld et al., 2016), making it a suitable location to test the effects of nutrient enrichment on corals. A total of 144 fragments of the staghorn coral *Acropora cervicornis* (three parental colonies, 7 to 13 cm in length) were obtained from a nearby offshore coral nursery operated by the Coral Restoration Foundation (permit no: FKNMS 2014-071). Each coral fragment was secured to a 50 cm tall section of PVC tubing (4 cm diameter) set in a base of concrete using nylon cable ties, for a total of 12 fragments per stand (Fig. 1B, C). Twelve experimental stands were distributed in a randomized block design across the study area with ≥ 2 m separation between them. Each stand (n = 4 per treatment) was randomly assigned to one of three treatment conditions as follows: Control (Ctrl), nitrogen enrichment (N), and nitrogen + phosphorus enrichment (N+P). Controls were replicated in the same way treatments were, to account for the potential environmental variability typical of field experiments. Coral fragments attached to stands were allowed to acclimate for more than 10 days without treatment until any visible wounds resulting from the fragmentation process healed. N enrichment was achieved using Florikan 0-19-0 slow-release ammonium nitrate fertilizer (300 g) as detailed by (Vega Thurber et al., 2014); N+P enrichment was obtained by combining 0-19-0 slow-release ammonium nitrate fertilizer

(300 g) with 80 g of 40-0-0 slow-release Superphosphate fertilizer. Ctrl stands were not exposed to any nutrient source. In both N and N+P treatments, nutrient exposure was achieved through the diffusion of nutrients in water by evenly dividing the fertilizer into two perforated PVC tubes, wrapped in mesh, and secured at opposing sides of each block via cable ties. This method was previously validated to triplicate the ambient levels of DIN and SRP for a period of 30 - 45 days in similar conditions (Heck, Pennock, Valentine, Coen, & Sklenar, 2000; Sotka & Hay, 2009; Vega Thurber et al., 2014).

Epigenetic modifications in invertebrates can occur rapidly after exposure to environmental stress (Gonzalez-Romero et al., 2017; Rivera-Casas et al., 2017; Suarez-Ulloa, Gonzalez-Romero, & Eirin-Lopez, 2015). Therefore, coral fragments were sampled at three different times during day 1 of exposure (1 h, 2 h, 5 h), day 2, day 7, and weekly thereafter for the next 4 weeks. For each sample, one coral fragment was randomly collected from each stand (n = 4 coral fragments per treatment, n = 12 fragments per sampling). Fragments were collected by cutting the cable ties securing them to the stands and were subsequently stored in individual sealed sterile plastic bags. Once all samples were collected, bags were transported to the surface and immediately flash-frozen in liquid nitrogen. Fragments were divided into sub-samples for nutrient analyses and for molecular analyses, finally stored at -80 ºC.

Nutrient Quantification

N and P content were quantified in tissue from coral fragments collected during the experiment, including increased sampling frequency during week 1. This sampling design is consistent with the findings of Achituv, Ben-Zion, & Mizrahi (1994) and

Muller-parker, Cook, & D'Elia, (1994), suggesting that the most significant nutrient changes in coral tissue occur within that period. Coral holobiont (the unit formed by the coral animal and its associated microorganisms consisting of bacteria, archaea, fungi, viruses, and protists including Symbiodiniaceae dinoflagellate algae) tissue was removed from a portion of each of the fragments sampled using an airbrush loaded with ultrapure water and was dried to a constant weight at 60 °C and homogenized to powder. Samples were subsequently fumed with HCl for 14 days to completely remove the skeletal inorganic carbon fraction (Szmant et al. 1990) and dried at 70 °C until no further weight change was observed. Carbon (C) and N content were measured in aliquots (10 mg) of dried and decalcified tissues using a FISONS elemental analyzer (NA1500, Loughborough, UK). P content was analyzed *sensu* Solórzano & Sharp, (1980) using a modification adapted for tissue (Fourqurean, Zieman, & Powell, 1992). Briefly, 5 to 10 mg of dried tissue were placed into glass scintillation vials, diluted with 0.5 mL of 0.17 M Na2SO4 and 2 mL of 0.017 M MgSO4, and dried again at 90 °C. The resulting powder was incubated at 500 °C for 3 h and cooled down to room temperature. A total of 5 mL of 0.2 N HCl was added to these oxidized and dried samples and incubated at 80 °C for 30 min, after which they were diluted with 10 mL of deionized water and allowed to stand overnight for the insoluble ash to settle. The phosphate concentration in the solution was determined as SRP using a colorimetric assay. The elemental content was calculated on a percentage of dry weight basis, and elemental ratios were calculated on a mole:mole basis. Data was collected following time frames reported in the literature, greater than or equal to 10 days (Godinot, Houlbrèque, Grover, & Ferrier-Pagès, 2011) but less than 8 weeks (Godinot, Ferrier-Pagès, & Grover, 2009), while considering the rapid initial

changes accounted in the sampling design (Achituv et al., 1994; Gisèle Muller-Parker et al., 1994). Accordingly, samples for the first three days were used as initial time (T1) and then organized into samples greater than 10 days but less than 8 weeks (T2 and T3) to ensure nutrient uptake representation.

Symbiont Density Analysis

The density of coral symbiont (Symbiodiniaceae) algae was quantified across treatments and exposure times by removing all tissue from the coral skeleton using the procedure detailed above. Upon extraction, tissue samples were homogenized using a tissue grinder and centrifuged for 5 minutes using a hand centrifuge to isolate symbiont cells. Each sample was subsequently divided into five technical replicates (100-300 µL each) and symbiont cells were quantified using a hemocytometer (Weber Scientific, Hamilton, NJ) in an inverted microscope (Leica, Buffalo Grove, IL). The extracted fragment's surface area (cm2) was estimated using the aluminum foil method (Marsh, 1970). Quantifications were averaged across technical replicates to produce mean symbiont density (cells x cm-2) for each fragment. To determine whether enrichments impacted Symbiodinaceae growth rates, we tested for differences in the symbiont density through time within each of the three treatments. To do so, we used linear mixed effects models with hours since enrichment began as a continuous predictor and included growth platform as a random factor to account for non-independence within the platforms (using $\chi 2$ with 1 d.f. to test whether symbiont growth rate significantly differs from zero through time). Tests were conducted using the *nlme* package in R (Pinheiro et al. 2018).

Normality and homogeneity of variance were confirmed via quantile-quantile plots and plots of fitted versus residual values.

Histone Isolation, Separation and Detection

Histone proteins were isolated as described elsewhere and adapted to coral tissue in the present work (Rivera-Casas et al., 2017). Accordingly, 5 mg of holobiont tissue were homogenized in a buffer consisting of 100 mM KCl, 50 mM Tris-HCl, 1 Mm MgCl2 and 0.5% Triton X-100 (pH 7.5) and containing a protease inhibitor mixture. After homogenization and incubation on ice for 5 min, samples were centrifuged at 12,000 g for 10 min at 4 ºC. The resulting pellets were resuspended in 0.6 N HCl, homogenized, and centrifuged again. The supernatant extracts were precipitated with six volumes of acetone at -20 ºC overnight and centrifuged at 12,000 g for 10 min at 4 ºC. The acetone pellets were dried using a Vacufuge concentrator (Eppendorf, Hamburg, Germany), and stored at -80 ºC. Histone protein separation was carried out in SDS-PAGE gels using ClearPAGE SDS gels 4-20% (C.B.S. Scientific, Del Mar, CA). Gels were stained with 0.2% (w/v) Coomassie blue in 25% (v/v) 2-propanol, 10% (v/v) acetic acid, and de-stained in 10% (v/v) 2-propanol, 10% (v/v) acetic acid. Additional histone separation was carried out using High Performance Liquid Chromatography (HPLC) as described in Rivera-Casas et al. (2017). Histone proteins were detected using commercial antibodies in western-blot analyses, including anti-H2A.X (H2A.X.ab, Abcam Cambridge, MA; H2A.Xry, Raybiotech, Norcross, GA) and anti-γH2A.X (γ-H2A.X ab, Rockland, Pottstown, PA; γ-H2A.Xry, Raybiotech, Norcross, GA). SDS-PAGE gels were electro transferred to a nitrocellulose membrane (C.B.S. Scientific, Del Mar, CA) and

processed as described elsewhere (Rivera-Casas et al., 2017). Membranes were incubated with a secondary goat anti-rabbit antibody (Rockland, Pottstown, PA) that was subsequently detected using enhanced chemiluminescence (Amershan ECL Prime Western Blotting Detection Reagent, GE Healthcare Life Sciences, Piscataway, NJ). Results were analyzed using the ChemiDoc-It TS2 Imager image analysis system (UVP Inc., San Gabriel, CA).

RNA Extraction, cDNA Synthesis and qPCR Reactions

Total RNA was extracted from coral holobiont tissue using Ribozol Reagent (Amresco, Solon, OH), and digested with PerfeCTa DNase I (Quanta Biosciences, Gaithersberg, MD) to eliminate residual genomic DNA. cDNA was synthesized using qScript cDNA Supermix (Quanta Biosciences, Gaithersberg, MD) and expression analyses were subsequently performed by means of quantitative PCR (qPCR). Primers specific for H2A.X and H4 histone genes were designed based on sequences retrieved from GenBank databases for *Acropora cervicornis* and *A. formosa* (Table 1) using the Primer-BLAST software (Ye et al., 2012). Histone H4 was used for normalization purposes. Primer efficiencies were calculated based on the slope of calibration curves constructed using ten-fold dilution steps, according to the formula $E = 10^{-1/slope}$. The resulting gene expression profiles were subsequently examined in *A. cervicornis* RNA samples by measuring SYBR green incorporation in a LightCycler 96 System (Roche, Mannheim, Germany). cDNA amplifications were carried out in 45 cycles under the following conditions: Preincubation at 95 °C for 10 min, denaturalization at 95 °C for 10 s, annealing at 60 °C for 10 s and elongation at 72 °C for 10 s, including a final

melting gradient up to 97 °C using a ramp of 4.4 °C x s-1 to confirm primer specificity. Each individual reaction was carried out in triplicate, including negative controls (No Template Control, NTC; Non-Reverse Transcription Control, NRTC). Results were recorded as normalized ratio values by the LightCycler 96 Software version 1.1 following the Pfaffl method (Pfaffl, 2001).

gamma-H2A.X/H2A.X Ratio Analysis

The quantification of histone H2A.X and its phosphorylated form (gamma-H2A.X) was implemented in coral samples from different experimental treatments by using a commercial ELISA kit (Raybiotech, Norcross, GA), providing a simultaneous semi-quantitative measure of the gamma-H2A.X/H2A.X ratio in a single experiment. For that purpose, 10 mg of coral tissue from each of three samples per treatment per time were solubilized in 500 µL of commercial lysis buffer and incubated on ice for 30 min. After centrifugation (18,000 g for 10 min at 4 °C), 100 µL of each lysate were loaded by duplicate in anti-H2A.X pre-coated microplate along with positive and negative controls provided in the kit, and samples were incubated overnight at 4 °C. Subsequently, 100 µL of detection antibodies [anti-H2A.X (S139) or anti-pan-H2A.X], HRP (Horseradish Peroxidase)-conjugated anti-rabbit IgG (against secondary antibodies) and TMB One-Step Substrate Reagent were added to the plate following manufacturer's indications. The TMB substrate was incubated for 30 min in the dark with shaking and 50 µL of Stop Solution were added to each well before reading absorbances in a ELx808IU microplate reader (Biotek, Winooski, VT) at 450 nm.

DNA Extraction and DNA Methylation Analysis

Genomic DNA was purified as described elsewhere and adapted to coral tissue in the present work. Briefly, tissue homogenates were incubated at 50 °C for 2 h with CTAB lysis buffer (100 mM Tris, 20mM EDTA, 1.2 M NaCl, 2% CTAB, pH 8.0) and proteinase K, completing DNA extraction following the phenol-chloroform protocol (Sambrook & Russell, 2006). DNA methylation was quantified in genomic DNA samples by measuring the amount of 5-methyl-Cytosines (5-mC), using the MethylFlash Global DNA Methylation (5-mC) ELISA kit (Epigentek, Farmingdale, NY). Accordingly, three genomic DNA samples per treatment/time were loaded in duplicate to ELISA plates, along with positive (polynucleotide with 50 % of 5-mC) and negative controls (polynucleotide with 50% of unmethylated Cytosine), all with binding solution. All samples were diluted to a final concentration of 9.645 ng/µL in NanoPure water, corresponding to 77.12 ng of DNA in each well. Once binding was completed, 100 µL of capture antibody, detection antibody, developer solution and stop solution were sequentially added, performing intercalated incubations and plate washes, following manufacturer indications. The absorbance (OD) resulting from the colorimetric reaction was quantified at 450 nm in a ELx808IU microplate reader (Biotek, Winooski, VT). Quantification of 5-methyl-Cytosine content (ng) was performed following the calculations suggested by the manufacturer.

Statistical Analyses

All results are presented as mean values of replicate samples ± standard error, unless indicated otherwise. All statistical analyses were performed with respect to

controls to separate the contributions of the experimental variables. The statistical significance of the effect of blocks, treatments and exposure time was evaluated by means of Two-Way ANOVA and One-Way ANOVA when required. This approach was appropriate for the analysis of P content, histone H2A.X quantification, and DNA methylation after transformation to natural logarithm. In all cases, data were confirmed to follow a normal distribution (Shapiro-Wilk Test, $p > 0.05$), and variance homogeneity (Brown-Forsythe Test, $p > 0.05$). The analysis of N content data (including N:P molar ratios) was done by means of a Two-Way PERMANOVA with Euclidean distance using 9,999 permutations (Anderson, 2001). Although this is primarily a multivariate method, it performs as a univariate test (equivalent to ANOVA) under the current experimental data conditions, avoiding the assumption of normality (Anderson, 2017) and allowing for the analysis of interactive effects (Doropoulos et al., 2014). PERMDISP was used to test for homogeneity of dispersion (equivalent to homoscedasticity). Post-hoc Tukey-HSD tests and the Holm-Sidak method were used for multiple comparisons when appropriate. All analyses were carried out using R 3.4.1 (R Core Team, 2017), except the Two-Way PERMANOVA that was performed using PAST 3.18 (Hammer, Harper, & Ryan, 2001) and the PERMDISP analysis that was performed with Primer v6 (Clarke & Gorley, 2006)

Results

Nutrient Quantification and Thermal Monitoring During Experimental Treatments.

The nutrient enrichment treatments implemented in the present work did not cause coral mortality, and no bleaching or disease were evident during the experiment. In addition, it was determined that the studied parameters were not influenced by the block

design ($p > 0.05$, Table 2). N and P levels in the holobiont displayed particularly low values (Fig. 2, Table 3), with %P around 0.4 and %N around 2.1 for all treatments. Nonetheless, while neither N or P content displayed significant differences among treatments (%P: $F(2, 34) = 0.744$, $p = 0.483$; %N: $F(2, 34) = 0.692$ $p = 0.427$), both parameters showed significant changes during the span of the experiment, decreasing in the case of P content ($F(4, 34) = 5.960$, $p = 0.007$, Fig. 2A), and increasing in the case of N content ($F(4, 34) = 10.527$, $p < 0.001$, Fig. 2B). As a result, N:P molar ratios displayed a significant dependence with time ($F(4, 34) = 13.62$, $p < 0.001$; Fig. 2C), as well as a statistical dependence with the nutrient enrichment treatments assayed ($F(2, 34) = 1.8245$ $p = 0.05$). Interestingly, although tissue nutrient analyses were not very sensitive to the nutrient addition treatments developed on the reef, results showed an antagonistic response of N and P through time, evidencing a mild nutrient enrichment in holobiont tissues.

Given that the present experiment was directly developed in the reef, factors other than nutrient exposure could be affecting the observed results, notably fluctuating thermal regimes. Consequently, temperature data corresponding to the experimental site (long-term monitoring station, 4 Km away and at similar depth, site 225, 25° 00.807', 80° 22.677') was subsequently analyzed to evaluate this possibility (Fig. 3). Results revealed a temperature increase in the lower portion of the water column (up to 40 cm from the bottom) from 28.39 ± 0.15 °C at the beginning of acclimatization period, to 30.52 ± 0.05 °C by the end of the experiment. This represents a net increase of more than 2 °C during the exposure period, reaching the bleaching threshold reported for *Acropora cervicornis* in the Florida Keys (30.5 °C; Manzello, Berkelmans, & Hendee, 2007). Based on this

observation, the effect of thermal stress was added to that of nutrient stress, in order to better evaluate their combined effect on coral epigenetic responses.

Changes in Symbiont Population Densities Across Nutrient Treatments.

Symbiont density analyses revealed a significant increase in the symbiont populations of *A. cervicornis* corals subject to nutrient enrichment treatments during the course of the present experiment (Table 4), as compared with the constant density levels observed in corals subject to control conditions. Additionally, the obtained results revealed that changes in symbiont densities were significantly influenced by the specific nature of the nutrient treatments as follows: on one hand, corals exposed to N only enrichment (treatment 1) displayed a twofold increase respect to control corals; on the other, a fourfold increase was observed in corals exposed to N+P enrichment (treatment 2). Along with nutrient quantification analyses, these results further support the efficiency of the nutrient exposures developed during the present work.

Changes in Histone H2A.X Phosphorylation During Nutrient and Thermal Stress.

Histones from *Acropora cervicornis* were extracted, isolated, and purified for the first time in the present work, including different fractions containing linker and core histones, as well as diverse histone-like proteins present in the coral holobiont (Fig. 4A, B). In addition, H2A.X and its phosphorylated form gamma-H2A.X were immuno-detected using western blot analyses (Fig. 4C), validating the use of different commercial antibodies for their detection in corals. The role of H2A.X during coral responses to nutrient and thermal stress was studied at two different functional levels. First, coral

H2A.X gene expression patterns were analyzed using coral-specific qPCR primers specifically designed using *A. cervicornis* and *A. formosa* sequences retrieved from GenBank databases as references (Table 1). The obtained results revealed homogeneous gene expression levels across the different nutrient treatments during the first 24 h of exposure ($F(2, 9) = 1.569$, $p = 0.265$, Fig. 5, Suppl. Fig. 1), suggesting that the main role of coral H2A.X during responses to nutrient stress (temperature was not high enough to cause stress during the first 24 h) does not take place at the transcriptional level.

The analysis of the epigenetic effects mediated by H2A.X was subsequently expanded to the post-translational level, based on the well-established link between H2A.X phosphorylation and DNA damage repair. For that purpose, gamma-H2A.X levels were quantified during coral 350 exposure to different nutrient treatments under increasing temperature, revealing significant differences between different treatments at specific sampling times ($F(14, 40) = 4.361$, $p < 0.001$) in spite of the high variability in the response of the controls. These results can be interpreted as indicative of DNA damage occurring in higher rates under enriched conditions, based on the stress marker nature of the gamma-H2A.X modification. Accordingly, the observed response can be divided into three major stages (Fig. 6A): first, an early rapid response consisting of a significant increase in gamma-H2A.X was observed during the first hour in corals subject to both N and N + P treatments (Tukey-HSD test, $q = 16.264$, $p = 0.003$); second, a suspended gamma-H2A.X response was observed in both treatments starting from hour 2 to day 7; and third, a late slow response in gamma-H2A.X over a longer period of time that was observed after day 7. In this last period, phosphorylation reached significantly different values in both enrichment treatments as follows: on one hand, gamma-H2A.X

became significantly greater than controls after a 20-day exposure to the N treatment (Tukey-HSD test, $q = 4.734$, $p = 0.036$) and after a 35-day exposure to N + P treatment (Holm-Sidak test, $t = 4.057$, $p < 0.001$); on the other, a reduction in gamma-H2A.X levels was observed in coral fragments subject to N enrichment for more than 20 days, displaying significant differences respect to controls upon reaching the 35-day mark (Holm-Sidak test, $t = 2.394$, $p = 0.021$).

Changes in DNA Methylation During Nutrient and Thermal Stress.

In addition to histone modifications, the role of DNA methylation during coral responses to nutrient stress was analyzed in the present work to account for the potential interaction among multiple mechanisms during epigenetic effects in response to environmental stress. In the present case, however, DNA methylation analyses did not detect significant differences among different nutrient treatments ($F(2, 44) = 2.505$, $p = 0.093$) or across different time points ($F(7, 44) = 2.081$, $p = 0.066$) (Fig. 6B). Nonetheless, the obtained results evidenced that the mean DNA methylation content in corals exposed to N enrichment was twice as much as that experienced by control corals at hour 1, hour 2, day 7, day 27 and day 35. The same was observed for corals exposed to N + P for day 27. Interestingly, this trend is similar (although no significant correlation was observed) to that observed for gamma-H2A.X (Fig. 6A), including an initial rapid response, followed by a suspended response and by a late slow response lasting until the end of the experiment.

Discussion

The present work constitutes one of the few pioneering efforts investigating the role of epigenetic mechanisms during environmental responses in corals, more precisely to nutrient and thermal stress. In doing so, this work also expands recent efforts combining the study of multiple epigenetic mechanisms during environmental epigenetic responses in marine invertebrates, including histone variants (and their modifications) and DNA methylation (Gonzalez-Romero et al., 2017; Li et al., 2018). The obtained results constitute the first description of the histone variant H2A.X and its phosphorylated form, gamma-H2A.X, in a stony coral species. Such findings, together with the histone diversity previously described in cnidarians (Reddy, Ubhe, Sirwani, Lohokare, & Galande, 2017; Török et al., 2016) as well as in Symbiodiniaceae dinoflagellates (Lin et al., 2015), unveil the potential contribution that chromatin-associated proteins convey during epigenetic effects and inheritance linked to environmental epigenetic responses in this group (Beal et al., 2018). Along with the study of DNA methylation levels, this work starts shaping our knowledge about the potential interactions among different epigenetic mechanisms mediating environmental responses, as well as their modulation by the combined action of different stressors (e.g., nutrients and temperature).

Coral Nutrient Content Does Not Predict Environmental Nutrient Exposure

Nutrient quantification analyses revealed a lack of correlation between nutrient content in the coral holobiont and the expected environmental nutrient levels derived from the experimental exposures. Nonetheless, a nutrient enrichment effect was evidenced by the N:P molar ratios estimated during exposures (Fig. 2C), as well as by the

increase in symbiont population densities across treatments (Table 4). Although nutrient content in water was not evaluated in this work, studies using the same enrichment strategy in the same location and season, successfully enriched the water column by approximately 3 μM N and 0.3 μM P in a 1 m radius around nutrient diffusers (Vega Thurber et al., 2014; Zaneveld et al., 2016), supporting the success of the present experimental approach in locally elevating nutrient concentrations available to experimental coral fragments. Indeed, it has been demonstrated that changes in environmental nutrient concentrations are not necessarily linked to changes in tissue content (Achituv et al., 1994; Godinot et al., 2009; Godinot, Ferrier-Pagès, Montagna, & Grover, 2011; 406 G Muller-Parker, Mccloskey, Hoegh-Guldberg, & Mcauley, 1994; Gisèle Muller-Parker et al., 1994). Accordingly, multiyear nutrient enrichment experiment (including both N and P) demonstrated a strong nutrient stoichiometric homeostasis and high constancy in coral holobiont tissue, regardless of elevated external nutrient levels, and even in the presence of a significant increase in the 15N isotope in corals exposed to N enrichment (Koop et al., 2001). Consequently, based on these observations as well as on the results obtained in the present work, the lack of a cause-effect relationship between environmental nutrient enrichment and the nutrient levels determined for coral tissues could be due to a rapid nutrient turnover in the holobiont.

On the other hand, nutrient content changed significantly with time and independently of nutrient treatment, suggesting that other factors may be influencing nutrient content in coral tissue. Among the different environmental parameters chiefly affecting coral fitness, it is well known that thermal stress can modify coral nutrient uptake ratios (Ezzat et al., 2016; Godinot, Houlbrèque, et al., 2011), and regulate

phosphate transfer to symbiotic vacuoles (Miller & Yellowlees, 1989). The analysis of thermal regimes during the present experiment revealed a progressive increase in water temperature in the area of study (Fig. 3), potentially affecting the observed nutrient dynamics. Accordingly, among the different reports addressing the effect of thermal stress on nutrient uptake ratios, at least one has described a sharp increase in N uptake (with no change in P intake) in corals subject to mild thermal stress (29 °C, Godinot et al., 2011), matching the observations described in the present work (Fig. 2A, B). On the other hand, alternative studies have described an inverse pattern in coral species subject to severe thermal stress (> 30 °C, Ezzat et al., 2016; Godinot et al., 2011). Altogether, these results are illustrative of the complexity of nutrient stress responses in corals, being possible that the thermal variation experienced by experimental corals (28 - 30°C) contributed to the observed trends in nutrient contents.

gamma-H2A.X Participates in Coral Epigenetic Responses to Nutrient and Thermal Stress

Coral exposure to elevated nutrient levels can promote the rapid proliferation of symbionts, leading to a potential increase in the production and export of ROS (Cunning & Baker, 2012; Ezzat et al., 2016; Marubini & Davies, 1996; Nesa & Hidaka, 2009; Wiedenmann et al., 2012; Wooldridge, 2 433 009), as well as in DNA damage (Lesser, 2006). Under conditions of nutrient imbalance and/or thermal stress, such deleterious effects are likely to be exacerbated by the damage experienced by the photosynthetic machinery (Pogoreutz et al., 2017), as well as by the disruption of the symbiont's membrane composition (Wiedenmann et al., 2012). Given the well-established role of

histone H2A.X and its phosphorylated form during the activation of DNA repair mechanisms in eukaryotes (Maré Chal & Zou, 2013; Suarez-Ulloa et al., 2015), the modifications observed in gamma-H2A.X/H2A.X levels are consistent with the role of this mechanism mediating epigenetic effects during coral responses to nutrient stress, supporting the link between exposure to nutrient/thermal stress and the presence of DNA damage.

The results from gene expression analyses indicate that the role played by H2A.X does not appear to take place at a transcriptional level (Fig. 5, Suppl. Fig. 1). Only two other studies have evaluated H2A.X gene expression in marine invertebrates, with contradictory results. On one hand, increased H2A.X.1 and H2A.X.2 mRNA levels were found in *Hydra* sp. exposed to the genotoxic agent bleomycin (Reddy et al., 2017). On the other, no expression changes were observed on variants H2A.X, H2A.Z and macroH2A during the exposure of the Eastern oyster *Crassostrea virginica* to marine toxins (Gonzalez-Romero et al., 2017). Nonetheless, both studies reported increased gamma-H2A.X levels upon exposure to environmental stress (Gonzalez-Romero et al., 2017; Reddy et al., 2017), supporting that the main functional role of this variant during DNA repair is regulated at a post-translational level.

The results obtained in this work suggest a link between environmental (nutrient/thermal) stress and histone H2A.X phosphorylation in corals. However, the observed patterns were complex. First, basal gamma-H2A.X levels (gamma-H2A.X/H2A.X ratio > 3) in corals are higher than those found in other eukaryotes including humans (Ji et al., 2017) and marine invertebrates (Gonzalez-Romero et al., 2017). Such peculiarity can be interpreted in the context of the recurrent state of

hyperoxia to which corals are subject during the day, resulting from the photosynthetic activity of symbiotic algae (Kuhl, Cohen, Dalsgaard, Jorgensen, & Revsbech, 1995; Shashar, Cohen, & Loya, 1993). This includes the production of ROS (Dykens, Shick, Benoit, Buettner, & Winston, 1992), requiring frequent 460 mitigation of the subsequent oxidative damage in the coral holobiont (Richier, Furla, Plantivaux, Merle, & Allemand, 2005; Roth, 2014). Precisely, such complex interaction between the coral host and the algal symbiont could also explain the high variability observed for gamma-H2A.X/H2A.X ratios in controls. Second, the transition from early rapid response, to suspended response, to late slow response periods in gamma-H2A.X levels (Fig. 6A) agrees with coral acclimatory responses, necessary to activate molecular and physiological mechanisms temporally restoring homeostasis until additional responses (usually more intense and persistent than the previous) are required. Indeed, a similar dynamic response was observed during coral exposure to thermal stress, involving two pulses in the expression of the heat shock protein hsp70 linked to acclimatization periods to different levels of stress (Gates & Edmunds, 1999). Similarly, Moya, Ganot, Furla, & Sabourault (2012) observed a rapid and transient transcriptomic response to stress in the anemone *Anemonia viridis*, followed by a second response after 5 or 21 days depending on the combination of thermal stress and UV exposure. The obtained results are further supported by the identification of pulse-like or transient responses in the expression and activity of stress proteins in coral larvae (Rodriguez-Lanetty, Harii, & Hoegh-Guldberg, 2009; Voolstra et al., 2009), as well as in molluscs exposed to thermal stress (Anestis, Lazou, Portner, & Michaelidis, 2007). The final stage of the experiment was particularly interesting regarding histone H2A.X dynamics, as gamma-H2A.X levels displayed

significant differences with respect to controls but with different signs depending on the nutrient treatment. Accordingly, gamma-H2A.X levels increased drastically in corals exposed to N + P by day 35, which not only agrees with a prolonged exposure to nutrient stress, but also with the increment in water temperature (more than 2 °C at this point). On the contrary, gamma-H2A.X levels decreased significantly by day 35 in corals exposed to N only enrichment, which is a remarkable observation considering that these individuals were also subject to thermal stress (and therefore require as much DNA repair as possible). This is probably one of the most interesting results in the present work, as it provides support for the hypothesis suggesting that N enrichment will promote P starvation in the coral holobiont (Wiedenmann et al., 2012), hampering the phosphorylation of H2A.X and subsequent activation of DNA repair mechanisms. In addition, P starvation has been proposed to increase thermally driven damage to photosystem II (Pogoreutz et al., 2017), as well as to limit the capacity of the thylakoid membrane to contain ROS (Wiedenmann et al. 2012), further exacerbating DNA damage in cells where DNA damage repair (by way of gamma-H2A.X formation) is already seriously impaired. On the other hand, a higher level of H2A.X phosphorylation (indicative of DNA damage sensing and repair) will be expected in corals exposed to N + P treatment after 35 days, as corroborated by the obtained results, thanks to the presence of P as part of that treatment, therefore preventing the harmful effects of P starvation.

Overall, the consequences of the impairment in H2A.X phosphorylation are enormous, as these will directly affect the ability of the coral holobiont to activate DNA damage repair mechanisms (Albino et al., 2009). Indeed, the alteration of this epigenetic mechanism could help explaining the synergistic effects of nutrient imbalance and

thermal stress on coral fitness, increasing bleaching and mortality (Ezzat et al., 2016; Wooldridge, 2009). Similarly, these results also support the positive effect of P addition in order to improve coral resilience to thermal stress (Ezzat et al., 2016).

Global DNA Methylation

Among the different epigenetic mechanisms known to date, DNA methylation is the best studied in marine organisms (Beal et al., 2018; Eirin-Lopez & Putnam, 2019). In the present work, the analysis of global DNA methylation did not detect significant differences among different nutrient treatments or across different time points (Fig. 6B). Such result is surprising, based on the multiple reports describing changes in DNA methylation levels in marine organisms subject to different environmental stimuli (Beal et al., 2018; Eirin-Lopez & Putnam, 2019). A possible explanation could involve the scale at which DNA methylation was quantified in the present work. Accordingly, DNA methylation was estimated at a global genomic level which provides little resolution, therefore, the marginal lack of significance observed could result from limited replication. In addition, DNA methylation was quantified for the coral holobiont (including both the coral host and the algal symbiont) introducing another potential source of variability affecting the results obtained. In addition, the canceling effect that specific local modifications may have on each other cannot be neglected. Lastly, both promoter and gene-body methylation (or the lack thereof) appear to contribute to phenotypic plasticity in marine invertebrates (Eirin-Lopez & Putnam, 2019; Gavery & Roberts, 2013; Li et al., 2018; Marsh & Pasqualone, 2014), making the study of this epigenetic mechanism extremely complex in this group. An illustration of such

complexity is exemplified by responses to stress involving an increase in DNA methylation at specific genomic regions accompanied by demethylation at others, resulting in a net genome-wide DNA methylation level similar to that present in controls (same number of DNA methylation marks but at different genomic regions). Despite the limitations of the method, the contribution of DNA methylation to coral stress responses is hinted by the trends observed, including pulsed changes in DNA methylation mirroring those observed in the case of gamma-H2A.X/H2A.X ratios. Since pulsed responses would facilitate immediate responses upon stress exposure, followed by the activation of other complementary mechanisms mediating longer-term responses, it would not be surprising if DNA methylation also follows such trend by regulating the expression of genes linked to other mechanisms involved in the maintenance of genome integrity. Further analyses addressing changes in DNA methylation variation at higher resolution (i.e., single nucleotide level) will be necessary in order to clarify that aspect.

Conclusions

This work constitutes a pioneering effort describing coral epigenetic modifications during responses to nutrient and thermal stress, including histone modifications and DNA methylation. The obtained results support the presence of the specialized histone variant H2A.X and its phosphorylated form (gamma-H2A.X) in stony corals. The relationship between gamma-H2A.X levels and coral exposure to stress appears to be consistent with the role of this histone modification activating DNA repair responses. Such function is further supported by the observed impairment of gamma-H2A.X formation after prolonged exposure to N enrichment, underscoring the

detrimental effects that P limitation bears on the epigenetic mechanisms preserving coral genome integrity. Although the observed modifications in DNA methylation during nutrient and thermal stress were not large enough to be statistically significant, the contribution of this epigenetic mechanism to coral stress responses should not be disregarded based on: a) the global nature of the DNA methylation estimations developed in this work; b) the similarity between the shape of DNA methylation trends (2 major pulses during the experiment), and that of the gamma-H2A.X response observed over the course of exposures; and c) the complexity of DNA methylation responses to environmental stress described in marine invertebrates. Overall, this effort constitutes a first step toward understanding the intricacies of the mechanisms regulating environmental epigenetic responses in marine organisms. Further efforts will be required to bring this research to the next level, including genome-wide, single-nucleotide resolution level studies to elucidate the regulatory relationships between different epigenetic mechanisms and the genes involved in acclimatory and adaptive responses. Similarly, the study of the interaction between the genome and the epigenome will help understand how population diversity shapes epigenetic responses in marine populations, along with the implications for the implementation of epigenetic selection methods. Although these goals will be even more challenging in the specific case of corals (given the contribution of the symbiont genome and epigenome to the phenotype of the holobiont) the potential benefits for improving restoration, management and conservation of coral reef ecosystems worldwide clearly justifies that effort.

References

Achituv, Y., Ben-Zion, M., & Mizrahi, L. (1994). Carbohydrate, lipid, and protein composition of zooxanthellae and animal fractions of the coral Pocillopora damicornis exposed to ammonium enrichment. Pacific Science, 48(3), 224–233. Retrieved from http://scholarspace.manoa.hawaii.edu/bitstream/10125/2231/1/v48n3-224-233.pdf

Anderson, M. J. (2001). A new method for non-parametric multivariate analysis of variance. Austral Ecol, 26(September), 32–46. https://doi.org/10.1111/j.1442-9993.2001.01070.pp.x

Anestis, A., Lazou, A., Portner, H. O., & Michaelidis, B. (2007). Behavioral, metabolic, and molecular stress responses of marine bivalve Mytilus galloprovincialis during long-term acclimation at increasing ambient temperature. AJP: Regulatory, Integrative and Comparative Physiology, 293(2), R911–R921. https://doi.org/10.1152/ajpregu.00124.2007

Ayre, D. J., & Hughes, T. P. (2000). Genotypic diversity and gene flow in brooding and spawning corals along the great barrier reef, Australia. Evolution, 54(5), 1590–1605. https://doi.org/10.1111/j.0014-3820.2000.tb00704.x

Ayre, D. J., & Hughes, T. P. (2004). Climate change, genotypic diversity and gene flow in reef-building corals. Ecology Letters, 7(4), 273–278. https://doi.org/10.1111/j.1461-0248.2004.00585.x

Barshis, D. J., Ladner, J. T., Oliver, T. A., Seneca, F. O., Traylor-Knowles, N., & Palumbi, S. R. (2013). Genomic basis for coral resilience to climate change. Proceedings of the National Academy of Sciences, 110(4), 1387–1392. https://doi.org/10.1073/pnas.1210224110

Baruch, R., Avishai, N., & Rabinowitz, C. (2005). UV incites diverse levels of DNA breaks in different cellular compartments of a branching coral species. The Journal of Experimental Biology, 208(Pt 5), 843–848. https://doi.org/10.1242/jeb.01496

Beal, A., Rodriguez-Casariego, J., Rivera-Casas, C., Suarez-Ulloa, V., & Eirín-López, J. M. (2018). Environmental epigenomics and its applications in marine organisms. In M. Oleksiak & O. Rajora (Eds.), Population Genomics: Marine Organisms (p. in press). Springer Nature.

Brown, B. E. (1997). Coral bleaching: causes and consequences. Coral Reefs, 16(0), 129–138. https://doi.org/10.1007/s003380050249

Bruno, J. F., & Edmunds, P. J. (1997). Clonal variation for phenotypic plasticity in the coral Madracis mirabilis. Ecology, 78(7), 2177–2190. https://doi.org/10.1890/0012-9658(1997)078[2177:cvfppi]2.0.co;2

Clarke, K. R., & Gorley, R. N. (2006). PRIMER v6: User Manual/Tutorial. Plymouth: PRIMER-E.

Cunning, R., & Baker, A. C. (2012). Excess algal symbionts increase the susceptibility of reef corals to bleaching. Nature Climate Change, 3(3), 259–262. Retrieved from http://www.nature.com/doifinder/10.1038/nclimate1711

D'Angelo, C., & Wiedenmann, J. (2014). Impacts of nutrient enrichment on coral reefs: New perspectives and implications for coastal management and reef survival. Current Opinion in Environmental Sustainability. https://doi.org/10.1016/j.cosust.2013.11.029

Deans, C., & Maggert, K. A. (2015). What Do You Mean, "Epigenetic"? Genetics, 199(4), 775–792. https://doi.org/10.1534/genetics.114.173492

Dimond, J. L., & Roberts, S. B. (2016). Germline DNA methylation in reef corals: Patterns and potential roles in response to environmental change. Molecular Ecology, 25(8), 1895–1904. https://doi.org/10.1111/mec.13414

Dixon, G. B., Bay, L. K., & Matz, M. V. (2014). Bimodal signatures of germline methylation are linked with gene expression plasticity in the coral Acropora millepora. BMC Genomics, 15(1), 1109. https://doi.org/10.1186/1471-2164-15-1109

Doropoulos, C., Roff, G., Zupan, M., Nestor, V., Isechal, A. L., & Mumby, P. J. (2014). Reef-scale failure of coral settlement following typhoon disturbance and macroalgal bloom in Palau, Western Pacific. Coral Reefs, 33(3), 613–623. https://doi.org/10.1007/s00338-014-1149-y

Downs, C. A., Fauth, J. E., Halas, J. C., Dustan, P., Bemiss, J., & Woodley, C. M. (2002). Oxidative stress and seasonal coral bleaching. Free Radical Biology and Medicine, 33(4), 533–543. https://doi.org/10.1016/S0891-5849(02)00907-3

Dunn, J. G., Sammarco, P. W., & LaFleur, G. (2012). Effects of phosphate on growth and skeletal density in the scleractinian coral Acropora muricata: A controlled experimental approach. Journal of Experimental Marine Biology and Ecology, 411, 34–44. https://doi.org/10.1016/j.jembe.2011.10.013

Dykens, J. A., Shick, J. M., Benoit, C., Buettner, G. R., & Winston, G. W. (1992). Oxygen Radical Production in the Sea Anemone Anthopleura Elegantissima and its Endosymbiotic Algae. Journal of Experimental Biology, 168(1), 219–241.

Eirin-Lopez, J. M., & Putnam, H. M. (2019). Marine Environmental Epigenetics. Annual Review of Marine Science, 11(1), annurev-marine-010318-095114. https://doi.org/10.1146/annurev-marine-010318-095114

Ezzat, L., Maguer, J.-F., Grover, R., & Ferrier-Pagès, C. (2016). Limited phosphorus availability is the Achilles heel of tropical reef corals in a warming ocean. Scientific Reports, 6(August), 31768. https://doi.org/10.1038/srep31768

Fabricius, K. E. (2005). Effects of terrestrial runoff on the ecology of corals and coral reefs: review and synthesis. Marine Pollution Bulletin, 50, 125–146.

Fourqurean, J. W., Zieman, J. C., & Powell, G. V. N. (1992). Phosphorus limitation of primary production in Florida Bay: Evidence from C: N: P ratios of the dominant seagrass Thalassia testudinum. Limnology and Oceanography, 37(1), 162–171. https://doi.org/10.4319/lo.1992.37.1.0162

Gates, R. D., & Edmunds, P. J. (1999). The Physiological Mechanisms of Acclimatization in Tropical Reef Corals. American Zoologist, 39(1), 30–43. https://doi.org/10.1093/icb/39.1.30

Gavery, M. R., & Roberts, S. B. (2013). Predominant intragenic methylation is associated with gene expression characteristics in a bivalve mollusc. PeerJ, 1, e215. https://doi.org/10.7717/peerj.215

Godinot, C., Ferrier-Pagès, C., & Grover, R. (2009). Control of phosphate uptake by zooxanthellae and host cells in the scleractinian coral Stylophora pistillata. Limnology and Oceanography, 54(5), 1627–1633. https://doi.org/10.4319/lo.2009.54.5.1627

Godinot, C., Ferrier-Pagès, C., Montagna, P., & Grover, R. (2011). Tissue and skeletal changes in the scleractinian coral Stylophora pistillata Esper 1797 under phosphate enrichment. Journal of Experimental Marine Biology and Ecology, 409(1–2), 200–207. https://doi.org/10.1016/j.jembe.2011.08.022

Godinot, C., Houlbrèque, F., Grover, R., & Ferrier-Pagès, C. (2011). Coral uptake of inorganic phosphorus and nitrogen negatively affected by simultaneous changes in temperature and pH. PLoS ONE, 6(9), e25024. https://doi.org/10.1371/journal.pone.0025024

González-Romero, R., Rivera-Casas, C., Fernández-Tajes, J., Ausió, J., Méndez, J., & Eirín-López, J. M. (2012). Chromatin specialization in bivalve molluscs: A leap forward for the evaluation of Okadaic Acid genotoxicity in the marine environment. Comparative Biochemistry and Physiology - C Toxicology and Pharmacology, 155(2), 175–181. https://doi.org/10.1016/j.cbpc.2011.09.003

Gonzalez-Romero, R., Suarez-Ulloa, V., Rodriguez-Casariego, J., Garcia-Souto, D., Diaz, G., Smith, A., … Eirin-Lopez, J. M. (2017). Effects of Florida Red Tides on histone variant expression and DNA methylation in the Eastern oyster Crassostrea virginica. Aquatic Toxicology, 186, 196–204. https://doi.org/10.1016/j.aquatox.2017.03.006

Hammer, Ø., Harper, D. A. T., & Ryan, P. D. (2001). PAST: Paleontological Statistics Software Package for Education and Data Analysis. Palaeontologia Electronica, 4(1), 9pp. Retrieved from https://www.uv.es/~pardomv/pe/2001_1/past/pastprog/past

Heck, K. L., Pennock, J. R., Valentine, J. F., Coen, L. D., & Sklenar, S. A. (2000). Effects of nutrient enrichment and small predator density on seagrass ecosystems: An experimental assessment. Limnology and Oceanography, 45(5), 1041–1057. https://doi.org/10.4319/lo.2000.45.5.1041

Hoegh-Guldberg, O., Mumby, J., Hooten, J., Steneck, S., Greenfield, P., Gomes, E., … Hatziolos, E. (2007). Coral reefs under rapid climate change and ocean acidification. Science, 318(5857), 1737.

Hughes, T. P., Kerry, J. T., Álvarez-Noriega, M., Álvarez-Romero, J. G., Anderson, K. D., Baird, A. H., … Wilson, S. K. (2017). Global warming and recurrent mass bleaching of corals. Nature, 543(7645). https://doi.org/10.1038/nature21707

Ji, J., Zhang, Y., Redon, C. E., Reinhold, W. C., Chen, A. P., Fogli, L. K., … Bonner, W. M. (2017). Phosphorylated fraction of H2AX as a measurement for DNA damage in cancer cells and potential applications of a novel assay. PLoS ONE, 12(2), e0171582. https://doi.org/10.1371/journal.pone.0171582

Koop, K., Booth, D., Broadbent, A., Brodie, J., Bucher, D., Capone, D., … Yellowlees, D. (2001). ENCORE: The effect of nutrient enrichment on coral reefs. Synthesis of results and conclusions. Marine Pollution Bulletin, 42(2), 91–120. https://doi.org/10.1016/S0025-326X(00)00181-8

Kuhl, M., Cohen, Y., Dalsgaard, T., Jorgensen, B. B., & Revsbech, N. P. (1995). Microenvironment and photosynthesis of zooxanthellae in scleractinian corals studied with microsensors for O2, pH and light. Marine Ecology Progress Series, 117(1–3), 159–177. https://doi.org/10.3354/meps117159

Leal, M. C., Hoadley, K., Pettay, D. T., Grajales, A., Calado, R., & Warner, M. E. (2015). Symbiont type influences trophic plasticity of a model cnidarian-dinoflagellate symbiosis. Journal of Experimental Biology, 218(6), 858–863. https://doi.org/10.1242/jeb.115519

Lesser, M. P. (2006). Oxidative Stress in Marine Environments: Biochemistry and Physiological Ecology. Annual Review of Physiology, 68(1), 253–278. https://doi.org/10.1146/annurev.physiol.68.040104.110001

Li, Y., Liew, Y. J., Cui, G., Cziesielski, M. J., Zahran, N., Michell, C. T., … Aranda, M. (2018). DNA methylation regulates transcriptional homeostasis of algal endosymbiosis in the coral model Aiptasia. Science Advances, 4(8), eaat2142. https://doi.org/10.1126/sciadv.aat2142

Liew, Y. J., Zoccola, D., Li, Y., Tambutte, E., Venn, A. A., Michell, C. T., … Aranda, M. (2018). Epigenome-associated phenotypic acclimatization to ocean acidification in a reef-building coral. Science Advances, 4(6), eaar8028. https://doi.org/10.1126/sciadv.aar8028

Lin, S., Cheng, S., Song, B., Zhong, X., Lin, X., Li, W., … Morse, D. (2015). The Symbiodinium kawagutii genome illuminates dinoflagellate gene expression and coral symbiosis. Science, 350(6261), 691–694. https://doi.org/10.1126/science.aad0408

Loya, Y., Lubinevsky, H., Rosenfeld, M., & Kramarsky-Winter, E. (2004). Nutrient enrichment caused by in situ fish farms at Eilat, Red Sea is detrimental to coral reproduction. Marine Pollution Bulletin, 49(4), 344–353. https://doi.org/10.1016/j.marpolbul.2004.06.011

Manzello, D. P., Berkelmans, R., & Hendee, J. C. (2007). Coral bleaching indices and thresholds for the Florida Reef Tract, Bahamas, and St. Croix, US Virgin Islands. Marine Pollution Bulletin, 54(12), 1923–1931. https://doi.org/10.1016/j.marpolbul.2007.08.009

Maré Chal, A., & Zou, L. (2013). DNA Damage Sensing by the ATM and ATR Kinases. Cold Spring Harb Perspect Biol, 5, a012716. https://doi.org/10.1101/cshperspect.a012716

Marsh, A. G., Hoadley, K. D., & Warner, M. E. (2016). Distribution of CpG motifs in upstream gene domains in a reef coral and sea anemone: Implications for epigenetics in cnidarians. PLoS ONE, 11(3), e0150840. https://doi.org/10.1371/journal.pone.0150840

Marsh, A. G., & Pasqualone, A. A. (2014). DNA methylation and temperature stress in an Antarctic polychaete, Spiophanes tcherniai. Frontiers in Physiology, 5, 173. https://doi.org/10.3389/fphys.2014.00173

Marubini, F., & Davies, P. S. (1996). Nitrate increases zooxanthellae population density and reduces skeletogenesis in corals. Marine Biology, 127(2), 319–328. https://doi.org/10.1007/BF00942117

McGinty, E. S., Pieczonka, J., & Mydlarz, L. D. (2012). Variations in reactive oxygen release and antioxidant activity in multiple Symbiodinium types in response to elevated temperature. Microbial Ecology, 64(4), 1000–1007. https://doi.org/10.1007/s00248-012-0085-z

Miller, D. J., & Yellowlees, D. (1989). Inorganic Nitrogen Uptake by Symbiotic Marine Cnidarians: A Critical Review. Proceedings of the Royal Society B: Biological Sciences, 237(1286), 109–125. https://doi.org/10.1098/rspb.1989.0040

Moya, A., Ganot, P., Furla, P., & Sabourault, C. (2012). The transcriptomic response to thermal stress is immediate, transient and potentiated by ultraviolet radiation in

the sea anemone Anemonia viridis. Molecular Ecology, 21(5), 1158–1174. https://doi.org/10.1111/j.1365-294X.2012.05458.x

Muller-Parker, G., Cook, C. B., & D'Elia, C. F. (1994). Elemental composition of the coral Pocillopora damicornis exposed to elevated seawater ammonium. Pacific Science, 48(3), 234–246.

Muller-Parker, G., Mccloskey, L. R., Hoegh-Guldberg, 0, & Mcauley, P. J. (1994). Effect of Ammonium Enrichment on Animal and Algal Biomass of the Coral Pocillopora damicornis. Pacific Science, 48(3), 273–283. Retrieved from http://hl-128-171-57-22.library.manoa.hawaii.edu/bitstream/10125/2236/1/v48n3-273-283.pdf

Nesa, B., Baird, A. H., Harii, S., Yakovleva, I., & Hidaka, M. (2012). Algal Symbionts Increase DNA Damage in Coral Planulae Exposed to Sunlight. Zoological Studies, 51(1), 12–17. Retrieved from http://zoolstud.sinica.edu.tw/Journals/51.1/12.pdf

Nesa, B., & Hidaka, M. (2009). High zooxanthella density shortens the survival time of coral cell aggregates under thermal stress. Journal of Experimental Marine Biology and Ecology, 368(1), 81–87. https://doi.org/10.1016/j.jembe.2008.10.018

Nielsen, D. A., Petrou, K., & Gates, R. D. (2018). Coral bleaching from a single cell perspective. The ISME Journal. https://doi.org/10.1038/s41396-018-0080-6

Palumbi, S. R., Barshis, D. J., Taylor-Knowles Nikki, & Bay, R. A. (2014). Mechanisms of reef coral resistance to future climate change. Science, 344(6186), 895–898. https://doi.org/10.1126/science.1251336

Pandolfi, J. M., Bradbury, R., Sala, E., Hughes, T. P., Bjorndal, K. A., Cooke, R., … Jackson, J. B. C. (2003). Climate change, human impacts, and the resilience of coral reefs. Science, 301(5635), 955–958. https://doi.org/10.1126/science.1085046

Pfaffl, M. W. (2001). A new mathematical model for relative quantification in real-time RT-PCR. Nucleic Acids Research, 29(9), e45. https://doi.org/10.1093/nar/29.9.e45

Pogoreutz, C., Rädecker, N., Cárdenas, A., Gärdes, A., Voolstra, C. R., & Wild, C. (2017). Sugar enrichment provides evidence for a role of nitrogen fixation in coral bleaching. Global Change Biology, 23(9), 3838–3848. https://doi.org/10.1111/gcb.13695

Putnam, H. M., Davidson, J., & Gates, R. D. (2016). Ocean acidification influences DNA methylation and phenotypic plasticity in environmentally susceptible corals. Evolutionary Applications, 56, E177–E177. https://doi.org/10.1111/eva.12408

Reddy, P. C., Ubhe, S., Sirwani, N., Lohokare, R., & Galande, S. (2017). Title: Rapid divergence of histones in Hydrozoa (Cnidaria) and evolution of a novel histone involved in DNA damage response in hydra. Zoology. https://doi.org/10.1016/j.zool.2017.06.005

Richier, S., Furla, P., Plantivaux, A., Merle, P., & Allemand, D. (2005). Symbiosis-induced adaptation to oxidative stress. Journal of Experimental Biology, 208(2), 277–285. https://doi.org/10.1242/jeb.01368

Rivera-Casas, C., Gonzalez-Romero, R., Garduño, R. A., Cheema, M. S., Ausio, J., & Eirin-Lopez, J. M. (2017). Molecular and biochemical methods useful for the epigenetic characterization of chromatin-associated proteins in bivalve molluscs. Frontiers in Physiology, 8(AUG), 490. https://doi.org/10.3389/fphys.2017.00490

Rodriguez-Lanetty, M., Harii, S., & Hoegh-Guldberg, O. (2009). Early molecular responses of coral larvae to hyperthermal stress. Molecular Ecology, 18(24), 5101–5114. https://doi.org/10.1111/j.1365-294X.2009.04419.x

Roth, M. S. (2014). The engine of the reef: Photobiology of the coral-algal symbiosis. Frontiers in Microbiology. https://doi.org/10.3389/fmicb.2014.00422

Sambrook, J., & Russell, D. W. (2006). Purification of nucleic acids by extraction with phenol:chloroform. Cold Spring Harb Protoc, 2006(1). https://doi.org/10.1101/pdb.prot4455

Saragosti, E., Tchernov, D., Katsir, A., & Shaked, Y. (2010). Extracellular production and degradation of superoxide in the coral stylophora pistillata and cultured symbiodinium. PLoS ONE, 5(9), 1–10. https://doi.org/10.1371/journal.pone.0012508

Schübeler, D. (2015, January 15). Function and information content of DNA methylation. Nature. Nature Publishing Group. https://doi.org/10.1038/nature14192

Shantz, A. A., & Burkepile, D. E. (2014). Context-dependent effects of nutrient loading on the coral-algal mutualism. Ecology, 95(7), 1995–2005. https://doi.org/10.1890/13-1407.1

Shashar, N., Cohen, Y., & Loya, Y. (1993). Extreme Diel Fluctuations of Oxygen in Diffusive Boundary Layers Surrounding Stony Corals. Biol. Bull, 185, 455–461. Retrieved from http://www.journals.uchicago.edu/t-and-c

Silverstein, R. N., Cunning, R., & Baker, A. C. (2015). Change in algal symbiont communities after bleaching, not prior heat exposure, increases heat tolerance of reef corals. Global Change Biology, 21(1), 236–249. https://doi.org/10.1111/gcb.12706

Silverstein, R. N., Cunning, R., & Baker, A. C. (2017). Tenacious D: Symbiodinium in clade D remain in reef corals at both high and low temperature extremes despite

impairment. The Journal of Experimental Biology, 220, 1192–1196. https://doi.org/10.1242/jeb.148239

Solórzano, L., & Sharp, J. H. (1980). Determination of total dissolved phosphorus and particulate phosphorus in natural waters. Limnology and Oceanography, 25(4), 754–758. https://doi.org/10.4319/lo.1980.25.4.0754

Sotka, E. E., & Hay, M. E. (2009). Effects of herbivores, nutrient enrichment, and their interactions on macroalgal proliferation and coral growth. Coral Reefs, 28(3), 555–568. https://doi.org/10.1007/s00338-009-0529-1

Souter, P. (2010). Hidden genetic diversity in a key model species of coral. Marine Biology, 157(4), 875–885. https://doi.org/10.1007/s00227-009-1370-3

Stillman, J. H., & Armstrong, E. (2015, March 1). Genomics are transforming our understanding of responses to climate change. BioScience. Oxford University Press. https://doi.org/10.1093/biosci/biu219

Suarez-Ulloa, V., Gonzalez-Romero, R., & Eirin-Lopez, J. M. (2015). Environmental epigenetics: A promising venue for developing next-generation pollution biomonitoring tools in marine invertebrates. Marine Pollution Bulletin, 98(1–2), 5–13. https://doi.org/10.1016/j.marpolbul.2015.06.020

Török, A., Schiffer, P. H., Schnitzler, C. E., Ford, K., Mullikin, J. C., Baxevanis, A. D., … Gornik, S. G. (2016). The cnidarian Hydractinia echinata employs canonical and highly adapted histones to pack its DNA. Epigenetics & Chromatin, 9(1), 36. https://doi.org/10.1186/s13072-016-0085-1

van Oppen, M. J. H., Oliver, J. K., Putnam, H. M., & Gates, R. D. (2015). Building coral reef resilience through assisted evolution. Proceedings of the National Academy of Sciences, 112(8), 1–7. https://doi.org/10.1073/pnas.1422301112

Vega Thurber, R. L., Burkepile, D. E., Fuchs, C., Shantz, A. A., Mcminds, R., & Zaneveld, J. R. (2014). Chronic nutrient enrichment increases prevalence and severity of coral disease and bleaching. Global Change Biology, 20(2), 544–554. https://doi.org/10.1111/gcb.12450

Voolstra, C. R., Schnetzer, J., Peshkin, L., Randall, C. J., Szmant, A. M., & Medina, M. (2009). Effects of temperature on gene expression in embryos of the coral Montastraea faveolata. BMC Genomics, 10(1), 627. https://doi.org/10.1186/1471-2164-10-627

Wagner, D., Kramer, P., & van Woesik, R. (2010). Species composition, habitat, and water quality influence coral bleaching in southern Florida. Marine Ecology Progress Series, 408, 65–78. https://doi.org/10.3354/meps08584

Wiedenmann, J., D 'angelo, C., Smith, E. G., Hunt, A. N., Legiret, F.-E., Postle, A. D., & Achterberg, E. P. (2012). Nutrient enrichment can increase the susceptibility of

reef corals to bleaching. Nature Climate Change, 3(2), 160–164. Retrieved from http://www.nature.com/doifinder/10.1038/nclimate1661

Wooldridge, S. A. (2009). Water quality and coral bleaching thresholds: Formalising the linkage for the inshore reefs of the Great Barrier Reef, Australia. Marine Pollution Bulletin, 58(5), 745–751. https://doi.org/10.1016/j.marpolbul.2008.12.013

Yakovleva, I. M., Baird, A. H., Yamamoto, H. H., Bhagooli, R., Nonaka, M., & Hidaka, M. (2009). Algal symbionts increase oxidative damage and death in coral larvae at high temperatures. Marine Ecology Progress Series, 378, 105–112. https://doi.org/10.3354/meps07857

Ye, J., Coulouris, G., Zaretskaya, I., Cutcutache, I., Rozen, S., & Madden, T. L. (2012). Primer-BLAST: A tool to design target-specific primers for polymerase chain reaction. BMC Bioinformatics, 13(1), 134. https://doi.org/10.1186/1471-2105-13-134

Zaneveld, J. R., Burkepile, D. E., Shantz, A. A., Pritchard, C. E., McMinds, R., Payet, J. P., … Vega Thurber, R. L. (2016). Overfishing and nutrient pollution interact with temperature to disrupt coral reefs down to microbial scales. Nature Communications, (May), 1–12. https://doi.org/10.1038/ncomms11833

Zaneveld, J. R., McMinds, R., & Thurber, R. V. (2017). Stress and stability: Applying the Anna Karenina principle to animal microbiomes. Nature Microbiology. https://doi.org/10.1038/nmicrobiol.2017.121

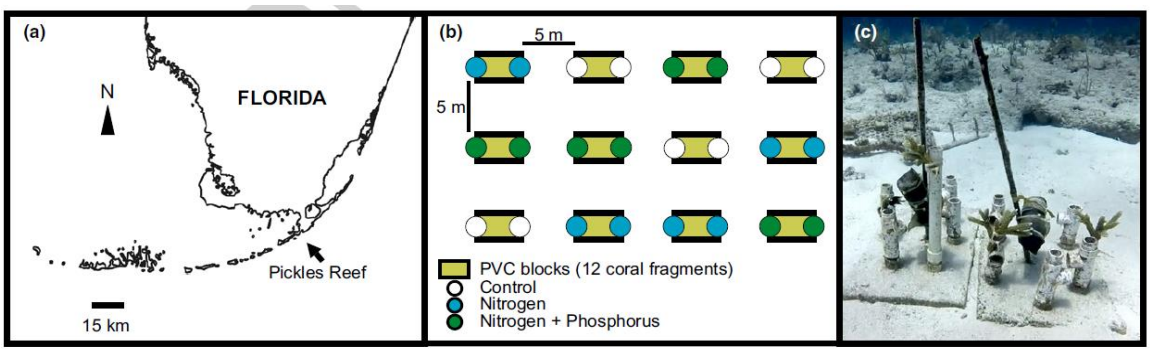

Fig. 1. A. Field experiment site location in Pickles Reef, Upper Florida Keys, Key Largo, FL (25°00′05″ N, 80°24′55″W). **B.** Nutrient exposure experiment design consisting of 12 blocks evenly distributed across the study area (n = 4 blocks per treatment), randomly assigned to one of three treatment conditions: control (C), Nitrogen enrichment (N), and Nitrogen and Phosphorous enrichment (N + P). **C.** Each coral fragment was secured to PVC tubing set in a base of concrete using nylon cable ties, for a total of 12 fragments per block.

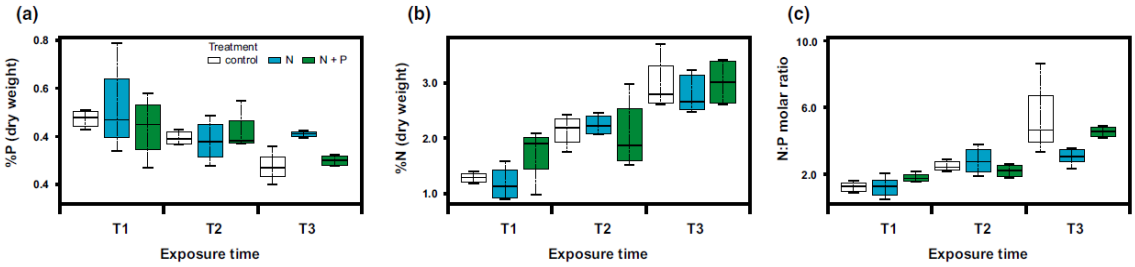

Fig. 2. Nutrient content in tissue from staghorn coral fragments exposed to the different enrichment treatments implemented in the present work. **A.** Phosphorus tissue content in coral fragments expressed as percent of dry mass of reactive phosphate; **B.** Nitrogen tissue content in coral fragments expressed as percent of dry mass; **C.** N:P molar ratio. Exposure times are defined as: T1, hour 1 to day 3; T2, day 3 to day 20; and T3, day 20 to day 35.

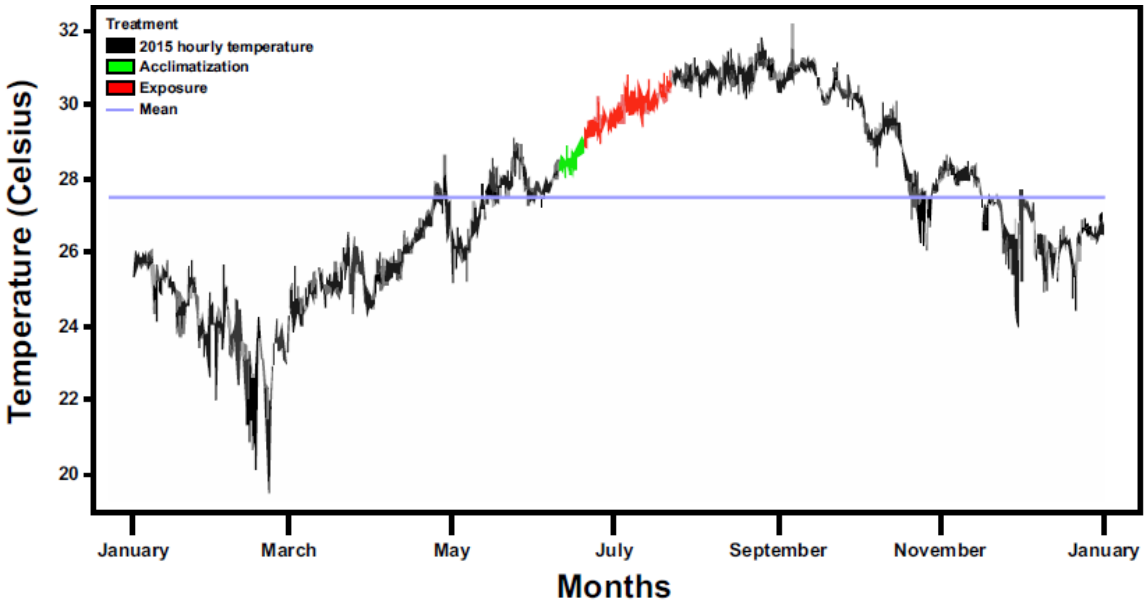

Fig. 3. Hourly water column temperatures in the Florida Keys National Marine Sanctuary, site 225, for the year 2015. The blue line represents the mean value for the temperature registered in this station for the year. The periods corresponding to the different stages of the experiment are indicated in green (acclimatization of coral fragments) and red (exposure of coral fragments to nutrient enrichment treatments).

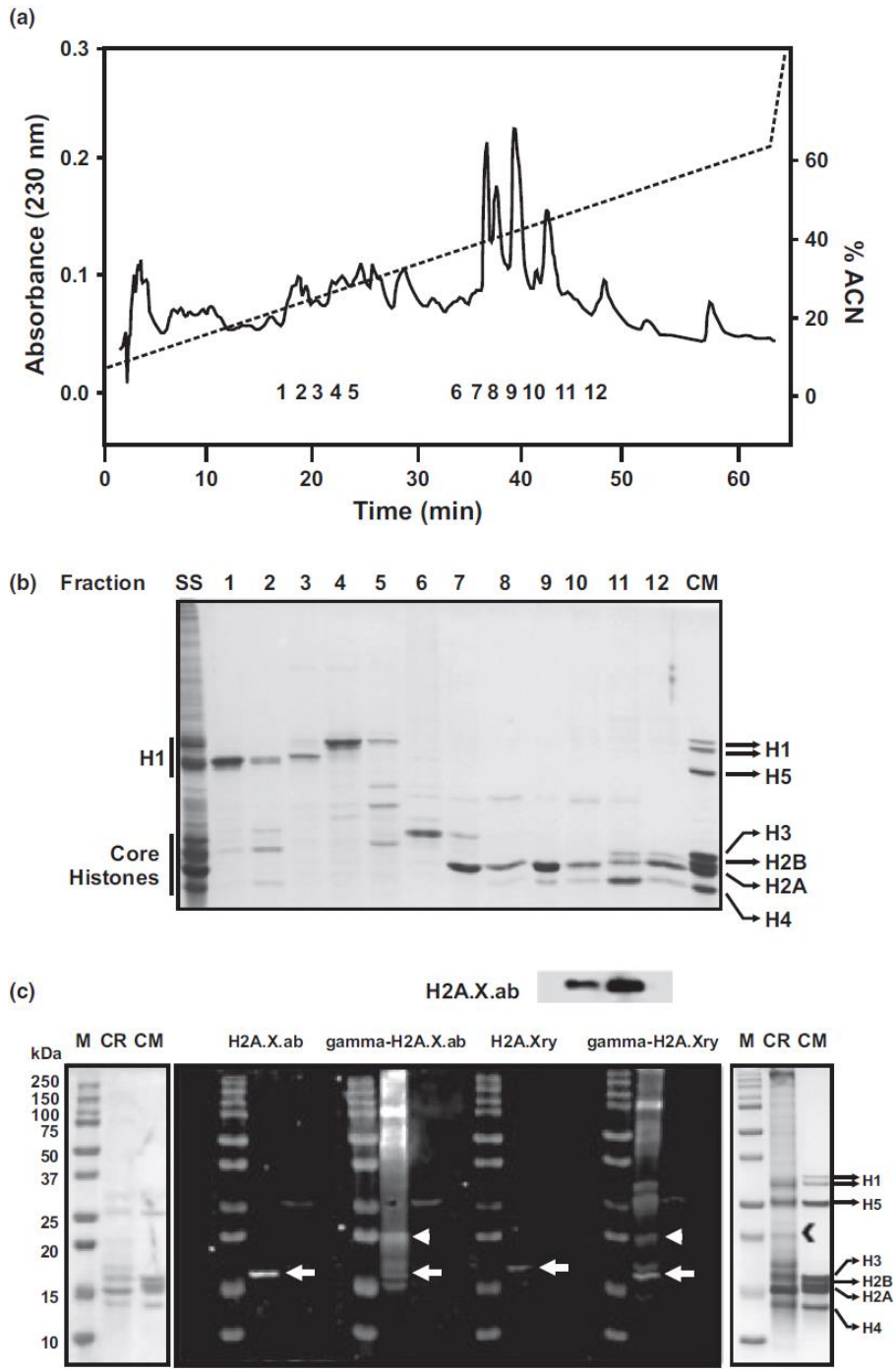

Fig. 4. A. Purification profile of acid-extracted staghorn coral histones across an acetonitrile gradient (ACN) using HPLC. The analyzed histone fractions are indicated by numbers 1-12. **B.** SDS-PAGE separation of HPLC histone fractions 1-12 revealing linker and core histones, as well as diverse histone like proteins present in the coral holobiont. **C.** Western blot immunodetection of histone variant H2A.X and its phosphorylated form (gamma-H2A.X) to validate antibody specificity (above) and of HCl-extracted histones

from *A. cervicornis* (below) using commercial antibodies H2A.X.ab (Abcam), γ-H2A.X ab (Abcam), H2A.Xry (RayBiotech) and γ-H2A.Xry (RayBiotech). ACN, acetonitrile; CM, chicken marker; M: molecular weight marker; CR, coral tissue extraction; SS, starting sample.

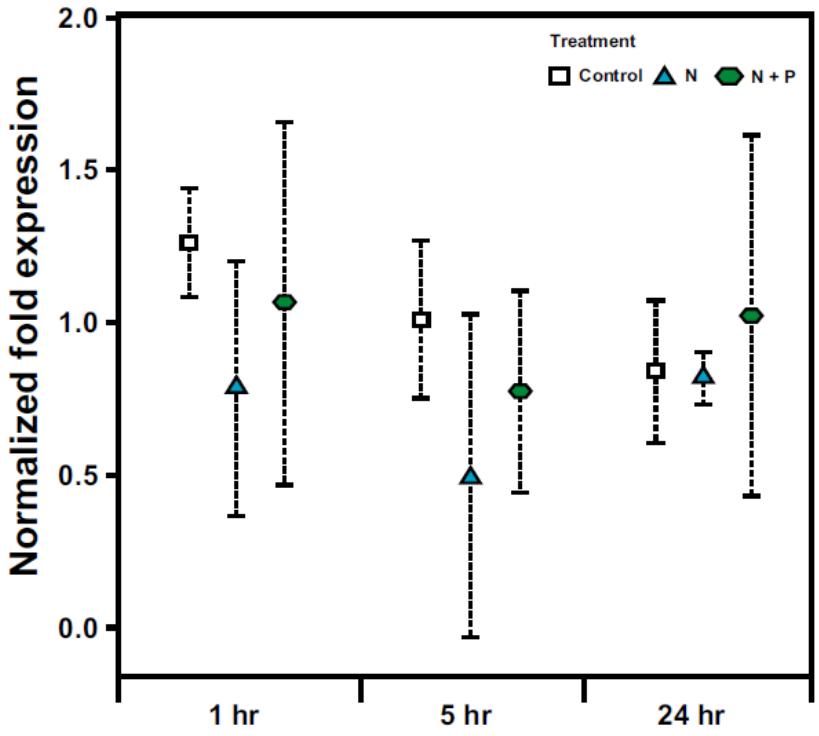

Fig. 5. Histone H2A.X gene expression levels in staghorn coral during the first 24 hours of exposure to different nutrient treatments. Plots represent mean normalized ratios in relation to the study calibrator (Histone H4) ± SE (n=2).

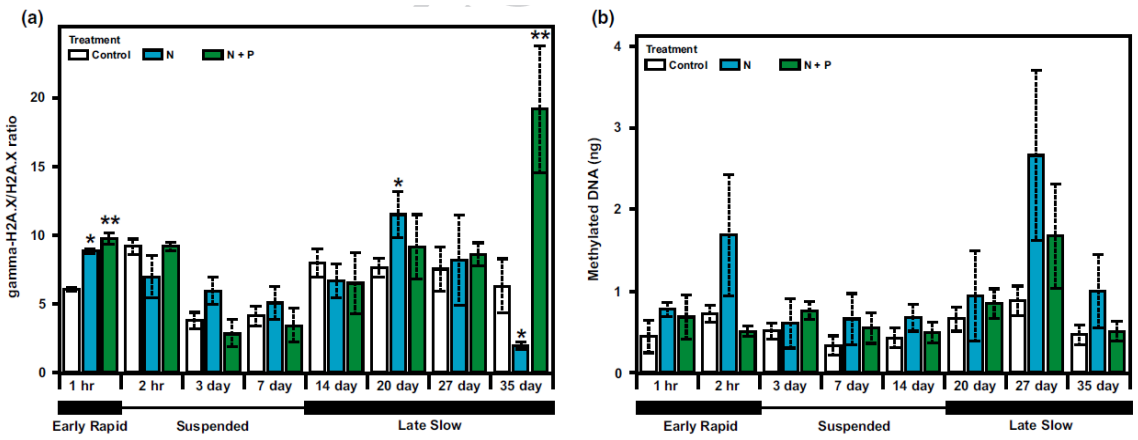

Fig. 6. A. Characterization of histone H2A.X phosphorylation levels in staghorn coral fragments across different nutrient treatments, estimated as the ratio between phosphorylated H2A.X (gamma-H2A.X) and its non-modified form (H2A.X). Each plot represents mean ± SE (n = 3). The level of significance of the post-hoc Holm-Sidak test is indicated as * $p < 0.05$, ** $p < 0.01$. The response was divided into three parts: early rapid response (hour 1), suspended response (hour 2 - day 7), and late slow response (after day 7). **B.** Characterization of global DNA methylation levels in staghorn coral fragments across different nutrient treatments, estimated as total mass of methylated (5-methyl-Cytosine) DNA. Each plot represents mean ± SE (n = 3, biological replicates). The response was divided in three parts mirroring gamma-H2A.X, defined as: early rapid response (hour 1 - 2), suspended response (hour 2 - day 14), and late slow response until the end of the experiment (after day 14).

Table 1. qPCR primers used in histone gene expression analyses and species used as references for their design.

Gene	Primer Name	Sequence (5' → 3')	Species
H2A.X	Ac-H2A.X-Fw	CTCAGGGAGGTGTTTTGCCA	*Acropora cervicornis*
	Ac-H2A.X-Rv	TGGCTTTGGGATGATTTCCCT	
H4	Af-H4-Fw	CCGGGCTCCCAGTAAAATGT	*Acropora formosa*
	Af-H4-Rv	TGTCGTATGGGGGAGGGATT	

Table 2. Two-way ANOVA analysis of the contribution of block design to the studied variables. %P and %N represent the percentage of dry weight for each element.

Variable	**Source of Variation**	**df**	**F**	***p***
%P	Block	3	0.574	0.636
	Treatment x Block	6	0.495	0.808
%N	Block	3	1.167	0.336
	Treatment x Block	6	0.407	0.869
gammaH2A.X/H2A.X	Block	3	1.128	0.345
	Treatment x Block	6	0.183	0.833
DNA methylation	Block	3	1.920	0.156
	Treatment x Block	6	0.883	0.419

Table 3. Nutrient content in corals (holobiont) exposed to control (C), enriched nitrogen (N), and enriched nitrogen and phosphorus (N+P) treatments. Values represent mean and standard deviation (in parentheses) for all samples collected during a 4 week-long exposure (n=24). N:P and C:N represent molar nitrogen:phosphorus and carbon:nitrogen ratios, respectively. %P, %N and %C represent the percentage of dry weight for each element.

Treatment	%P	%N	%C	N:P	C:N
C	0.382 (0.096)	2.136 (0.790)	15.592 (5.049)	3.011 (2.163)	6.350 (0.498)
N	0.420 (0.148)	2.135 (0.755)	15.298 (4.665)	2.875 (2.310)	6.286 (0.731)
N+P	0.404 (0.106)	2.116 (0.715)	15.791 (4.615)	2.493 (1.132)	6.480 (0.556)

Table 4. Mixed effects models analysis of modifications in symbiont population densities in *A. cervicornis* during the course of the present experiment under control (C), enriched nitrogen (N), and enriched nitrogen and phosphorus (N+P) treatments*.

Treatment	**$\chi 2$**	**Slope ± SE**	***p***
C	2.184	0.00034 ± 0.00023	0.140
N	4.400	0.00084 ± 0.00040	0.036
N+P	14.061	0.00100 ± 0.00028	<0.001

* The slope represents the linear estimate of how the symbiont population changes through time (106 cell x hour-1) in the different treatments. See Statistical Methods in the Methods section of this work for additional details on symbiont density analyses.

CHAPTER III

GENOME-WIDE DNA METHYLATION ANALYSIS REVEALS A CONSERVED EPIGENETIC RESPONSE TO SEASONAL ENVIRONMENTAL VARIATION IN THE STAGHORN CORAL *ACROPORA CERVICORNIS*

This manuscript was published in Frontiers in Marine Science 2020 and formatted according to the publisher's requirements.

Abstract

Epigenetic modifications such as DNA methylation have been shown to participate in plastic responses to environmental change in a wide range of organisms, including scleractinian corals. Unfortunately, the current understanding of the links between environmental signals, epigenetic modifications, and the subsequent consequences for acclimatory phenotypic changes remain obscure. Such a knowledge gap extends also to the dynamic nature of epigenetic changes, hampering our ability to ascertain the magnitude and extent of these responses under natural conditions. The present work aims to shed light on these subjects by examining temporal changes in genome-wide patterns of DNA methylation in the staghorn coral *Acropora cervicornis* in the island of Culebra, PR. During a 17-month period, a total of 162 polymorphic loci were identified using Methylation-Sensitive Amplified Polymorphism (MSAP). Among them, 83 of these fragments displayed changes in DNA methylation changes that were significantly correlated to seasonal variation as determined mostly by changes in sea water temperature. Remarkably, the observed time-dependent change in DNA methylation patterns is consistent across coral genets, coral source sites and site-specific conditions studied. Overall, these results are consistent with a conserved epigenetic response to seasonal environmental variation. These findings highlight the importance of including seasonal variability into experimental designs investigating the role of epigenetic mechanisms such as DNA methylation in responses to stress.

Introduction

Hermatypic (i.e., reef-building) corals play a critical role as ecosystem foundation species. Hence, it is not surprising that continuous reductions in their populations for the last 30 years have caused the collapse of many coral reef ecosystems worldwide, and a drastic deterioration in the ones still remaining (Birkeland 2019; O. Hoegh-Guldberg et al. 2007; Pandolfi et al. 2003). Among the different potential drivers for this decrease, the increase in average temperature in the upper layers of the ocean (Abraham et al. 2013; Hansen, Sato, and Ruedy 2012) and changes in ocean chemistry (Feely, Doney, and Cooley 2009) caused by human-driven global change (Ove Hoegh-Guldberg and Bruno 2010; Rosenzweig et al. 2008) are considered among the most important factors. It is well known that corals are particularly sensitive to water temperature fluctuations (Cai et al. 2016; Hume et al. 2016), with current conditions provoking frequent bleaching events in reefs worldwide when temperature increases 1–2°C above normal summer maximum (Ove Hoegh-Guldberg 1999; Hughes et al. 2003). This susceptibility, along with the fast-paced progression of global change has generated concerns about the ability of corals to acclimatize and adapt to these conditions.

Temperature and light represent the main environmental factors responsible for the collapse (i.e., bleaching) of the coral holobiont (the unit formed by the symbiosis between the coral animal and its associated microorganisms, including dinoflagellate algae of the family Symbiodinaceae). In addition, seasonal changes in these parameters also drive subsequent variation in coral physiology (Scheufen et al. 2017). Contrary to the case of random environmental variation, the predictability of seasonal fluctuations can be conducive to the development and inheritance of plastic transcriptional profiles

mediating phenotypic responses, regulated by epigenetic mechanisms [e.g., seasonal DNA methylation changes in bivalve mollusks (Suarez-Ulloa, Rivera-Casas, and Michel 2019; Ito et al. 2019) and birds (Viitaniemi et al. 2019)]. Indeed, seasonality produces dramatic physiological adjustments in corals, including changes in symbiont's abundance and pigmentation (Fitt et al. 2000; Thornhill et al. 2006), modifications of microbial community composition (Sharp et al. 2017), as well as the alteration of transcriptional profiles (Edge, Morgan, and Snell 2008; Brady, Snyder, and Vize 2011; Brener-Raffalli et al., 2019; Parkinson et al. 2018). On one hand, the different sensitivities to heat stress and bleaching displayed by winter and summer coral phenotypes (Berkelmans and Willis 1999; Scheufen et al. 2017) seem to support the notion that these changes could prepare corals to respond to increased temperature and light stress during the summer months. On the other hand, recent experiments in *A. cervicornis* have failed to find additional support for this idea (Parkinson et al. 2018). Nevertheless, even if these adjustments were to occur, they may fall short when facing altered seasonal regimes and unprecedented stress events caused by global change. Consequently, understanding the shared mechanisms underlying thermal and seasonal acclimatization in corals will improve our capacity to model coral population trajectories, and enhance coral preconditioning and assisted evolution approaches (van Oppen et al. 2015).

As sessile organisms, corals rely exclusively on phenotypic plasticity to respond to their environment (López-Maury, Marguerat, and Bähler 2008), a response that is largely mediated by the interaction between the coral's genome and intrinsic and extrinsic environmental signals modulating its expression (West-Eberhard 2003). Although the role of this plasticity is mostly observed during the life of an organism (IntraGenerational

Plasticity, IGP), it has been suggested that parents can "prime" their offspring to better respond to changes in their specific environments (InterGenerational Plasticity, ItGP) (Salinas and Munch 2012) and even produce phenotypes that will persist for generations even in the absence of the initial stressor triggering that phenotype (TransGenerational Plasticity TGP) (Perez and Lehner 2019). Based on the current evidence for the inheritance of acquired epigenetic marks, it seems plausible that epigenetic mechanisms play a critical role providing a mechanistic framework for the acquisition and intergenerational inheritance of phenotypes optimized to the prevailing environmental conditions (Vignet et al. 2015; Marsh and Pasqualone 2014; Navarro-Martín et al. 2011; Vandegehuchte et al. 2009; Eirin-Lopez and Putnam 2019), increasing the resilience and resistance of corals to global change. However, in order to disentangle the role of epigenetic mechanisms on IGP, ItGP and TGP, there is an urgent need to better understand how these epigenetic mechanisms interact with environmental factors.

Epigenetic mechanisms display extremely dynamic responses to environmental changes (Cortessis et al. 2012), serving as a "sensory" interface between the environmental condition and the genome function. Therefore, understanding exposure-response relationships of these molecular mechanisms could potentially allow the quantification of the effects of the environment on phenotypic variation (Etchegaray and Mostoslavsky 2016; Cortessis et al. 2012; Suarez-Ulloa, Gonzalez-Romero, and Eirin-Lopez 2015), increasing our capacity to predict population responses after environmental change. While increasing evidence points to a relevant role of DNA methylation and other epigenetic mechanisms in plastic responses to environmental change in corals (Putnam, Davidson, and Gates 2016; Dixon et al. 2018b; Dimond and Roberts 2020;

Liew et al. 2018) and other marine organisms (Eirin-Lopez and Putnam 2019; Ryu et al. 2018), there is limited understanding of the factors influencing dynamic epigenetic changes under non-stressed conditions, confounding the ability to determine the magnitude and extent of epigenetic responses under natural conditions (Suarez-Ulloa, Rivera-Casas, and Michel 2019). In addition, solid baseline data of "natural response" to seasonal and diel cycles in most ecologically important organisms is lacking (Suarez-Ulloa, Rivera-Casas, and Michel 2019). This gap can be bridged by developing seasonal monitoring of coral epigenetic signatures, helping disentangle the molecular underpinnings of such epigenetic responses, their involvement in seasonal acclimatization, and their capacity to respond to factors driving global change in the Anthropocene. The present work aims to do so by characterizing temporal changes in DNA methylation patterns using the staghorn coral *A. cervicornis* as model system.

Methods

Study site, experimental and sampling design

A total of n=200 staghorn coral (*Acropora cervicornis*) fragments (naturally generated by hurricanes Irma and Maria between August and October 2017) were collected from 4 reefs around Culebra Island, Puerto Rico (Figure 1). Naturally occurring fragments were used to minimize the effect of sampling on standing colonies of *A. cervicornis*. Therefore, sampling effort was not standardized among sites, and analyses on genotypic diversity of the sample pool cannot be extrapolated to compare natural levels of sexual recruitment among sites. Fragments were stabilized by immediate outplanting into two natural reefs located in the Canal Luis Peña No-Take Marine

Reserve: Luis Peña (LP: 18°18'45.0"N, 65°20'08.4"W) and Carlos Rosario (CR: 18°19'30.2"N, 65°19'52.7"W) reefs. At the time of outplanting, genotyping information was not available. Thus, in order to homogenize the distribution of putative genets and avoid biases from local adaptation in the site-specific response, fragments from different sources were further subdivided before fixing them to the substrate using nails and plastic ties at two different depths (5 and 15 m). This yielded an equal representation of putative genets at both depths. The outplanting sites were named LP shallow (LPs), LP deep (LPd), CR shallow (CRs), and CR deep (CRd). Coral fragments were organized into 5x5 m plots containing 20 fragments per plot, for a total of 5 plots per site (n=100 fragments per site, total=400 fragments outplanted). The size of outplanted fragments ranged between 10 and 30 cm in length.

The characterization of depth-associated changes in dissolved oxygen, pH, salinity, and pressure (tides) was performed by deploying YSI EXO2 multiparameter sondes (YSI, Yellow Springs, OH) and photosynthetically active radiation (PAR) sensors (Sea Bird, Bellevue, WA) at the two studied depths in Luis Peña reef. Sensors were deployed for a month in September 2018 and January 2019 in order to capture summer and winter seasonal peaks. Daily water temperature (3 m below Mean Lower Low Water) records were gathered from NOAA Data Buoy Center, Station CLBP4 located in Culebra, PR, approximately 3.8 and 4 km from LP and CR, respectively (Figure 1). Regional light data was obtained from the integration of 25 climatological models (CMIP5 IPCC) for Puerto Rico (San Juan PR, 18°26'24.0"N 66°07'48.0"W).

Tissue samples were clipped from coral fragments using bone cutters at the beginning of the experiment (April 2018), and subsequently stored in 95% non-denatured

ethanol for DNA genotyping. Tissue samples were further collected from selected fragments at LP and CR reefs after 3, 5, 6, 9, 12, and 17 months-post-outplanting (hereafter referred to as T+ month post outplanting), resampling fragments when possible. Repetitive samples were collected from grown branches, discarding the actively growing tip (generally without symbionts). The selection of specific fragments for sampling was determined based on the availability of healthy branches not previously disturbed. Coral samples were immediately flash-frozen, shipped on dry ice to Florida International University and stored at -80°C. In order to assess seasonal variation of healthy corals during the study period, only corals that survived the 17-month period and were sampled at least 4 times were included in DNA methylation analysis. This ensured replication at each sampling event. Overall, a total of n=205 samples from the four outplanting sites were analyzed for DNA methylation (n=55 for LPs, n=38 for LPd, n=64 for CRs, and n=48 for CRd).

Coral genotyping and genomic DNA isolation

We define a collection of fragments sharing the same multilocus genotype as belonging to the same ‘‘genet’’, and each of the fragments is referred to as a “ramet”. Coral host genotyping was based on DNA isolated using a standard phenol-chloroform protocol (Sambrook and Russell 2006) from the samples collected at the beginning of the experiment. A panel of 6 microsatellite loci was applied (Baums, Hughes, and Hellberg 2005). Since these markers were demonstrated to be highly heterozygous, the probability of wrongfully identifying ramets as clonemates of the same genet is consequently extremely low (Baums, Miller, and Hellberg 2005). Only samples sharing the same

alleles at all six loci were classified as ramets of the same genet. The descriptors of coral genotypic structure at the sampled sites, genotypic richness, diversity and evenness were calculated following (Stoddart and Taylor 1988) and (Baums, Miller, and Hellberg 2006). Briefly, genotypic richness was calculated as the number of genets (N_g) over the number of colonies sampled (N). Genotypic diversity refers to the diversity of genets in a population. Here, it was calculated as the observed over the expected genotypic diversity (Baums, Miller, and Hellberg 2006). Observed genotypic diversity (G_o) was calculated as per the equation (Stoddart and Taylor 1988):

$$G_o = \frac{1}{\sum_{i}^{k} g_i^2}$$

where g_i is the relative frequency of each genet. Expected genotypic diversity (Ge) was equal to the total number of colonies analyzed (N), assuming a population with only sexual reproduction. This index of genotypic diversity, therefore, indicates the contribution of sexual reproduction to the population (Baums, Miller, and Hellberg 2006). Evenness was calculated as the fraction of the observed genotypic diversity (G_o) over the number of genets (N_g).

Coral holobiont's genomic DNA (82.0 ± 41.1 ng/µL, final concentration) was purified from flash-frozen tissue using the Quick DNA/RNA Mini-Prep kit (Zymo Research, Irvine, CA) with some modifications: Briefly, coral fragments were pulverized in liquid nitrogen and approximately 100 mg of the resulting powder was resuspended in 2 mL vials containing 500 mg of Zirconia/Silica beads (0.5 mm diameter) and 1 mL of DNA/RNA Shield (Zymo Research, Irvine, CA). Coral host cells were lysed using two pulses of 30 sec in a vortex, in an attempt to leave most of the symbiont cells intact, thus

enriching host DNA. However, a significant contribution of symbiont DNA to the final sample was assumed. After centrifugation (12,000 x g for 5 min), the supernatant was carefully transferred to a new tube and DNA isolation continued following the manufacturer's instructions. DNA quality was assessed by gel electrophoresis for integrity and spectrophotometric analysis (NanoVue GE Healthcare, Chicago, IL) for quality as described elsewhere (Rivera-Casas et al. 2017). DNA concentration was measured using a Qubit 2.0 Fluorometer (Thermo Fisher, Waltham, MA) following the instructions provided by the manufacturer. Samples with concentrations under 40 ng/µL or low quality (i.e., ethanol contamination) were processed using a DNA Clean & Concentrator kit (Zymo Research, Irvine, CA) until requirements were met.

Symbiodiniaceae ITS2 Amplicon Sequencing and analysis

The ITS2 region was sequenced in coral samples in order to assess changes in symbiont community composition throughout the experiment. Accordingly, a total of n = 30 samples, consisting of 10 randomly selected coral fragments from the 4 outplanting and three representative time points (T3, T12 and T17), were used in the analysis. The isolated genomic DNA was quantified using the Qubit 2.0 DNA HS Assay (ThermoFisher, Massachusetts, USA) and the quality assessed by the Tapestation genomic DNA Assay (Agilent Technologies, California, USA). Library preparation and sequencing was performed by Admera Health (South Plainfield, NJ). Briefly, ITS2 spacer regions of the ribosomal DNA of the family Symbiodinaceae were amplified from 50 ng of isolated genomic DNA via PCR, using Symbiodinaceae-specific primers [ITS2alg-F, 5'-GTGAATTGCAGAACTCCGTG-3'; ITS2alg-R, 3'-

TTCGTATATTCATTCGCCTCC-5' (Pochon et al. 2001)] modified to include Illumina® adapters. The resulting libraries were quantified and assessed for quality before sequencing as detailed above and barcoded for multiplexing using Illumina® 8-nt dual-indices. An equimolar pooling of the libraries was performed based on QC values and sequenced on an Illumina® MiSeq (Illumina, California, USA) with a read length configuration of 2x250 for 0.1 M pairs of reads per sample (500K in each direction).

Symbiodinaceae community composition was analyzed using the SymPortal Pipeline (Hume et al. 2019). Untrimmed demultiplexed forward and reverse sequences (fastq) were submitted directly into SymPortal for quality control and taxonomic assignment as described in Hume et al. (2019). Identified sequence variants per sample was used to characterize ITS2 type profiles (Hume et al., 2019). The abundance of ITS2 type profile and sequencing reads representative of putative Symbiodiniaceae taxa were used to evaluate changes in symbiont communities through time (T3, T12, T17). Differences of ITS2 profiles between collection times was evaluated by Permutational multivariate analysis of variance (PERMANOVA) with the *adonis* function in vegan (Oksanen et al. 2019) fragment identity as strata in the model and performing 9,999 permutations of residuals from Bray-Curtis dissimilarities.

Genome-wide DNA methylation analysis

Genome-wide DNA methylation was assessed on coral host-enriched-DNA samples using an amplified polymorphism approach specific for DNA methylation states (Methylation Sensitive Amplified Polymorphism, MSAP; (Reyna-Lopez, Simpson, and Ruiz-Herrera 1997; Xiong et al. 2013; Covelo-Soto, Saura, and Morán 2015). This

method is based on the use of isoesquizomeric endonucleases, HpaII and MspI, with shared sequence targets (CCGG sites) but differential sensitivities to their DNA methylation. More precisely, HpaII cleavage is blocked by methylation on either the internal cytosine methylation of the target site (i.e., 5'-C^{m}CGG-3'/3'-GG^{m}CC-5') or its hypermethylation (i.e., 5'-^{m}C^{m}CGG-3'/3'-GG^{m}C^{m}C-5'). MspI, on the other hand, is sensitive to external cytosine methylation, including hemimethylation (i.e., 5'-^{m}CCGG-3'/3'-GGCC-5') and hypermethylation states. This allows the establishment of global cytosine methylation patterns by comparing both amplified restriction profiles (Díaz-Freije et al. 2014). Accordingly, coral genomic DNA was digested using EcoRI/HpaII and EcoRI/MspI endonuclease mixes in parallel reactions. In the same step, the resulting fragments were ligated to EcoRI and HpaII/MspI adapters (Table 1). Digestion-ligation reactions were performed for 2 h at 37 ºC in a solution consisting of 200 ng DNA, 4 U of EcoRI (NEB, Ipswich, MA), 1 U of either HpaII (NEB, Ipswich, MA) or MspI (NEB, Ipswich, MA), 1 U T4 DNA ligase (Thermo Fisher Scientific, Waltham, MA), 1X ligase buffer (Thermo Fisher Scientific, Waltham, MA) and 1X CutSmart Buffer (NEB, Ipswich, MA). The resulting restriction fragments were selectively amplified through two consecutive PCR reactions. First, a pre-selective reaction containing 2 µL of diluted (1:7) restriction-ligation product, 20 pM of each HpaII/MspI and EcoRI primers combination (Table 1), 1X PCR buffer, 0.5 mM dNTPs (Thermo Fisher Scientific, Waltham, MA), 2.5 mM MgCl2, and 1 U DreamTAQ DNA polymerase (Thermo Fisher Scientific, Waltham, MA). Second, a selective reaction used 0.5 µL of 1:9 of the pre-selective PCR product, 0.83 pM of each labelled selective primer (Table 1), 1X PCR buffer, 0.5 mM dNTPs, 2.5 mM $MgCl_2$ and 1 U DreamTaq DNA polymerase. PCR conditions were identical to the

original protocol (Reyna-Lopez, Simpson, and Ruiz-Herrera 1997), and the amplified products (2 per enzyme/sample combination, 4 selective combinations multiplexed, Table 1) were diluted to 1:10 for 6-FAM and 1:5 for 6-HEX prior to multiplexing and run on an ABI Prism 310 Genetic Analyzer (Applied Biosystems, Foster City, CA) with a MapMarker 1000 ROX marker at Florida International University's DNA Core facility.

Data and Statistical analysis

MSAP restriction profiles were scored to a binary matrix for each primer combination with GeneMapper v.3.7 (Applied Biosystems, Foster City, CA), retaining fragments between 50 and 500 bp and above 25 Relative Fluorescent Units for 6-HEX and 50 for 6-FAM. The matrices were filtered utilizing a 5% error rate (loci with one methylation state in more than 95% of the samples) and a 2% occurrence of any DNA methylation state to remove uninformative loci and analyzed using the R-package *msap* (Pérez-Figueroa 2013). For a given animal, loci were scored according to the presence or absence of EcoRI-HpaII and EcoRI-MspI bands as either Non-Methylated (NMT, 0/0), Hemimethylated (HMM, 1/0), Internal Cytosine Methylated (ICM, 0/1) or Hypermethylated (HPM, 0/0). Hypermethylation was assumed on 0/0 loci due to the low genetic diversity on our dataset, which comprised the repetitive sampling of ramets of 7 genets. Loci were further classified as susceptible (MSL) or not susceptible to methylation (NML). The resulting data matrix of scored methylation states was subjected to further analysis.

Epigenetic variation on MSL was analyzed with Permutational Multivariate Analysis of Variance [PERMANOVA] (Anderson 2001), considering genet, outplant site

and collection time as grouping variables in the model *genet*fragment*time + site* as implemented on the R-package *vegan* [*adonis* function (Oksanen et al. 2019)]. Fragment identity was included in the model and as *strata* to assess the effect of repeated measurements. A Euclidean distance matrix was generated with 9,999 permutations. Pairwise PERMANOVA (Martinez-Arbizu 2019) with Holm's correction (Holm 1979) was performed to evaluate which variables had significant effects on DNA methylation. Statistical significance of each MSL was assessed by means of multiple comparisons between the experimental groups by Fisher's exact tests with Benjamini and Hochberg multi-test corrections(Benjamini and Hochberg 2000); adjusted $p<0.05$, $pFDR<0.05$), identifying loci with non-random distribution of DNA methylation states for each experimental variable. Using these significant MSL, pairwise distances between all analysed coral fragments with Gower's Coefficient of Similarity were computed. The resulting distance matrix was clustered with UPGMA (unweighted pair group method with arithmetic mean) and visualized as a heatmap with *ComplexHeatmap (Gu, Eils, and Schlesner 2016).*

A Discriminant Analysis of Principal Components (DAPC, (Pritchard et al. 2000; Jombart, Devillard, and Balloux 2010; Grünwald and Goss 2011) was performed to assess the epigenetic discrimination between groups using *adegenet* (Jombart 2008). The number of principal components (PCs) retained for the analysis was evaluated with two rounds of cross-validation [Xval.dapc function, (Jombart and Collins 2015)]. All discriminant functions (K-1= 5) were retained in the analysis. Correlation between the independent variables (Temperature and light) and DAPC coordinates of temporal variation in DNA methylation was evaluated. Appropriate Lag shifts were calculated [*ccf*

function, (Brockwell and Davis 2009)] to determine the cross correlation between each of the univariate series. Next, the lag corrected series (Lag corrected +1 shift for temperature) were input into a matrix of Pearson's r rank correlation coefficients using *rcorr* in the *Hmisc* library (Harrell and Harrell 2019).

Non-Metric Multidimensional Scaling Analysis (NMDS) was performed utilizing Gower's distances, and environmental parameters were fitted as vectors in the ordination (*envfit* function) with *vegan* (Oksanen et al. 2019) to represent their effect on DNA methylation. Monthly mean values, maximum, standard deviations and differences for each environmental factor were employed as vectors. For temperature and light irradiance long-term data sets, a coefficient of variation of the previous three months (CV3) to each sampling month was calculated and employed as an additional vector to evaluate a possible response to the relative change in the parameter and not the actual magnitude. Significance and coefficient of determination was calculated for each of these parameters.

Fragment sequencing and identification

Preselective products from 10 samples with high band representation for each selective (SL1-4) and enzyme (Hpall and Mspl) combination were pooled and amplified with non-labelled selective primers. Resulting products (n=8) were cleaned with a DNA Clean & Concentrator kit (Zymo Research, Irvine, CA), quality checked with a TapeStation D1000 ScreenTape (Agilent Technologies Inc., California, USA) on a Tapestation 4200 system and multiplexed with a Native barcoding expansion kit (EXP-NBD104, Oxford Nanopore Technologies). Libraries for Oxford NanoPore sequencing were constructed with a ligation library kit (SQK-LSK109, Oxford Nanopore

Technologies, Oxford, UK) and sequenced to a total of 20GB on MinION R9.4 flowcells. The resulting sequences were base-called and demultiplexed with the MinKNOW software, trimmed with Porechop (https://github.com/rrwick/Porechop) to eliminate PCR adapters, and mapped to the genomes of *A. digitifera* (Shinzato et al. 2011) and *Symbiodinium microadriaticum* (Aranda et al. 2016) using Minimap2 (H. Li 2018).

Results

Abiotic characterization and seasonality

Hourly data (n=824) was recorded for temperature, photosynthetic active radiation (PAR), dissolved oxygen (DO), and salinity at two sites at a depth of 5 and 15 m (LPs and LPd, respectively) during two monthly deployments to capture peak summer and winter signals in sites representative of studied depths (Table S1). Greater values (two tailed t-test $p<0.05$) for pH, PAR and Salinity were observed at LPs as opposed to LPd. However, as expected, both depths showed greater values of temperature and PAR as well as lower pH, DO and salinity during the summer (two tailed t-test $p<0.05$). Temperature daily mean for each month was analyzed for seasonality, revealing a trend for the period through 2018 and 2019 (Mann-Kendall trend test $p=0.007$). This is graphically confirmed (Figure S1) by applying a moving average to the data set to extract the seasonal component from the trend and error terms assuming an additive model because the variance structure remained homogeneous throughout the periods observed (decompose function in the Stats package R). Solar Radiation is reported as W/m^{-2} with peak values in April and lowest values reported in December.

Genotypic composition of source reefs

A total of n=81 *A. cervicornis* host genets were identified in 186 of the 200 initial fragments analyzed (14 samples failed): 45 from Los Corchos (LC), 15 from Carlos Rosario (CR), 14 from Luis Peña (LP), and 7 from Culebritas (CUL) (Figure 1). All genets were exclusive to their corresponding sampling site, and three to four prevalent genets accounted for 67-75% of the collected fragments at each site, with the exception of LC, where most genets had only one or two ramets. The genotypic structure was subsequently described for each site (Table 2), resulting in an overall genotypic richness [number of genets (N_g)/number of samples (N)] of 0.38 ± 0.21 for all sites combined. LC showed the highest richness amongst all sampled sites. Genotypic diversity [observed genotypic diversity (G_o)/expected genotypic diversity (G_e)] followed the same pattern with combined values of 0.24 ± 0.16 and 0.47 for LC. For evenness (G_o/N_g) however, both sites in the east of the island (LC and CUL) showed similar values (around 0.68) while the sites on the west were lower (around 0.5).

Symbiodinaceae community composition and dynamic

In order to evaluate symbiotic community dynamics through the duration of the study, ITS2 amplicon sequences for the Symbiodinaceae family were analyzed. The 30 samples generated 5,415,404 sequencing reads, producing 2,707,680 sequences after quality filtering into the SymPortal pipeline (50%). A total of 57 operational taxonomic units were identified from ITS2 sequences, with the majority of filtered ITS2 sequences being of the genus *Symbiodinium* (formerly Clade A), and a minor representation of genuses *Brevolium* (formerly Clade B) and *Cladocopium* (formerly Clade C) (Figure S2).

Four ITS2 type profiles were identified across samples, all uniquely composed by *Symbiodinium* spp. sequences. ITS2 profile shifts were observed in some of the samples. However, no significant dynamic changes were evidenced between collection times (PERMANOVA; $F = 0.2552$, $p = 0.6646$; Table S2).

Global genome-wide DNA methylation variability

A total of 7 genets were selected among those represented by the transplanted fragments for DNA methylation analyses. Genet selection was based on the number of ramets of each genet surviving the 17-month period, allowing appropriate replication between outplanting sites and source sites. The availability of a minimum of 3 ramets of each genet per outplanting site at the end of the 17-month period were used as criteria for selection. Selected genets were n=3 from CR (C1708, C1732 and C1739), n=2 from LP (C1727 and C1733), and n=2 from CUL (C1706 and C1734), representing most of the highly represented genets at each source site (Figure 1). Unfortunately, no genet from LC satisfied the criteria to be included in the DNA methylation analyses.

MSAP analyses were performed to assess changes in whole-genome DNA methylation profiles of corals depending on their outplant site, genet and/or collection time. The four combinations of primers tested yielded a total of n=199 loci after quality-filtering, among which 192 were categorized as methylation-susceptible loci (MSL, 96%) and the remaining 7 were non-methylated (NML, 4%) loci. Primer combinations SL2 and SL4 (Table 1) showed the highest number of methylation-susceptible loci with 93 (46.7%) and 81 (40.7%), respectively. The overall epigenetic diversity within methylation-susceptible loci, based on the occurrence of the different DNA methylation

states by means of Shannon's diversity index (SDI), was 0.33 ± 0.22, while non-methylated loci showed a Shannon diversity index of 0.22 ± 0.08. A total of 162 (84%) of the methylation-susceptible loci were characterized as polymorphic, showing at least two occurrences for each DNA methylation state, either NMT, ICM, HMM or HPM. These polymorphic loci were subsequently used for further analyses aimed to describe the influence of collection time, outplant sites, and genet on the DNA methylation patterns.

The results indicate a dynamic fluctuation in coral DNA methylation states over time (Table 3, Figure S3). Accordingly, HPM and NMT trended upwards from July 2018 (T3, i.e., three months post-outplanting) to April 2019 (T12), then decreased by September 2019 (T17). ICM and HMM showed the opposite trend, with an absolute minimum value by T12 and a subsequent increase by September 2019 (T17). This variation of DNA methylation patterns over time was significant, as revealed by PERMANOVA (Table S3, $F=4.1524$, $p<0.0001$). Further post-hoc analyses (Table 4) revealed significantly different DNA methylation patterns between all pairwise sampling time comparisons except for October 2018 with September 2018 (T5-T6, $F=1.6992$, $p=0.0994$) and October 2018 with Jan 2019 (T6-T9, $F=1.2757$, Adjusted $p=0.1782$) respectively.

The contribution of genet and outplanting sites to the variability observed in DNA methylation states was also evaluated using PERMANOVA analyses (Table S3). While no significant differences were observed between outplanting sites ($F=0.8735$, $p=0.6637$), genets influenced DNA methylation significantly ($F=2.3315$, $p=0.0131$). Accordingly, post-hoc analyses (Table 5) revealed significant pairwise differences of genet C1739 with C1733 ($F=3.2225$, Adjusted $p=0.0084$) and marginally significant with C1732 ($F=2.539$,

Adjusted p=0.0494) and C1727 (F=2.449, Adjusted p=0.0494). Additional marginal significance was found between genets C1732 and C1708 (F=2.4780, Adjusted p=0.0494), and between C1734 and C1708 (F=2.4824, Adjusted p=0.0440). It is interesting to note that most genet pairs showing significant differences in DNA methylation originated from the same source reefs or from reefs located near each other (i.e., CR and LP), making it less likely that similarities in DNA methylation patterns displayed by most genets were determined by epigenetic memory or local adaptation. Fragment (ramet) identity also had a significant effect on DNA methylation patterns (F=1.1037, p=0.0131).

Seasonal influence on global DNA methylation patterns

Considering the significant fluctuation observed on DNA methylation patterns throughout the studied time series, detailed analyses were performed to ascertain the exact contribution of seasonality to such variation. First, Fisher's exact test analyses were conducted to identify significant MSL, resulting in n=83 MSL with both significant differences among experimental times (Adjusted $p<0.05$) and low probability of false positives (pFDR<0.05). As shown in Figure 2, the clustering analyses of identified loci organized the samples into two major groups based on similar distribution of DNA methylation profiles, discriminating between cold (T12) and warm (T3, T5 and T17) months. Samples from T6 and T9 showed a scattered distribution across these two clusters, while most T17 specimens constituted a well-defined sub-cluster within the warm group.

In order to further assess epigenetic discrimination among sampling times, a Discriminant Analysis of Principal Components (DAPC) analysis was employed (Figure 3). As evidenced by the first discriminant function (LD1, x-axis, horizontal, Figures 3A, B), T17 samples constituted a well-defined cluster with distinct epigenetic signatures respective to the remaining samples. In contrast, the second discriminant function (LD2, y-axis, verticals Figure 3A, C) split the samples into warm (T3, T5 and T17) and cold (T6, T9 and T12) months, with each of these sampling times forming a discrete cluster. Along this axis, T17 occupied a position between T5 and T6 corresponding to the same period in the previous year. Analysis of the individual contribution of each locus to the group separation [(Jombart and Collins 2015); Figure 3D, E] resulted in the identification of different groups of loci mediating the separation of each discriminant function. Marked differences in the frequency of occurrence of each DNA methylation status in these loci through time (Figure 3F, G) were observed, with loci contributing to LD1 showing stable frequencies with a drastic change at T17, while LD2 loci showed a variable temporal response. These differences could indicate the occurrence of different overlapping responses mediated by DNA methylation changes.

To further investigate this, discriminant 3 (LD3) was also evaluated (Figure 4), in spite of its lower discriminant power (hence significant; $F=76.29$, $p<0.0001$). In this function, the marked separation of T17 was no longer evident and a clearer seasonal pattern emerged (Figure 4A, B). Remarkably, LD3 pattern s correlated significantly to Temperature (+1 lag, $r = 0.91$, $p = 0.0310$), but not with irradiance ($r = -0.76$, $p = 0.0783$) that showed significance only for $\alpha = 0.1$. Although LD3 has lower discriminant power (Figure 4B), the temporal changes of DNA methylation status in the main contributing

loci showed a dynamic variation as in LD2 (Figure 4C). Altogether, these results show an orderly transition of DNA methylation profiles during the months after the introduction of corals in their new environment, apparently driven by a warm-cold seasonality, but experiencing a pronounced change from T12 to T17 maybe related with a heat-stress event throughout this period.

Contribution of coral host vs. symbiont to MSAP-amplified loci

Considering the limitations to separate symbiont and host DNA efficiently, additional analyses were performed to evaluate the contribution of the symbionts to the methylation pattern observed. Therefore, MSAP products were sequenced and aligned against the genomes of the closely related acroporid coral *A. digitifera* (the *A. cervicornis* genome was not available at the time of this analysis) and a representative symbiont (*S. microadriaticum*, formerly clade A). All MSAP selective-enzyme combinations (n=8) produced a total of 30,519,266 reads after trimming. From those, 27,696,330 reads mapped to the coral genome (90.75%), while only 388,363 reads mapped to the symbiont genome (1.27%). This result indicates that although contamination with symbiont DNA is present, its contribution to MSAP loci is negligible.

Environmental parameters driving seasonal variability in global DNA methylation patterns

Given the observed seasonal trend in DNA methylation and its link with regional temperature and light irradiance patterns, further analyses were performed to evaluate such relationship. Accordingly, the contribution of different environmental parameters

was assessed by conducting non-metric multidimensional scaling (NMDS), fitting vectors to the ordination using the function *envfit*. Considering the abiotic data available and the lack of difference between the DNA methylation response among outplanting sites, two separate analyses were implemented. First, only samples from T5 (September 2018) and T12 (April 2019) for sites LPs and LPd (where site-specific environmental data was collected) were included (Figure 5A). This dataset allowed the evaluation of the contribution of temperature, pH, DO, salinity, and PAR to DNA methylation patterns. Results revealed that temperature, pH and DO correlated significantly with the NMDS ordination of the DNA methylation patterns driven by collection time (Figure 5B; Table S4), while surprisingly PAR did not. Despite clear abiotic differences between depths, these parameters correlate to DNA methylation differences across sampling time points instead of sampling sites, indicating that seasonal variation in these environmental parameters was more relevant than site specific conditions in modulating DNA methylation patterns.

The second analysis fitted regional temperature and light irradiance to the ordination of all sampling times, but only for shallow sites in both reefs. This was performed to determine the influence of these parameters during the duration of the experiment without introducing errors derived by differences in irradiance between depths. We tested the contribution of monthly averages together with the coefficient of variation of the previous three months (CV3) for each variable. The NMDS ordination with all the data corroborated the DAPC analysis by showing T17 as an independent cluster (Figure 5C). All vectors analyzed showed a significant correlation with the ordination (Figure 5D, Table S5), with temperature mean and CV3 of the irradiance

showing the highest coefficients of determination (R^2). Interestingly, it seemed that light and temperature were sensed differently by DNA methylation mechanisms, with rapid responses to temperature and a potentially lagged response to light (Figure 5D).

Discussion

This work constitutes the first attempt to characterize seasonal epigenetic changes in stony corals, providing support for the role of DNA methylation during seasonal acclimatization in the coral *A. cervicornis*. The results presented in this work suggest that DNA methylation profiles in this species vary following a season-dependent trend, with similar temporal changes in DNA methylation patterns in all inspected coral fragments, regardless of their genotype, source reef or outplanting site. This concurs with the frequently proposed notion of a seasonal variation in the phenotype of corals, including the presence of winter and summer ecotypes (Scheufen et al. 2017), likely driven by observed transcriptional changes (DeSalvo et al. 2008; Kenkel, Meyer, and Matz 2013). These findings underscore the importance of including seasonal variability in environmental epigenetic studies in marine (especially sessile) organisms (Parkinson et al. 2018).

Variability and seasonal trends in environmental abiotic parameters

Describing changes in environmental conditions is a prerequisite for the establishment of a seasonal dependence in any organismal response. Since DNA methylation data did not differ among sites, it was possible to use data from NOAA's weather buoy (CLBP4) to describe changes in temperature for all study sites, and data

derived from climatological models (CMIP5 IPCC) for light irradiance. A limited *in-situ* dataset was used to corroborate the responsiveness of DNA methylation to regional seasonal environmental variation, therefore validating the use of regional data and models to describe the general seasonal patterns as evidenced in temperature correlation with DNA methylation patterns with both datasets (Figure 5). Given the resolution of the regional light dataset with a limited sensitivity to differences in depth, it is not possible to categorically invoke interactive effects with depth and season based on the obtained data. Nonetheless, these results strongly support the interest of future research to understand the interactive effects of seasonality and depth differences on global DNA methylation.

Genotypic composition of source reefs

Genotypic variation is correlated with diverse stress responses, disease resistance, epigenetic patterns and reproductive output in Caribbean acroporids (Parkinson and Baums 2014; Drury et al. 2019; Durante et al. 2019; Baums et al. 2013). In this experiment, fragments were collected using an opportunistic sampling approach that favors the collection of dominant genets. It is thus encouraging that multiple genets were collected at each site, indicating that the genotypic diversity of *A. cervicornis* around Culebra is not low (Figure 1, Table 2). Genets were restricted to one collection site each, and thus there was no evidence of long-distance dispersal of asexually derived fragments. This is not surprising, considering that asexual fragmentation (Tunnicliffe 1981; Drury et al. 2019), restricts dispersion to a few hundred meters under natural conditions (including hurricane impacts), restricting genet distributions. Therefore, genotypic diversity observed on each site was mostly based in sexual recruitment.

Temporal differences dominate patterns of DNA methylation

Epigenetic landmarks, such as histone variants and DNA methylation, influence phenotypic plasticity in response to changes in environmental conditions and are, therefore, predictors of the general state of the organism in the face of environmental alterations and natural cycles (Rivière 2014). Emerging evidence suggests that these mechanisms play an important role during responses to environmental changes, likely by regulating gene expression and maintaining DNA integrity throughout the entire lifespan of an organism (Liew et al. 2018; Roberts and Gavery 2012; Dimond and Roberts 2016; Rodriguez-Casariego et al. 2018). Recent studies on marine invertebrates [reviewed in (Eirin-Lopez and Putnam 2019)] have shown that DNA methylation exerts a role on phenotypic acclimatization (Liew et al. 2018; Putnam, Davidson, and Gates 2016; Durante et al. 2019) by modulating gene expression (Dixon et al. 2018a). Moreover, epigenetic marks acquired throughout the lifespan of coral can be inherited intergenerationally, promoting acclimatized phenotypes in the offspring and thus increasing their fitness (Liew et al. 2020; Putnam et al. 2020). In addition, seasonal patterns of DNA methylation have been observed in vertebrates (Stevenson and Prendergast 2013; Viitaniemi et al. 2019), invertebrates (Pegoraro et al. 2016; Suarez-Ulloa, Rivera-Casas, and Michel 2019) and plants (Finnegan et al. 1998; Ito et al. 2019; Bastow et al. 2004). Based on these elements, it is not surprising that DNA methylation could play an active role during coral responses to seasonal variation.

The PERMANOVA analysis of all loci susceptible to DNA methylation showed clear differences in DNA methylation patterns between sampled months and genets, while no differences were observed between, sources or outplant sites in this study. This

is a remarkable result, considering the significant differences in environmental conditions and habitat type between deep and shallow sites (see Table S1), although the seasonal variation is larger for most parameters, including temperature. In corals, several studies have also found clear changes in DNA methylation in response to experimental manipulation in environmental conditions (Putnam, Davidson, and Gates 2016; Liew et al. 2018; Cziesielski, Schmidt-Roach, and Aranda 2019). On the other hand, a study aimed to evaluate the components of phenotypic divergence between clonemates of *A. palmata* under natural conditions (Durante et al. 2019), attributed most of the variation in DNA methylation to difference among genets followed by micro-environmental conditions, rather than between study sites. Nonetheless, this study was still able to observe small differences between sites. In the present work, *A. cervicornis* fragments were transplanted to new locations and only sampled after an acclimation period, hence source-site specific differences in DNA methylation profiles could have been diluted after a rapid acclimation. Still, evidence here suggests that seasonality remains as a stronger modulator of DNA methylation patterns. Coral genotype also exerts a significant effect over DNA methylation variability, although to a lesser extent than the aforementioned temporal influence, as evidenced by PERMANOVA (Table S3). This observation is consistent with the dependence of DNA methylation on the presence of CpG sites in the DNA, and is further supported by previous evidence that DNA methylation in corals (or in any other eukaryotic organism) directly relies on sequence features of the genome, also supporting its heritability (Dixon, Bay, and Matz 2014; Liew et al. 2018; Durante et al. 2019).

Coral DNA methylation displays seasonal trends in response to environmental changes

Seasonal environmental variation, similar to diel cycles, triggers the adjustment of physiological functions in corals (Hill and Ralph 2005; Brady, Snyder, and Vize 2011; Sorek et al. 2014; Ulstrup et al. 2008). The obtained results support the role of DNA methylation on the seasonal acclimatization of *A. cervicornis,* as evidenced by a clear temporal effect over the MSAP methylation patterns. DNA methylation seems to follow seasonal trends in temperature, light, DO and pH, as evidenced by the significant correlation between DNA methylation ordination and the vectors representing mean-value variation of these parameters and coefficient of variations in the case of light and temperature (Figure 5), hinting a possible lagged response. However, analysis of the complete dataset with specific methylation patterns (DAPC) showed that temperature (1+ lagged) significantly correlates with changes in DNA methylation, while light was significant only under α=0.1. Yet, interactive effects of light seasonality and depth differences on global DNA methylation require additional analyses. Overall, it seems that seasonal variation in temperature, light, pH, and dissolved oxygen modulate DNA methylation patterns.

This seasonal trend, however, seems to be masked by other phenomena occurring in the temporal scale. For example, samples collected during September 2019 have homogeneous DNA methylation profiles, markedly differentiated from the remaining sampling times by the first discriminant function of the DAPC analysis (Figure 3A). However, as revealed by the second and third linear discriminant functions (LD2 & LD3) of the DAPC analysis (Figures 3C, 4), these samples are more related to September and October 2018. Although this may sound incompatible with an annual periodicity in DNA

methylation profiles (considering there is just one replicated time point in both years), this change may simply reflect either coral acclimation to the experimental environment within the possibilities of its genetic and epigenetic backgrounds, or more likely, a response to stress.

Under an acclimation scenario, the switch in DNA methylation patterns would be immediate and then progressively undergo a resilience period after which the epigenome would be reprogrammed, resulting in the activation (or repression) of genes previously silenced (or activated) under native conditions. Unfortunately, the DNA methylation trends characterized in the present work do not support this notion. While rapid epigenetic changes were observed by our own previous research in coral (Rodriguez-Casariego et al. 2018), the constant change in DNA methylation patterns observed in the present work is not consistent with a linear progression towards an acclimated state. Indeed, several loci follow a seasonal-like pattern returning to DNA methylation values similar to those measured during the same season in the previous year (Figure 3G, 4). This is especially evident in the loci driving the divergence of T17, which display a rather abrupt change instead of a progressive transition towards an acclimated state (Figure 3F).

A stress response hypothesis, on the other hand, would be consistent with the occurrence of an abnormal event in September 2019, justifying the dramatic change observed in the aforementioned loci. Abiotic monitoring data seem to validate this idea, including extremely high seawater temperatures during the summer of 2019 (+0.5-1.3 °C, between July and October) compared to the same period of 2018. Indeed, a moderate bleaching event was observed in the area in subsequent months following an accumulation of 7 Degree Heat Weaks (Weil et al. 2019). Thermal-stress has been linked

to significant changes in coral transcriptional profiles (Voolstra et al. 2009; DeSalvo et al. 2008; Kenkel, Meyer, and Matz 2013), and to rapid epigenetic responses (Palumbi et al. 2014; Barshis et al. 2013), even at stress levels not high enough to produce bleaching (Rodriguez-Casariego et al. 2018). However, the anticipation of the response observed in T17 to the heat-stress event opens the possibility that DNA methylation could represent an early indicator of a changing thermal environment.

Overall, the evidence of a seasonal-driven response of DNA methylation presented by this work is in agreement with observed seasonal changes in gene expression in *A. cervicornis* (Parkinson et al. 2018), and phenotypic changes described in the coral holobiont (DeSalvo et al. 2008; Kenkel et al. 2013). Given the proposed role of DNA methylation mediating transcriptional plasticity (Dixon, Bay, and Matz 2014; J. L. Dimond and Roberts 2016), it is not surprising to find such a seasonal response. Previous studies have also highlighted significant responses in the holobiont physiology, supporting seasonal variations (Chen et al. 2005; Ulstrup et al. 2008; Carballo-Bolaños et al. 2019). Bacterial community composition has been also described to follow a certain seasonal pattern in several coral species (Li et al. 2014; Sharp et al. 2017; Cai et al. 2018). Changes in symbiont cell density, pigment composition, and photosynthetic capacity following annual periods have also been reported (Fitt et al. 2000; Warner et al. 2002; Ulstrup et al. 2008). While the proposed role of temperature mediating seasonal changes in coral physiology (Brown et al. 1999; Fitt et al. 2000; Dimond and Carrington 2007) was confirmed for DNA methylation here, non-conclusive evidence of the significant effect of other environmental factors with seasonal trends like pH, DO and light was obtained and will require further study. Given the marked seasonality observed

in calcification rates and photosynthetic production (Samiei et al. 2016; Hinrichs et al. 2013), it is not surprising that these factors would also influence DNA methylation patterns potentially involved in the establishment of these seasonal phenotypes.

Conclusions

The present work provides support for the role of DNA methylation during seasonal acclimatization of the coral *A. cervicornis*, based on its correlation with seasonal environmental variation independently of genotypic and site-specific differences. The emergence of these patterns, despite the complexity of DNA methylation responses to environmental stress described in marine invertebrates and the limited resolution of the method employed here (when compared to sequencing techniques), support the relevance of this phenomena for epigenetic regulation in corals. Given the ecological importance of coral acclimatization in the Anthropocene and the potential similarities between seasonal adjustments and heat-stress responses, the evidence generated by the present effort constitutes an initial approach to understanding the dynamicity and the potential for intergenerational inheritance of this epigenetic mechanism. Further studies will be instrumental to decipher the extent in which seasonally driven epigenetic patterns are indicative of IGP, ItGP or even TGP, encompassing critical implications on the current understanding of the epigenetic regulation of phenotypic plasticity. Overall, the data generated with this work will serve as a baseline to filter the contribution of seasonal-driven DNA methylation changes in studies addressing epigenetic responses to stressors, and as background for the study of environmental disturbances caused by extreme weather episodes (e.g., hurricanes).

References

Abraham, John P., M. Baringer, N. L. Bindoff, T. Boyer, L. J. Cheng, J. A. Church, J. L. Conroy, et al. 2013. "A Review of Global Ocean Temperature Observations: Implications for Ocean Heat Content Estimates and Climate Change." *Reviews of Geophysics* 51 (3): 450–83.

Anderson, Marti J. 2001. "A New Method for Non-Parametric Multivariate Analysis of Variance." *Austral Ecology* 26 (1): 32–46.

Aranda, M., Y. Li, Y. J. Liew, S. Baumgarten, O. Simakov, M. C. Wilson, J. Piel, et al. 2016. "Genomes of Coral Dinoflagellate Symbionts Highlight Evolutionary Adaptations Conducive to a Symbiotic Lifestyle." *Scientific Reports*. https://doi.org/10.1038/srep39734.

Barshis, Daniel J., Jason T. Ladner, Thomas A. Oliver, François O. Seneca, Nikki Traylor-Knowles, and Stephen R. Palumbi. 2013. "Genomic Basis for Coral Resilience to Climate Change." *Proceedings of the National Academy of Sciences*. https://doi.org/10.1073/pnas.1210224110.

Bastow, Ruth, Joshua S. Mylne, Clare Lister, Zachary Lippman, Robert A. Martienssen, and Caroline Dean. 2004. "Vernalization Requires Epigenetic Silencing of FLC by Histone Methylation." *Nature* 427 (6970): 164–67.

Baums, I. B., M. K. Devlin-Durante, N. R. Polato, D. Xu, and S. Giri. 2013. "Genotypic Variation Influences Reproductive Success and Thermal Stress Tolerance in the Reef Building Coral, Acropora Palmata." *Coral Reefs* . https://link.springer.com/article/10.1007/s00338-013-1012-6.

Baums, I. B., C. R. Hughes, and M. E. Hellberg. 2005. "Mendelian Microsatellite Loci for the Caribbean Coral Acropora Palmata." *Marine Ecology Progress Series* 288: 115–27.

Baums, Iliana B., Margaret W. Miller, and Michael E. Hellberg. 2005. "Regionally Isolated Populations of an Imperiled Caribbean Coral, Acropora Palmata." *Molecular Ecology*. https://doi.org/10.1111/j.1365-294x.2005.02489.x.

———. 2006. "Geographic Variation in Clonal Structure in a Reef-Building Caribbean Coral, Acropora Palmata." *Ecological Monographs* 76 (4): 503–19.

Benjamini, Yoav, and Yosef Hochberg. 2000. "On the Adaptive Control of the False Discovery Rate in Multiple Testing with Independent Statistics." *Journal of Educational and Behavioral Statistics*. https://doi.org/10.2307/1165312.

Berkelmans, R., and B. L. Willis. 1999. "Seasonal and Local Spatial Patterns in the Upper Thermal Limits of Corals on the Inshore Central Great Barrier Reef." *Coral Reefs* 18 (3): 219–28.

Birkeland, Charles. 2019. "Global Status of Coral Reefs: In Combination, Disturbances and Stressors Become Ratchets." *World Seas: An Environmental Evaluation*. https://doi.org/10.1016/b978-0-12-805052-1.00002-4.

Brady, Aisling K., Kevin A. Snyder, and Peter D. Vize. 2011. "Circadian Cycles of Gene Expression in the Coral, Acropora Millepora." *PloS One* 6 (9): e25072.

Brener-Raffalli, K., J. Vidal-Dupiol, M. Adjeroud, O. Rey, P. Romans, F. Bonhomme, M. Pratlong, et al. 2019. "Gene Expression Plasticity and Frontloading Promote Thermotolerance in Pocillopora Corals." https://doi.org/10.1101/398602.

Brockwell, Peter J., and Richard A. Davis. 2009. *Time Series: Theory and Methods*. Springer Science & Business Media.

Brown, B. E., R. P. Dunne, I. Ambarsari, M. D. A. Le Tissier, and U. Satapoomin. 1999. "Seasonal Fluctuations in Environmental Factors and Variations in Symbiotic Algae and Chlorophyll Pigments in Four Indo-Pacific Coral Species." *Marine Ecology Progress Series* 191: 53–69.

Cai, Lin, Ren-Mao Tian, Guowei Zhou, Haoya Tong, Yue Him Wong, Weipeng Zhang, Apple Pui Yi Chui, et al. 2018. "Exploring Coral Microbiome Assemblages in the South China Sea." *Scientific Reports* 8 (1): 2428.

Cai, Wei-Jun, Yuening Ma, Brian M. Hopkinson, Andréa G. Grottoli, Mark E. Warner, Qian Ding, Xinping Hu, et al. 2016. "Microelectrode Characterization of Coral Daytime Interior pH and Carbonate Chemistry." *Nature Communications* 7 (April): 11144.

Carballo-Bolaños, Rodrigo, Vianney Denis, Ya-Yi Huang, Shashank Keshavmurthy, and Chaolun Allen Chen. 2019. "Temporal Variation and Photochemical Efficiency of Species in Symbiodinaceae Associated with Coral Leptoria Phrygia (Scleractinia; Merulinidae) Exposed to Contrasting Temperature Regimes." *PloS One* 14 (6): e0218801.

Chen, Chaolun Allen, Ya-Wen Yang, Nuwei Vivian Wei, Wan-Shen Tsai, and Lee-Shing Fang. 2005. "Symbiont Diversity in Scleractinian Corals from Tropical Reefs and Subtropical Non-Reef Communities in Taiwan." *Coral Reefs*. https://doi.org/10.1007/s00338-004-0389-7.

Cortessis, Victoria K., Duncan C. Thomas, A. Joan Levine, Carrie V. Breton, Thomas M. Mack, Kimberly D. Siegmund, Robert W. Haile, and Peter W. Laird. 2012. "Environmental Epigenetics: Prospects for Studying Epigenetic Mediation of Exposure–response Relationships." *Human Genetics* 131 (10): 1565–89.

Covelo-Soto, Lara, María Saura, and Paloma Morán. 2015. "Does DNA Methylation Regulate Metamorphosis? The Case of the Sea Lamprey (Petromyzon Marinus) as an Example." *Comparative Biochemistry and Physiology Part B: Biochemistry and Molecular Biology*. https://doi.org/10.1016/j.cbpb.2015.03.007.

Cziesielski, Maha J., Sebastian Schmidt-Roach, and Manuel Aranda. 2019. "The Past, Present, and Future of Coral Heat Stress Studies." *Ecology and Evolution* 9 (17): 10055–66.

DeSalvo, M. K., C. R. Voolstra, S. Sunagawa, J. A. Schwarz, J. H. Stillman, M. A. Coffroth, A. M. Szmant, and M. Medina. 2008. "Differential Gene Expression during Thermal Stress and Bleaching in the Caribbean Coral Montastraea Faveolata." *Molecular Ecology* 17 (17): 3952–71.

Díaz-Freije, Eva, Camino Gestal, Sheila Castellanos-Martínez, and Paloma Morán. 2014. "The Role of DNA Methylation on Octopus Vulgaris Development and Their Perspectives." *Frontiers in Physiology* 5 (February): 62.

Dimond, James L., and Steven B. Roberts. 2016. "Germline DNA Methylation in Reef Corals: Patterns and Potential Roles in Response to Environmental Change." *Molecular Ecology* 25 (8): 1895–1904.

———. 2020. "Convergence of DNA Methylation Profiles of the Reef Coral Porites Astreoides in a Novel Environment." *Frontiers in Marine Science* 6: 792.

Dimond, J., and E. Carrington. 2007. "Temporal Variation in the Symbiosis and Growth of the Temperate Scleractinian Coral Astrangia Poculata." *Marine Ecology Progress Series* 348 (October): 161–72.

Dixon, Groves B., Line K. Bay, and Mikhail V. Matz. 2014. "Bimodal Signatures of Germline Methylation Are Linked with Gene Expression Plasticity in the Coral Acropora Millepora." *BMC Genomics* 15 (December): 1109.

Dixon, Groves, Yi Liao, Line K. Bay, and Mikhail V. Matz. 2018a. "Role of Gene Body Methylation in Acclimatization and Adaptation in a Basal Metazoan." *Proceedings of the National Academy of Sciences*. https://doi.org/10.1073/pnas.1813749115.

———. 2018b. "Role of Gene Body Methylation in Acclimatization and Adaptation in a Basal Metazoan." *Proceedings of the National Academy of Sciences of the United States of America* 115 (52): 13342–46.

Drury, Crawford, Justin B. Greer, Iliana Baums, Brooke Gintert, and Diego Lirman. 2019. "Clonal Diversity Impacts Coral Cover in Acropora Cervicornis Thickets: Potential Relationships between Density, Growth, and Polymorphisms." *Ecology and Evolution* 9 (8): 4518–31.

Durante, Meghann K., Iliana B. Baums, Dana E. Williams, Sam Vohsen, and Dustin W. Kemp. 2019. "What Drives Phenotypic Divergence among Coral Clonemates of Acropora Palmata?" *Molecular Ecology* 28 (13): 3208–24.

Edge, Sara E., Michael B. Morgan, and Terry W. Snell. 2008. "Temporal Analysis of Gene Expression in a Field Population of the Scleractinian Coral Montastraea

Faveolata." *Journal of Experimental Marine Biology and Ecology* 355 (2): 114–24.

Eirin-Lopez, Jose M., and Hollie M. Putnam. 2019. "Marine Environmental Epigenetics." *Annual Review of Marine Science* 11 (January): 335–68.

Etchegaray, Jean-Pierre, and Raul Mostoslavsky. 2016. "Interplay between Metabolism and Epigenetics: A Nuclear Adaptation to Environmental Changes." *Molecular Cell* 62 (5): 695–711.

Feely, Richard A., Scott C. Doney, and Sarah R. Cooley. 2009. "Ocean Acidification: Present Conditions and Future Changes in a High-CO_2 World." *Oceanography* 22 (4): 36–47.

Finnegan, E. J., R. K. Genger, K. Kovac, W. J. Peacock, and E. S. Dennis. 1998. "DNA Methylation and the Promotion of Flowering by Vernalization." *Proceedings of the National Academy of Sciences of the United States of America* 95 (10): 5824–29.

Fitt, W. K., F. K. McFarland, M. E. Warner, and G. C. Chilcoat. 2000. "Seasonal Patterns of Tissue Biomass and Densities of Symbiotic Dinoflagellates in Reef Corals and Relation to Coral Bleaching." *Limnology and Oceanography* 45 (3): 677–85.

Grünwald, Niklaus J., and Erica M. Goss. 2011. "Evolution and Population Genetics of Exotic and Re-Emerging Pathogens: Novel Tools and Approaches." *Annual Review of Phytopathology* 49: 249–67.

Gu, Zuguang, Roland Eils, and Matthias Schlesner. 2016. "Complex Heatmaps Reveal Patterns and Correlations in Multidimensional Genomic Data." *Bioinformatics* 32 (18): 2847–49.

Hansen, James, Makiko Sato, and Reto Ruedy. 2012. "Perception of Climate Change." *Proceedings of the National Academy of Sciences of the United States of America* 109 (37): E2415–23.

Harrell, Frank E., Jr, and Maintainer Frank E. Harrell Jr. 2019. "Package 'Hmisc.'" *CRAN2018* 2019: 235–36.

Hill, Ross, and Peter J. Ralph. 2005. "Diel and Seasonal Changes in Fluorescence Rise Kinetics of Three Scleractinian Corals." *Functional Plant Biology: FPB* 32 (6): 549–59.

Hinrichs, S., N. L. Patten, R. J. N. Allcock, S. M. Saunders, D. Strickland, and A. M. Waite. 2013. "Seasonal Variations in Energy Levels and Metabolic Processes of Two Dominant Acropora Species (A. Spicifera and A. Digitifera) at Ningaloo Reef." *Coral Reefs* 32 (3): 623–35.

Hoegh-Guldberg, O., P. J. Mumby, A. J. Hooten, R. S. Steneck, P. Greenfield, E. Gomez, C. D. Harvell, et al. 2007. "Coral Reefs under Rapid Climate Change and Ocean Acidification." *Science* 318 (5857): 1737–42.

Hoegh-Guldberg, Ove. 1999. "Climate Change, Coral Bleaching and the Future of the World's Coral Reefs." *Marine and Freshwater Research* 50 (8): 839–66.

Hoegh-Guldberg, Ove, and John F. Bruno. 2010. "The Impact of Climate Change on the World's Marine Ecosystems." *Science* 328 (5985): 1523–28.

Holm, Sture. 1979. "A Simple Sequentially Rejective Multiple Test Procedure." *Scandinavian Journal of Statistics, Theory and Applications* 6 (2): 65–70.

Hughes, T. P., A. H. Baird, D. R. Bellwood, M. Card, S. R. Connolly, C. Folke, R. Grosberg, et al. 2003. "Climate Change, Human Impacts, and the Resilience of Coral Reefs." *Science* 301 (5635): 929–33.

Hume, Benjamin C. C., Edward G. Smith, Maren Ziegler, Hugh J. M. Warrington, John A. Burt, Todd C. LaJeunesse, Joerg Wiedenmann, and Christian R. Voolstra. 2019. "SymPortal: A Novel Analytical Framework and Platform for Coral Algal Symbiont Next-generation Sequencing ITS2 Profiling." *Molecular Ecology Resources* 19 (4): 1063–80.

Hume, Benjamin C. C., Christian R. Voolstra, Chatchanit Arif, Cecilia D'Angelo, John A. Burt, Gal Eyal, Yossi Loya, and Jörg Wiedenmann. 2016. "Ancestral Genetic Diversity Associated with the Rapid Spread of Stress-Tolerant Coral Symbionts in Response to Holocene Climate Change." *Proceedings of the National Academy of Sciences of the United States of America* 113 (16): 4416–21.

Ito, Ito, Nishio, Tarutani, Emura, Honjo, Toyoda, Fujiyama, Kakutani, and Kudoh. 2019. "Seasonal Stability and Dynamics of DNA Methylation in Plants in a Natural Environment." *Genes*. https://doi.org/10.3390/genes10070544.

Jombart, Thibaut. 2008. "Adegenet: A R Package for the Multivariate Analysis of Genetic Markers." *Bioinformatics*. https://doi.org/10.1093/bioinformatics/btn129.

Jombart, Thibaut, and Caitlin Collins. 2015. "A Tutorial for Discriminant Analysis of Principal Components (DAPC) Using Adegenet 2.0. 0." *Imp Coll London-MRC Cent Outbreak Anal Model* 43: 1–43.

Jombart, Thibaut, Sébastien Devillard, and François Balloux. 2010. "Discriminant Analysis of Principal Components: A New Method for the Analysis of Genetically Structured Populations." *BMC Genetics* 11 (October): 94.

Kenkel, C. D., E. Meyer, and M. V. Matz. 2013. "Gene Expression under Chronic Heat Stress in Populations of the Mustard Hill Coral (Porites Astreoides) from Different Thermal Environments." *Molecular Ecology* 22 (16): 4322–34.

Liew, Yi Jin, Emily J. Howells, Xin Wang, Craig T. Michell, John A. Burt, Youssef Idaghdour, and Manuel Aranda. 2020. "Intergenerational Epigenetic Inheritance in Reef-Building Corals." *Nature Climate Change* 10 (3): 254–59.

Liew, Yi Jin, Didier Zoccola, Yong Li, Eric Tambutté, Alexander A. Venn, Craig T. Michell, Guoxin Cui, et al. 2018. "Epigenome-Associated Phenotypic Acclimatization to Ocean Acidification in a Reef-Building Coral." *Science Advances* 4 (6): eaar8028.

Li, Heng. 2018. "Minimap2: Pairwise Alignment for Nucleotide Sequences." *Bioinformatics* 34 (18): 3094–3100.

Li, Jie, Qi Chen, Li-Juan Long, Jun-De Dong, Jian Yang, and Si Zhang. 2014. "Bacterial Dynamics within the Mucus, Tissue and Skeleton of the Coral Porites Lutea during Different Seasons." *Scientific Reports* 4 (December): 7320.

López-Maury, Luis, Samuel Marguerat, and Jürg Bähler. 2008. "Tuning Gene Expression to Changing Environments: From Rapid Responses to Evolutionary Adaptation." *Nature Reviews. Genetics* 9 (8): 583–93.

Marsh, Adam G., and Annamarie A. Pasqualone. 2014. "DNA Methylation and Temperature Stress in an Antarctic Polychaete, Spiophanes Tcherniai." *Frontiers in Physiology* 5 (May): 173.

Martinez-Arbizu, P. 2019. "pairwiseAdonis: Pairwise Multilevel Comparison Using Adonis." *R Package Version 0. 0* 1.

Navarro-Martín, Laia, Jordi Viñas, Laia Ribas, Noelia Díaz, Arantxa Gutiérrez, Luciano Di Croce, and Francesc Piferrer. 2011. "DNA Methylation of the Gonadal Aromatase (cyp19a) Promoter Is Involved in Temperature-Dependent Sex Ratio Shifts in the European Sea Bass." *PLoS Genetics* 7 (12): e1002447.

Oksanen, Jari, F. Guillaume Blanchet, Michael Friendly, Roeland Kindt, Pierre Legendre, Dan McGlinn, Peter R. Minchin, et al. 2019. "Vegan: Community Ecology Package. 2018." *R Package Version* 1: 17–14.

Oppen, Madeleine J. H. van, James K. Oliver, Hollie M. Putnam, and Ruth D. Gates. 2015. "Building Coral Reef Resilience through Assisted Evolution." *Proceedings of the National Academy of Sciences*. https://doi.org/10.1073/pnas.1422301112.

Palumbi, Stephen R., Daniel J. Barshis, Nikki Traylor-Knowles, and Rachael A. Bay. 2014. "Mechanisms of Reef Coral Resistance to Future Climate Change." *Science* 344 (6186): 895–98.

Pandolfi, John M., Roger H. Bradbury, Enric Sala, Terence P. Hughes, Karen A. Bjorndal, Richard G. Cooke, Deborah McArdle, et al. 2003. "Global Trajectories of the Long-Term Decline of Coral Reef Ecosystems." *Science* 301 (5635): 955–58.

Parkinson, J. E., and I. B. Baums. 2014. "The Extended Phenotypes of Marine Symbioses: Ecological and Evolutionary Consequences of Intraspecific Genetic Diversity in Coral–algal Associations." *Frontiers in Microbiology*. https://www.frontiersin.org/articles/10.3389/fmicb.2014.00445.

Parkinson, John Everett, Erich Bartels, Meghann K. Devlin-Durante, Caitlin Lustic, Ken Nedimyer, Stephanie Schopmeyer, Diego Lirman, Todd C. LaJeunesse, and Iliana B. Baums. 2018. "Extensive Transcriptional Variation Poses a Challenge to Thermal Stress Biomarker Development for Endangered Corals." *Molecular Ecology* 27 (5): 1103–19.

Pegoraro, Mirko, Akanksha Bafna, Nathaniel J. Davies, David M. Shuker, and Eran Tauber. 2016. "DNA Methylation Changes Induced by Long and Short Photoperiods in Nasonia." *Genome Research* 26 (2): 203–10.

Pérez-Figueroa, A. 2013. "Msap: A Tool for the Statistical Analysis of Methylation-Sensitive Amplified Polymorphism Data." *Molecular Ecology Resources* 13 (3): 522–27.

Perez, Marcos Francisco, and Ben Lehner. 2019. "Intergenerational and Transgenerational Epigenetic Inheritance in Animals." *Nature Cell Biology* 21 (2): 143–51.

Pochon, X., J. Pawlowski, L. Zaninetti, and R. Rowan. 2001. "High Genetic Diversity and Relative Specificity among Symbiodinium-like Endosymbiotic Dinoflagellates in Soritid Foraminiferans." *Marine Biology* 139 (6): 1069–78.

Pritchard, Jonathan K., Matthew Stephens, Noah A. Rosenberg, and Peter Donnelly. 2000. "Association Mapping in Structured Populations." *The American Journal of Human Genetics*. https://doi.org/10.1086/302959.

Putnam, Hollie M., Jennifer M. Davidson, and Ruth D. Gates. 2016. "Ocean Acidification Influences Host DNA Methylation and Phenotypic Plasticity in Environmentally Susceptible Corals." *Evolutionary Applications* 9 (9): 1165–78.

Putnam, Hollie M., Raphael Ritson-Williams, Jolly Ann Cruz, Jennifer M. Davidson, and Ruth D. Gates. 2020. "Environmentally-Induced Parental or Developmental Conditioning Influences Coral Offspring Ecological Performance." *Scientific Reports*. https://doi.org/10.1038/s41598-020-70605-x.

Reyna-Lopez, G. E., J. Simpson, and J. Ruiz-Herrera. 1997. "Differences in DNA Methylation Patterns Are Detectable during the Dimorphic Transition of Fungi by Amplification of Restriction Polymorphisms." *Molecular & General Genetics: MGG* 253 (6): 703–10.

Rivera-Casas, Ciro, Rodrigo Gonzalez-Romero, Rafael A. Garduño, Manjinder S. Cheema, Juan Ausio, and Jose M. Eirin-Lopez. 2017. "Molecular and Biochemical Methods Useful for the Epigenetic Characterization of Chromatin-

Associated Proteins in Bivalve Molluscs." *Frontiers in Physiology* 8 (August): 490.

Rivière, Guillaume. 2014. "Epigenetic Features in the Oyster Crassostrea Gigas Suggestive of Functionally Relevant Promoter DNA Methylation in Invertebrates." *Frontiers in Physiology* 5 (April): 129.

Roberts, Steven B., and Mackenzie R. Gavery. 2012. "Is There a Relationship between DNA Methylation and Phenotypic Plasticity in Invertebrates?" *Frontiers in Physiology* 2. https://doi.org/10.3389/fphys.2011.00116.

Rodriguez-Casariego, Javier A., Mark C. Ladd, Andrew A. Shantz, Christian Lopes, Manjinder S. Cheema, Bohyun Kim, Steven B. Roberts, et al. 2018. "Coral Epigenetic Responses to Nutrient Stress: Histone H2A. X Phosphorylation Dynamics and DNA Methylation in the Staghorn Coral Acropora Cervicornis." *Ecology and Evolution* 8 (23): 12193–207.

Rosenzweig, Cynthia, David Karoly, Marta Vicarelli, Peter Neofotis, Qigang Wu, Gino Casassa, Annette Menzel, et al. 2008. "Attributing Physical and Biological Impacts to Anthropogenic Climate Change." *Nature* 453 (7193): 353–57.

Ryu, Taewoo, Heather D. Veilleux, Jennifer M. Donelson, Philip L. Munday, and Timothy Ravasi. 2018. "The Epigenetic Landscape of Transgenerational Acclimation to Ocean Warming." *Nature Climate Change* 8 (6): 504–9.

Salinas, Santiago, and Stephan B. Munch. 2012. "Thermal Legacies: Transgenerational Effects of Temperature on Growth in a Vertebrate." *Ecology Letters*. https://doi.org/10.1111/j.1461-0248.2011.01721.x.

Sambrook, Joseph, and David W. Russell. 2006. "Isolation of High-Molecular-Weight DNA from Mammalian Cells Using Proteinase K and Phenol." *Cold Spring Harbor Protocols*. https://doi.org/10.1101/pdb.prot4036.

Samiei, Jahangir Vajed, Abolfazl Saleh, Arash Shirvani, Neda Sheijooni Fumani, Mehri Hashtroudi, and Morgan Stuart Pratchett. 2016. "Variation in Calcification Rate of Acroporadowningi Relative to Seasonal Changes in Environmental Conditions in the Northeastern Persian Gulf." *Coral Reefs* 35 (4): 1371–82.

Scheufen, Tim, Wiebke E. Krämer, Roberto Iglesias-Prieto, and Susana Enríquez. 2017. "Seasonal Variation Modulates Coral Sensibility to Heat-Stress and Explains Annual Changes in Coral Productivity." *Scientific Reports* 7 (1): 4937.

Sharp, Koty H., Zoe A. Pratte, Allison H. Kerwin, Randi D. Rotjan, and Frank J. Stewart. 2017. "Season, but Not Symbiont State, Drives Microbiome Structure in the Temperate Coral Astrangia Poculata." *Microbiome* 5 (1): 120.

Shinzato, C., E. Shoguchi, T. Kawashima, and M. Hamada. 2011. "Using the Acropora Digitifera Genome to Understand Coral Responses to Environmental Change." *Nature*. https://www.nature.com/articles/nature10249/.

Sorek, Michal, Erika M. Díaz-Almeyda, Mónica Medina, and Oren Levy. 2014. "Circadian Clocks in Symbiotic Corals: The Duet between Symbiodinium Algae and Their Coral Host." *Marine Genomics* 14 (April): 47–57.

Stevenson, Tyler J., and Brian J. Prendergast. 2013. "Reversible DNA Methylation Regulates Seasonal Photoperiodic Time Measurement." *Proceedings of the National Academy of Sciences of the United States of America* 110 (41): 16651–56.

Stoddart, J. A., and J. F. Taylor. 1988. "Genotypic Diversity: Estimation and Prediction in Samples." *Genetics* 118 (4): 705–11.

Suarez-Ulloa, Victoria, Rodrigo Gonzalez-Romero, and Jose M. Eirin-Lopez. 2015. "Environmental Epigenetics: A Promising Venue for Developing next-Generation Pollution Biomonitoring Tools in Marine Invertebrates." *Marine Pollution Bulletin* 98 (1-2): 5–13.

Suarez-Ulloa, Victoria, Ciro Rivera-Casas, and Michelot Michel. 2019. "Seasonal DNA Methylation Variation in the Flat Tree Oyster Isognomon Alatus from a Mangrove Ecosystem in North Biscayne Bay, Florida." *Journal of Shellfish Research* 38 (1): 79.

Thornhill, Daniel J., Todd C. LaJeunesse, Dustin W. Kemp, William K. Fitt, and Gregory W. Schmidt. 2006. "Multi-Year, Seasonal Genotypic Surveys of Coral-Algal Symbioses Reveal Prevalent Stability or Post-Bleaching Reversion." *Marine Biology* 148 (4): 711–22.

Tunnicliffe, V. 1981. "Breakage and Propagation of the Stony Coral Acropora Cervicornis." *Proceedings of the National Academy of Sciences of the United States of America* 78 (4): 2427–31.

Ulstrup, K. E., R. Hill, M. J. H. van Oppen, A. W. D. Larkum, and P. J. Ralph. 2008. "Seasonal Variation in the Photo-Physiology of Homogeneous and Heterogeneous Symbiodinium Consortia in Two Scleractinian Corals." *Marine Ecology Progress Series* 361 (June): 139–50.

Vandegehuchte, Michiel B., Tina Kyndt, Bartel Vanholme, Annelies Haegeman, Godelieve Gheysen, and Colin R. Janssen. 2009. "Occurrence of DNA Methylation in Daphnia Magna and Influence of Multigeneration Cd Exposure." *Environment International* 35 (4): 700–706.

Vignet, Caroline, Lucette Joassard, Laura Lyphout, Tiphaine Guionnet, Manon Goubeau, Karyn Le Menach, François Brion, et al. 2015. "Exposures of Zebrafish through Diet to Three Environmentally Relevant Mixtures of PAHs Produce Behavioral

Disruptions in Unexposed F1 and F2 Descendant." *Environmental Science and Pollution Research International* 22 (21): 16371–83.

Viitaniemi, Heidi M., Irene Verhagen, Marcel E. Visser, Antti Honkela, Kees van Oers, and Arild Husby. 2019. "Seasonal Variation in Genome-Wide DNA Methylation Patterns and the Onset of Seasonal Timing of Reproduction in Great Tits." *Genome Biology and Evolution* 11 (3): 970–83.

Voolstra, Christian R., Julia Schnetzer, Leonid Peshkin, Carly J. Randall, Alina M. Szmant, and Mónica Medina. 2009. "Effects of Temperature on Gene Expression in Embryos of the Coral Montastraea Faveolata." *BMC Genomics* 10 (December): 627.

Warner, M., G. Chilcoat, F. McFarland, and W. Fitt. 2002. "Seasonal Fluctuations in the Photosynthetic Capacity of Photosystem II in Symbiotic Dinoflagellates in the Caribbean Reef-Building Coral Montastraea." *Marine Biology* 141 (1): 31–38.

Weil, E., E. Hernández-Delgado, M. Gonzalez, S. Williams, S. Suleimán Ramos, M. Figuerola, and T. and Metz-Estrella. 2019. "Spread of the New Coral Disease 'SCTLD' into the Caribbean: Implications for Puerto Rico." *Reef Encounter* 34 (1): 38–43.

West-Eberhard, Mary Jane. 2003. *Developmental Plasticity and Evolution*. Oxford University Press.

Xiong, Wanshan, Xiaorong Li, Donghui Fu, Jiaqin Mei, Qinfei Li, Guanyuan Lu, Lunwen Qian, et al. 2013. "DNA Methylation Alterations at 5'-CCGG Sites in the Interspecific and Intraspecific Hybridizations Derived from Brassica Rapa and B. Napus." *PloS One* 8 (6): e65946.

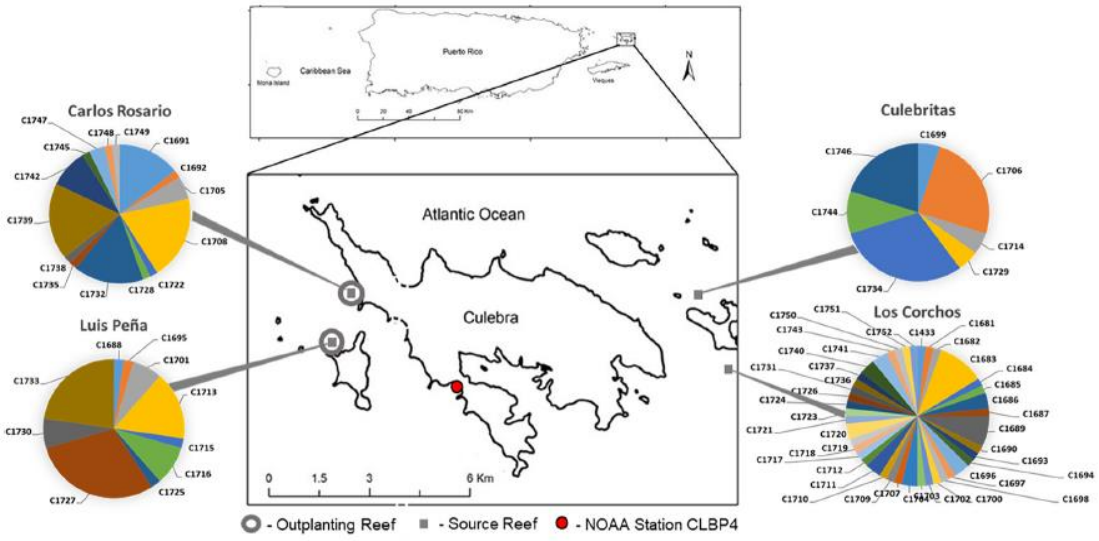

Fig. 1. Field experiment locations in Culebra, Puerto Rico. Four source sites are denoted with gray squares, Luis Peña (LP: 18°18'45.0"N, 65°20'08.4"W), Carlos Rosario (CR: 18°19'30.2"N, 65°19'52.7"W), Culebritas (18°19'19.4"N 65°14'14.5"W) and Los Corchos (18°18'33.0"N 65°13'44.3"W). The genotypic composition was obtained using 6 microsatellite loci as in (Baums et al. 2005a) and is shown in pie charts. Outplant sites (gray circles) consisted of five 5 x 5m plots located at each site at two depths (5 and 15m). A total of n=20 fragments from each source site were outplanted in each plot for a total of n=400 fragments. Temperature records were gathered from NOAA Data Buoy Center, Station CLBP4 (red circle) located 3.8 and 4 km from LP and CR respectively.

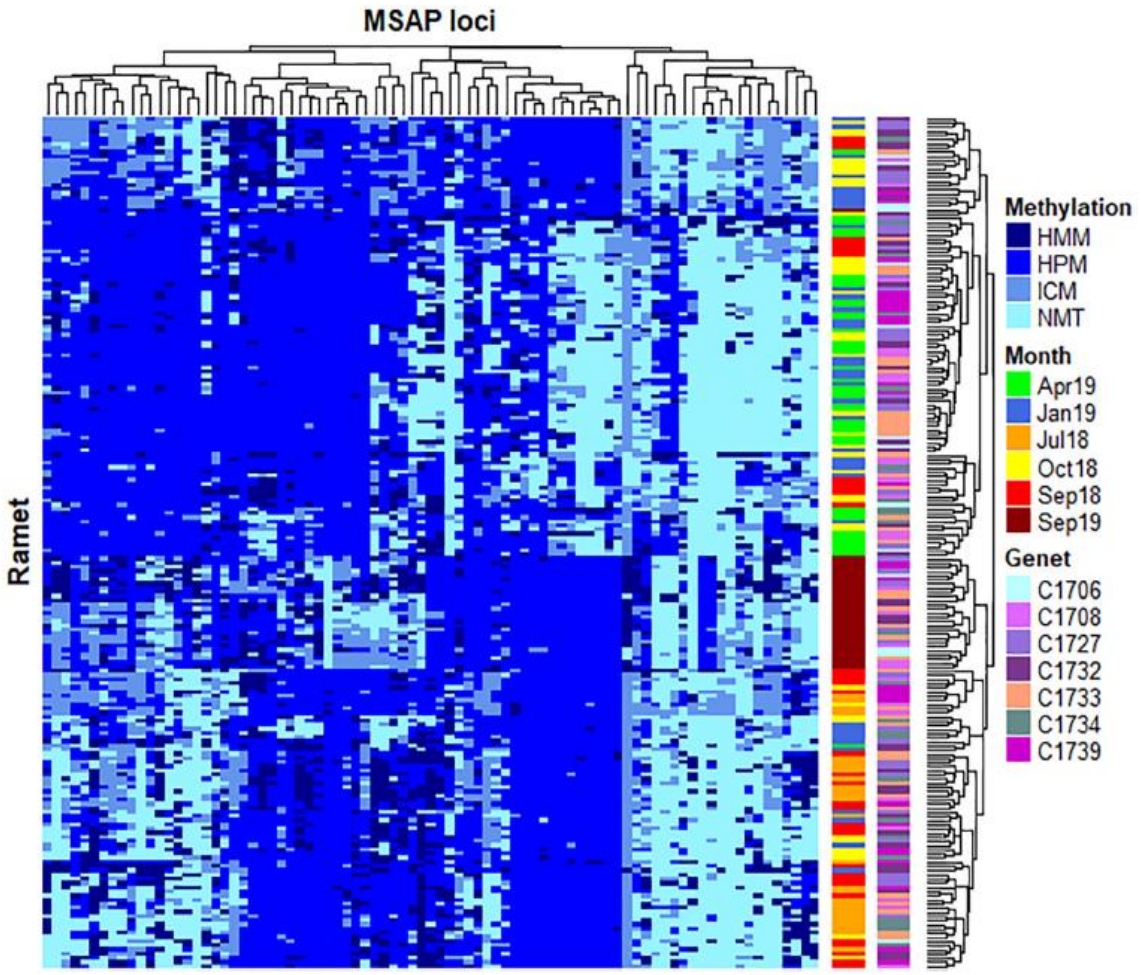

Fig. 2. Heatmap representing temporal changes in 83 loci showing a significant non-random distribution of DNA methylation patterns ($p<0.05$, $pFDR<0.05$). Two distinctive clusters separate DNA methylation between cold (Apr 2019) and warm (Jul 2018, Sep 2018, and Sep 2019) months. Samples from Oct 2018 and Jan 2019 show a scattered distribution across these two clusters, while most Sep 2019 specimens constituted a well-defined sub-cluster within the warm group. No clear clustering is observed for specific genets. Rows (samples) and columns (MSAP loci) were clustered using Gower's Coefficient of Similarity. The methylation status of each locus is indicated in the right margin of the figure: **HMM**, hemimethylated, **HPM**, hypermethylated; **ICM**, internal cytosine methylation; **NMT**, non-methylated (unmethylated).

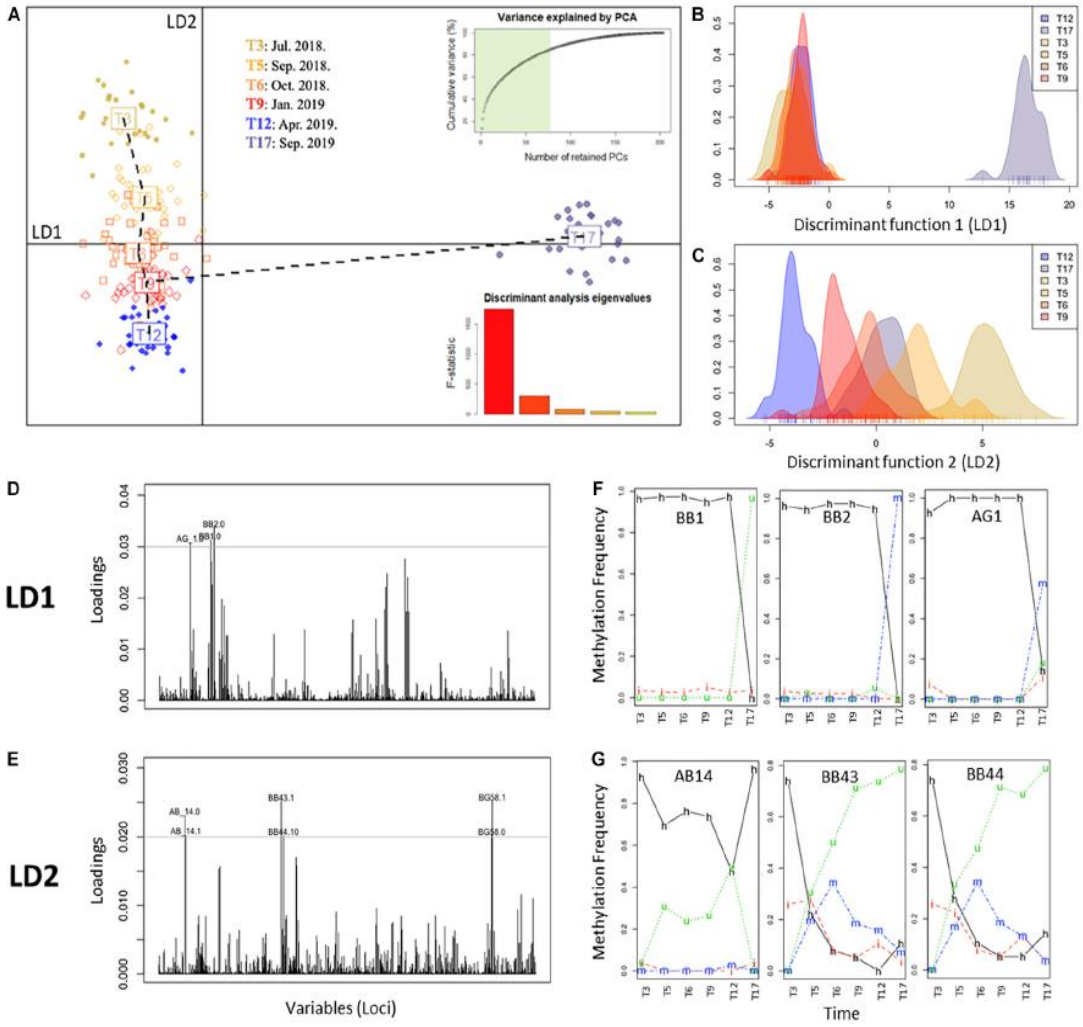

Fig. 3. Discriminant analysis of principal components (DAPC) of complete MSAP profiles representing the different groups (i.e., time points). **A:** scatterplot of monthly clusters resolved by DAPC. Barplot shows the significance of each of the five discriminant functions retained. In the upper-left corner the variance explained by the 77 PCs retained for the study. Horizontal line: x-axis, first discriminant function (LD1) and vertical line: y-axis, second discriminant function (LD2). **B and C:** density of methylation profiles of each *A. cervicornis* fragment against discriminant function 1 (LD1) and discriminant function 2 (LD2), respectively. **D and E:** loading plot of MSAP loci that most contributed to LD1 and LD2 respectively. **F and G:** temporal variation of the frequency of each methylation status of loci with high contribution to LD1 (BB1, BB2, AG1) and LD2 (AB14, BB43, BB44), respectively. Methylation status is indicated in the lines of the figure: **h**, hemimethylated, **m**, hypermethylated; **i**, internal cytosine methylation; **u**, non-methylated (unmethylated).

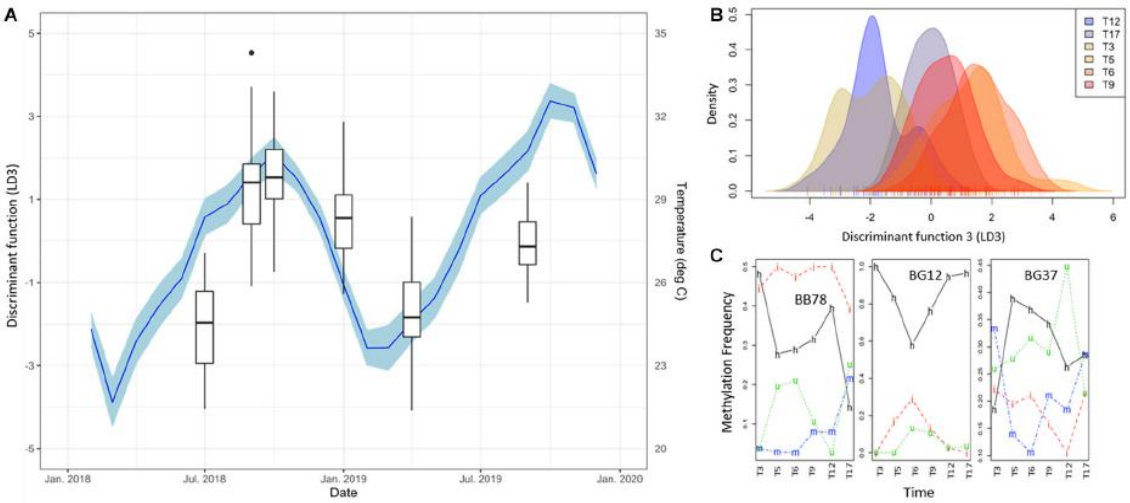

Fig. 4. A: time series of DNA methylation pattern separation as given by the DAPC discriminant function 3 (LD3, Box Plots). Black dots indicate outliers. Monthly average of daily mean temperature (NOAA Buoy CLBP4, blue line), lagg corrected +1 as calculated with the *ccf* function in R, is shown as additional y-axes. Blue shadings indicate 95% confidence intervals of temperature variability. Note the clear seasonal variation of the DNA methylation patterns evidenced by this discriminant function and its significant correlation with temperature changes (Pearson's rank correlation: $r = 0.91$, $p = 0.0310$). **B:** density of DNA methylation profiles of each *A. cervicornis* fragment against discriminant function 3 (LD3) **C:** temporal variation of the frequency of each methylation status of three loci with high contribution to LD3 (BB78, BG12, BG37). Methylation status is indicated in the lines of the figure: **h**, hemimethylated; **m**, hypermethylated; **i**, internal cytosine methylation; **u**, non-methylated (unmethylated).

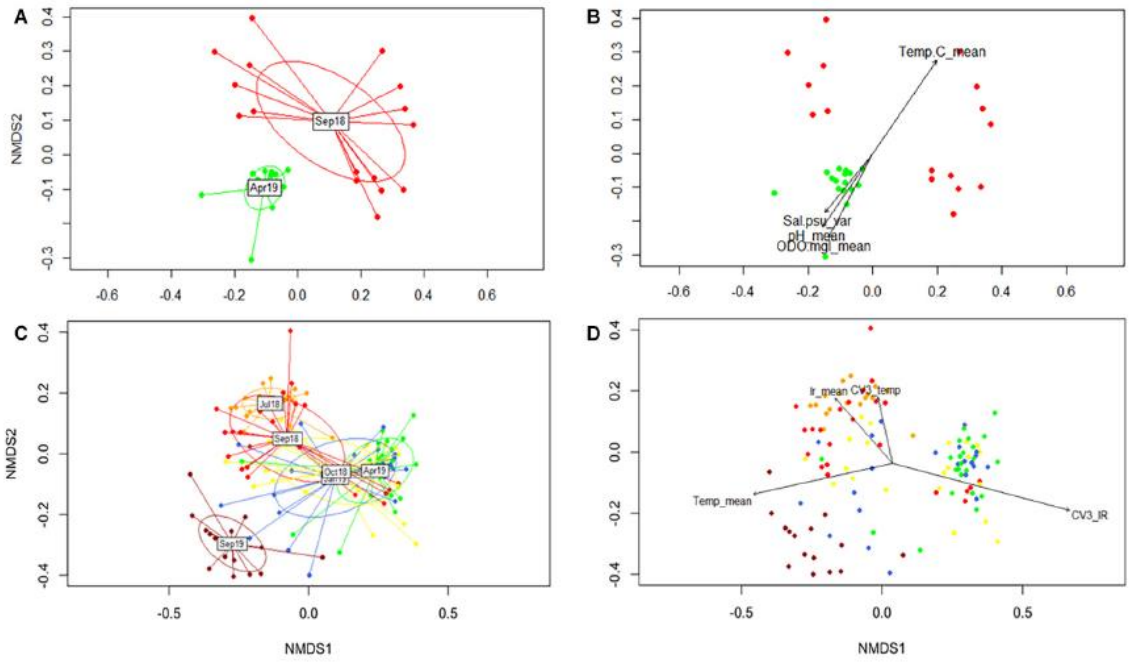

Fig. 5. Non-metric multidimensional scaling (NMDS) of global DNA methylation patterns using Gower distances. **A:** temporal separation for T5 and T12 for LP sites. **C:** representation of all sampling times for both shallow sites (LP and CR). **B and D**: significant correlations of environmental parameters to DNA methylation patterns ($P < 0.05$). Colors correspond to collection times.

Table 1. Adapters and Primers used for MSAP analysis in *A. cervicornis*.

Step	Adapter/ Primer	Sequence (5'→ 3')	Combinations*
Digestion/ ligation	EcoRI	3'CTCGTAGACTGCGTACC5' 5'CTGACGCATGGTTAA 3'	**DL**
	HpaII/MspI	3'CGACTCAGGACTCAT5' 5'TGAGTCCTGAGTAGCAG 3'	
Pre-selective PCR	EcoRI+A	GACTGCGTACCAATTCA	**PA**
	M/H+T	GATGAGTCTAGAACGGT	
	EcoR1+C	GACTGCGTACCAATTCC	**PB**
	M/H + A	GATGAGTCTAGAACGGA	
Selective PCR	SL1-TTG	FAM-GATGAGTCTAGAACGGTTG	**SL1**
	SL1-TCT	FAM-GATGAGTCTAGAACGGTCT	
	SL2-TCA	FAM-GATGAGTCTAGAACGGTCA	**SL2**
	SL2-AAC	FAM-GATGAGTCTAGAACGGAAC	
	SL3-TTA	HEX-GATGAGTCTAGAACGGTTA	**SL3**
	SL3-TAA	HEX-GATGAGTCTAGAACGGTAA	
	SL4-AGT	HEX-GATGAGTCTAGAACGGAGT	**SL4**
	SL4-ATC	HEX-GATGAGTCTAGAACGGATC	

* adapters or primers were combined in one PCR reaction for digestion/ligation, pre-selective, and selective combinations.

Table 2. Genotypic diversity of *A. cervicornis* at source sites around Culebra, PR.

	N	**Ng**	**N_g/N**	**G_o**	**G_o/G_e**	**G_o/N_g**
Los Corchos (LC)	60	41	0.683	28	0.467	0.683
Culebrita (CUL)	20	7	0.350	4.762	0.238	0.680
Carlos Rosario (CR)	50	11	0.220	5.438	0.109	0.494
Luis Peña (LP)	56	15	0.268	7.612	0.136	0.507
Average	46.500	18.500	0.380	11.453	0.237	0.591
Std. Dev	18.138	15.351	0.209	11.098	0.163	0.105

N = sample size, N_g = number of genets, G_o = observed genotypic diversity, G_e = expected genotypic diversity.

Table 3. DNA methylation status of target sequences (percentages) from each time point.

Band pattern (target state)	**T3**	**T5**	**T6**	**T9**	**T12**	**T17**
HPA+/MSP+(Non-methylated)	17.69	15.48	15.75	17.48	17.45	13.49
HPA+/MSP-(Hemimethylated)	10.92	13.15	11.57	9.49	8.64	15.68
HPA-/MSP+(Internal C methylation)	13.39	13.98	13.31	11.45	7.95	15.98
HPA-/MSP-(Hypermethylation)	58.01	57.39	59.38	61.60	65.97	54.85

Table 4. Pairwise PERMANOVA of global DNA methylation patterns between time points.

	T3	T5	T6	T9	T12	T17
T3		**0.0660**	**0.0015**	**0.0015**	**0.0015**	**0.0015**
T5	2.7247		0.0994	**0.0015**	**0.0015**	**0.0015**
T6	5.5726	1.6992		0.1782	**0.0015**	**0.0015**
T9	7.7282	3.5977	1.2757		**0.0015**	**0.0015**
T12	14.6953	9.6050	5.4069	3.4001		**0.0015**
T17	13.3517	9.1919	8.0027	8.4736	16.2329	

Values of F below the diagonal. Adjusted p-values (Holm's method) above the diagonal. Values of $p < 0.05$ are in bold.

Table 5. Pairwise PERMANOVA of global DNA methylation patterns between coral genets.

	C1706	C1708	C1727	C1732	C1733	C1734	C1739
C1706		0.4536	0.4536	0.2744	0.2744	0.1344	0.2744
C1708	0.9931		0.2744	**0.0494**	0.1837	**0.0440**	0.0765
C1727	1.1813	1.5936		0.1837	0.2744	0.0688	**0.0494**
C1732	1.4882	2.4780	1.9408		0.0765	0.2744	**0.0494**
C1733	1.8353	2.1118	1.7832	2.5051		0.1926	**0.0084**
C1734	1.9702	2.4824	2.2012	1.6745	1.9121		0.0765
C1739	1.7727	2.4298	2.4494	2.5393	3.2224	2.2206	

Values of F below the diagonal. Adjusted p-values (Holm's method) above the diagonal. Values of $p < 0.05$ are in bold.

CHAPTER IV

SYMBIONT SHUFFLING INDUCES DIFFERENTIAL DNA METHYLATION RESPONSES TO THERMAL STRESS IN THE CORAL *MONTASTRAEA CAVERNOSA*.

This manuscript was submitted and is under revision for publication at Molecular Ecology. Accordingly, it was formatted following publisher's requirements

Abstract

Algal symbiont shuffling in favor of more thermo-tolerant species has been shown to enhance coral resistance to heat-stress. Yet, the mechanistic underpinnings and long-term implications of these changes are poorly understood. This work studied the modifications in coral DNA methylation, an epigenetic mechanism involved in coral acclimatization, in response to symbiont manipulation and subsequent heat stress exposure. Symbiont composition was manipulated in the great star coral *Montastraea cavernosa* through controlled thermal bleaching and recovery, producing paired ramets of three genets dominated by either their native symbionts (genus *Cladocopium*) or the thermotolerant species (*Durusdinium trenchii*). Single-base genome-wide analyses showed significant modifications in DNA methylation concentrated in intergenic regions, introns, and transposable elements. Remarkably, DNA methylation changes in response to heat stress were dependent on the dominant symbiont, with twice as many differentially methylated regions found in heat-stressed corals hosting different symbionts (*Cladocopium* vs. *D. trenchii*) compared to all other comparisons. Interestingly, while differential gene body methylation was not correlated with gene expression, an enrichment in differentially methylated regions was evident in repetitive genome regions. Overall, these results suggest that changes in algal symbionts favoring heat tolerant associations are accompanied by changes in DNA methylation in the coral host. The implications of these results for coral adaptation, along with future avenues of research based on current knowledge gaps, are discussed in the present work.

Introduction

The obligate symbiosis between corals and dinoflagellates in the family Symbiodinaceae constitutes one of the most successful biological strategies supporting remarkable biodiversity in very oligotrophic waters. This highly efficient symbiosis, however, is sensitive to elevated temperatures, among other stressors, leading to the disruption of the partnership in a stress response known as "coral bleaching" (Weis 2008; Baker and Cunning 2015), often resulting in mortality. Bleaching is the main cause of the accelerated decline of coral populations, mainly caused by the anthropogenic alteration of the planet's climate (Pandolfi et al. 2003; Hughes et al. 2017), with dire consequences for marine ecosystems and coastal populations. Hence, great efforts have been placed in understanding the dynamics and the mechanisms regulating this symbiosis as a way to develop strategies to increase coral resilience to global change (National Academies of Sciences, Engineering, and Medicine et al. 2019; Bay et al. 2019).

Several factors have been shown to modulate coral sensitivity to heat stress and promote acclimation/adaptation responses [i.e., genetic, epigenetic, symbiotic community composition and microbiome (Barshis 2015; Quigley et al. 2018; Eirin-Lopez and Putnam 2019)], leading to a wide spectrum of bleaching susceptibility patterns. Focusing on the symbiotic relationship, both the identity and population density of the symbiont appear to affect thermal sensitivity (Baker 2004; Cunning and Baker 2013; Silverstein, Cunning, and Baker 2015; Swain et al. 2020). Particularly, corals hosting symbionts in the genus *Durusdinium* often display higher tolerances to heat stress (Berkelmans and van Oppen 2006; Silverstein, Cunning, and Baker 2015) and improved overall survival to bleaching events (Glynn et al. 2001; Jones et al. 2008). Current evidence of an increase

and persistence of *Durusdinium* in natural coral populations, with a recent and rapid expansion through the Caribbean (Pettay et al. 2015), suggests a positive selection of this symbiotic partner under increasingly frequent thermal anomalies. Consequently, increasing efforts have been placed to study the mechanisms underlying coral symbiotic interactions under stress conditions (Yuyama et al. 2018; Helmkampf et al. 2019; Cunning and Baker 2020). Yet, with the exception of a single study investigating the epigenetic regulation of transcriptional changes upon the establishment of symbiosis (Li et al. 2018), the role of epigenetic mechanisms regulating molecular responses to changes in coral symbiont composition under thermal stress remains unknown.

Accumulating evidence suggests that epigenetic modifications [i.e., molecules and mechanisms able to regulate gene expression through the generation of alternative gene activity states in the context of the same DNA sequence (Cavalli and Heard 2019)] are involved in conveying environmental signals to the genome, and thus participating in the regulation of subsequent phenotypic responses. Epigenetic regulation is ubiquitous in all eukaryotes, based on the fundamental role that epigenetic mechanisms play in genome packing and functional organization within the cell nucleus. In corals, several studies have already reported evidence of epigenetic responses to different types of environmental stressors such as thermal stress, ocean acidification, and eutrophication, among others (Putnam, Davidson, and Gates 2016; Liew et al. 2018; Rodriguez-Casariego et al. 2018), as well as to broad environmental change (Rodríguez-Casariego et al. 2020; Dimond and Roberts 2020), with links to transcriptional plasticity (Dixon et al. 2018; Li et al. 2018). Since the symbiotic partners of corals also constitute part of (and therefore shape) their environment, the present work hypothesizes that transitions in these

populations will require phenotypic acclimatory responses in the coral host, facilitated by epigenetic modifications. Indeed, coral symbiont variants and abundance have been shown to significantly modulate gene expression in the host (Barfield et al. 2018; Helmkampf et al. 2019), including experiments where the inter-genet variability [genet refers to the collection of fragments or “ramets" originating from the same colony (DeSalvo et al. 2010; Cunning and Baker 2020)] was eliminated. In order to elucidate the role of epigenetic regulation during symbiont transitions, the present work builds on the experimental design developed by Cunning and Baker (2020) in which symbionts were manipulated to produce paired ramets with different symbionts to subsequently expose them to thermal stress. Epigenetic changes in DNA methylation occurring in response to symbiont manipulation and subsequent thermal stress exposure are examined, as well as their relationship with gene expression. The obtained results suggest that DNA methylation response to thermal stress is symbiont-specific, with accumulation of differentially methylated sites in repetitive regions of the genome and evidence of gene-body methylation reducing spurious transcription but not mediating changes in gene expression.

Materials and Methods

Experimental Design

Detailed description of coral collection, fragmentation, and subsequent symbiont manipulation and short-term thermal stress exposure can be found in Cunning and Baker (2020). Briefly, wild colonies of the great star coral *Montastraea cavernosa* were collected near Key Biscayne, FL, fragmented by coring into 2.5-cm diameter ramets, and

acclimated to the University of Miami's Marine Technology and Life Sciences Seawater Complex water systems for 3.5 months (26°C, ~230 μmol photons m−2 s−1 in a 12-hr:12-hr light–dark cycle, Reef Chilli twice a week). After this period, half of the ramets were maintained in control conditions while the other half were subjected to controlled bleaching (temperature was raised from 26 to 32°C at 0.5°C day-1 and kept at 32°C for 14 days) and recovery (fragments were transferred to control conditions at 26°C), which encouraged symbiont community changes in favor of *Durusdinium*. After a 4-month recovery period, coral symbiotic composition was assessed through qPCR (Cunning and Baker 2013), confirming symbiont shuffling from *Cladocopium* to *Durusdinium* dominance. Paired (same coral genotype) *Cladocopium*- and *Durusdinium*-dominated ramets were then exposed to control (26°C) or short-term heat-stress conditions for 4.8 days (~3 degree heating weeks, DHWs) and subsequently flash frozen in liquid nitrogen for long-term preservation of samples. Manipulations resulted in 4 groups, control corals hosting *Cladocopium* (C_C), control corals hosting *Durusdinium* (D_C), heat-stressed corals hosting *Cladocopium* (C_H) and heat-stressed corals hosting *Durusdinium* (D_H).

Coral DNA Extraction and MBD-BS Library Preparation

In the present work, DNA methylation was studied using a Methyl-binding domain capture approach coupled with bisulfite sequencing (MBD-BS). This method allows the enrichment of methylated DNA (as low as 1% of the genome in some invertebrates) to reduce sequencing requirements, while maintaining base-pair resolution of the resulting data. From the subset of flash-frozen samples (see above), a total of n=2 replicates per genotype, n=3 genotypes, for all 4 symbiont/temperature combinations

were randomly selected for methylation analyses (n=24 samples). Genomic DNA was isolated from flash frozen coral cores after pulverization in liquid nitrogen. Approximately 100 mg of the resulting powder was resuspended in 2 mL vials containing 500 mg of Zirconia/Silica beads (0.5 mm diameter) and 1 mL of DNA/RNA Shield buffer (Zymo Research, Irvine, CA). Coral cells were gently lysed with two 30 s vortex pulses to enrich host DNA by maintaining symbiont cells intact (Rodríguez-Casariego et al. 2020). After centrifugation (12,000 x g for 5 min), 800 µL of the supernatant were transferred to a new tube and DNA isolation was continued using the *Quick*-DNA/RNA Mini-Prep kit (Zymo Research, Irvine, CA) as per manufacturer's instructions. DNA quality was assessed by gel electrophoresis and spectrophotometric analysis as described in our previous work (Rivera-Casas et al., 2017). DNA concentration was measured using a Qubit 2.0 fluorometer (Thermo Fisher, Waltham, MA). Samples with concentrations under 20 ng/µL and/or low quality (i.e., ethanol contamination) were re-processed using a DNA Clean & Concentrator kit (Zymo Research, Irvine, CA) until proper concentration and quality were achieved.

DNA samples ranging from 36.2 to 119 ng/µL (100 µL) were placed in 1.5ml polystyrene tubes and sheared in a Bioruptor (Diagenode, Philadelphia, PA) using 25 cycles of 30s ON and 30s OFF in low power. Shearing size (~350 bp) was confirmed using a 2100 Bioanalyzer with High Sensitivity DNA Assay Kit (Agilent Technologies, Santa Clara, CA). Capture of methylated DNA was performed with the MethylCap Kit (Diagenode, Ougrée, Belgium). A single-fraction elution was performed with 150 µL of high-salt buffer to obtain captured DNA only. Purification of the captured DNA was performed with the DNA Clean & Concentrator kit (Zymo Research, Irvine, CA), and

eluted in 25 μL. Bisulfite conversion and library preparation was performed using the Pico Methyl-Seq Library Prep Kit (Zymo Research, Irvine, CA). Libraries were barcoded and shipped for pooling and sequencing at Admera Health Biopharma Services (South Plainfield, NJ), generating 150bp paired-end reads on two lanes of a HiSeq-X sequencer.

DNA methylation quantification

Sequences were trimmed with 10 bp removed from both the 5′ and 3′ ends using TrimGalore! v.0.4.5 (Krueger 2012). Sequence quality was assessed using FastQC v.0.11.7 (Andrews, 2010) before and after trimming. The *M. cavernosa* genome assembly was obtained from Dr. M. Matz's Laboratory (https://matzlab.weebly.com/data--code.html) and was prepared for downstream use with the Bismark genome_preparation function (Bismark v.0.19.0, Krueger and Andrews, 2011) using Bowtie 2-2.3.4 (Langmead and Salzberg, 2012) as aligner. Trimmed sequences were then aligned to the prepared genome using Bismark with non-directionality and alignment score of L,0,-1.2. Alignment files (i.e., bam files) were deduplicated (using deduplicate_bismark), sorted and indexed [using SAMtools v.1.9 (Li et al., 2009)]. Methylation calls were extracted from deduplicated files using bismark_methylation_extractor and separated by context (i.e., CpG, CHG, CHH).

Genomic feature tracks for downstream analyses were derived directly from the *M. cavernosa* genome annotation (https://matzlab.weebly.com/data--code.html) or created using BEDtools v2.26.0 (Quinlan and Hall, 2010). Genes, mRNA, exons, coding sequences (CDS), and flanking untranslated regions (3'-UTR and 5'-UTR) were obtained directly from the genome annotation file while putative promoter regions, intergenic

regions and repetitive regions were created following previously developed pipelines (Venkataraman et al. 2020). Introns were derived by subtracting exons from gene tracks. Gene body methylation includes CpGs overlapping with intron, CDS and UTRs, but not promoters.

Statistical Analyses

Statistical analyses were all completed in R (v4.0.2; R Core Team 2020) with RStudio (v1.3.959; R Studio Team 2020). R scripts used for all analysis were stored in Github (see data accessibility statement).

Describing the DNA methylation landscape

Sequences from all samples were used to characterize general DNA methylation patterns in *M. cavernosa*. Methylation calls per CpG loci (i.e., .cov files) were merged, corrected using a 1% miss-call rate (based on non CpG methylation calls) and filtered to maintain individual CpG dinucleotides with at least 5x coverage in each sample. Individual loci (i.e., CpG dinucleotides) were classified based on methylation percent in unmethylated (<10% methylation), sparsely methylated (10-50% methylation) and methylated (> 50% methylation). The genomic feature where they locate was also characterized (i.e., CDS, intron, UTRs, putative promoters, transposable elements, and other intergenic regions). The significant association between genomic features and methylation status was evaluated through a chi-squared test (*prop.test* R function) using a CpG track extracted from the genome assembly. A similar approach was followed for the feature overlap of differentially methylated regions (DMR).

Genome-wide DNA methylation response

The genome-wide DNA methylation response induced by the experimental manipulation (symbiont and temperature) was visualized through principal coordinates analysis (PCoA) of Manhattan distances. A variance partitioning analysis was performed using the R package *variancepartition* (Hoffman and Schadt 2016), to visualize the variance components within each coral genet. Treatment associated variance across all genets was analyzed through a Discriminant Analysis of Principal Components (DAPC) using the R package *adegenet* v2.1.3 (Jombart, Devillard, and Balloux 2010). The effect of experimental manipulations in Global percent DNA methylation was also tested by ANOVA with the model *aov(median~Treatment*Symb*feature*).

Describing DNA methylation in repetitive regions

Repetitive regions in *M. cavernosa* were annotated using RepeatMasker v4.1.1 (A.F.A. Smit, R. Hubley & P. Green RepeatMasker at http://repeatmasker.org). Python scripts developed by Dr. Yi Jin Liew (https://github.com/lyijin/smic_dna_meth) were used to calculate methylation levels (average % methylation for all sites overlapping repeats) and methylation densities (number of methylated Cs) per repeat type. The correlation between treatment combinations and DNA methylation density on repeats was evaluated through two-way ANOVA and pairwise t-test.

Determining expression of repetitive elements

The expression of transcripts originating from repeat elements was quantified utilizing the RNA-seq dataset developed by Cunning and Baker (2020). Reads from each sample included in the methylation analysis (n=24) were mapped against the genome of *M. cavernosa* with HISAT2 v2.1.0 (Kim, Langmead, and Salzberg 2015). The resulting

aligned reads (between 75-90% mapping efficiency) were processed using *samtools depth* (Li et al. 2009) to create a per-base coverage file. RNA-seq reads counts for each repeat type were parsed utilizing a python script developed by Dr. Yi Jin Liew (https://github.com/lyijin/smic_dna_meth). The significance of the effect of experimental manipulations on the expression of repetitive regions was evaluated through paired t-tests.

Identification of differentially methylated regions and genes

Differentially methylated regions (DMRs) were identified using the methylpy pipeline (Schultz et al. 2015) (https://github.com/shellytrigg/methylpy). This method first identifies differentially methylated CpGs between all samples using a mean square root test, and then collapses neighboring sites across a specific window size. CpG sites with at least 5x coverage were subject to DMR analysis across a 250bp window. DMRs were identified from all samples together, and between relevant symbiont/temperature combinations. Regions with less than 3 CpGs and present in less than 75% of the samples in each treatment were discarded. Significant differences of DMRs between treatments was further tested through ANOVA after arcsine-square-root transformation. Two-way ANOVA with the model *~symbiont*temperature* was applied for DMRs identified from all samples together, and One-way ANOVA was employed for combination contrasts (i.e., C_H vs C_C; D_C vs C_C; etc.).

Differentially methylated genes (DMG) were identified though a generalized linear model implemented in R. CpG methylation (>5x coverage) across gene-body (intron, CDS and UTRs) was summarized for each gene as the sum of all methylated and

unmethylated reads for a particular position across the gene. The model *glm(meth, unmeth~ sym*temp, family=binomial)* was applied to all samples, while models including only *sym* or *temp* were applied to individual combination contrasts as described before. Only positions shared by all samples were included in the analyses.

Functional enrichment of methylated genes and association with gene expression

Gene ontology (GO) and eukaryotic orthologous groups (KOG) categories enrichment in relation to gene-level DNA methylation was performed using GO-MWU (Wright et al. 2015) and KOG-MWU (Matz 2016) respectively. Methylation change between treatment contrasts used for both enrichment analyses was calculated as log2 fold of the methylated/unmethylated fraction per gene. *M. cavernosa* KOG and GO categories used here are the same as in (Cunning and Baker 2020) and were obtained from https://github.com/mstudiva/Mcav-Annotated-Transcriptome. Additional GO enrichment analysis, using topGO (Alexa, Rahnenführer, and Lengauer 2006), was performed to identify categories significantly overrepresented in DMGs. Similarities between the methylation responses of group contrasts were evaluated by correlation of KOG delta-ranks

Gene expression data, as counts per sample/gene, was obtained from (Cunning and Baker 2020) (https://github.com/jrcunning/mcav_shuffle) and filtered to include only the samples for which DNA methylation data was generated here. The correlation between these datasets was tested with linear regression, including gene-body methylation mean (methylated/unmethylated CpGs), gene expression mean (log2-cpm) and its respective coefficient of variance (methCV and expressionCV). Variable

generation was based on code developed by (Downey-Wall et al. 2020) (https://github.com/epigeneticstoocean/AE17_Cvirginica_MolecularResponse).

Results

The DNA methylation landscape of M. cavernosa

Sequencing of 24 MBD-captured bisulfite libraries resulted in a total of ~800 million paired-end 150 bp-long reads (Pending NCBI data info, Supplementary Figure S1), among which ~779 million passed the quality filtering, and 192 million mapped to the genome of *M. cavernosa*. Across all samples, 9,993,450 CpG sites (~36% of 28,118,336 CpGs in the genome) passed error filtration (1% miss-called Cs) and 8,412,240 (~30% of all CpGs in the genome) had at least 5x coverage. Although mapping and coverage varied between samples, the patterns were not treatment-specific (Supplementary Figures S2).

All CpG sites, after error and coverage filtering, were used to characterize the general DNA methylation landscape (Fig. 1). As expected from the enrichment caused by the MBD method, most of the CpGs covered by sequencing were either methylated (5,226,176; 62.1%) or sparsely methylated (2,881,642; 34.3%) with only 304,422 (3.6%) being unmethylated (Gavery and Roberts 2013; Olson and Roberts 2014). The observed CpG-methylation level was dependent on genomic location ($p < 0.001$; Table S1), with introns and repetitive regions having proportionally higher methylated CpGs (>50% median methylation) compared to all CpGs in the genome (Fig. 1A, Table S1). Methylated CpGs overlapped primarily with intergenic regions (including repeats), with only ~30% overlapping with genic and flanking regions (Fig. 1A). Introns and exons, however, showed higher methylation levels (%) than intergenic regions (Fig. 1B).

DNA methylation response to symbiont shuffling and heat stress

Only CpG positions with >5x coverage that were present in at least 80% of samples per treatment were used for evaluating epigenetic changes caused by symbiont manipulation and/or thermal stress. Principal coordinate analysis (Fig. 2A) revealed that samples clustered primarily by genotype along the PC2 axis, with the effect of treatment groups somewhat evident across PC1, although the separation along this axis is not consistent between genotypes. Variance partitioning analysis (Fig. 2B) also confirmed that the effects of the symbiont manipulation and heat stress were not homogeneous across genotypes, with the effects of symbiont manipulations and thermal exposure contributing differently among colonies. Across all genotypes, however, most of the variance was explained by the interaction between symbiont and temperature, indicating variable methylation responses to heat stress in corals hosting different symbionts. Significant differences in global methylation (calculated as median methylation of all CpGs) due to thermal stress (F = 5.943, *p.value* = 0.0171), but not to symbiont manipulation (F = 0.572, *p.value* = 0.4519) or its interaction with thermal stress (F = 0.648, *p.value* = 0.4234) were observed using a two-way ANOVA, indicating that the loci specific response observed in the PCoA and variance partitioning, is not evident at a global methylation level.

The discriminant analysis of principal components (Fig. 2C for all CpGs; Supplementary Fig. S3 by feature) identified consistent differences in DNA methylation profiles corresponding to the experimental variables across genets. Along the first discriminant axis (LD1) corals hosting *Durusdinium*, towards the right, separate from those hosting *Cladocopium*, towards the left. Heat stress response was evident along the

second discriminant function (LD2), with control corals hosting *Durusdinium* separating from control corals hosting *Cladocopium* in the same direction of the heat stress response. Remarkably, *Durusdinium*-dominated corals exposed to thermal stress move very little along LD2 but separate from control along LD1. This pattern of methylation in response to symbiont change, resembling the *Cladocopium*-dominated corals thermal response, as well as the different DNA methylation response to temperature in corals hosting *Durusdinium*, was also evident across genomic features such as gene bodies, introns, intergenic regions, and transposable elements (Supplementary Fig. S3).

Overlapping between differential DNA methylation and genomic features

Regional changes in DNA methylation are more likely to affect genomic functioning than variation in individual CpGs. Consequently, DMRs were identified by combining differentially methylated cytosines (*methylpy* pipeline) across 250bp windows. DMRs (Table 1) were determined by either comparing samples from all four treatment combinations (*all*-DMR) or from each of the four individual treatment contrasts, such as symbiont shuffling under control temperature (D_C vs C_C), heat stress response for both symbiont types (C_H vs C_C, and D_H vs D_C), and the combination of both symbiont manipulation and temperature (D_H vs C_H). Symbiont manipulation produced the highest number of DMRs (80), but it was mostly contributed by the D_H vs C_H contrast with almost 10 times the number of DMR's produced by the D_C vs C_C contrast. Interestingly, *Cladocopium*-dominated corals heat-stress response involves almost three times more DMRs than that of *Durusdinium*-dominated, hinting a potential "milder" methylation response to heat-stress in corals hosting *Durusdinium*.

Heatmaps were used to illustrate methylation changes caused by symbiont manipulation and thermal exposure on significant DMRs (Fig 3A). Across all 206 significant DMRs responding to *symbiont*, *temperature* and *symbiont:temperature* interaction (Fig 3A), five distinctive clusters (*a* to *e*) were defined. DMRs in cluster *a* show DNA methylation changes that are responsive to both symbiont and temperature, with a reduction in methylation from control-corals hosting *Cladocopium* to both heated-corals hosting the same symbiont and control corals hosting *Durusdinium*. DNA methylation response to temperature of corals hosting *Durusdinium* show an opposite direction than that of *Cladocopium* dominated corals in this cluster, confirming a different response to stress in corals dominated by each symbiont. Clusters *b* and *d* comprise DMRs responding exclusively to symbiont manipulation but with opposite directions of methylation change. DMRs in cluster *c* show a shared methylation response to temperature for corals hosting both symbionts. In cluster *e*, DMRs show little change between control corals hosting both symbionts, but the demethylation response to heat stress is smaller in corals hosting *Durusdinium*. Overall, DNA methylation seems to be responding differently to symbiont manipulation and heat stress, with some evidence of a milder response to temperature in corals dominated by *Durusdinium* symbionts.

Significant DMRs in all clusters mostly overlap with intergenic regions, although gene bodies of 68 genes were represented (Table S2). DMRs in each cluster showed dependence on genomic regions. Intergenic regions were enriched in DMRs for cluster *c* (chi square *p*.value < 0.1), while repetitive regions were significantly overrepresented in cluster *d* (chi square *p*.value <0.0001; Fig. 3B). Intronic regions were overrepresented in cluster *e*, but this enrichment was not significant. These marked differences in DMRs

localization also support a differential response to symbiont manipulation and thermal stress.

DNA methylation and expression of repetitive regions

Given the observed prevalence of methylated positions across repetitive regions and the significant representation of these genomic elements in DMRs, a more detailed analysis of DNA methylation distribution and variation across these features was performed, as well as the evaluation of their expression. No significant change in global methylation density or expression was observed between treatment combinations when all repeat types were combined (Fig. 4). However, significant changes in the expression of long terminal repeats (LTR; Fig 4B) were observed for both thermal stress contrasts [*Ch vs Cc* (t-test: *p*.value = 0.0238); *Dh vs Dc* (t-test: *p*.value = 0.0169)]. Although methylation density in these repeats showed a similar trend (Fig 4A), these changes were not significant. However, DMRs overlapping with repeats showed a significant proportional enrichment in LTR for both *Dc vs Cc* (prop_test; *p*.value = 0.0360) and *Dh vs Ch* (prop_test; *p*.value < 0.0001). Combined, these results are indicative that DNA methylation in repetitive regions is responsive to environmental change, and that transposable elements are activated under thermal stress.

Gene body methylation and functional enrichment

Gene methylation information was obtained for 1040 genes represented across all groups and covered by at least 3 CpGs. Differentially methylated genes (DMGs) were determined through a binomial generalized linear model with *symbiont type*, *temperature,*

and the interaction as levels, and also as 1v1 comparisons for the contrasts described before. Across all 430 DMGs obtained, there was a significant reduction in global DNA methylation between control and heated *Cladocopium*-dominated corals (t-test, $p.adj_{BH}$= 0.047; Fig 5A) and a non-significant increase in control corals hosting *Durusdinium* when compared with *Cladocopium* dominated controls (t-test, $p.adj_{BH}$= 0.912). There was also a slight reduction in global DNA methylation in response to temperature for *Durusdinium*-dominated corals, but it was not significant (t-test, $p.adj_{BH}$= 0.486). The contrast D_H vs C_H produced the largest number of DMGs (286, Fig 5D) while D_H vs D_C produced less than half of all other contrasts (106 DMGs). Comparisons including different symbionts (D_C vs C_C and D_H vs C_H) shared 130 DMGs, while only 62 were shared between temperature contrasts for both symbionts (C_H vs C_C and D_H vs D_C). Overall, these results suggest that corals hosting *Durusdinium* respond to thermal stress with substantially less and different methylation changes than those of *Cladocopium*-hosting corals.

Functional enrichment analysis of DMGs identified 34 overrepresented GO terms across significant DMGs in all contrasts (Table 2). However, GO_MWU analysis using all 1040 genes with methylation data available, did not find any GO significantly hypo- or hyper-methylated for any of the treatment groups. Similarly, KOG_MWU analysis showed no significantly hypo- or hyper-methylated category across contrasts (Fig. S4A). KOG delta ranks (Fig. S4B), however, were significantly correlated between the symbiont shuffling contrast (D_C vs C_C) and the responses to heat stress of both, *Cladocopium*-dominated corals (C_H vs C_C; R = -0.74, CI95% [-0.47, -0.89]) and *Durusdinium*-dominated corals (*(*D_H vs D_C; R = 0.61, CI95% [0.25, 0.81]) but in opposite

directions. No correlation was observed between the heat stress responses of both symbionts. Similar to the case of individual genes, results from DMGs support that DNA methylation responses to heat stress are dependent on the dominant symbiont.

Interaction between DNA methylation and gene expression.

Using a gene expression dataset previously produced for the same set of samples (Cunning and Baker 2020), hypotheses were tested about the correlation between DNA methylation and gene expression. No linear correlation was observed between mean gene-body methylation and gene expression for control corals ($R^2 = 0.0019$, *p*.value = 0.348, Fig. 5B). DNA methylation, however, did show a marginally significant (for $a = 0.1$) negative correlation with gene expression CV ($R^2 = 0.0066$, *p*.value = 0.0766, Fig. 5C), hinting a decrease in DNA methylation in genes with more variable expression. Finally, the association between the responses of DNA methylation and gene expression to the symbiont and temperature manipulations was also evaluated using linear regression (Fig. S5). Again, no significant correlation was observed for any of the contrasts, neither for all covered genes nor for DMGs only, in correspondence with the lack of shared DMGs/DEGs (i.e., differentially expressed genes) found for all contrasts (Fig. 5D). Overall, these results are consistent with a DNA methylation response to experimental manipulations, showing certain similarities to the transcriptome, although lacking evidence of a direct association between gene expression and DNA methylation at the gene level.

Discussion

This work constitutes the first evaluation of the epigenetic responses to symbiont manipulations in stony corals, and the first description of the DNA methylation landscape of the great star coral *M. cavernosa*, including its response to heat stress. The complementarity between the datasets developed in this work and the transcriptional plasticity data developed by Cunning and Baker (2020), allowed the analysis of the interactions between gene expression and DNA methylation in response to symbiont manipulations and thermal stress. Differential DNA methylation in response to both symbiont and temperature manipulations was identified at single nucleotide, region, and gene levels, following a global pattern similar to that observed in the transcriptional response (Cunning and Baker 2020). Both differentially methylated regions and genes (DMRs and DMGs) indicate a divergent response to heat stress for corals dominated by *Cladocopium* or *Durusdinium* symbionts. However, no clear evidence of direct interaction between gene body methylation (gbM) and expression was observed, and only inconclusive evidence supporting a role of DNA methylation in decreasing spurious transcription was found.

The DNA methylation landscape of M. cavernosa depicts a relatively stress resistant coral

About 19% of all CpGs in the genome of *M. cavernosa* were methylated and primarily located in intergenic regions (>60% for all CpGs and methylated CpGs). This is comparable with the DNA methylation levels observed in other marine invertebrates (Gavery and Roberts 2013; Venkataraman et al. 2020; Strader, Kozal, and Leach 2020),

including the relatively stress resistant corals *Porites astreoides* (Dimond and Roberts 2020) and *Montipora capitata* (Dr. Hollie Putnam, unpublished data). Remarkably, methylation levels are significantly higher than those reported for the cnidarian model *Aiptasia* sp. [6.7%; (Li et al. 2018)], the stress-sensitive coral *Stylophora pistillata* [7%, (Liew et al. 2018)], and other corals of the robust clade like *Pocillopora damicornis* (<10%; Dr. H. Putnam, unpublished data) and *Acropora cervicornis* (<10%; J. A. Rodriguez-Casariego, unpublished data).

Methylated CpGs in *M. cavernosa* significantly concentrate in introns and transposable elements (on both genic and intergenic regions) when compared to the global distribution of CpGs in the genome. While gene-body methylation is characteristic of invertebrates (Gavery and Roberts 2013; Feng et al. 2010), including corals (Dixon et al. 2018; Liew et al. 2018), the presence of similar DNA methylation levels in intergenic regions and transposable elements represents a new evidence never observed before in corals. An increased DNA methylation of transposable elements has been previously observed in plants (Cantu et al. 2010), mammals (Jansz 2019) and other invertebrates (Venkataraman et al. 2020), and has been attributed to the defense role of DNA methylation by selectively inhibiting mobile elements in the genome (Choi et al. 2020). It thus may be plausible that, also in the case of corals, DNA methylation participates in the regulation of mobile element activity in the genome, potentially generating new genetic combinations. Lastly, Exons displayed higher methylation levels and lower methylation variability than introns and intergenic regions. This aligns with DNA methylation patterns observed in other invertebrates (Lyko et al. 2010; Downey-Wall et al. 2020), and could be related with a role of this epigenetic mechanism in the regulation of differential

splicing (Lyko et al. 2010; Flores et al. 2012). Nonetheless, since other studies have described higher DNA methylation levels in the introns of the coral *S. pistillata* (Liew et al. 2018), further studies will be required in order to fully elucidate the linkages between DNA methylation and genome metabolism.

Symbiont manipulation and thermal stress produce distinctive DNA methylation responses

Symbiont manipulation and thermal stress triggered particular environmentally responsive changes in the methylome of *M. cavernosa*, suggesting the existence of distinctive responses for the different types of manipulations used in the present work. Estimates of global DNA methylation levels, however, failed to detect differences between treatment groups, consistent with previous reports suggesting that this approach provides a poor descriptor of environmental responsiveness in corals [i.e., "seesaw" patterns with increases and decreases in DNA methylation canceling each other to produce invariant values (Dixon et al. 2018; Dimond and Roberts 2020)]. This is further supported by the identification of DMRs and DMGs between symbiont compositions and thermal treatments reported in the present work, suggesting significant differences in DNA methylation.

The present work evidences a genet- and treatment-specific DNA methylation response that is influenced by the coral genotype, in agreement with previous studies in other scleractinian species (Liew et al. 2018; Durante et al. 2019; Rodríguez-Casariego et al. 2020). In this case, genets also responded differently to symbiont and temperature manipulations. However, across all genets, a clear treatment-specific response and

symbiont-driven heat stress pattern was indicated by ordination analyses and variance partitioning. Given that symbiont shuffling was achieved by thermal bleaching, there is a possibility that the observed differences between symbionts are due to that previous bleaching and not the effect of the symbiont identity. In their study, Cunning and Baker (2020) discarded carry-over effects by analyzing the transcriptome of corals that bleached and recovered with the native symbiont before being subject to heat-stress. Since that analysis was not possible in the present work, the contribution of DNA methylation changes maintained through epigenetic memory cannot be fully neglected. However, the differences between the genomic location of DNA methylation changes resulting from symbiont manipulation (at repetitive elements and intergenic regions) from those triggered by thermal treatments [at introns and putative promoters, (Liew et al. 2018; Dixon et al. 2018)]. strongly suggest that symbiont manipulation shapes the coral DNA methylome in ways yet to be known. Overall, it is evident that shifts in symbiont dominance from *Cladocopium* to *Durusdinium* drive DNA methylation changes influencing subsequent responses to thermal stress, in agreement with the transcriptomic (Cunning and Baker 2020) and phenotypic features (i.e., thermal resistance) conferred to corals by this shift (Silverstein, Cunning, and Baker 2015).

Gene body DNA methylation does not correlate with gene expression.

Epigenetic modifications play a central role in phenotypic plasticity during environmental responses (Eirin-Lopez and Putnam 2019). However, the underpinnings of how epigenetic mechanisms convey environmental signals to the genome and the resulting shaping of its function is still uncertain, especially in the case of non-model

organisms (Eirin-Lopez and Putnam 2019). Accordingly, invertebrate genomes are significantly less methylated than vertebrate genomes, with DNA methylation accumulating in gene bodies in the former as opposed to promoters in the latter (Gavery and Roberts 2013; Dixon, Bay, and Matz 2016). Such differences have generated multiple hypotheses describing the role of gene body methylation regulating gene expression (Duncan, Gluckman, and Dearden 2014). In cnidarians, the hypothesis most widely supported is the reduction of spurious transcription through the blocking of intragenomic initiation positions (Roberts and Gavery 2012; Dixon et al. 2018; Li et al. 2018). The results obtained in the present work provide additional support to this hypothesis, based on the higher levels of methylation detected in *M. cavernosa* genes displaying less variable transcription. However, the links between differentially methylated genes and changes in gene expression remained elusive, with significant changes in gene-body methylation occurring in genes with no differential expression regardless of the similarities of the global responses of both mechanisms to the experimental manipulations.

The present work found a significant accumulation of DMRs in transposable elements (TEs, including repetitive regions), consistent with the proposed role of DNA methylation mediating TE transcriptional silencing (Feschotte, Jiang, and Wessler 2002; Choi et al. 2020). Remarkably, the expression of LTRs [retrotransposons linked to transcriptional regulation in plants (Jia et al. 2014)], was significantly different between thermal treatments regardless of the dominant symbiont. Based on these results, it is tempting to hypothesize a link between DNA methylation and the regulation of repetitive regions, constituting a very attractive direction for future analyses.

Conclusions

The present work provides evidence suggesting that DNA methylation plays an important role mediating the interaction between holobiont composition and phenotypic responses in the coral *M. cavernosa*. Importantly, such a role does not seem to involve a direct influence (at least necessarily) on gene expression regulation. Both symbiont manipulation and heat stress elicited DNA methylation responses that were not homogeneous across genotypes, but consistently showed a treatment-specific pattern. DNA methylation response to heat stress was dependent on the dominant symbiont, with twice as many significant DMRs found between heated corals hosting different symbionts (D_H vs C_H contrast). Similar to the transcriptional response of *M. cavernosa* to these manipulations (Cunning and Baker 2020), *Durusdinium*-dominated corals displayed a potentially "milder" DNA methylation response to thermal stress. On the other hand, no evidence of a direct association between gene expression and DNA methylation at the gene level was found, other than the previously described reduction of transcriptional variability on highly methylated genes (Liew et al. 2018; Li et al. 2018). Remarkably, our analyses showed significant accumulation of methylated and differentially methylated loci in transposable elements. Given the activation of some of these elements in response to heat stress, the obtained results could provide new research avenues to link DNA methylation with transcriptional and phenotypic plasticity involving the regulation of repetitive regions in the genome.

References

Alexa, Adrian, Jörg Rahnenführer, and Thomas Lengauer. 2006. "Improved Scoring of Functional Groups from Gene Expression Data by Decorrelating GO Graph Structure." *Bioinformatics* 22 (13): 1600–1607.

Åsman, Anna K. M., Johan Fogelqvist, Ramesh R. Vetukuri, and Christina Dixelius. 2016. "Phytophthora Infestans Argonaute 1 Binds microRNA and Small RNAs from Effector Genes and Transposable Elements." *The New Phytologist* 211 (3): 993–1007.

Baker, Andrew C. 2004. "Symbiont Diversity on Coral Reefs and Its Relationship to Bleaching Resistance and Resilience." *Coral Health and Disease*. https://doi.org/10.1007/978-3-662-06414-6_8.

Baker, Andrew C., and Ross Cunning. 2015. "Coral 'bleaching' as a Generalized Stress Response to Environmental Disturbance." *Diseases of Coral*, 396–409.

Barfield, Sarah J., Galina V. Aglyamova, Line K. Bay, and Mikhail V. Matz. 2018. "Contrasting Effects of Symbiodinium Identity on Coral Host Transcriptional Profiles across Latitudes." *Molecular Ecology* 27 (15): 3103–15.

Barshis, Daniel J. 2015. "Genomic Potential for Coral Survival of Climate Change." *Coral Reefs in the Anthropocene*. https://doi.org/10.1007/978-94-017-7249-5_7.

Berkelmans, Ray, and Madeleine J. H. van Oppen. 2006. "The Role of Zooxanthellae in the Thermal Tolerance of Corals: A 'nugget of Hope' for Coral Reefs in an Era of Climate Change." *Proceedings of the Royal Society B: Biological Sciences*. https://doi.org/10.1098/rspb.2006.3567.

Bourc'his, Déborah, and Timothy H. Bestor. 2004. "Meiotic Catastrophe and Retrotransposon Reactivation in Male Germ Cells Lacking Dnmt3L." *Nature* 431 (7004): 96–99.

Cantu, Dario, Leonardo S. Vanzetti, Adam Sumner, Martin Dubcovsky, Marta Matvienko, Assaf Distelfeld, Richard W. Michelmore, and Jorge Dubcovsky. 2010. "Small RNAs, DNA Methylation and Transposable Elements in Wheat." *BMC Genomics* 11 (June): 408.

Cavalli, Giacomo, and Edith Heard. 2019. "Advances in Epigenetics Link Genetics to the Environment and Disease." *Nature* 571 (7766): 489–99.

Choi, Jaemyung, David B. Lyons, M. Yvonne Kim, Jonathan D. Moore, and Daniel Zilberman. 2020. "DNA Methylation and Histone H1 Jointly Repress Transposable Elements and Aberrant Intragenic Transcripts." *Molecular Cell* 77 (2): 310–23.e7.

Cunning, R., P. Gillette, T. Capo, K. Galvez, and A. C. Baker. 2015. "Growth Tradeoffs Associated with Thermotolerant Symbionts in the Coral Pocillopora Damicornis Are Lost in Warmer Oceans." *Coral Reefs* 34 (1): 155–60.

Cunning, Ross, and Andrew C. Baker. 2013. "Excess Algal Symbionts Increase the Susceptibility of Reef Corals to Bleaching." *Nature Climate Change* 3 (3): 259–62.

———. 2020. "Thermotolerant Coral Symbionts Modulate Heat Stress-responsive Genes in Their Hosts." *Molecular Ecology*. https://doi.org/10.1111/mec.15526.

DeSalvo, M. K., S. Sunagawa, P. L. Fisher, C. R. Voolstra, R. Iglesias-Prieto, and M. Medina. 2010. "Coral Host Transcriptomic States Are Correlated with Symbiodinium Genotypes." *Molecular Ecology* 19 (6): 1174–86.

Dimond, James L., and Steven B. Roberts. 2020. "Convergence of DNA Methylation Profiles of the Reef Coral Porites Astreoides in a Novel Environment." *Frontiers in Marine Science* 6: 792.

Dixon, Groves B., Line K. Bay, and Mikhail V. Matz. 2016. "Evolutionary Consequences of DNA Methylation in a Basal Metazoan." *Molecular Biology and Evolution* 33 (9): 2285–93.

Dixon, Groves, Yi Liao, Line K. Bay, and Mikhail V. Matz. 2018. "Role of Gene Body Methylation in Acclimatization and Adaptation in a Basal Metazoan." *Proceedings of the National Academy of Sciences of the United States of America* 115 (52): 13342–46.

Downey-Wall, Alan M., Louise P. Cameron, Brett M. Ford, Elise M. McNally, Yaamini R. Venkataraman, Steven B. Roberts, Justin B. Ries, and Katie E. Lotterhos. 2020. "Ocean Acidification Induces Subtle Shifts in Gene Expression and DNA Methylation in Mantle Tissue of the Eastern Oyster (Crassostrea Virginica)." *Frontiers in Marine Science* 7: 828.

Duncan, Elizabeth J., Peter D. Gluckman, and Peter K. Dearden. 2014. "Epigenetics, Plasticity, and Evolution: How Do We Link Epigenetic Change to Phenotype?" *Journal of Experimental Zoology. Part B, Molecular and Developmental Evolution* 322 (4): 208–20.

Eirin-Lopez, Jose M., and Hollie M. Putnam. 2019. "Marine Environmental Epigenetics." *Annual Review of Marine Science* 11 (January): 335–68.

Feng, Suhua, Shawn J. Cokus, Xiaoyu Zhang, Pao-Yang Chen, Magnolia Bostick, Mary G. Goll, Jonathan Hetzel, et al. 2010. "Conservation and Divergence of Methylation Patterning in Plants and Animals." *Proceedings of the National Academy of Sciences of the United States of America* 107 (19): 8689–94.

Feschotte, Cédric, Ning Jiang, and Susan R. Wessler. 2002. “Plant Transposable Elements: Where Genetics Meets Genomics.” *Nature Reviews. Genetics* 3 (5): 329–41.

Gavery, Mackenzie R., and Steven B. Roberts. 2013. “Predominant Intragenic Methylation Is Associated with Gene Expression Characteristics in a Bivalve Mollusc.” *PeerJ* 1 (November): e215.

He, Jiangping, Xiuling Fu, Meng Zhang, Fangfang He, Wenjuan Li, Mazid Md Abdul, Jianguo Zhou, et al. 2019. “Transposable Elements Are Regulated by Context-Specific Patterns of Chromatin Marks in Mouse Embryonic Stem Cells.” *Nature Communications* 10 (1): 34.

Helmkampf, Martin, M. Renee Bellinger, Monika Frazier, and Misaki Takabayashi. 2019. “Symbiont Type and Environmental Factors Affect Transcriptome-Wide Gene Expression in the Coral Montipora Capitata.” *Ecology and Evolution* 9 (1): 378–92.

Hoffman, Gabriel E., and Eric E. Schadt. 2016. “variancePartition: Interpreting Drivers of Variation in Complex Gene Expression Studies.” *BMC Bioinformatics* 17 (1): 483.

Hughes, Terry P., James T. Kerry, Mariana Álvarez-Noriega, Jorge G. Álvarez-Romero, Kristen D. Anderson, Andrew H. Baird, Russell C. Babcock, et al. 2017. “Global Warming and Recurrent Mass Bleaching of Corals.” *Nature* 543 (7645): 373–77.

Jansz, Natasha. 2019. “DNA Methylation Dynamics at Transposable Elements in Mammals.” *Essays in Biochemistry* 63 (6): 677–89.

Jombart, Thibaut, Sébastien Devillard, and François Balloux. 2010. “Discriminant Analysis of Principal Components: A New Method for the Analysis of Genetically Structured Populations.” *BMC Genetics* 11 (October): 94.

Kim, Daehwan, B. Langmead, and S. L. Salzberg. 2015. “hisat2.” *Nature Methods* 944.

Liew, Yi Jin, Didier Zoccola, Yong Li, Eric Tambutté, Alexander A. Venn, Craig T. Michell, Guoxin Cui, et al. 2018. “Epigenome-Associated Phenotypic Acclimatization to Ocean Acidification in a Reef-Building Coral.” *Science Advances* 4 (6): eaar8028.

Li, Heng, Bob Handsaker, Alec Wysoker, Tim Fennell, Jue Ruan, Nils Homer, Gabor Marth, Goncalo Abecasis, Richard Durbin, and 1000 Genome Project Data Processing Subgroup. 2009. “The Sequence Alignment/Map Format and SAMtools.” *Bioinformatics* 25 (16): 2078–79.

Li, Yong, Yi Jin Liew, Guoxin Cui, Maha J. Cziesielski, Noura Zahran, Craig T. Michell, Christian R. Voolstra, and Manuel Aranda. 2018. "DNA Methylation Regulates Transcriptional Homeostasis of Algal Endosymbiosis in the Coral Model Aiptasia." *Science Advances* 4 (8): eaat2142.

Lyko, Frank, Sylvain Foret, Robert Kucharski, Stephan Wolf, Cassandra Falckenhayn, and Ryszard Maleszka. 2010. "The Honey Bee Epigenomes: Differential Methylation of Brain DNA in Queens and Workers." *PLoS Biology* 8 (11): e1000506.

Matz, M. V. 2016. "KOGMWU: Functional Summary and Meta-Analysis of Gene Expression Data." *R Package Version* 1.

McGinnis, W., A. W. Shermoen, and S. K. Beckendorf. 1983. "A Transposable Element Inserted Just 5' to a Drosophila Glue Protein Gene Alters Gene Expression and Chromatin Structure." *Cell* 34 (1): 75–84.

National Academies of Sciences, Engineering, and Medicine, Division on Earth and Life Studies, Board on Life Sciences, Ocean Studies Board, and Committee on Interventions to Increase the Resilience of Coral Reefs. 2019. *A Research Review of Interventions to Increase the Persistence and Resilience of Coral Reefs*. National Academies Press.

Olson, Claire E., and Steven B. Roberts. 2014. "Genome-Wide Profiling of DNA Methylation and Gene Expression in Crassostrea Gigas Male Gametes." *Frontiers in Physiology* 5 (June): 224.

Pandolfi, John M., Roger H. Bradbury, Enric Sala, Terence P. Hughes, Karen A. Bjorndal, Richard G. Cooke, Deborah McArdle, et al. 2003. "Global Trajectories of the Long-Term Decline of Coral Reef Ecosystems." *Science* 301 (5635): 955–58.

Pettay, D. Tye, Drew C. Wham, Robin T. Smith, Roberto Iglesias-Prieto, and Todd C. LaJeunesse. 2015. "Microbial Invasion of the Caribbean by an Indo-Pacific Coral Zooxanthella." *Proceedings of the National Academy of Sciences of the United States of America* 112 (24): 7513–18.

Putnam, Hollie M., Jennifer M. Davidson, and Ruth D. Gates. 2016. "Ocean Acidification Influences Host DNA Methylation and Phenotypic Plasticity in Environmentally Susceptible Corals." *Evolutionary Applications*. https://doi.org/10.1111/eva.12408.

Quigley, K. M., A. C. Baker, M. A. Coffroth, B. L. Willis, and M. J. H. van Oppen. 2018. "Bleaching Resistance and the Role of Algal Endosymbionts." *Ecological Studies*. https://doi.org/10.1007/978-3-319-75393-5_6.

Roberts, Steven B., and Mackenzie R. Gavery. 2012. "Is There a Relationship between DNA Methylation and Phenotypic Plasticity in Invertebrates?" *Frontiers in Physiology* 2. https://doi.org/10.3389/fphys.2011.00116.

Rodriguez-Casariego, Javier A., Mark C. Ladd, Andrew A. Shantz, Christian Lopes, Manjinder S. Cheema, Bohyun Kim, Steven B. Roberts, et al. 2018. "Coral Epigenetic Responses to Nutrient Stress: Histone H2A.X Phosphorylation Dynamics and DNA Methylation in the Staghorn Coral Acropora Cervicornis." *Ecology and Evolution* 8 (23): 12193–207.

Rodríguez-Casariego, Javier A., Alex E. Mercado-Molina, Daniel Garcia-Souto, Ivanna M. Ortiz-Rivera, Christian Lopes, Iliana B. Baums, Alberto M. Sabat, and Jose M. Eirin-Lopez. 2020. "Genome-Wide DNA Methylation Analysis Reveals a Conserved Epigenetic Response to Seasonal Environmental Variation in the Staghorn Coral Acropora Cervicornis." *Frontiers in Marine Science* 7: 822.

Schultz, Matthew D., Yupeng He, John W. Whitaker, Manoj Hariharan, Eran A. Mukamel, Danny Leung, Nisha Rajagopal, et al. 2015. "Human Body Epigenome Maps Reveal Noncanonical DNA Methylation Variation." *Nature*. https://doi.org/10.1038/nature14465.

Silverstein, Rachel N., Ross Cunning, and Andrew C. Baker. 2015. "Change in Algal Symbiont Communities after Bleaching, Not Prior Heat Exposure, Increases Heat Tolerance of Reef Corals." *Global Change Biology*. https://doi.org/10.1111/gcb.12706.

Slotkin, R. Keith, and Robert Martienssen. 2007. "Transposable Elements and the Epigenetic Regulation of the Genome." *Nature Reviews. Genetics* 8 (4): 272–85.

Strader, M. E., L. C. Kozal, and T. S. Leach. 2020. "Examining the Role of DNA Methylation in Transcriptomic Plasticity of Early Stage Sea Urchins: Developmental and Maternal Effects in a Kelp Forest Herbivore." *Frontiers in Marine Science* 7:205.

Swain, Timothy D., Simon Lax, Vadim Backman, and Luisa A. Marcelino. 2020. "Uncovering the Role of Symbiodiniaceae Assemblage Composition and Abundance in Coral Bleaching Response by Minimizing Sampling and Evolutionary Biases." *BMC Microbiology* 20 (1): 124.

Tompa, Rachel, Claire M. McCallum, Jeffrey Delrow, Jorja G. Henikoff, Bas van Steensel, and Steven Henikoff. 2002. "Genome-Wide Profiling of DNA Methylation Reveals Transposon Targets of CHROMOMETHYLASE3." *Current Biology: CB* 12 (1): 65–68.

Tran, Robert K., Daniel Zilberman, Cecilia de Bustos, Renata F. Ditt, Jorja G. Henikoff, Anders M. Lindroth, Jeffrey Delrow, et al. 2005. "Chromatin and siRNA Pathways Cooperate to Maintain DNA Methylation of Small Transposable Elements in Arabidopsis." *Genome Biology* 6 (11): R90.

Venkataraman, Yaamini R., Alan M. Downey-Wall, Justin Ries, Isaac Westfield, Samuel J. White, Steven B. Roberts, and Kathleen E. Lotterhos. 2020. "General DNA Methylation Patterns and Environmentally-Induced Differential Methylation in the Eastern Oyster (Crassostrea Virginica)." *Frontiers in Marine Science* 7: 225.

Weis, Virginia M. 2008. "Cellular Mechanisms of Cnidarian Bleaching: Stress Causes the Collapse of Symbiosis." *The Journal of Experimental Biology* 211 (Pt 19): 3059–66.

Wright, Rachel M., Galina V. Aglyamova, Eli Meyer, and Mikhail V. Matz. 2015. "Gene Expression Associated with White Syndromes in a Reef Building Coral, Acropora Hyacinthus." *BMC Genomics* 16 (May): 371.

Yuyama, Ikuko, Masakazu Ishikawa, Masafumi Nozawa, Masa-Aki Yoshida, and Kazuho Ikeo. 2018. "Transcriptomic Changes with Increasing Algal Symbiont Reveal the Detailed Process Underlying Establishment of Coral-Algal Symbiosis." *Scientific Reports* 8 (1): 16802.

Zhang, Zhongge, and Milton H. Saier Jr. 2009. "A Novel Mechanism of Transposon-Mediated Gene Activation." *PLoS Genetics* 5 (10): e1000689.

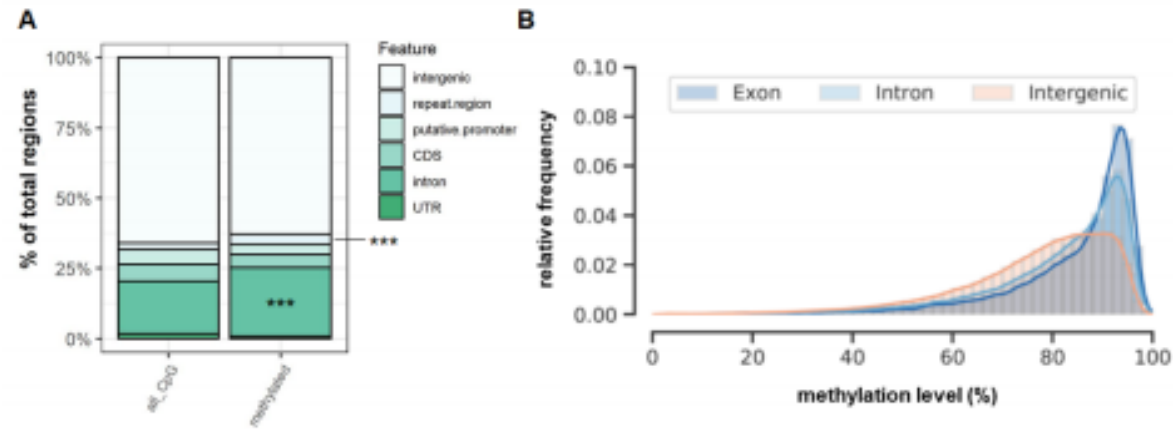

Fig. 1. DNA methylation characteristics of *M. cavernosa*. **(A)** CpG overlap with genomic features: "all_CpG" refers to all positions in the genome of *M. cavernosa* regardless of their methylation status; "methylated" refers to CpG showing over 50% median methylation. Significant interaction between methylation and features was obtained (p.value < 2.2e-16). Significant proportional enrichment is represented with asterisks (*** represents $p < 0.001$, see Table S1 for details). **(B)** Distribution of DNA methylation levels (% methylation) in exons, introns, and intergenic regions.

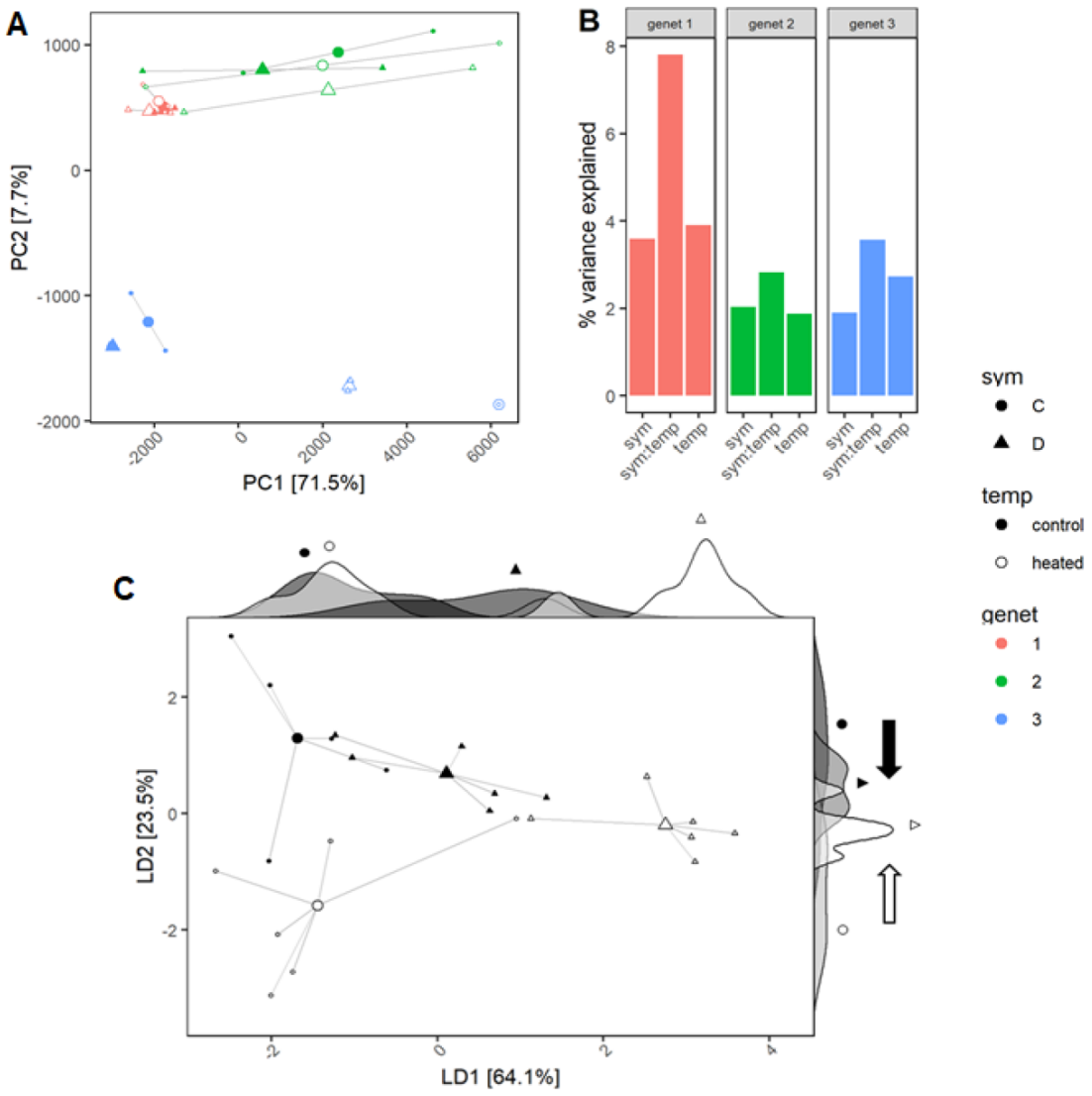

Fig. 2. DNA methylation variation in *M. cavernosa* corals (N=3 genets) manipulated to host different symbionts (sym) and then exposed to thermal stress (temp). **(A)** Principal coordinate analysis of percent DNA methylation at single CpGs (>5x coverage) shared by all samples after variance-stabilization (n = 22,953 loci). **(B)** Sources of variance in DNA methylation calculated as a percentage of the total variance within each coral genet. **(C)** Discriminant analysis of principal components (DAPC) of single CpG methylation profiles. Density plots showing the distribution of samples across each discriminant function (LD1 and LD2) are shown across the top and left of the figure. Arrows illustrate the different position of corals dominated by *Durusdinium* symbionts compared with those dominated by *Cladocopium* of the same thermal treatment. C refers to native

symbionts in the genus *Cladocopium* and D refers to manipulated symbionts (*D. trenchii*). Small symbols represent coral samples and larger symbols represent centroids of two replicates.

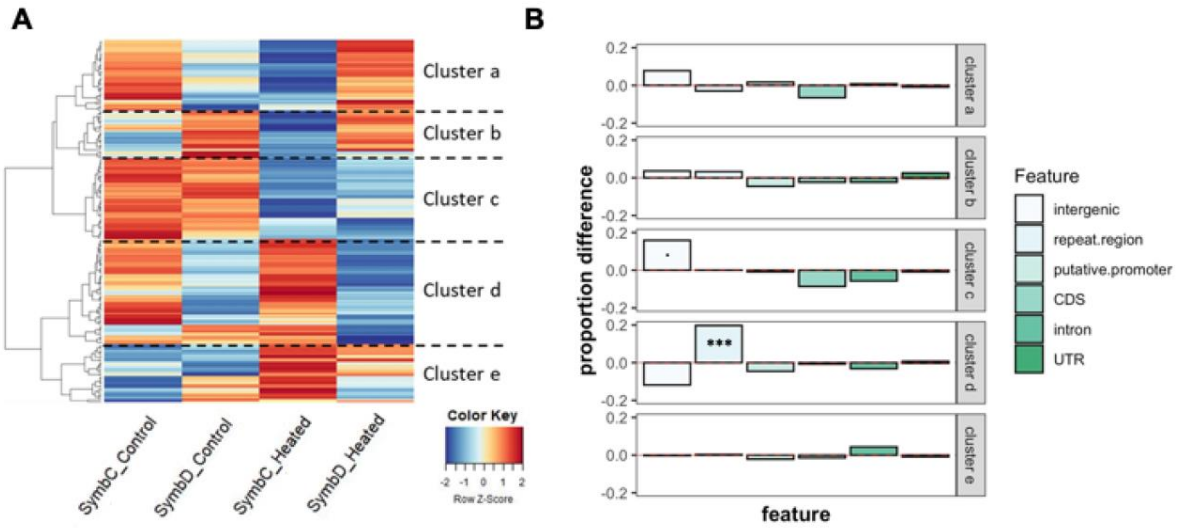

Fig 3. DNA methylation across differentially methylated regions (DMRs). **(A)** Heatmap of DNA methylation variation (as deviation from the mean; z-score) of significant DMRs for all experimental contrasts. Clusters represent groups of DMRs with similar patterns of methylation change. **(B)** Genomic features overlapping with DMRs and differences between proportions of CpGs overlapping with each feature within each DMR and through all the regions analyzed. Significance of a chi-square proportion test are represented for enriched regions (· = p.adj < 0.1; * = p.adj < 0.05; ** = p.adj < 0.001; *** = p.adj < 0.0001)

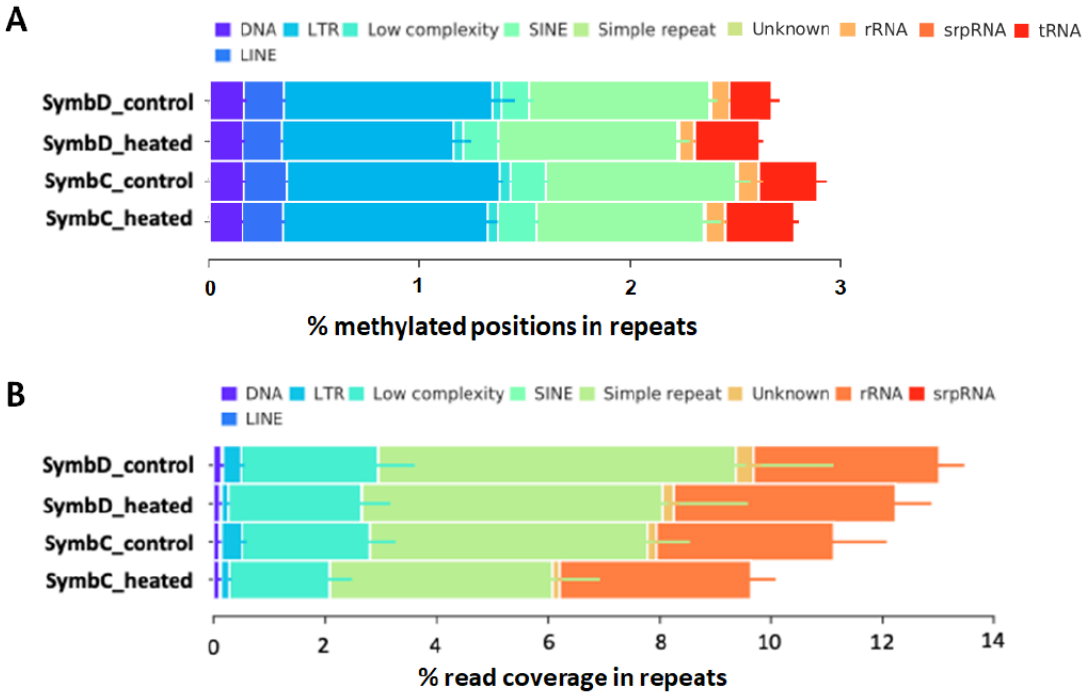

Fig. 4 Transposable elements methylation and expression by treatment combination **(A)** Density of methylated positions in repeat region types by treatment combination **(B)** Expression of repeat elements for each of the treatment combinations. Error bars denote 1 SE. DNA: DNA transposons; LINE: long interspersed nuclear elements; LTR: long terminal repeat; SINE: short interspersed nuclear elements; srpRNA: signal recognition particle RNA.

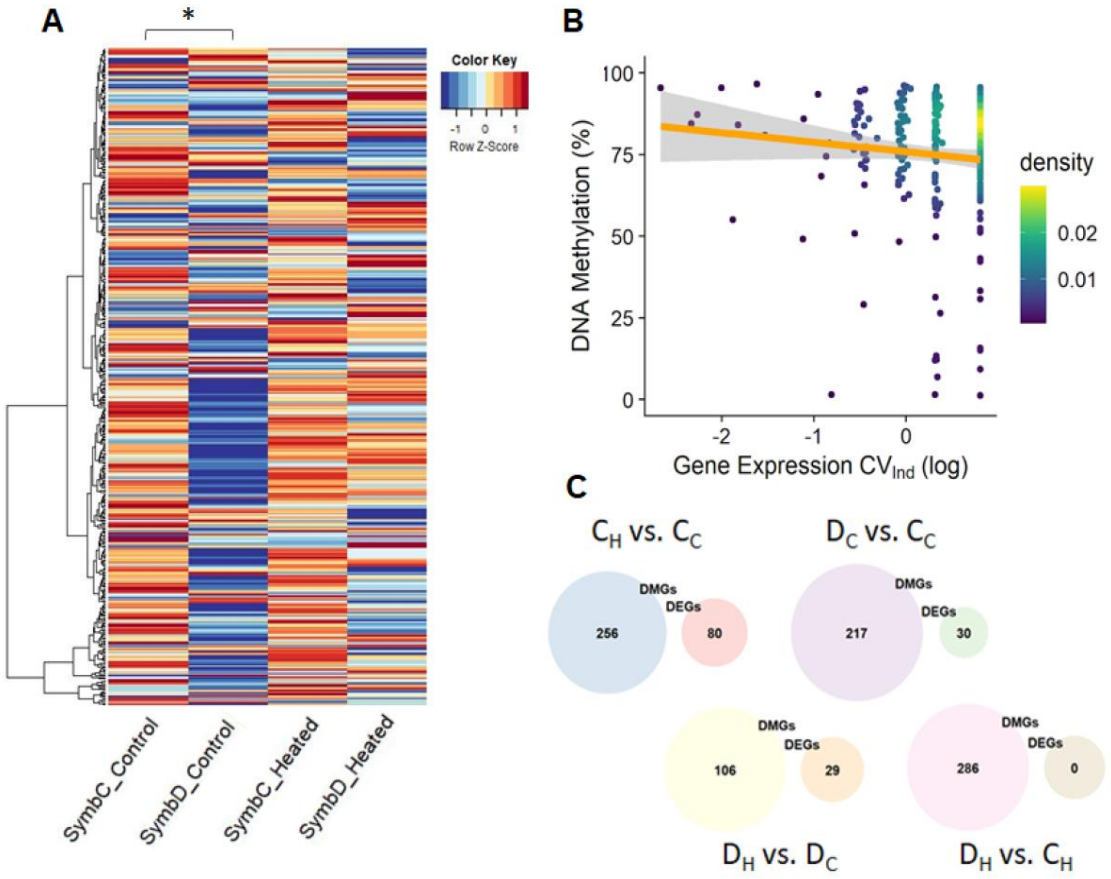

Fig. 5 Differentially methylated genes (DMGs) and correlation with gene expression. **A.** Heatmap representing methylation changes for all significant DMGs across all treatments. (*) represent significant differences (p.adj = 0.0429) in total gene-body methylation mean evaluated through pairwise t-test with Benjamini-Hochberg correction. **B.** represents the level of gene DNA methylation compared with gene expression CV across individuals in the control-*Cladocopium* group. DNA methylation was not significantly correlated with gene expression (R2 = 0.0053, p.value = 0.3265), but it was marginally significantly correlated with Gene Expression CVind (R2 = 0.0219, p.value < 0.0441). Given the low coverage (Supplementary Fig. S2) no filter was applied and n=185 genes were included. **C.** Venn diagram comparing differentially methylated genes (DMG) and differentially expressed genes (DEG, data obtained from Cunning and Baker, 2020) for each of the contrasts between experimental groups (Ch = *Cladocopium*/heated, Cc = *Cladocopium*/control, Dh = *Durusdinium*/heated, Dc = *Durusdinium*/control).

Table 1. Differentially methylated regions (DMRs) for general model output and across treatment contrasts. Total significant DMRs [hypermethylated, hypomethylated] are represented for contrasts.

Contrast	**all**	**sig_symb**	**sig_temp**	**sig_inter**
all-DMRs	34,419	80	68	62
$D_C C_C$-DMRs	15,598	15 [6, 9]		
$C_H C_C$-DMRs	17,000		73 [30, 43]	
$D_H D_C$-DMRs	18,353		26 [8, 18]	
$D_H C_H$-DMRs	21,585	132 [73, 59]		

Table 2. Gene ontology (GO) categories overrepresented in differentially methylated genes (DMGs)

Contrast	Ontology	Genes	GO term	*p*.value
Cc.vs.Ch	BP	3/3	endoplasmic reticulum to Golgi vesicle-mediated transport	0.0178
	BP	4/6	ion transport	0.0327
	BP	4/6	**Golgi organization**	0.0378
	BP	3/4	autophagosome assembly	0.0462
	MF	5/8	**RNA-directed DNA polymerase activity**	0.0246
	MF	3/4	ARF guanyl-nucleotide exchange factor activity	0.0474
Cc.vs.Dc	BP	4/4	positive regulation of I-kappaB kinase/NF-kappaB signaling	0.0022
	BP	5/10	apoptotic process	0.0391
	BP	4/7	actin cytoskeleton organization	0.0430
	BP	2/2	histone deacetylation	0.0446
	BP	2/2	chemotaxis	0.0493
	BP	2/2	cellular response to testosterone stimulus	0.0496
	CC	11/21	extracellular region	0.0018
	CC	2/2	retrotransposon nucleocapsid	0.0364
	CC	2/2	mitotic spindle pole	0.0437
	CC	2/2	spindle pole centrosome	0.0496
	MF	3/4	RNA-DNA hybrid ribonuclease activity	0.0348
	MF	2/2	ribonuclease activity	0.0364
	MF	2/2	tumor necrosis factor receptor binding	0.0415
Ch.vs.Dh	BP	5/6	**Golgi organization**	0.0089
	BP	5/8	G protein-coupled receptor signaling pathway	0.0414
	BP	5/8	negative regulation of apoptotic process	0.0459
	CC	12/23	**integral component of plasma membrane**	0.0086
	MF	4/5	thiol-dependent ubiquitin-specific protease activity	0.0178
	MF	4/5	cysteine-type endopeptidase activity	0.0270
	MF	4/5	microtubule motor activity	0.0314
Dc.vs.Dh	BP	2/2	regulation of protein localization	0.0092
	BP	2/3	cerebellar Purkinje cell differentiation	0.0371
	BP	2/3	negative regulation of autophagy	0.0418
	BP	2/4	positive regulation of angiogenesis	0.0472
	CC	8/23	**integral component of plasma membrane**	0.0011
	CC	2/2	cell projection	0.0175
	MF	2/2	kinesin binding	0.0122
	MF	3/8	**RNA-directed DNA polymerase activity**	0.0375

CHAPTER V

MULTI-OMIC ANALYSIS REVEALS MARKED PHENOTYPIC PLASTICITY IN CORAL CLONES OUTPLANTED TO DIVERGENT ENVIRONMENTS.

Abstract

Phenotypic plasticity, defined as a property of individual genotypes to produce different phenotypes when exposed to different environmental conditions, may be expressed at the behavioral, biochemical, physiological, or developmental levels and have direct influence over species' demographic performance. How different mechanisms modulate phenotypic plasticity and what is the adaptive potential of their effects is mostly unknown. In reef-building corals, a group particularly affected by anthropogenic global change, non-genetic mechanisms have been shown to participate in responses to environmental change. However, the contribution of different non-genetic mechanisms (i.e., Epigenetic and microbiome changes) to plastic physiological responses in corals is not clear. This work aimed to aid filling this gap by studying the epigenetic, microbiome, and physiological divergence of coral clones outplanted to different natural environments. A rapid phenotypic response to the conditions imposed to the outplanting site allowing the survival of the fragments, was observed in the lipidome, methylome and transcriptome. Remarkably, the symbiotic community remained unchanged, indicating that *A. cervicornis* does not rely on symbiotic changes to acclimatize to divergent conditions. Obtained evidence indicates a shift towards a more heterotrophic feeding behavior under the lower pH conditions imposed by the deep site.

Introduction

The persistence of coral reefs will fundamentally depend on the capacity of stony corals, the main builders of these ecosystems, to acclimatize and adapt to a rapidly changing environment. Paleontological and paleoclimatic evidence indicates that modern

corals have successfully survived dramatic shifts in environmental conditions (Allmon 2001; Pandolfi 2002; Jackson 2008), supporting the notion that they have evolved effective mechanisms for acclimatization and adaptation. However, the unprecedented frequency of occurrence of extreme conditions, and the overall accelerated pace of global change may exceed coral adaptability. Sustained anthropogenic disturbances to the planet's climate (The Royal Society and National Academy of Sciences 2014), ocean chemistry (Feely, Doney, and Cooley 2009; Regnier et al. 2013), and biological organization and processes (Rosenzweig et al. 2008; Doney et al. 2012; Poloczanska et al. 2013), have caused dramatic declines in coral cover and regime shifts in many reefs worldwide (Hoegh-Guldberg et al. 2017; Robinson et al. 2019). Such an alarming scenario has elicited the interest to study mechanisms with the potential to produce rapid acclimatization and adaptation responses (Eirin-Lopez and Putnam 2019; Putnam 2021)

Organisms have the capacity to rapidly modulate different physiological, morphological and behavioral traits (phenotype) in response to environmental change (Bonamour et al. 2019), allowing adjustments within the limits imposed by the genome (Li et al. 2018). This phenotypic plasticity serves as a base for selection to act upon (Yanagida et al. 2015), therefore facilitating population survival under rapid environmental change until genetic adaptation can occur. Considering the life history traits of stony corals (i.e., sessile, long lifespan) and the rapid pace of current anthropogenically driven environmental change, mechanisms enhancing phenotypic plasticity may be critical for their long-term survival (Payne and Wagner 2018). Several mechanisms have been proposed to generate phenotypic divergence independently of genetic mutation [see (Payne and Wagner 2018)]. Among those, epigenetic modifications

have been shown to generate heritable alternative gene activity states from the same DNA sequence (Cavalli and Heard 2019; Deans and Maggert 2015) in response to environmental change, receiving special attention in marine invertebrates including corals (Eirin-Lopez and Putnam 2019). Substantial transcriptional plasticity has been observed in corals facing environmental stress (Bellantuono et al. 2012; Bay and Palumbi 2015; Kenkel and Matz 2016; Traylor-Knowles, Rose, and Palumbi 2017; Yetsko et al. 2020), including the accumulation of stress-related transcripts (e.g., heat shock proteins) in anticipation of a recurrent stress ["frontloading" (Palumbi et al. 2014; Kenkel and Matz 2016; Brener-Raffalli et al. 2019)]. Given the rapid induction and persistence of these transcriptional responses, it is likely that epigenetic mechanisms are involved in its regulation (Torda et al. 2017; Putnam 2021). However, although there is evidence of epigenetic regulation of gene expression in corals (Li et al. 2018; Dixon et al. 2018; Baumgarten et al. 2018), these mechanisms are not clear. Crosstalk between epigenetic mechanisms regulating gene expression (Li et al. 2018; Weizman and Levy 2019) and the transient and non-deterministic nature of epigenetic marks make the mechanistic association difficult (Adrian-Kalchhauser et al. 2020).

Additionally, as metaorganisms composed by a multitude of functionally connected members (Bosch and McFall-Ngai 2011; Ainsworth et al. 2020), corals have further sources of plasticity provided by host-microbiome interactions (Putnam 2021). Consistently, ecological, genetic, epigenetic and physiological changes occurring in either of the components of the metaorganism (i.e., dinoflagellates, bacteria, viruses, fungi, archaea) or in their interaction with the host [i.e., changes in metabolite translocation (Cui et al. 2019; Matthews et al. 2017)] can have significant effects on the

phenotype of the colony (Silverstein, Cunning, and Baker 2015; Del Campo et al. 2017; van Oppen and Blackall 2019), making the overall colony plasticity a complex multi-mechanism process. Evidence of this complex interplay is the modulation of the host transcriptome and epigenome elicited by the composition of the symbiotic community (DeSalvo et al. 2010; Cunning and Baker 2020; Rodriguez-Casariego et al., *submitted*). Targeting the complexity and interconnection of the components modulating phenotypic plasticity, this work aims to utilize a multi-omics approach to evaluate the acclimatory response of coral clones exposed to divergent environments. The main hypothesis evaluated here predicts the correlated divergence of the transcriptome, methylome, lipidome and symbiotic community to adjust to specific environmental conditions after a year post-transplantation in either a shallow (3m) or a deep (15m) site.

Materials and Methods

Study sites and experimental design

A detailed description of the study sites, coral collection and host genotyping can be found in (Rodríguez-Casariego et al. 2020). Briefly, a total of n=200 naturally fragmented colonies of the staghorn coral (*Acropora cervicornis*) were collected, subdivided into two similarly sized ramets and directly outplanted into experimental 5 x 5 m plots at two depths (5 and 15 m). Initial colonies were genotyped using 6 microsatellite loci (Baums, Hughes, and Hellberg 2005), resulting in n=81 genets (Rodríguez-Casariego et al. 2020). For this study, and in order to evaluate the phenotypic divergence of ramets under different environmental conditions (determined by depth), a subset of (n=13) initial colonies outplanted as part of the experiment described in Rodríguez-Casariego et al.

(2020) with ramets surviving at both depths for a year, were monitored and sampled. All colonies included in this work were ouplanted to Luis Peña reef (LP: 18°18'45.0"N, 65°20'08.4"W), Culebra Island, PR. This site was chosen given the availability of detailed environmental datasets along the study period (Rodríguez-Casariego et al. 2020). Such dataset includes depth-associated differences in temperature, dissolved oxygen, pH, and salinity, recorded using YSI EXO2 multiparameter sondes (YSI, Yellow Springs, OH), and photosynthetically active radiation (PAR), measured with PAR sensors (Sea Bird, Bellevue, WA). Duplicated sets of sensors were deployed simultaneously at both depths during September 2018 and January 2019.

Phenotypic and molecular datasets

Sample collection, DNA and RNA extraction.

Branches of ~5 cm in length, were collected from each fragment (n=26 ramets of 13 colonies located at both depths) one-year post-outplanting. Coral tissue was immediately flash frozen in liquid nitrogen and stored at -80°C. To perform a detailed analysis of the symbiont community in addition to the characterization of the coral host molecular response, two parallel nucleic acid extraction strategies, "hard" and "soft", were applied to each coral sample. In both cases, DNA and RNA were purified from flash-frozen tissue using the Quick DNA/RNA Mini-Prep kit (Zymo Research, Irvine, CA) as described before (Rodríguez-Casariego et al. 2020). Briefly, 100 mg of tissue, previously powdered in liquid nitrogen, was resuspended in 2 mL vials containing 500 mg of Zirconia/Silica beads (0.5 mm diameter) and 1 mL of DNA/RNA Shield (Zymo Research, Irvine, CA) in duplicate. For the "soft" extraction, coral host cells were gently

lysed using two pulses of 30 sec in a vortex, leaving most of the symbiont cells intact and enriching host DNA (Rodríguez-Casariego et al. 2020). For the "hard" extraction, complete tissue homogenization was achieved with a MiniBead Beater (BioSpec, Bartlesville, OK, USA). After centrifugation (12,000 x g for 5 min), DNA isolation continued following the manufacturer's instructions. RNA was extracted following the kit's protocol, but only for the set of samples subject to "soft" homogenization. DNA and RNA were assessed by gel electrophoresis for integrity and spectrophotometric analysis (NanoVue GE Healthcare, Chicago, IL) for quality as described elsewhere (Rivera-Casas et al. 2017). Concentrations were measured using a Qubit 2.0 Fluorometer (Thermo Fisher, Waltham, MA) using appropriate reagent sets and following the instructions provided by the manufacturer. RNA quality was also assessed using a 2100 Bioanalyzer (Agilent Technologies, Santa Clara, CA).

Symbiodiniaceae ITS2 Amplicon Sequencing

The internal transcribed spacer 2 (ITS2) region of nuclear ribosomal DNA of the symbionts was analyzed to identify changes in the symbiotic community (Pochon et al. 2001). Genomic DNA, resulting from the "hard" extraction, was shipped to the Genomic Sequencing and Analysis Facility at University of Texas at Austin for amplification, library preparation and sequencing on an Illumina® MiSeq (Illumina, California, USA), with a read length configuration of 2x250 bp. Symbiodinaceae community composition was analyzed using the SymPortal Pipeline (Hume et al. 2019).

Lipid extraction and quantification.

The extraction and characterization of *A. cervicornis* lipidome was performed following methods previously developed for this coral species in (Lugo Charriez et al. 2021), and methodological details can be found there. Briefly, 1g of powder resulting from the maceration of a coral fragment (including skeleton) was extracted following the BUME method (Löfgren, Forsberg, and Ståhlman 2016). After overnight incubation in 3 mL BUME solvent, samples were centrifuged at 3500 rpm for 10 min and the supernatant collected. Two additional re-extractions with 3 mL of BUME solvent were performed to the pellets, with 10 min incubations. A total supernatant volume of 9 mL was homogenized, and 1 mL aliquot of each sample was transferred to LC vial in duplicate for analysis.

Lipid samples were analyzed by liquid chromatography followed by high resolution mass spectrometry (LC-HRMS) in a Thermo Q-Exactive Orbitrap equipped with a heated electrospray ionization (HESI) source. Mass spectrometry and liquid chromatography separation were performed using the same conditions described in (Lugo Charriez et al. 2021)), with 0.1% formic acid instead of ammonium formate in the mobile phase. Lipid identification and relative quantitation was performed using the Lipid Search Software™ (Thermo Scientific, version 4.2.21). Lipid Search parameters were adjusted to include only compounds classified into 8 lipid classes: cholesterol esters (ChE), fatty acids (FA), monoacylglycerols (MG), monogalactosyldiacylgylcerols (MGDG), phosphatidylcholines (PC), phosphatidylethanolamines (PE), triglycerides (TG), and wax esters (WE). These classes were previously described as important components of the lipidomes of corals and their symbionts (Harland et al. 1993; Imbs et al. 2010; Lin et al.

2013; Rosset et al. 2019; Stien et al. 2020), including *A. cervicornis* (Lugo Charriez et al. 2021). Data was blank subtracted and filtered to eliminate all peaks with signal to noise ratio < 3 and a delta ppm of ± 10. Peak area was normalized using internal standards (Lugo Charriez et al. 2021).

DNA Methylation Library Preparation and Quantification

Coral host genomic DNA, isolated through the "soft" extraction method previously described, was sent to Genewiz (Genewiz, South Plainfield, NJ) for whole genome bisulfite sequencing (WGBS) processing. Bisulfite conversion was performed with the EZ DNA Methylation-Gold kit (Zymo,CA,USA) and library preparation was completed with the NEBNext Ultra DNA Library Preparation Kit (New England Biolabs, Ipswich, MA). Resulting libraries were sequenced on a HiSeq platform, generating 150bp paired-end reads.

Quality trimming of the resulting sequences was performed using TrimGalore! (v0.6.4; Martin, 2011), removing 10 bp from both the 5′ and 3′ ends. After quality control with FastQC v.0.11.7 (Andrews, 2010), trimmed sequences were aligned to the *Acropora cervicornis* genome (Dr. I. B. Baums assembly) using Bismark (v0.22.3; Krueger and Andrews, 2011) with non-directionality and an optimized alignment score of L,0,-0.9. The Bismark platform was also used to quantify methylated or unmethylated CpGs in all samples. Resulting .cov files were filtered to keep only CpG loci with at least 5x coverage for each sample. CpG loci were annotated by feature. Genes, mRNA, exons, coding sequences (CDS), flanking untranslated regions (3'-UTR and 5'-UTR) and tRNAs were obtained directly from the genome annotation file while putative promoter regions,

intergenic regions, introns and repetitive regions were created following previously developed pipelines (Venkataraman et al. 2020). Gene body methylation (gbM) includes CpGs overlapping with intron, CDS and UTRs, but not promoters. Combined methylation calls per CpG loci (i.e., cov files) for all samples were filtered to maintain individual CpG dinucleotides with at least 10x coverage and used to characterize the methylome of *A. cervicornis*. Repetitive regions in the genome of *A. cervicornis* were annotated using RepeatMasker v4.1.1 (A.F.A. Smit, R. Hubley & P. Green RepeatMasker at http://repeatmasker.org), and methylation levels (average % methylation for all sites overlapping repeats) and methylation densities (number of methylated Cs) per repeat type were calculated using Python scripts developed by Dr. Yi Jin Liew (https://github.com/lyijin/smic_dna_meth).

RNA Library Preparation and Quantification

Host-enriched RNA, normalized to a concentration of 44 ng/uL (30 uL), was shipped to the Genomic Sequencing and Analysis Facility, University of Texas at Austin, for tag-based RNA-seq (tagSeq) library preparation and sequencing on an Illumina HiSeq 2500 (Lohman, Weber, and Bolnick 2016). Gene expression quantification was performed following code developed by M. Matz (github.com/z0on/tag-based_RNAseq). TagSeq demultiplexed raw reads were trimmed of adaptors and quality filtered using fastx-toolkit (http://hannonlab.cshl.edu/fastx_toolkit/). PCR duplicates were removed, and the resulting reads were mapped to the *A. cervicornis* transcriptome (Libro, Kaluziak, and Vollmer 2013) using bowtie2 (v.2.3.4; (Langmead and Salzberg 2012). Successfully mapped reads were compiled into a count table for downstream analysis.

To evaluate the expression of transcripts originating from repeat elements trimmed RNA reads were mapped against the genome of *A. cervicornis* using HISAT2 v2.1.0 (Kim, Langmead, and Salzberg 2015). For the aligned reads, a per-base coverage file was created using samtools depth (Li et al. 2009). Per-repeat read counts were parsed utilizing a python script developed by Dr. Yi Jin Liew (https://github.com/lyijin/smic_dna_meth).

Statistical Analyses

All statistical analyses were completed in R (v4.0.2; R Core Team 2020) with RStudio (v1.3.959; R Studio Team 2020). Analysis code is available on Github (see data accessibility statement).

Divergence of the symbiotic community

SymPortal output, including the absolute abundance of each ITS2 type profile and sequenced reads representative of putative Symbiodinaceae taxa, were analyzed to evaluate symbiont community divergence between depths. The hypothesis that Symbiodinaceae communities differ between outplant depth was evaluated by Permutational multivariate analysis of variance (PERMANOVA) with the *adonis* function in the R-package *vegan* (Oksanen et al. 2019). Fragment identity was used as strata in the models for both ITS2 type profiles and individual taxa distributions, and 9,999 permutations of residuals from Bray-Curtis dissimilarities were employed.

Differences in lipid profiles

The differentiation of the lipidome in response to depth was evaluated with two variables describing the lipidome of each sample, the number of different compounds per class and the proportional abundance of lipids in each class per sample. Hypothesis linking these variables with outplanting depths were evaluated through PERMANOVA and proportion using chi-squared tests (*prop.test* R function).

Global molecular response

To evaluate the hypothesis that transcriptome and methylome are influenced by the outplanting environment, genome-wide gene expression and DNA methylation was visualized through principal coordinates analysis (PCoA) of Manhattan distances, and differences between sites were tested through ANOVA. Treatment associated variance in DNA methylation and gene expression across all colonies was further analyzed through a Discriminant Analysis of Principal Components (DAPC) using the R package *adegenet* v2.1.3 (Jombart, Devillard, and Balloux 2010). Gene expression count data were previously filtered to exclude genes with a mean count <1 and normalized using the variance stabilizing transformation implemented in DESEQ2 (Love, Anders, and Huber 2014). DNA methylation data were previously filtered to include only CpGs with at least 10x coverage and were present in all samples. Methylation was further summarized keeping CpGs with potential differential methylation between all samples (regardless of treatment) at a regional level (100bp windows) using the methylpy *DMRfind* function (Schultz et al. 2015) (https://github.com/yupenghe/methylpy).

Differential responses of DNA methylation and gene expression.

Hypotheses testing the influence of the outplanting environment over DNA methylation and the expression of individual genes were evaluated through differential methylation analysis at regional and gene levels, and differential gene expression analysis, respectively. Differentially methylated regions (DMRs) were identified through ANOVA on arcsine-square-root transformed methylation data. Differentially methylated genes (DMG) were identified using a generalized linear model implemented in R, with the model *glm(meth, unmeth~ site, family=binomial)*. Regions and genes with p-adjusted values < 0.05 were considered differentially methylated. Only shared CpG positions, with at least 10x coverage, were included in the differential methylation analyses. Differentially expressed genes were identified using a generalized linear model approach implemented with the R package DESEQ2 with site as fixed effects. Genes with FDR ≤ 0.1 were considered differentially expressed.

Functional enrichment analysis.

Analyses of gene ontology (GO) and eukaryotic orthologous groups (KOG) enrichments associated with gene expression and methylation were performed using GO-MWU (Wright et al. 2015) and KOG-MWU (Matz 2016) respectively. These were based on log2 fold of the methylated/unmethylated fraction of all CpG loci per gene for gene-level DNA methylation, and on signed log(p-values) for gene expression. *A. cervicornis* KOG and GO categories used for the functional analysis of gene expression were obtained from a previously published transcriptome for the species (Libro, Kaluziak, and Vollmer 2013). GO terms used for DNA methylation functional analysis was derived

from the annotation of the genome (I. B. Baums assembly) Additional GO enrichment analysis, using topGO (Alexa, Rahnenführer, and Lengauer 2006), was performed to identify categories significantly overrepresented in DMGs.

Results

Coral Holobiont physiological divergence

Symbiodinaceae community composition

The sequencing and analysis (SymPortal) of the ITS2 region of Symbiodinaceae members of the holobiont identified 69 symbiont types and 6 profiles across all analyzed samples (n = 26, Fig. 1). ANOVA analyses found a significant effect of colony identity on the beta diversity of ITS type profiles ($F = 1.0259e31$, $df = 12$, p-value < 2.2e-16), but no changes between outplanting sites ($F = 0.2188$, $df = 1$, p-value = 0.6442). Similarly, no effect of outplanting depth was found for ITS2 sequence distribution (PERMANOVA, $R^2 = 0.00535$, $df = 1$, p-value = 0.7703). In summary, the symbiotic community seems to remain stable regardless of the marked differences of the environmental conditions of the outplanting sites.

Lipidome differentiation

A total of 3,062 lipidic compounds were identified across all samples for eight lipid classes previously shown to be the major components of coral lipidomes (Harland et al. 1993; Imbs et al. 2010; Rosset et al. 2019; Stien et al. 2020; Lugo Charriez et al. 2021). The class of monogalactosyldiacylgylcerols (MGDG) presented the highest number of compounds, with a mean of 217.5 compounds per sample (Fig. 2A). However,

the most abundant lipid classes were triglycerides (TG) followed by monoacylglycerols (MG) (Fig. 2B). As evidenced by PERMANOVA (Table S1), there was a significant effect of the outplanting site and its interaction with the lipid class in the number of compounds found, with significant changes in TG (Paired t-test: $t = -3.9567$, $df = 12$, p-value = 0.002) and WE (Paired t-test: $t = -2.5695$, $df = 12$, p-value = 0.0246) classes, and marginally significant in MGDG (Paired t-test: $t = -2.1071$, $df = 12$, p-value = 0.0568) and PC (Paired t-test: $t = -2.0694$, $df = 12$, p-value = 0.0608; Fig. 2A).

Similar to the number of compounds, relative abundances of lipids of each class were dependent on the coral colony (PERMANOVA: $R^2 = 0.59617$, $df = 12$, p-value = 0.0029; Fig. 2B). However, for this variable, all classes were dependent on the outplanting site (Contingency tests, Table S2), with the most dramatic changes occurring in PE (reduced in half on the deep site) and MGDG (doubled in the deep site) (Fig. 2B).

Differential molecular response

Gene expression divergence

RNA sequencing (Tag-Seq, n = 26 samples) produced a total of 309,224,452 reads, with a median of 11,497,504 reads per sample. Trimming, quality filtering and PCR duplicate removal resulted in 5,313,517 (median) sequences per sample. A median of 3,757,251 reads per sample, mapped to the transcriptome assembly of *A. cervicornis* (Table S1, Fig. S1), covering 69,954 of the 95,390 predicted genes in the assembly. Finally, 45,518 genes had mean counts >1 and were utilized for downstream analyses.

Significant inter-genet variability was evidenced through PCoA analysis of variance-stabilized gene counts (Fig. 3A), with samples clustering primarily by colony.

However, a clear divergence between ramets by outplanting site can be observed across PC1 (explaining 12.6% of the total variance). This separation between depths was corroborated by DAPC regardless of the high variability between genets (Fig. 3B).

Given the high variability observed in the PCoA analysis, differentially expressed genes (DEGs) between corals outplanted to each depth were identified by genotype and across all samples. The number of DEGs was highly dependent on the genotype (Table 1), with half of the genets having <1 DEGs and the rest ranging from 10-65 DEGs each. Combining all samples, 300 DEGs were identified, with up- and down-regulated genes almost evenly distributed.

GO (Table S4) and KOG (Fig. 4, Table S5) functional analyses, revealed significant responses across all genets regardless of the substantial variability between genets. Corals outplanted to the shallow reef (LP15) significantly up-regulated KOG categories "replication, recombination and repair", "RNA processing and modification" and "signal transduction mechanisms"; while corals maintained in the deep reef up-regulated the categories "translation, ribosomal structure and biogenesis", "nucleotide transport and metabolism", "energy production and conversion" and "post-translational modification, protein turnover, chaperones" (Fig 4, Table S5). Similar functional categories were also evidenced in the GO analysis (Table S4), with corals outplanted to the deep site upregulating mostly components and functions of the cellular energetic metabolism, and corals in the shallow reef up-regulating mostly RNA processing and signal transduction elements and functions.

DNA methylation landscape.

Sequencing of WGBS libraries (n = 26) produced a median of 40,706,732 reads after trimming and quality filtering. From those, 30,465,974 reads per sample (median) mapped to the genome of *A. cervicornis*, for a mean overall mapping efficiency of 74.7%. Sequencing and mapping statistics were homogeneous (low inter-sample variation), reducing potential biases for comparisons between treatments (Fig. S2). After error (1% miss-called Cs) and coverage (5x) filtration, 17,428,204 CpGs (91% of all CpGs in the *A. cervicornis* genome) in total were used for methylome characterization.

Most of the CpGs in the *A. cervicornis* genome were unmethylated (82.9%), with 1,981,493 CpGs (11.4%) displaying methylation levels over 50%, and only a 5.7 % showing sparse methylation (between 10-50% of the reads methylated). As commonly found in invertebrates, methylated cytosines were accumulated in gene bodies, with significantly higher methylation levels (% methylation) when compared with intergenic regions (Fig. 5A, B). Introns showed significantly higher methylation levels that exons (Fig. 5B). Although, across a gene model, methylated CpGs were more frequent at the gene boundaries, including the first and last exons, and flanking regions (Fig. 5C).

A total of 146,849 methylation islands were identified in the genome of *A. cervicornis*, containing between 11 and 13,212 CpGs (mean = 42 CpGs) and a length ranging from 500 to 395,513 bp (mean = 1,576 bp). Methylation islands majoritarily overlapped with gene bodies (50,751, 34.56% with exons; 48,494, 33.02% with introns). Interestingly, the proportion of methylation islands overlapping with genomic features was significantly different when compared with the general distribution of CpGs in the genome (Contingency test; p-value < 0.001, Fig. S3), with a 3x enrichment in exons and

a 26x enrichment in repetitive regions (transposable elements). Remarkably, repetitive regions in the genome of *A. cervicornis* account only for approximately 1.4% of the genome (less than half of the regions in the genome of *Montastraea cavernosa*, Rodriguez-Casariego et al. *submitted*), with only 145 retroelements and 45 DNA transposons.

Divergence of DNA methylation patterns

Significant differentially methylated regions (DMRs) were evaluated across genomic windows of 100 bp between all samples regardless of their treatment. Similar to gene expression, DNA methylation patterns were highly influenced by the genotype as evidenced through PCoA analysis (Fig. 6A), but the effect of depth of outplant was not clear. Only through DAPC (Fig. 6B) the divergence of the methylation patterns on a subset of samples was evident along LD1, explaining 30.4% of the total variance. To further evaluate treatment-induced differences, ANOVA analyses identified 149 DMRs ($p < 0.05$) across all samples, between corals in deep and shallow sites. Substantial variability across genets was also evidenced in the methylation level of DMRs (Fig S4A). A significant portion of these DMRs occurred in gene bodies (71 overlapped with genes) and flanking regions (39 overlapped with 3'UTRs and 18 with putative promoters). Compared with the general distribution of methylated CpGs across genomic features, coding regions (CDS) and 3'UTRs were proportionally enriched in DMRs (Fig S4B), although these differences were not significant (chi square *adjusted p*.value > 0.1).

In correspondence with the prevalence of differential methylation in gene bodies and flanking regions, differential methylation (identification of DMGs) was evaluated on

a set of 22,258 genes containing at least 5 CpG positions covered at least 10x in all samples. Gene body methylation was significantly influenced by the outplanting site ($F = 5.776$, $df = 1$, p-value = 0.0163), genotype ($F = 39.656$, $df = 11$, p-value < 2e-16) and their interaction ($F = 2.430$, $df = 11$, p-value = 0.0050), in correspondence with the previously observed inter-genet response variability. 1,316 genes were identified as differentially methylated across all genets, with a general increase in methylation in corals maintained in the deep reef (Fig. 7A). Only 2 genes were both differentially methylated and expressed (Fig. 7B).

Two KOG categories showed differential methylation between sites, with "amino acid transport and metabolism" significantly (p-adj < 0.1) under-methylated in the shallow reef and "transcription" under-methylated in the deep reef (Fig 7C). GO-MWU analysis did not find any term significantly (FDR < 0.1) over- or under-methylated. Interestingly, both functional categories with significant changes in methylation were slightly up-regulated (in terms of gene expression) in the shallow reef but non-significant. Overall, a clear relationship between gene expression and gene body methylation was not evident, although both mechanisms seem to diverge in response to environmental change.

Discussion

With a multi-omics approach, this work attempted to discern the response of different mechanisms potentially involved in rapid acclimatization responses of stony corals under divergent natural conditions. Pioneering is such an approach, datasets covering the responses of the symbiotic community, the lipidome, the transcriptome and the methylome were generated for the first time in a single experiment. Building on the

complementarity of these datasets, further analysis (beyond the scope of this work) will allow the study of the interaction between these mechanisms and their combined role modulating phenotypic plasticity under predicted future conditions [i.e., sea level rise scenario (Rahmstorf 2010)]. Phenotypic divergence in response to global environmental change, as provided by experimental outplanting at reefs located at 5 and 15 m of depth, was evidenced in the lipidome, transcriptome and methylome, but no significant shifts in the symbiotic community was observed.

Stability of the symbiotic community.

Stability rather than plasticity was observed in the Symbioninaceae community (Fig. 1) under divergent environmental conditions [pH, salinity, and irradiance (Rodríguez-Casariego et al. 2020)]. Symbiont identity has been shown to affect coral phenotype (Mieog et al. 2009; Silverstein, Cunning, and Baker 2015; Cunning and Baker 2020), with dynamic changes in the symbiotic community composition potentially contributing to plastic holobiont responses to environmental change, mostly thermal stress. Although the genus *Acropora* has been described to host a highly diverse symbiotic community when compared to other coral genera (Putnam et al. 2012), remarkable stability of the consortia has been observed through seasons (Thornhill et al. 2006; Rodríguez-Casariego et al. 2020) and experimental manipulations (O'Donnell et al. 2018), with minimum and only transient changes under thermal stress (Thornhill et al. 2006). Maintaining such stability under divergent environmental conditions, yet not thermal (Rodríguez-Casariego et al. 2020), recreated by outplanting *A. cervicornis* fragments below the depth they commonly inhabit, indicates either a limited role of the

symbiotic composition modulating phenotypic plasticity in this species, or a remarkable plasticity of the symbiome to maintain appropriate interactions under such divergent conditions without affecting the community structure.

Divergence of lipidic profiles indicate increased energetic demands in deep-outplanted corals

Significant changes in the lipidome were observed under divergent environmental conditions in the coral *A. cervicornis* (Fig. 2, Supplementary Tables S1 and S2). Despite a large inter-genet variability, consistent changes in both diversity and abundance of compounds included in the eight lipid classes studied were observed. MGDG galactolipids were the most diverse class across all samples (Fig. 2A). As one of the main components of thylakoid membranes (Guschina and Harwood 2009), the diversity of this class can be directly linked with the high symbiont diversity characteristic of this group (Putnam et al. 2012). Significant increases in MGDG lipids proportional abundance were observed in deep-outplanted corals (Fig 2B). Increases of this class of lipids have been previously linked with enhanced responses to thermal stress (Rosset et al. 2019) through the strengthening of thylakoid membranes in the symbionts. Considering that the deep reef displayed lower and less variable temperatures during the study period (Rodríguez-Casariego et al. 2020), this enrichment can constitute a "frontloading" strategy based on the previous stress exposure of these fragments now faced with more favorable conditions in the deep reef. Competing hypotheses could include an increase in the symbiont population to compensate for lower carbon translocation under lower irradiance (Tremblay et al. 2014), or the activation of heterotrophy in response to the lower pH of

the deep site (Edmunds 2011; Towle, Enochs, and Langdon 2015). While the first two hypotheses could explain the increase in proportional abundance of this lipid group, the increase in diversity of compounds is difficult to accommodate given the observed stability of the symbiont community. However, the activation of heterotrophy, including items from the phytoplankton, could explain both changes observed in the MGDG class. Similarly, triglycerides (TG) and wax esters (WE) classes presented a significantly higher number of compounds for corals outplanted to the deep site.

WE abundance was proportionally higher in the shallow site and TG was more abundant in the deep site (Fig. 2B). Reductions in the abundance of WE have been linked to stress (Yamashiro et al. 2001; Grottoli, Rodrigues, and Juarez 2004), and "frontloading" of both WE and TG lipid classes have been shown to reduce thermal stress-related mortality (Anthony, Connolly, and Hoegh-Guldberg 2007). Accordingly, this pattern could be indicative of the different stress conditions imposed by each site during the year, requiring specific metabolic responses. Additional reductions in monoacylglycerols (MG) and phosphatidylethanolamines (PE) in the deep reef (Fig. 2B), could be indicative of a response to stress (Grottoli, Rodrigues, and Juarez 2004; Solomon et al. 2019), but also of a lower energetic budget given the lower irradiance of this site or the demand of calcification under lower pH . In all cases, changes in diversity and relative abundance of lipid classes with depth seem to indicate different strategies to meet energetic demands and respond to stress under different environmental conditions.

Depth-associated transcriptional plasticity indicates more favorable conditions in the deep site.

Gene expression was evaluated in ramets of the same initial fragments, allowing the discrimination between the effects of divergent environmental exposure and the host genotype. High inter-genet variability has been previously observed for gene expression (Granados-Cifuentes et al. 2013; Parkinson et al. 2018; Cunning and Baker 2020) and was evidenced here with half of the genets included in the analysis showing reduced transcriptional variability (Table 1). However, given the design of the experiment, common divergent transcriptional profiles were described in response to transplantation to different environments (Fig. 3).

The largest effect of transplantation in the transcriptome was the differential regulation of ribosomal biosynthesis, translation, and energetic metabolism (Fig. 4). This response was evident in both the KOG and GO enrichments (Supplementary Table S4), and was consistent across genets, with 8 out of the 12 genets in the study significantly up-regulating "translation, ribosomal structure and biogenesis" when placed in the deep reef. Increases in these categories are often related with cellular proliferation (López-Maury, Marguerat, and Bähler 2008) and therefore coral growth. This could indicate a more favorable energetic conditions in the deep reef since ribosomal synthesis constitutes an important proxy for energetic metabolism (Grummt and Ladurner 2008), but it seems counter to the notion that lower irradiance produces a reduction in carbon translocation from the symbionts (P. Tremblay et al. 2014). Increased protein synthesis can also be related with the activation of mechanisms to counteract the lower carbon translocation by hosting larger symbiotic populations (Cunning and Baker 2020), or by activating

heterotrophic nutrition in response to a higher energetic demand. As hypothesized based on the lipidic profiles, the lower pH of the deep site could have also produced the activation of heterotrophy (Towle, Enochs, and Langdon 2015), and explain the up-regulation of the energetic metabolism in deep-outplanted corals. Although low pH generally produces metabolic depression in marine invertebrates (Strader, Wong, and Hofmann 2020), several studies have shown increases in metabolic processes under ocean acidification (Ogawa et al. 2013; Vidal-Dupiol et al. 2013; Davies et al. 2016). Although most of these studies were performed in laboratory settings and used unrealistic CO_2 levels, their findings were corroborated by the study of coral populations inhabiting natural CO_2 seeps (Kenkel et al. 2018). Similar to the results obtained in this work, these authors found a significant up-regulation of ribonuclear protein biosynthesis and energetic metabolism (Kenkel et al. 2018).

Given that the experimental design lacks real controls, the proportional increase of these transcripts in the deep corals could also be related to its down-regulation in the shallow corals. Shallow corals upregulated repair mechanisms and signal transduction, and downregulated ribosomal and energetic metabolism (Supplementary Tables S4 and S5), all hallmarks of corals environmental stress response (López-Maury, Marguerat, and Bähler 2008), potentially related with the higher thermal variability and light irradiance of the shallow site. This is consistent with the observed transcriptional responses to transplantation in *Porites astreoides* between inshore and offshore reefs (Kenkel and Matz 2016) and their conclusion that inshore reefs constitute more stressful environments. In addition, "G protein-coupled receptor signaling pathway", a GO term linked with coral bleaching (Rose, Seneca, and Palumbi 2015) was significantly up-

regulated in shallow corals (Table S4). However, very similar patterns of expression of stress response components were observed in coral populations inhabiting CO_2 seeps (Kenkel et al. 2018), with a downregulation of protein folding and stress response functions. These remarkable similarities could indicate that differences in pH between the outplanting sites (Rodríguez-Casariego et al. 2020) are driving the transcriptional response observed. Nevertheless, being conservative, a combination of differential responses to stress in the shallow (light and thermal probably) and deep (pH) reefs could explain both the divergence of the lipidome and transcriptome observed here.

DNA methylation pattern and divergence

A single-base resolution methylome of *A. cervicornis* was described for the first time in this work utilizing WGBS. With a high read depth and mapping efficiency (Supplementary Fig. S2), over 90% of all the CpG sites in the genome of the species were appropriately characterized.

Recent findings seem to indicate that interspecific differences in genome-wide DNA methylation correlates with the level of sensitivity to environmental stress in corals (Trigg et al. 2021). Correspondingly, relatively stress resistant corals such as *Porites astreoides* (Dimond and Roberts 2020), *Montipora capitata (Trigg et al. 2021)* and *Montastraea cavernosa* (Rodriguez-Casariego et al., *submitted*) show higher methylation levels than sensitive species [*Stylophora pistillata* (Liew et al. 2018), and *Pocillopora damicornis* (Trigg et al. 2021)]. Surprisingly, methylation levels of *A. cervicornis* (11.4% of CpGs are methylated) observed here place the species among more resistant corals like *M. capitata* (Trigg et al. 2021), although in terms of other aspects like genome size,

repeat content and overall energetic capacity [see discussion in (Trigg et al. 2021)], relevant to DNA methylation, *A. cervicornis* is very different from resistant species [*M. capitata* (Shumaker et al. 2019) and *M. cavernosa* (Rodriguez-Casariego et al., *submitted*)]. A possible explanation of this contrast could be related with the seasonality of DNA methylation demonstrated in this species (Rodríguez-Casariego et al. 2020), as samples used to describe this and other methylomes could have been collected at different seasons. Other characteristics of the methylome such as the distribution of methylated CpGs across genomic features and the frequency distribution of methylation levels (Fig. 5) was very similar to other previously described coral methylomes (Li et al. 2018; Liew et al. 2020; Trigg et al. 2021).

DNA methylation pattern across 100 bp genome windows was dependent on the genotype as previously described (Dimond and Roberts 2020; Liew et al. 2020; Rodríguez-Casariego et al. 2020) with most samples grouping by genet in a multidimensional space (Fig. 6A). Regardless of this variability, significant differences at regional and gene levels were observed (Fig. 7, Supplementary Fig. S4), with a consistent increase in the level of gene body methylation in corals outplanted to the deep reef. An energetically favorable environment in the deep reef, as somehow evidenced by the transcriptome and lipidome analyses, could allow higher methyltransferase activities (Donohoe and Bultman 2012) reducing spurious transcription (Li et al. 2018), and therefore allowing cellular proliferation as evidenced in the transcriptional profile of deep-outplanted corals. Alternatively, and similarly to the lipidome and transcriptome responses, the consistently lower pH levels occurring in the deep site for the duration of the experiment (Rodríguez-Casariego et al. 2020), could potentially influence the

methylation state of the fragments exposed to these conditions. Increases in global DNA methylation and gene body methylation levels has been consistently observed in corals exposed to low pH (Putnam, Davidson, and Gates 2016; Liew et al. 2018).

Regardless of the commonalities between the general responses of the transcriptome and methylome, we could not find evidence supporting a direct interaction between both mechanisms as has previously been described in cnidarians (Li et al. 2018; Dixon et al. 2018). However, given the current state of the bioinformatic resources available for *A. cervicornis,* a detailed analysis allowing the correlation between gene expression and DNA methylation was not possible at this moment. However, the limited number of shared differentially expressed and methylated genes (Fig. 7B), and the different functional enrichment of the methylation and expression datasets (Fig. 4 and Fig. 7C), do not allow any mechanistic inference of the interconnection between DNA methylation and gene expression. Nevertheless, the differential methylation observed in genes involved in transcription (enriched KOG term) could hint an indirect interaction between methylation and gene expression.

Conclusions

Overall, the evidence provided by the analysis of the lipidome, transcriptome and methylome indicate a rapid phenotypic response to the conditions imposed to the outplanting sites, allowing the survival of the fragments. Remarkably, the observed stability of the symbiotic community indicates that *A. cervicornis* adjustments to acclimatize to divergent conditions rely heavily on other mechanisms, potentially including nutritional plasticity. Corals have been proposed to modulate their feeding

modes under different environments, providing a potential adaptive mechanism to sustain growth under stressful conditions (Anthony and Fabricius 2000; Ferrier-Pagès et al. 2011; Tremblay et al. 2014; Pascale Tremblay et al. 2016). Both lipidomic and transcriptional responses seem to indicate a change to a more heterotrophic habit in the corals exposed to a lower pH in the deep site. Although the DNA methylation response was also consistent with a response to elevated pH, evidence of its correlation with gene expression was not observed. However, technical limitations did not allow an appropriate interaction analysis at this time, and it will be included in the near future clarifying these interactions.

References

Adrian-Kalchhauser, Irene, Sonia E. Sultan, Lisa N. S. Shama, Helen Spence-Jones, Stefano Tiso, Claudia Isabelle Keller Valsecchi, and Franz J. Weissing. 2020. "Understanding Non-genetic Inheritance: Insights from Molecular-Evolutionary Crosstalk." *Trends in Ecology & Evolution*. https://www.sciencedirect.com/science/article/pii/S0169534720302263.

Ainsworth, Tracy D., Catriona L. Hurd, Ruth D. Gates, and Philip W. Boyd. 2020. "How Do We Overcome Abrupt Degradation of Marine Ecosystems and Meet the Challenge of Heat Waves and Climate Extremes?" *Global Change Biology* 26 (2): 343–54.

Alexa, Adrian, Jörg Rahnenführer, and Thomas Lengauer. 2006. "Improved Scoring of Functional Groups from Gene Expression Data by Decorrelating GO Graph Structure." *Bioinformatics* 22 (13): 1600–1607.

Allmon, W. D. 2001. "Nutrients, Temperature, Disturbance, and Evolution: A Model for the Late Cenozoic Marine Record of the Western Atlantic." *Palaeogeography, Palaeoclimatology, Palaeoecology* 166 (1): 9–26.

Anthony, Kenneth R. N., Sean R. Connolly, and Ove Hoegh-Guldberg. 2007. "Bleaching, Energetics, and Coral Mortality Risk: Effects of Temperature, Light, and Sediment Regime." *Limnology and Oceanography* 52 (2): 716–26.

Anthony, K. R., and K. E. Fabricius. 2000. "Shifting Roles of Heterotrophy and Autotrophy in Coral Energetics under Varying Turbidity." *Journal of Experimental Marine Biology and Ecology* 252 (2): 221–53.

Baumgarten, Sebastian, Maha J. Cziesielski, Ludivine Thomas, Craig T. Michell, Lisl Y. Esherick, John R. Pringle, Manuel Aranda, and Christian R. Voolstra. 2018. "Evidence for Mi RNA-Mediated Modulation of the Host Transcriptome in Cnidarian--Dinoflagellate Symbiosis." *Molecular Ecology* 27 (2): 403–18.

Baums, I. B., C. R. Hughes, and M. E. Hellberg. 2005. "Mendelian Microsatellite Loci for the Caribbean Coral Acropora Palmata." *Marine Ecology Progress Series* 288: 115–27.

Bay, Rachael A., and Stephen R. Palumbi. 2015. "Rapid Acclimation Ability Mediated by Transcriptome Changes in Reef-Building Corals." *Genome Biology and Evolution* 7 (6): 1602–12.

Bellantuono, Anthony J., Camila Granados-Cifuentes, David J. Miller, Ove Hoegh-Guldberg, and Mauricio Rodriguez-Lanetty. 2012. "Coral Thermal Tolerance: Tuning Gene Expression to Resist Thermal Stress." *PLoS ONE*. https://doi.org/10.1371/journal.pone.0050685.

Bonamour, Suzanne, Luis-Miguel Chevin, Anne Charmantier, and Céline Teplitsky. 2019. "Phenotypic Plasticity in Response to Climate Change: The Importance of Cue Variation." *Philosophical Transactions of the Royal Society B: Biological Sciences*. https://doi.org/10.1098/rstb.2018.0178.

Bosch, Thomas C. G., and Margaret J. McFall-Ngai. 2011. "Metaorganisms as the New Frontier." *Zoology* 114 (4): 185–90.

Brener-Raffalli, K., J. Vidal-Dupiol, M. Adjeroud, O. Rey, P. Romans, F. Bonhomme, M. Pratlong, et al. 2019. "Gene Expression Plasticity and Frontloading Promote Thermotolerance in Pocillopora Corals." *bioRxiv*. https://doi.org/10.1101/398602.

Cavalli, Giacomo, and Edith Heard. 2019. "Advances in Epigenetics Link Genetics to the Environment and Disease." *Nature* 571 (7766): 489–99.

Cui, Guoxin, Yi Jin Liew, Yong Li, Najeh Kharbatia, Noura I. Zahran, Abdul-Hamid Emwas, Victor M. Eguiluz, and Manuel Aranda. 2019. "Host-Dependent Nitrogen Recycling as a Mechanism of Symbiont Control in Aiptasia." *PLoS Genetics* 15 (6): e1008189.

Cunning, Ross, and Andrew C. Baker. 2020. "Thermotolerant Coral Symbionts Modulate Heat Stress-responsive Genes in Their Hosts." *Molecular Ecology*. https://doi.org/10.1111/mec.15526.

Cziesielski, Maha J., Yi Jin Liew, Guoxin Cui, Sebastian Schmidt-Roach, Sara Campana, Claudius Marondedze, and Manuel Aranda. 2018. "Multi-Omics Analysis of Thermal Stress Response in a Zooxanthellate Cnidarian Reveals the Importance of Associating with Thermotolerant Symbionts." *Proceedings. Biological Sciences / The Royal Society* 285 (1877). https://doi.org/10.1098/rspb.2017.2654.

Davies, Sarah W., Adrian Marchetti, Justin B. Ries, and Karl D. Castillo. 2016. "Thermal and pCO2 Stress Elicit Divergent Transcriptomic Responses in a Resilient Coral." *Frontiers in Marine Science* 3: 112.

Deans, Carrie, and Keith A. Maggert. 2015. "What Do You Mean, 'Epigenetic'?" *Genetics* 199 (4): 887–96.

Del Campo, Javier, Jean-François Pombert, Jan Šlapeta, Anthony Larkum, and Patrick J. Keeling. 2017. "The 'Other' Coral Symbiont: Ostreobium Diversity and Distribution." *The ISME Journal* 11 (1): 296–99.

DeSalvo, M. K., S. Sunagawa, P. L. Fisher, C. R. Voolstra, R. Iglesias-Prieto, and M. Medina. 2010. "Coral Host Transcriptomic States Are Correlated with Symbiodinium Genotypes." *Molecular Ecology* 19 (6): 1174–86.

Dimond, James L., and Steven B. Roberts. 2020. "Convergence of DNA Methylation Profiles of the Reef Coral Porites Astreoides in a Novel Environment." *Frontiers in Marine Science* 6: 792.

Dixon, Groves, Yi Liao, Line K. Bay, and Mikhail V. Matz. 2018. "Role of Gene Body Methylation in Acclimatization and Adaptation in a Basal Metazoan." *Proceedings of the National Academy of Sciences of the United States of America* 115 (52): 13342–46.

Doney, Scott C., Mary Ruckelshaus, J. Emmett Duffy, James P. Barry, Francis Chan, Chad A. English, Heather M. Galindo, et al. 2012. "Climate Change Impacts on Marine Ecosystems." *Annual Review of Marine Science* 4: 11–37.

Donohoe, Dallas R., and Scott J. Bultman. 2012. "Metaboloepigenetics: Interrelationships between Energy Metabolism and Epigenetic Control of Gene Expression." *Journal of Cellular Physiology* 227 (9): 3169–77.

Edmunds, Peter J. 2011. "Zooplanktivory Ameliorates the Effects of Ocean Acidification on the Reef coralPoritesspp." *Limnology and Oceanography* 56 (6): 2402–10.

Eirin-Lopez, Jose M., and Hollie M. Putnam. 2019. "Marine Environmental Epigenetics." *Annual Review of Marine Science*. https://doi.org/10.1146/annurev-marine-010318-095114.

Feely, Richard A., Scott C. Doney, and Sarah R. Cooley. 2009. "Ocean Acidification: Present Conditions and Future Changes in a High-CO_2 World." *Oceanography* 22 (4): 36–47.

Ferrier-Pagès, C., A. Peirano, M. Abbate, S. Cocito, A. Negri, C. Rottier, P. Riera, R. Rodolfo-Metalpa, and S. Reynaud. 2011. "Summer Autotrophy and Winter Heterotrophy in the Temperate Symbiotic coralCladocora Caespitosa." *Limnology and Oceanography* 56 (4): 1429–38.

Granados-Cifuentes, Camila, Anthony J. Bellantuono, Tyrone Ridgway, Ove Hoegh-Guldberg, and Mauricio Rodriguez-Lanetty. 2013. "High Natural Gene Expression Variation in the Reef-Building Coral Acropora Millepora: Potential for Acclimative and Adaptive Plasticity." *BMC Genomics* 14 (April): 228.

Grottoli, A. G., L. J. Rodrigues, and C. Juarez. 2004. "Lipids and Stable Carbon Isotopes in Two Species of Hawaiian Corals, Porites Compressa and Montipora Verrucosa, Following a Bleaching Event." *Marine Biology* 145 (3): 621–31.

Grummt, Ingrid, and Andreas G. Ladurner. 2008. "A Metabolic Throttle Regulates the Epigenetic State of rDNA." *Cell* 133 (4): 577–80.

Guschina, Irina A., and John L. Harwood. 2009. "Algal Lipids and Effect of the Environment on Their Biochemistry." In *Lipids in Aquatic Ecosystems*, edited by Martin Kainz, Michael T. Brett, and Michael T. Arts, 1–24. New York, NY: Springer New York.

Harland, A. D., J. C. Navarro, P. Spencer Davies, and L. M. Fixter. 1993. "Lipids of Some Caribbean and Red Sea Corals: Total Lipid, Wax Esters, Triglycerides and Fatty Acids." *Marine Biology* 117 (1): 113–17.

Hoegh-Guldberg, Ove, Elvira S. Poloczanska, William Skirving, and Sophie Dove. 2017. "Coral Reef Ecosystems under Climate Change and Ocean Acidification." *Frontiers in Marine Science* 4 (May): 321.

Hume, Benjamin C. C., Edward G. Smith, Maren Ziegler, Hugh J. M. Warrington, John A. Burt, Todd C. LaJeunesse, Joerg Wiedenmann, and Christian R. Voolstra. 2019. "SymPortal: A Novel Analytical Framework and Platform for Coral Algal Symbiont Next-generation Sequencing ITS2 Profiling." *Molecular Ecology Resources* 19 (4): 1063–80.

Imbs, A. B., N. A. Latyshev, T. N. Dautova, and Y. Y. Latypov. 2010. "Distribution of Lipids and Fatty Acids in Corals by Their Taxonomic Position and Presence of Zooxanthellae." *Marine Ecology Progress Series* 409 (June): 65–75.

Jackson, Jeremy B. C. 2008. "Ecological Extinction and Evolution in the Brave New Ocean." *Proceedings of the National Academy of Sciences of the United States of America* 105 (Supplement 1): 11458–65.

Jombart, Thibaut, Sébastien Devillard, and François Balloux. 2010. "Discriminant Analysis of Principal Components: A New Method for the Analysis of Genetically Structured Populations." *BMC Genetics* 11 (October): 94.

Kenkel, Carly D., and Mikhail V. Matz. 2016. "Gene Expression Plasticity as a Mechanism of Coral Adaptation to a Variable Environment." *Nature Ecology & Evolution* 1 (1): 14.

Kenkel, Carly D., Aurelie Moya, Julia Strahl, Craig Humphrey, and Line K. Bay. 2018. "Functional Genomic Analysis of Corals from Natural CO2 -Seeps Reveals Core Molecular Responses Involved in Acclimatization to Ocean Acidification." *Global Change Biology* 24 (1): 158–71.

Langmead, Ben, and Steven L. Salzberg. 2012. "Fast Gapped-Read Alignment with Bowtie 2." *Nature Methods* 9 (4): 357–59.

Libro, Silvia, Stefan T. Kaluziak, and Steven V. Vollmer. 2013. "RNA-Seq Profiles of Immune Related Genes in the Staghorn Coral Acropora Cervicornis Infected with White Band Disease." *PloS One* 8 (11): e81821.

Liew, Yi Jin, Emily J. Howells, Xin Wang, Craig T. Michell, John A. Burt, Youssef Idaghdour, and Manuel Aranda. 2020. "Intergenerational Epigenetic Inheritance in Reef-Building Corals." *Nature Climate Change* 10 (3): 254–59.

Liew, Yi Jin, Didier Zoccola, Yong Li, Eric Tambutté, Alexander A. Venn, Craig T. Michell, Guoxin Cui, et al. 2018. "Epigenome-Associated Phenotypic Acclimatization to Ocean Acidification in a Reef-Building Coral." *Science Advances* 4 (6): eaar8028.

Lin, Chiahsin, Li-Hsueh Wang, Pei-Jie Meng, Chii-Shiarng Chen, and Sujune Tsai. 2013. "Lipid Content and Composition of Oocytes from Five Coral Species: Potential Implications for Future Cryopreservation Efforts." *PloS One* 8 (2): e57823.

Li, Xin, Tingting Guo, Qi Mu, Xianran Li, and Jianming Yu. 2018. "Genomic and Environmental Determinants and Their Interplay Underlying Phenotypic Plasticity." *Proceedings of the National Academy of Sciences of the United States of America* 115 (26): 6679–84.

Li, Yong, Yi Jin Liew, Guoxin Cui, Maha J. Cziesielski, Noura Zahran, Craig T. Michell, Christian R. Voolstra, and Manuel Aranda. 2018. "DNA Methylation Regulates Transcriptional Homeostasis of Algal Endosymbiosis in the Coral Model Aiptasia." *Science Advances* 4 (8): eaat2142.

Löfgren, Lars, Gun-Britt Forsberg, and Marcus Ståhlman. 2016. "The BUME Method: A New Rapid and Simple Chloroform-Free Method for Total Lipid Extraction of Animal Tissue." *Scientific Reports* 6 (June): 27688.

Lohman, Brian K., Jesse N. Weber, and Daniel I. Bolnick. 2016. "Evaluation of TagSeq, a Reliable Low-Cost Alternative for RNA Seq." *Molecular Ecology Resources* 16 (6): 1315–21.

López-Maury, Luis, Samuel Marguerat, and Jürg Bähler. 2008. "Tuning Gene Expression to Changing Environments: From Rapid Responses to Evolutionary Adaptation." *Nature Reviews Genetics*. https://doi.org/10.1038/nrg2398.

Love, Michael, Simon Anders, and Wolfgang Huber. 2014. "Differential Analysis of Count Data--the DESeq2 Package." *Genome Biology* 15 (550): 10–1186.

Lugo Charriez, Kathleen, Leila Soledade Lemos, Yailee Carrazana, Javier A. Rodríguez-Casariego, Jose M. Eirin-Lopez, Rachel Ann Hauser-Davis, Piero Gardinali, and Natalia Quinete. 2021. "Application of an Improved Chloroform-Free Lipid Extraction Method to Staghorn Coral (Acropora Cervicornis) Lipidomics Assessments." *Bulletin of Environmental Contamination and Toxicology*, January. https://doi.org/10.1007/s00128-020-03078-3.

Matthews, Jennifer L., Camerron M. Crowder, Clinton A. Oakley, Adrian Lutz, Ute Roessner, Eli Meyer, Arthur R. Grossman, Virginia M. Weis, and Simon K. Davy. 2017. "Optimal Nutrient Exchange and Immune Responses Operate in Partner Specificity in the Cnidarian-Dinoflagellate Symbiosis." *Proceedings of the National Academy of Sciences*. https://doi.org/10.1073/pnas.1710733114.

Matz, M. V. 2016. "KOGMWU: Functional Summary and Meta-Analysis of Gene Expression Data." *R Package Version* 1.

Mieog, Jos C., Jeanine L. Olsen, Ray Berkelmans, Silvia A. Bleuler-Martinez, Bette L. Willis, and Madeleine J. H. van Oppen. 2009. "The Roles and Interactions of Symbiont, Host and Environment in Defining Coral Fitness." *PloS One* 4 (7): e6364.

O'Donnell, Kelli E., Kathryn E. Lohr, Erich Bartels, Iliana B. Baums, and Joshua T. Patterson. 2018. "Acropora Cervicornis Genet Performance and Symbiont Identity throughout the Restoration Process." *Coral Reefs* 37 (4): 1109–18.

Ogawa, D., T. Bobeszko, T. Ainsworth, and W. Leggat. 2013. "The Combined Effects of Temperature and CO2 Lead to Altered Gene Expression in Acropora Aspera." *Coral Reefs* 32 (4): 895–907.

Oksanen, Jari, F. Guillaume Blanchet, Michael Friendly, Roeland Kindt, Pierre Legendre, Dan McGlinn, Peter R. Minchin, et al. 2019. "Vegan: Community Ecology Package. 2018." *R Package Version* 1: 17–14.

Oppen, Madeleine J. H. van, and Linda L. Blackall. 2019. "Coral Microbiome Dynamics, Functions and Design in a Changing World." *Nature Reviews. Microbiology* 17 (9): 557–67.

Palumbi, Stephen R., Daniel J. Barshis, Nikki Traylor-Knowles, and Rachael A. Bay. 2014. "Mechanisms of Reef Coral Resistance to Future Climate Change." *Science* 344 (6186): 895–98.

Pandolfi, J. 2002. "Coral Community Dynamics at Multiple Scales." *Coral Reefs* 21 (1): 13–23.

Parkinson, John Everett, Erich Bartels, Meghann K. Devlin-Durante, Caitlin Lustic, Ken Nedimyer, Stephanie Schopmeyer, Diego Lirman, Todd C. LaJeunesse, and Iliana B. Baums. 2018. "Extensive Transcriptional Variation Poses a Challenge to Thermal Stress Biomarker Development for Endangered Corals." *Molecular Ecology* 27 (5): 1103–19.

Payne, Joshua L., and Andreas Wagner. 2018. "The Causes of Evolvability and Their Evolution." *Nature Reviews. Genetics* 20 (1): 24–38.

Pochon, X., J. Pawlowski, L. Zaninetti, and R. Rowan. 2001. "High Genetic Diversity and Relative Specificity among Symbiodinium-like Endosymbiotic Dinoflagellates in Soritid Foraminiferans." *Marine Biology* 139 (6): 1069–78.

Poloczanska, Elvira S., Christopher J. Brown, William J. Sydeman, Wolfgang Kiessling, David S. Schoeman, Pippa J. Moore, Keith Brander, et al. 2013. "Global Imprint of Climate Change on Marine Life." *Nature Climate Change* 3 (10): 919–25.

Putnam, Hollie M. 2021. "Avenues of Reef-Building Coral Acclimatization in Response to Rapid Environmental Change." *The Journal of Experimental Biology* 224 (Pt Suppl 1). https://doi.org/10.1242/jeb.239319.

Putnam, Hollie M., Jennifer M. Davidson, and Ruth D. Gates. 2016. "Ocean Acidification Influences Host DNA Methylation and Phenotypic Plasticity in Environmentally Susceptible Corals." *Evolutionary Applications*. https://doi.org/10.1111/eva.12408.

Putnam, Hollie M., Michael Stat, Xavier Pochon, and Ruth D. Gates. 2012. "Endosymbiotic Flexibility Associates with Environmental Sensitivity in Scleractinian Corals." *Proceedings. Biological Sciences / The Royal Society* 279 (1746): 4352–61.

Rahmstorf, Stefan. 2010. "A New View on Sea Level Rise." *Nature Climate Change* 1 (1004): 44–45.

Regnier, Pierre, Pierre Friedlingstein, Philippe Ciais, Fred T. Mackenzie, Nicolas Gruber, Ivan A. Janssens, Goulven G. Laruelle, et al. 2013. "Anthropogenic Perturbation of the Carbon Fluxes from Land to Ocean." *Nature Geoscience* 6 (8): 597–607.

Rivera-Casas, Ciro, Rodrigo Gonzalez-Romero, Rafael A. Garduño, Manjinder S. Cheema, Juan Ausio, and Jose M. Eirin-Lopez. 2017. "Molecular and Biochemical Methods Useful for the Epigenetic Characterization of Chromatin-Associated Proteins in Bivalve Molluscs." *Frontiers in Physiology* 8 (August): 490.

Robinson, James P. W., Shaun K. Wilson, Jan Robinson, Calvin Gerry, Juliette Lucas, Cindy Assan, Rodney Govinden, Simon Jennings, and Nicholas A. J. Graham. 2019. "Productive Instability of Coral Reef Fisheries after Climate-Driven Regime Shifts." *Nature Ecology & Evolution* 3 (2): 183–90.

Rodríguez-Casariego, Javier A., Alex E. Mercado-Molina, Daniel Garcia-Souto, Ivanna M. Ortiz-Rivera, Christian Lopes, Iliana B. Baums, Alberto M. Sabat, and Jose M. Eirin-Lopez. 2020. "Genome-Wide DNA Methylation Analysis Reveals a Conserved Epigenetic Response to Seasonal Environmental Variation in the Staghorn Coral Acropora Cervicornis." *Frontiers in Marine Science* 7: 822.

Rodríguez-Casariego, Javier A., Ross Cunning, Andrew C. Baker, Jose M. Eirin-Lopez. *Submitted*. Symbiont shuffling induces differential DNA methylation responses to thermal stress in the coral Montastraea cavernosa. *Molecular Ecology*, under review.

Rose, Noah H., Francois O. Seneca, and Stephen R. Palumbi. 2015. "Gene Networks in the Wild: Identifying Transcriptional Modules That Mediate Coral Resistance to Experimental Heat Stress." *Genome Biology and Evolution* 8 (1): 243–52.

Rosenzweig, Cynthia, David Karoly, Marta Vicarelli, Peter Neofotis, Qigang Wu, Gino Casassa, Annette Menzel, et al. 2008. "Attributing Physical and Biological Impacts to Anthropogenic Climate Change." *Nature* 453 (7193): 353–57.

Rosset, S., G. Koster, J. Brandsma, A. N. Hunt, A. D. Postle, and C. D'Angelo. 2019. "Lipidome Analysis of Symbiodiniaceae Reveals Possible Mechanisms of Heat Stress Tolerance in Reef Coral Symbionts." *Coral Reefs* 38 (6): 1241–53.

Schultz, Matthew D., Yupeng He, John W. Whitaker, Manoj Hariharan, Eran A. Mukamel, Danny Leung, Nisha Rajagopal, et al. 2015. "Human Body Epigenome Maps Reveal Noncanonical DNA Methylation Variation." *Nature*. https://doi.org/10.1038/nature14465.

Shumaker, Alexander, Hollie M. Putnam, Huan Qiu, Dana C. Price, Ehud Zelzion, Arye Harel, Nicole E. Wagner, Ruth D. Gates, Hwan Su Yoon, and Debashish Bhattacharya. 2019. "Genome Analysis of the Rice Coral Montipora Capitata." *Scientific Reports* 9 (1): 2571.

Silverstein, Rachel N., Ross Cunning, and Andrew C. Baker. 2015. "Change in Algal Symbiont Communities after Bleaching, Not Prior Heat Exposure, Increases Heat Tolerance of Reef Corals." *Global Change Biology*. https://doi.org/10.1111/gcb.12706.

Solomon, Sarah L., Andréa G. Grottoli, Mark E. Warner, Stephen Levas, Verena Schoepf, and Agustí Muñoz-Garcia. 2019. "Lipid Class Composition of Annually Bleached Caribbean Corals." *Marine Biology* 167 (1): 7.

Stien, Didier, Marcelino Suzuki, Alice M. S. Rodrigues, Marion Yvin, Fanny Clergeaud, Evane Thorel, and Philippe Lebaron. 2020. "A Unique Approach to Monitor Stress in Coral Exposed to Emerging Pollutants." *Scientific Reports* 10 (1): 9601.

Strader, Marie E., Juliet M. Wong, and Gretchen E. Hofmann. 2020. "Ocean Acidification Promotes Broad Transcriptomic Responses in Marine Metazoans: A Literature Survey." *Frontiers in Zoology* 17 (February): 7.

The Royal Society, and National Academy of Sciences. 2014. *Climate Change: Evidence and Causes*. National Academies Press.

Thornhill, Daniel J., Todd C. LaJeunesse, Dustin W. Kemp, William K. Fitt, and Gregory W. Schmidt. 2006. "Multi-Year, Seasonal Genotypic Surveys of Coral-Algal Symbioses Reveal Prevalent Stability or Post-Bleaching Reversion." *Marine Biology* 148 (4): 711–22.

Torda, Gergely, Jennifer M. Donelson, Manuel Aranda, Daniel J. Barshis, Line Bay, Michael L. Berumen, David G. Bourne, et al. 2017. "Rapid Adaptive Responses to Climate Change in Corals." *Nature Climate Change* 7 (9): 627–36.

Towle, Erica K., Ian C. Enochs, and Chris Langdon. 2015. "Threatened Caribbean Coral Is Able to Mitigate the Adverse Effects of Ocean Acidification on Calcification by Increasing Feeding Rate." *PLOS ONE*. https://doi.org/10.1371/journal.pone.0123394.

Traylor-Knowles, Nikki, Noah H. Rose, and Stephen R. Palumbi. 2017. "The Cell Specificity of Gene Expression in the Response to Heat Stress in Corals." *The Journal of Experimental Biology* 220 (Pt 10): 1837–45.

Tremblay, Pascale, Andrea Gori, Jean François Maguer, Mia Hoogenboom, and Christine Ferrier-Pagès. 2016. "Heterotrophy Promotes the Re-Establishment of Photosynthate Translocation in a Symbiotic Coral after Heat Stress." *Scientific Reports*. https://doi.org/10.1038/srep38112.

Tremblay, P., R. Grover, J. F. Maguer, M. Hoogenboom, and C. Ferrier-Pagès. 2014. "Carbon Translocation from Symbiont to Host Depends on Irradiance and Food Availability in the Tropical Coral Stylophora Pistillata." *Coral Reefs* 33 (1): 1–13.

Trigg, S. A., Y. R. Venkataraman, M. Gavery, and S. B. Roberts. 2021. "Invertebrate Methylomes Provide Insight into Mechanisms of Environmental Tolerance and Reveal Methodological Biases." *bioRxiv*. https://www.biorxiv.org/content/10.1101/2021.03.29.437539v1.abstract.

Venkataraman, Yaamini R., Alan M. Downey-Wall, Justin Ries, Isaac Westfield, Samuel J. White, Steven B. Roberts, and Kathleen E. Lotterhos. 2020. "General DNA Methylation Patterns and Environmentally-Induced Differential Methylation in the Eastern Oyster (Crassostrea Virginica)." *Frontiers in Marine Science* 7: 225.

Vidal-Dupiol, Jeremie, Didier Zoccola, Eric Tambutté, Christoph Grunau, Céline Cosseau, Kristina M. Smith, Michael Freitag, Nolwenn M. Dheilly, Denis Allemand, and Sylvie Tambutté. 2013. "Genes Related to Ion-Transport and

Energy Production Are Upregulated in Response to CO2-Driven pH Decrease in Corals: New Insights from Transcriptome Analysis." *PloS One* 8 (3): e58652.

Wright, Rachel M., Galina V. Aglyamova, Eli Meyer, and Mikhail V. Matz. 2015. "Gene Expression Associated with White Syndromes in a Reef Building Coral, Acropora Hyacinthus." *BMC Genomics* 16 (May): 371.

Yamashiro, Hideyuki, Hirosuke Oku, Kyoko Onaga, Hironori Iwasaki, and Kensaku Takara. 2001. "Coral Tumors Store Reduced Level of Lipids." *Journal of Experimental Marine Biology and Ecology* 265 (2): 171–79.

Yanagida, Hayato, Ariel Gispan, Noam Kadouri, Shelly Rozen, Michal Sharon, Naama Barkai, and Dan S. Tawfik. 2015. "The Evolutionary Potential of Phenotypic Mutations." *PLoS Genetics* 11 (8): e1005445.

Yetsko, K., M. Ross, A. Bellantuono, and D. Merselis. 2020. "Genetic Differences in Thermal Tolerance among Colonies of Threatened Coral Acropora Cervicornis: Potential for Adaptation to Increasing Temperature." *Marine Ecology* . https://www.int-res.com/abstracts/meps/v646/p45-68/.

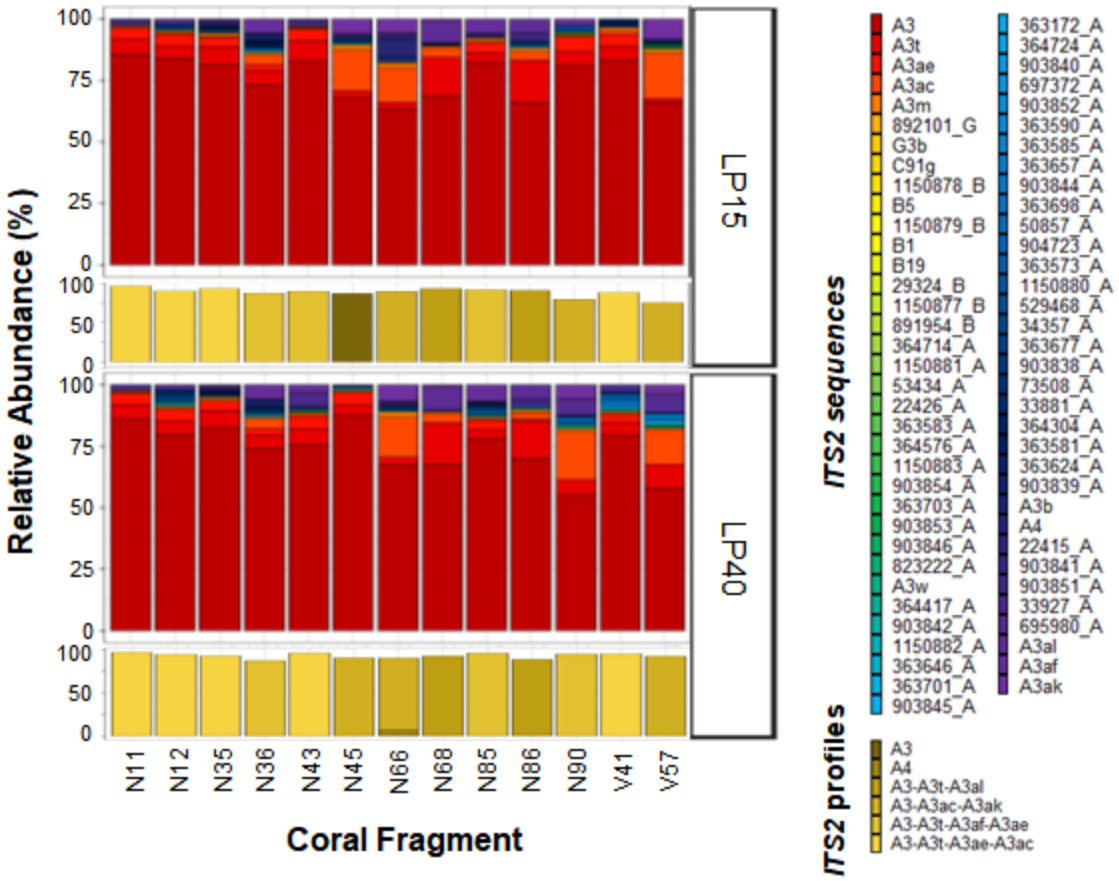

Fig. 1. Relative abundance of ITS2 sequences and predicted profiles of symbiont types for *A. cervicornis* ramets outplanted to sites located at 3 m (LP15) and 15 m (LP40) depths in Luis Peña Reef, Culebra, PR, and sampled one-year post-outplanting. Each column in the stacked bar plots represents a colony with ramets sampled from the depth specified on the right-hand side. For each section the relative abundance of ITS2 sequences (top) and relative abundance of ITS2 type profiles (bottom) are represented. Only ITS2 sequences contributing >0.01% in at least 1 sample are labeled. Named sequences (e.g., A3ae or A4) refer to sequences used to characterize the ITS2 type profiles, or sequences commonly found in previous analysis through SymPortal (Hume et al. 2019). Other lesser representative sequences are shown with their database ID and their clade identifier (e.g., 29324_B).

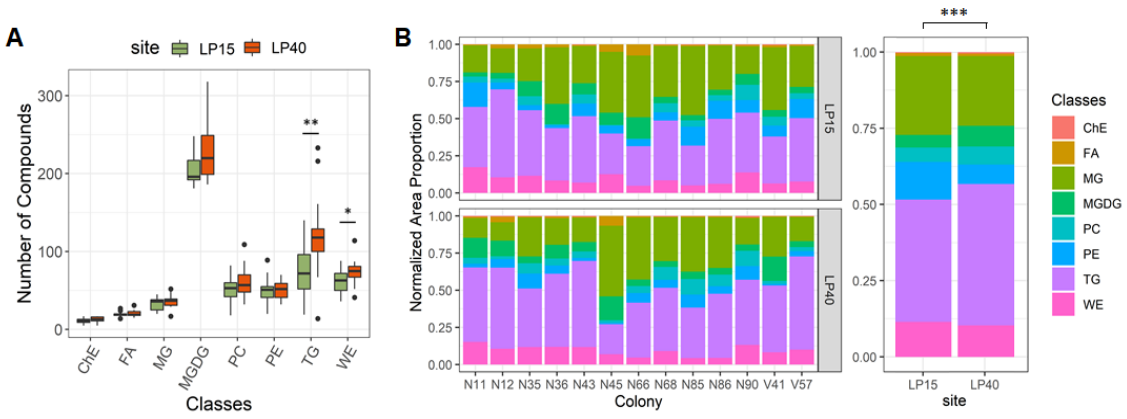

Fig. 2 Lipid profiles derived from coral ramets maintained at depths of 3m (LP15) or 15m (LP40) in Luis Peña reef, Culebra. PR. for a year. **(A)** Lipid extraction results for the butanol:methanol methods expressed as number of compounds per each of eight lipid classes. Results of pairwise comparisons through t-test between sites are represented by asterisks: (*****) $p < 0.05$; (******) $p < 0.01$. **(B)** Proportional abundance of lipids (calculated from normalized peak areas) per class across all genets and outplanting sites. Asterisks represent significance of chi-square tests for each class ($p < 0.001$). **ChE** cholesterol ester, **FA** Fatty acid, **MG** mono-acyl glycerol, **MGDG** Monogalactosyldiacylgylcerol, **PC** Phosphatidylcholine, **PE** Phosphatidylethanolamine, **TG** Triglyceride and **WE** Wax ester.

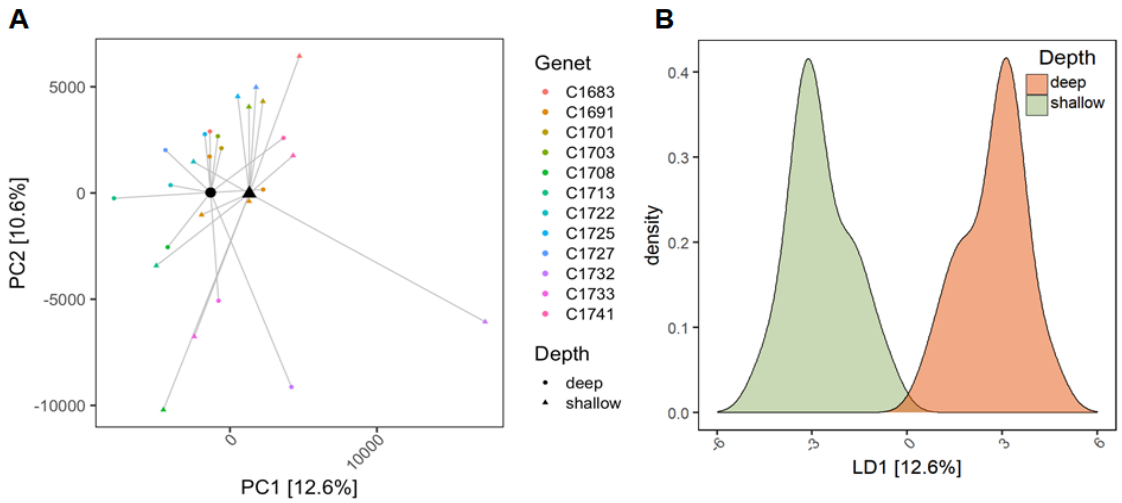

Fig. 3. Divergence of transcriptional state in *A. cervicornis* ramets maintained at 3m or 15m for a year. **(A)** Principal Coordinate Analysis (PCoA) of "manhattan" distances based on variance-stabilized gene counts. Larger symbols represent the centroid of the sample distribution for each depth **(B)** Discriminant analysis of principal components (DAPC).

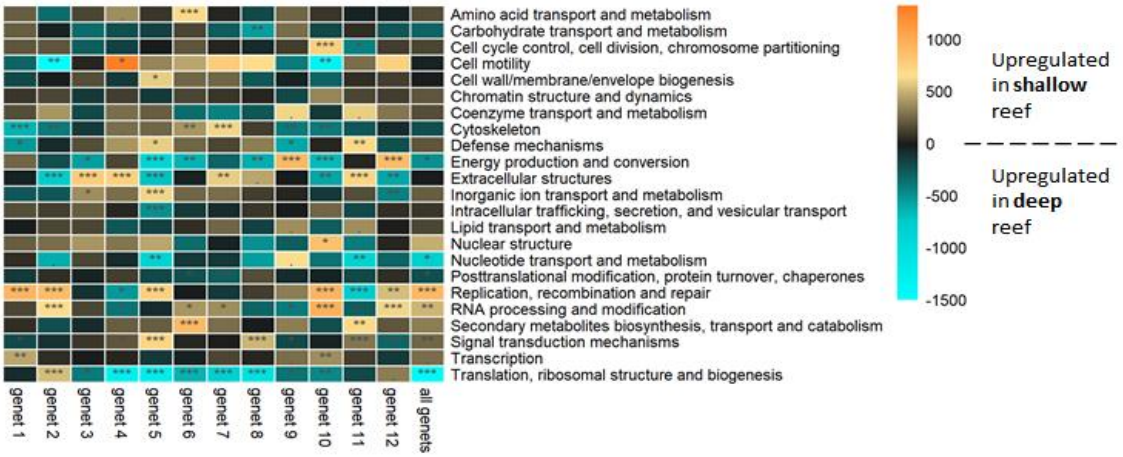

Fig. 4. Eukaryotic ortholog group (KOG) enrichment analysis results. KOG functional categories up- or down-regulated (indicated by color) for the contrast shallow vs deep reef of each individual genet and the combination of all genets. Statistical significance is represented as: (**.**) FDR < 10%; (*) FDR < 5%; (**) FDR < 1%; (***) FDR < 0.1 %.

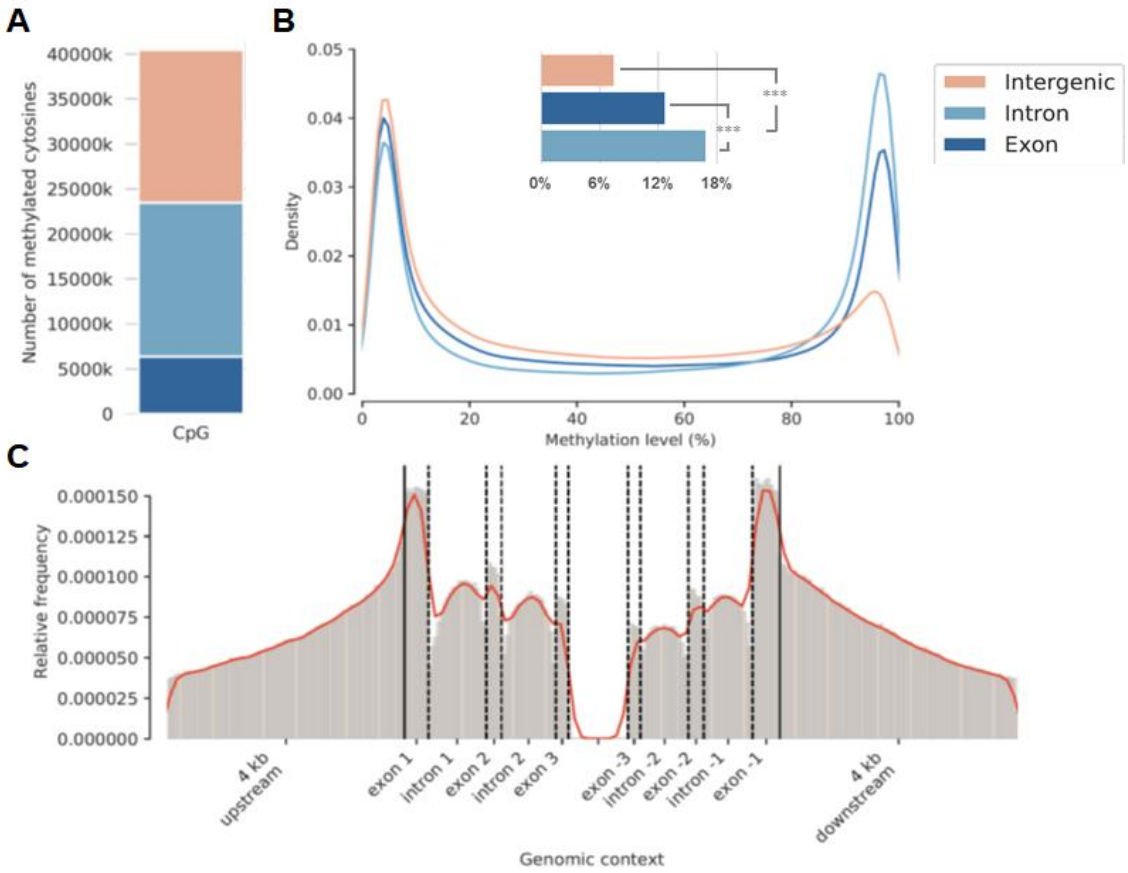

Fig. 5. DNA methylation characteristics of *A. cervicornis*. **(A)** Number of Methylated cytosines overlapping with genic and intergenic regions. **(B)** Distribution of DNA methylation levels (% methylation) in exons, introns, and intergenic regions. Significant differences in methylation levels between features is represented by asterisks: (***) p-value < 0.001. **(C)** Frequency of methylated CpGs across a gene model with 4-kb flanking regions. Solid lines represent start and end transcription sites. Genic region lengths were normalized in correspondence with mean lengths in the genome of *A. cervicornis*.

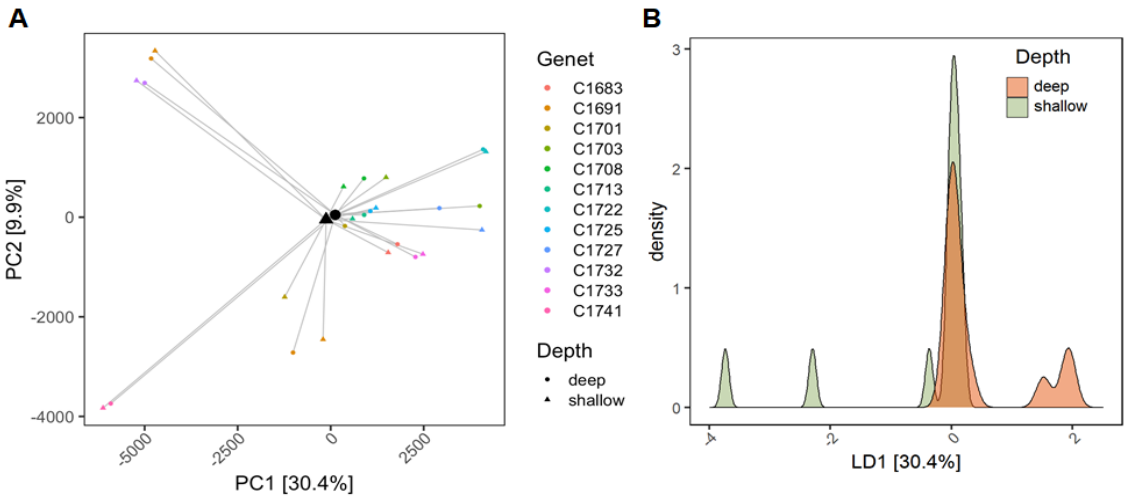

Fig 6. General DNA methylation patterns in *A. cervicornis* ramets maintained at 3m or 15m for a year. (**A**) Plot of the first two principal components from a principal coordinate analysis (PCoA) by depth and genotype, based on "manhattan" distances of percent methylation of 100bp windows. (**B**) Density plot of a discriminant analysis of principal components.

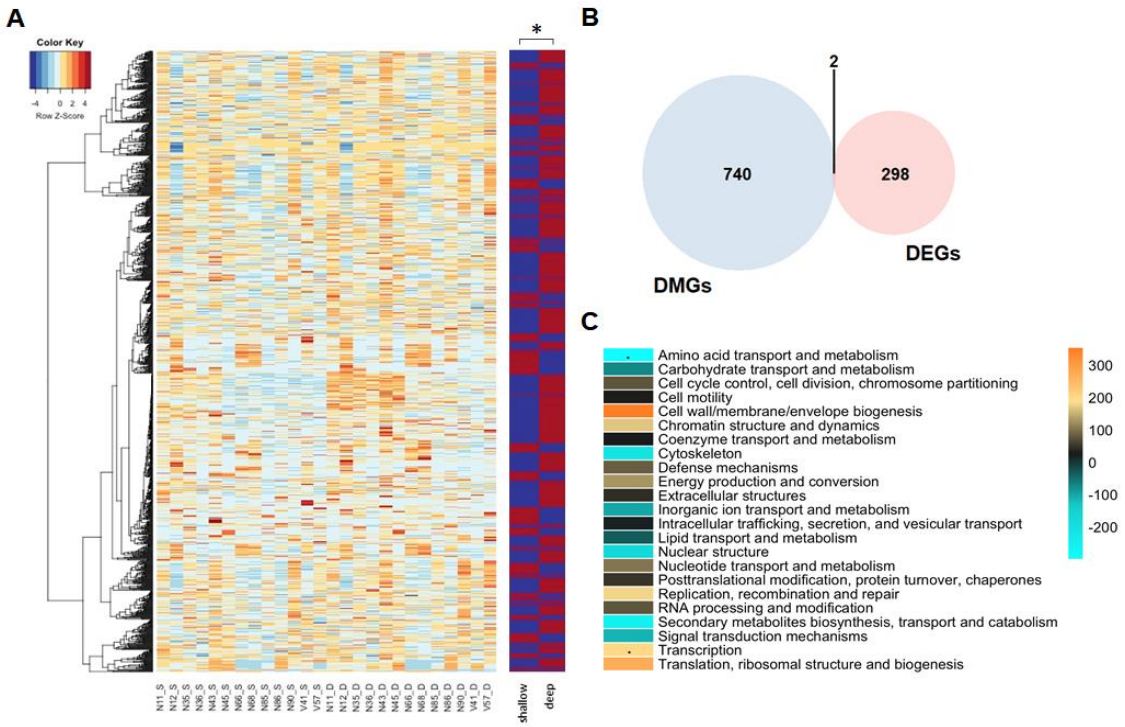

Fig. 7. Divergence of gene body methylation in *A. cervicornis* ramets maintained at 3m or 15m for a year. **(A)** Heatmap of methylation level for 742 differentially methylated genes (DMGs) by sample (left) and grouped by site (right). Asterisk represents significant differences in gene methylation level between sites (PERMANOVA, p-value = 0.0163). **(B)** Venn Diagram showing relationship between DMGs and differentially expressed genes (DEGs). Only 2 genes were differentially expressed and methylated: an ATP-dependent RNA helicase DDX41, and a tyrosine-protein kinase Fyn. **(C)** KOG functional categories hyper- or hypo-methylated (indicated by color) for the contrast shallow (num) vs deep (den) reefs. Statistical significance is represented as: (**.**) FDR < 10%.

Table 1. Number of differentially expressed genes (DEGs) within individual genets and across all genets identified using DESeq with an adjusted p-value < 0.1. In brackets are the numbers of significantly up- and down-regulated genes.

All genets	genet 1	genet 2	genet 3	genet 4	genet 5	genet 6	genet 7	genet 8	genet 9	genet 10	genet 11	genet 12
300 [111, 189]	1 [1, 0]	10 [7, 3]	32 [19, 13]	37 [18, 19]	16 [6, 10]	0 [0, 0]	0 [0, 0]	0 [0, 0]	42 [10, 32]	64 [15, 49]	0 [0, 0]	0 [0, 0]

CHAPTER VI

GENERAL CONCLUSIONS

Oceans bear the brunt of human industrial development, with dramatic increases in atmospheric CO_2 warming and acidifying surface waters, and pollution disrupting biogeochemical cycles and biological processes, and resulting in biodiversity losses and ecosystem collapse. The unprecedented rate of disturbance imposed by human-driven global change has the potential to overwhelm natural eco-evolutionary mechanisms mediating organism's adaptation and allowing ecosystem resilience. The survival of marine ecosystems will therefore depend not only on the capacity of natural ecosystems to accelerate their acclimatization/adaptation rates, but on our understanding of the mechanisms involved in such responses allowing appropriate interventions to mitigate the detrimental effects of climate change when necessary.

Corals reefs represent the most diverse ecosystems in the oceans providing critical services and goods for human society (e.g., fisheries and aquaculture production, shoreline protection, and recreation). Unfortunately, coral reef's decline has been documented for decades, with substantial mechanistic evidence linking such collapses to the effects of global change on stony corals. A remarkable capacity for phenotypic plasticity and acclimation of corals has been observed at molecular, physiological, and morphological levels. Despite these elements and the critical ecological and economic importance of coral reefs, it wasn't until very recently that the scientific community started focusing on the study of molecular mechanisms mediating such plasticity, and their potential to drive corals rapid acclimatization and adaptation (Eirin-Lopez and Putnam 2019; Putnam 2021). For example, it was not until 2011 that the first coral genome was completed (Shinzato et al. 2011), limiting the application of molecular biology tools in this group. This dissertation contributes to filling this gap by pioneering the characterization of epigenetic mechanisms involved in responses to varied environmental stressors,

employing an array of field and laboratory-based experiments to describe the functionality and dynamics of such mechanisms, and their interaction with the genome and other components of the coral holobiont.

Accordingly, details of several epigenetic mechanisms were described for the first time in corals. In Chapter II we described the histone repertoire at the protein level for the first time for corals and demonstrated the functionality of the histone variant H2A.X mediating responses to nutrient pollution and thermal stress in the coral *Acropora cervicornis*. Regardless of the limitations of the methodology used to evaluate DNA methylation in this chapter, the observed changes in global DNA methylation hinted at the possibility of its role in the stress response, and of a cross-talk between epigenetic mechanisms, further evidenced in other cnidarians (Li et al. 2018; Weizman and Levy 2019).

Focusing on DNA methylation, detailed methylomes for two coral species; *Montastraea cavernosa* in Chapter IV and *Acropora cervicornis* in Chapter V, were characterized for the first time in this work. General methylation landscapes showed substantial differences between species, potentially related to differential sensitivity to environmental stress (Trigg et al. 2021). Although links between methylation and gene expression in corals have been described before (Liew et al. 2018; Dixon et al. 2018), the results of these two chapters evidence that other mechanisms might be interacting with DNA methylation so the regulation of gene expression can be the results of multi-mechanism crosstalk. Both inducible DNA methylation and differential gene expression [see Cunning and Baker (2020) for gene expression results in *M. cavernosa*] was observed in response to environmental change, adding symbiont shuffling, thermal stress,

and depth-linked environmental divergence as drivers of epigenetic change and gene expression plasticity. However, very little overlapping occurred between differentially methylated and expressed genes, only confirming previous evidence of a reduction of spurious transcription mediated by increased DNA methylation (Liew et al. 2018; Dixon et al. 2018).

Substantial genotype-driven variability in DNA methylation between corals exposed to shared environmental conditions was evidenced at various resolutions (global, fragment, base-pair) though all chapters of the dissertation. Adding to previous results in *A. palmata* (Durante et al. 2019), this tight dependence of DNA methylation on the genome sequence indicates that at least a portion of the methylation pattern is inherited. However, substantial evidence was also found in this dissertation of similarly induced DNA methylation changes between genets in response to shared environmental exposure. Chapter III, for example, demonstrated dynamic seasonal variability in DNA methylation patterns linked to seasonal changes in temperature for the corals *A. cervicornis* irrespective of their genotype and stress exposure history. So, is inducible DNA methylation inherited trans-generationally? Although evidence of the inheritance of specific methylation patterns in genes functionally enriched under specific environmental conditions was observed before in corals (Liew et al. 2020), it is hard to separate inducible from stable methylation. Similar to the findings in the coral *P. daedalea* (Liew et al. 2020), global methylation patterns of *A. cervicornis* and *M. cavernosa* tend to be very similar between ramets or genetically closer individuals, and it's only at the regional or gene levels that clear evidence of environmentally inducible patterns arise. Additional work focusing on clonal lines exposed to divergent environments in a multigenerational

design will be required to elucidate the inheritance of inducible DNA methylation and its role modulating gene expression plasticity.

Coral's symbiotic community composition, abundance and physiology may also influence host epigenetic responses. In Chapter II, we evidenced the effect of symbiont-host nutritional interactions modulating epigenetic mechanisms, demonstrating the interaction between host epigenetic machinery and the symbiont physiology. Impairment of the phosphorylation of the histone H2A.X, involved in DNA repair and cell cycle regulation (Fernandez-Capetillo et al. 2004; Orlando et al. 2021), was observed as a result of phosphorus starvation driven by symbiont population growth under nitrogen enrichment. Additional evidence of such interaction was provided by the results of Chapter IV where DNA methylation responses to thermal stress in *M. cavernosa* were dependent on the dominant clade of Symbiodinacea, similar to the previously described changes in gene expression (Cunning and Baker 2020).

Overall, this dissertation contributes to better understand the epigenetic mechanisms and their role modulating plastic responses to environmental variations. Through the initial characterization of chromatin associated proteins and DNA chemical modifications, their response when faced to various environmental conditions, and their interaction with other non-genetic mechanisms to mediate phenotypic responses, this work provides significant contributions to the understanding of the mechanisms of rapid acclimatization and adaptation in corals. Moreover, this knowledge provides a better basis to evaluate the feasibility of intervention strategies aimed at the manipulation of these modulators of phenotypic plasticity.

Further research is needed to identify the interaction between epigenetic mechanisms, other non-genetic mechanisms, and expression changes in these organisms. Taking into consideration the dynamic response of these mechanisms and the variability in their temporal stabilities evidenced in our results, it is very likely that a combination of non-genetic mechanisms acting in a probabilistic rather than a deterministic way, interact to regulate transcriptional and posttranscriptional processes (Adrian-Kalchhauser et al. 2020). Recent studies, including that in Chapter II, have found evidence of this epigenetic crosstalk in cnidarians (Li et al. 2018; Rodriguez-Casariego et al. 2018), supporting the idea that phenotypic responses to environmental variation will depend on the establishment of a multi-mechanism epigenetic landscape. However, only the analysis of multi-omic data sets resulting from specific tissue types, or even individual cells (Levy et al. 2021), will allow the disentangling of such a complex process by reducing variability.

References

Cunning, Ross, and Andrew C. Baker. 2020. "Thermotolerant Coral Symbionts Modulate Heat Stress-responsive Genes in Their Hosts." *Molecular Ecology*. https://doi.org/10.1111/mec.15526.

Dixon, Groves, Yi Liao, Line K. Bay, and Mikhail V. Matz. 2018. "Role of Gene Body Methylation in Acclimatization and Adaptation in a Basal Metazoan." *Proceedings of the National Academy of Sciences of the United States of America* 115 (52): 13342–46.

Durante, Meghann K., Iliana B. Baums, Dana E. Williams, Sam Vohsen, and Dustin W. Kemp. 2019. "What Drives Phenotypic Divergence among Coral Clonemates of Acropora Palmata?" *Molecular Ecology* 28 (13): 3208–24.

Eirin-Lopez, Jose M., and Hollie M. Putnam. 2019. "Marine Environmental Epigenetics." *Annual Review of Marine Science*. https://doi.org/10.1146/annurev-marine-010318-095114.

Fernandez-Capetillo, Oscar, Alicia Lee, Michel Nussenzweig, and André Nussenzweig. 2004. "H2AX: The Histone Guardian of the Genome." *DNA Repair* 3 (8-9): 959–67.

Levy, Shani, Anamaria Elek, Xavier Grau-Bové, Simón Menéndez-Bravo, Marta Iglesias, Amos Tanay, Tali Mass, and Arnau Sebé-Pedrós. 2021. "A Stony Coral Cell Atlas Illuminates the Molecular and Cellular Basis of Coral Symbiosis, Calcification, and Immunity." *Cell*. https://doi.org/10.1016/j.cell.2021.04.005.

Liew, Yi Jin, Emily J. Howells, Xin Wang, Craig T. Michell, John A. Burt, Youssef Idaghdour, and Manuel Aranda. 2020. "Intergenerational Epigenetic Inheritance in Reef-Building Corals." *Nature Climate Change* 10 (3): 254–59.

Liew, Yi Jin, Didier Zoccola, Yong Li, Eric Tambutté, Alexander A. Venn, Craig T. Michell, Guoxin Cui, et al. 2018. "Epigenome-Associated Phenotypic Acclimatization to Ocean Acidification in a Reef-Building Coral." *Science Advances* 4 (6): eaar8028.

Li, Yong, Yi Jin Liew, Guoxin Cui, Maha J. Cziesielski, Noura Zahran, Craig T. Michell, Christian R. Voolstra, and Manuel Aranda. 2018. "DNA Methylation Regulates Transcriptional Homeostasis of Algal Endosymbiosis in the Coral Model Aiptasia." *Science Advances* 4 (8): eaat2142.

Orlando, Luca, Borko Tanasijevic, Mio Nakanishi, Jennifer C. Reid, Juan L. García-Rodríguez, Kapil Dev Chauhan, Deanna P. Porras, et al. 2021. "Phosphorylation State of the Histone Variant H2A.X Controls Human Stem and Progenitor Cell Fate Decisions." *Cell Reports* 34 (10): 108818.

Putnam, Hollie M. 2021. "Avenues of Reef-Building Coral Acclimatization in Response to Rapid Environmental Change." *The Journal of Experimental Biology* 224 (Pt Suppl 1). https://doi.org/10.1242/jeb.239319.

Shinzato, Chuya, Eiichi Shoguchi, Takeshi Kawashima, Mayuko Hamada, Kanako Hisata, Makiko Tanaka, Manabu Fujie, et al. 2011. "Using the Acropora Digitifera Genome to Understand Coral Responses to Environmental Change." *Nature* 476 (7360): 320–23.

Trigg, S. A., Y. R. Venkataraman, M. Gavery, and S. B. Roberts. 2021. "Invertebrate Methylomes Provide Insight into Mechanisms of Environmental Tolerance and Reveal Methodological Biases." *bioRxiv*. https://www.biorxiv.org/content/10.1101/2021.03.29.437539v1.abstract.

Weizman, Eviatar, and Oren Levy. 2019. "The Role of Chromatin Dynamics under Global Warming Response in the Symbiotic Coral Model Aiptasia." *Communications Biology* 2 (August): 282.

Appendix A: Supplementary materials for Chapter II

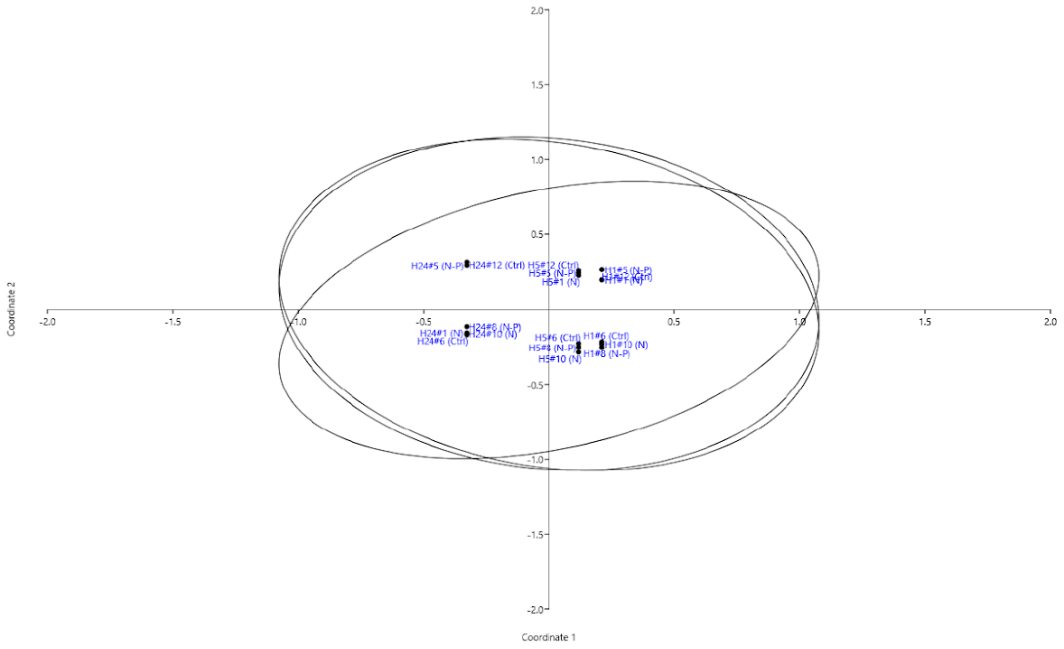

Suppl. Fig. 1, Rodriguez-Casariego et al. 2018

Appendix B: Supplementary materials for Chapter III

Supplementary Table S1. Environmental parameters summary statistics. Data corresponding to deployments in summer (Sept) and winter (Jan) peaks of multiprobe sensors at Luis Peña reef, Culebra, PR. Shallow (5 m) and deep (15 m) sites were included.

	Depth		**Season**		**Total**
	Deep | A	**Shallow | B**	**Summer | A**	**Winter | B**	
Temperature °C | Mean	27	26.9	28.9 > B	26.2 < A	26.9
Temperature °C | Std. dev.	1.2	1.2	0.2	0.2	1.2
Temperature °C | Unw. valid N	824	824	437	1211	1648
pH | Mean	8.0 < B	8.1 > A	8.0 < B	8.1 > A	8.1
pH | Std. dev.	0	0.1	0	0.1	0.1
pH | Unw. valid N	824	824	437	1211	1648
PAR | Mean	99.0 < B	243.5 > A	201.9 > B	161.8 < A	172.4
PAR | Std. dev.	143.9	348.6	320.8	258.6	276.8
PAR | Unw. valid N	819	819	434	1209	1643
ODO mg L^{-1} | Mean	6.4	6.4	6.3 < B	6.5 > A	6.4
ODO mg L^{-1} | Std. dev.	0.2	0.4	0.3	0.3	0.3
ODO mg L^{-1} | Unw. valid N	824	824	437	1211	1648
Salinity psu | Mean	37.1 > B	37.0 < A	36.1 < B	37.4 > A	37
Salinity psu | Std. dev.	0.7	0.9	0.1	0.6	0.8
Salinity psu | Unw. valid N	824	824	437	1211	1648

only significant differences ($p < 0.05$) were represented as > or < the corresponding factor labeled as A or B as in table header. PAR: Photosynthetically Active Radiation. ODO: Dissolved Oxygen derived from an optical sensor.

Supplementary Table S2. PERMANOVA results of Symbiodiniaceae ITS2 sequences and type profiles derived from ten *A. cervicornis* fragments sampled at three times during the 17-month experiment (T3, T12 & T17).

Dataset		df	SS	MS	F.model	R^2	p (>F)
ITS2 sequences	time	2	0.0114	0.0057	0.2360	0.0172	0.7807
	Residuals	27	0.6500	0.0241		0.9828	
	Total	29	0.6614			1.0000	
ITS2 type profiles	time	2	0.2004	0.10019	0.2552	0.0185	0.6646
	Residuals	27	10.6014	0.3926		0.9815	
	Total	29	10.8018				

analysis based on Bray-Curtis Dissimilarities. Model ~ *time*, *strata* = *fragments* and 9,999 permutations to estimate p-values were used in the *adonis* function (vegan R package). **df**: degrees of freedom, **SS**: Sum of Squares, **MS**: Mean Squares, **F.model**: pseudo F statistics, $\mathbf{R^2}$: coefficient of determination.

Supplementary Table S3. PERMANOVA Partitioning and Analysis of DNA Methylation patterns in *A. cervicornis* in Culebra, PR.

	df	SS	MS	F.model	R^2	p (>F)
genet	6	204.2	34.036	2.3315	0.0593	**0.0131**
fragment	35	563.9	16.112	1.1037	0.1636	**0.0131**
time	5	454.2	90.838	6.2223	0.1318	**0.0001**
site	2	25.5	12.752	0.8735	0.0074	0.6637
genet:time	29	425.5	14.672	1.0050	0.1234	0.4083
frag:time	107	1481.5	12.846	0.9485	0.4298	0.6828
Residuals	20	292.0	14.599		0.0847	
Total	204	3446.8		1.0000		

analysis based on MSAP-patterns-derived Euclidean Distances. Model ~ *genet*fragment*time + Site, strata = fragments* and 9,999 permutations to estimate p-values were used in the *adonis* function (vegan R package). **df**: degrees of freedom, **SS**: Sum of Squares, **MS**: Mean Squares, **F.model**: pseudo F statistics, **R^2**: coefficient of determination.

Supplementary Table S4. Envfit vector adjustment (permutations = 999) of site-specific abiotic parameters in Luis Peña deep and shallow sites to the Non-metric Multidimensional Scaling (NMDS) ordination of the DNA methylation patterns of T5 and T12.

	NMDS1	NMDS2	R^2	p (>r)
PAR_mean	0.0516	-0.9985	0.0066	0.9150
Temp_mean	0.5829	0.8126	0.6474	**0.0010**
pH_mean	-0.5790	-0.8156	0.4008	**0.0010**
ODO_mean	-0.4781	-0.8783	0.4532	**0.0010**
Sal.psu_mean	-0.4382	-0.8989	0.1047	0.2000
Pressure	-0.8157	0.5785	0.0048	0.9350
PAR_var	0.6951	-0.7189	0.0041	0.9480
Temp_var	0.6128	0.7903	0.0537	0.4370
pH_var	0.1491	0.9888	0.0132	0.8150
ODO_var	-0.5851	-0.8109	0.0903	0.2310
Sal.psu_var	-0.6465	-0.7630	0.2946	**0.0120**

values of $p < 0.05$ are in bold. R^2, proportion of variance explained. NMDS 1 and NMDS 2, vector orientation respective to first and second axes of NMDS, respectively. **PAR_mean**, monthly average of daily mean photosynthetically active radiation (µmol (photons) m^{-2} s^{-1}); **Temp_mean**, monthly average of daily mean temperature (°C); **pH_mean**, monthly average of daily mean pH; **ODO_mean**, monthly average of daily means of dissolved oxygen (mg L^{-1}, optical sensor); **Sal.psu_mean**, monthly average of daily mean salinity (psu). **_var**, total variance. All environmental variables were measured *in-situ*.

Supplementary Table S5. Envfit vector adjustment (permutations = 999) of regional temperature and irradiance variables in the NMDS ordination of the DNA methylation patterns of all samples in shallow sites for both study reefs.

	NMDS1	NMDS2	R^2	p(>r)
Temp_mean	-0.9795	-0.2017	0.2335	**0.0010**
IR_mean	-0.6901	0.7237	0.0810	**0.0060**
CV3_temp	-0.2340	0.9722	0.0459	**0.0700**
CV3_IR	0.9710	-0.2391	0.3855	**0.0010**

values of $p < 0.05$ are in bold. **Temp_mean**, monthly average of daily mean temperature (°C); **IR_mean**, monthly average of daily mean of surface solar irradiance (W/m^{-2}). **CV3_** refers to the coefficient of variation of temperature of irradiance for the three months previous to each sample point.

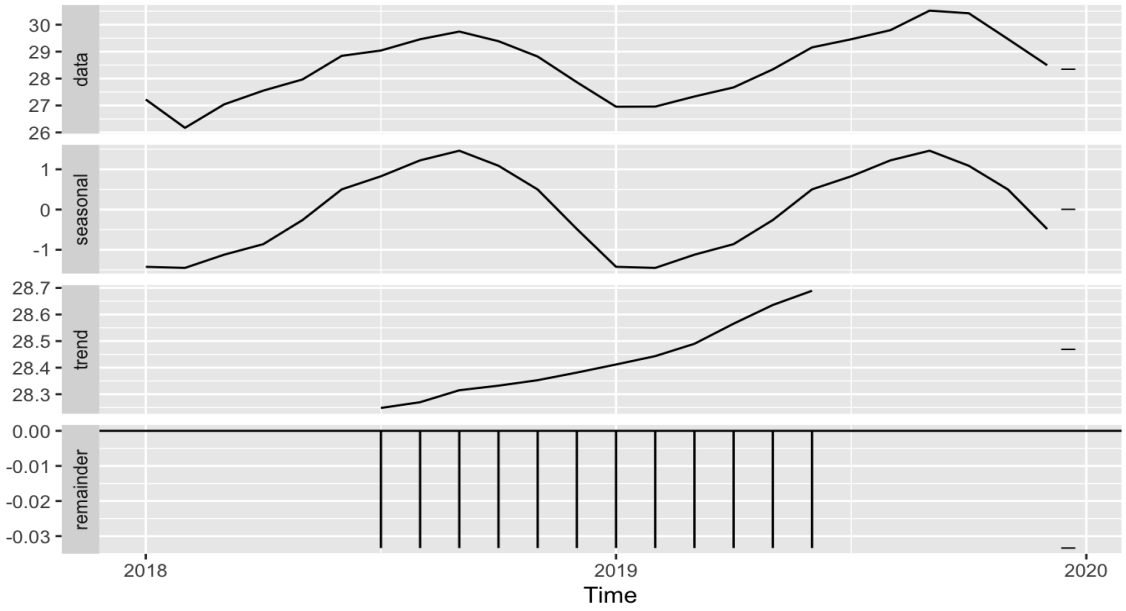

Supplementary Fig S1. Decomposition of additive temperature time series of monthly daily means to show the trend from 2018-2019 in Culebra, PR. Data records were gathered from NOAA Data Buoy Center, Station CLBP4 located 3.8 and 4 km from Luis Peña and Carlos Rosario reefs, respectively.

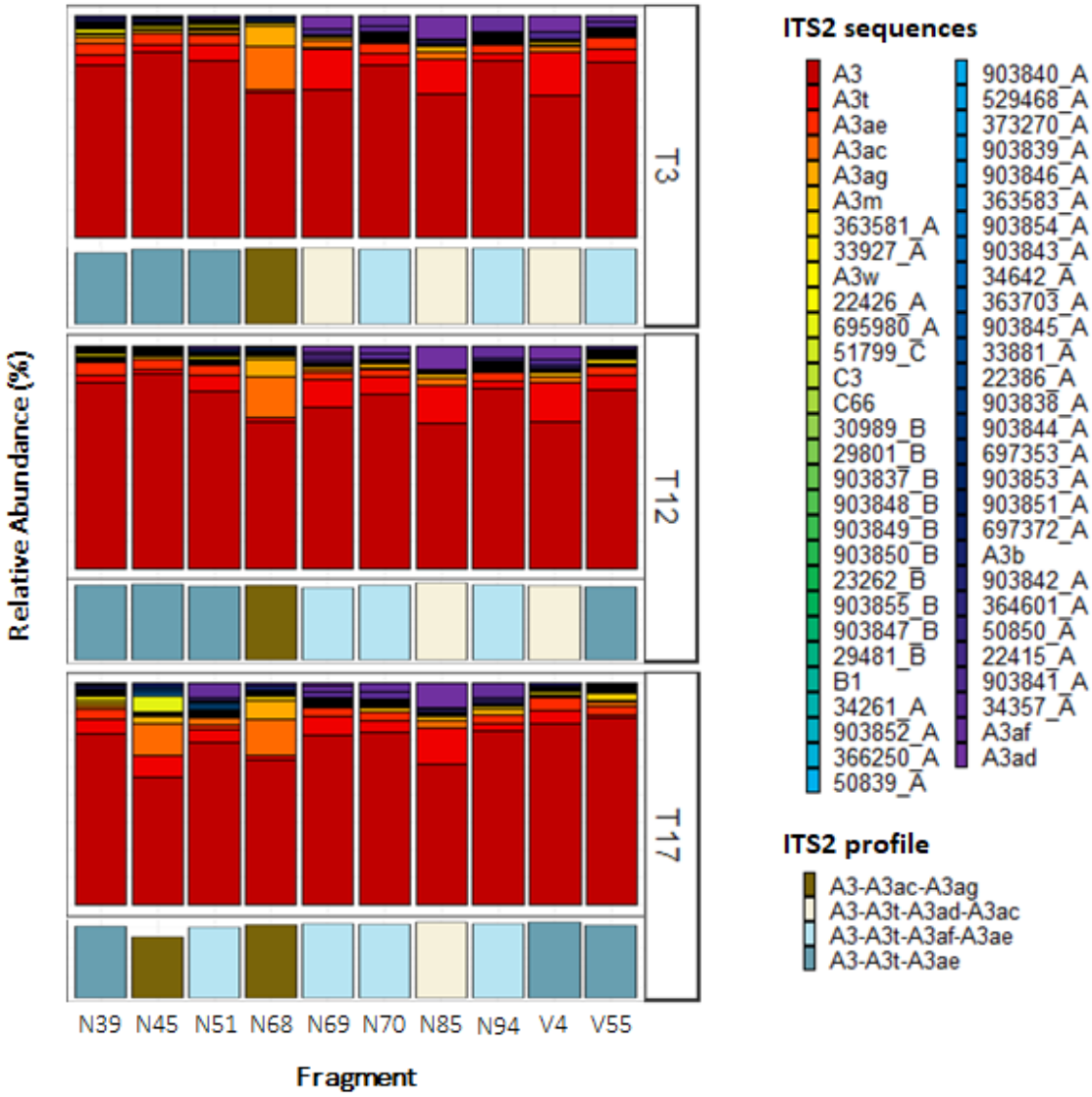

Supplementary Fig S2. Relative abundance of ITS2 sequences and predicted profiles from *A. cervicornis* samples collected in July 2018 (T3), April 2019 (T12) and September 2019 (T17) from Luis Peña and Carlos Rosario Reefs, Culebra, PR. Each column in the stacked bar plots represents a fragment sampled at the collection time specified on the right-hand side. For each section the relative abundance of ITS2 sequences (top) and relative abundance of ITS2 type profiles (bottom) are represented. Only ITS2 sequences contributing >0.01% in at least 1 sample are labeled. Named sequences (e.g. A3, A3t, or C3) refer to sequences used to characterize ITS2 type profiles or commonly found in previous analysis through SymPortal (Hume et al. 2019). Other lesser representative sequences are shown with their database ID and their clade identifier (e.g. 50839_A).

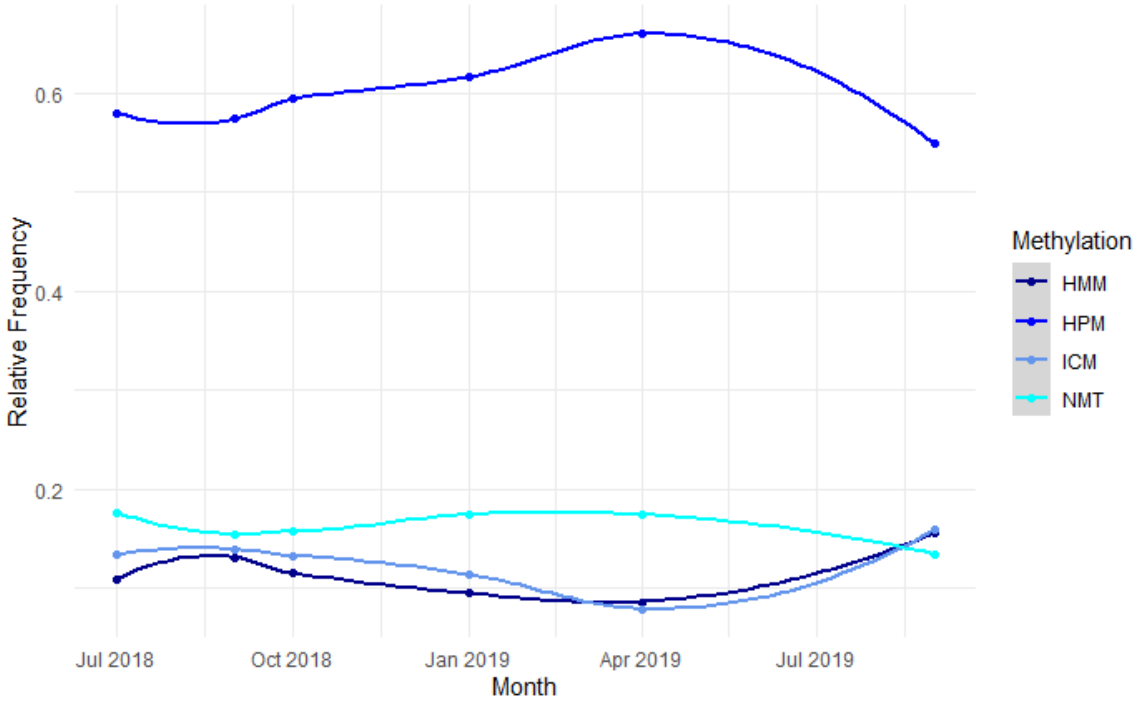

Supplementary Fig. S3. Temporal trend in DNA methylation states along the 17-month period of the study. DNA methylation states are based on differential cuts of MSAP restriction enzymes (Reyna-Lopez et al. 1997). Relative frequency of each methylation state is composed of all samples (n=205) and the 162 loci showing methylation polymorphism.

Appendix C: Supplementary materials for Chapter IV

Supplementary Table S1: Proportion test results for genomic features overlap between all genomic CpGs and methylated (>50% methylation) CpGs.

Feature	meth CpG	all CpG	stat	conf.low	conf.high	*p*.adj	Odds ratio
CDS	257654	1810701	16791.61	0.013616	0.013999	$<10^{-10}$	0.756755
5'-UTR	9188	120261	7177.284	0.002282	0.002362	$<10^{-10}$	0.41132
Intergenic	3548193	20107691	20990.3	0.031124	0.031989	$<10^{-100}$	0.871237
Intron	1375120	5733932	92345.16	-0.05578	-0.05502	$<10^{-100}$	**1.388957**
Promoter	208084	1628282	27158.44	0.016427	0.016777	$<10^{-10}$	0.677723
Repeat	204824	680559	38706.82	-0.01412	-0.01379	$<10^{-10}$	**1.647602**
3'-UTR	38199	360414	11189.37	0.00499	0.005146	$<10^{-100}$	0.569014

Stat: Pearson's chi-squared test statistic; **conf.low/high**: 95% confidence intervals; ***p*.adj**: Benjamini-Hochberg adjusted *p*.value

Supplementary Table S2: Gene annotation details of genes overlapping with differentially methylated regions DMRs.

gene	sprot_Top_BLASTP_hit	gene_ontology_blast
Mcavernosa00583	UBXN4_BOVIN\UBXN4_BOVIN\Q:181-379,H:307-508\41.67%ID\E:1e-38\RecName: Full=UBX domain-containing protein 4;\Eukaryota; Metazoa; Chordata; Craniata; Vertebrata; Euteleostomi; Mammalia; Eutheria; Laurasiatheria; Cetartiodactyla; Ruminantia; Pecora; Bovidae; Bovinae; Bos|||UBXN4_RAT\UBXN4_RAT\Q:181-379,H:305-506\40.58%ID\E:4e-37\RecName: Full=UBX domain-containing protein 4;\Eukaryota; Metazoa; Chordata; Craniata; Vertebrata; Euteleostomi; Mammalia; Eutheria; Euarchontoglires; Glires; Rodentia; Myomorpha; Muroidea; Muridae; Murinae; Rattus|||UBXN4_PONAB\UBXN4_PONAB\Q:190-379,H:314-508\41.38%ID\E:2e-36\RecName: Full=UBX domain-containing protein 4;\Eukaryota; Metazoa; Chordata; Craniata; Vertebrata; Euteleostomi; Mammalia; Eutheria; Euarchontoglires; Primates; Haplorrhini; Catarrhini; Hominidae; Pongo|||UBXN4_PONAB\UBXN4_PONAB\Q:1-149,H:1-134\43.62%ID\E:7e-36\RecName: Full=UBX domain-containing protein 4;\Eukaryota; Metazoa; Chordata; Craniata;	GO:0005829\cellular_component\cytosol|||GO:0005789\cellular_component\endoplasmic reticulum membrane|||GO:0005635\cellular_component\nuclear envelope|||GO:0006986\biological_process\response to unfolded protein|||GO:0030433\biological_process\ubiquitin-dependent ERAD pathway

gene	sprot_Top_BLASTP_hit	gene_ontology_blast
	Vertebrata; Euteleostomi; Mammalia; Eutheria; Euarchontoglires; Primates; Haplorrhini; Catarrhini; Hominidae; Pongo|||\UBXN4_RAT\UBXN4_RAT\Q:1-130,H:1-133\47.01%ID\E:3e-35\RecName: Full=UBX domain-containing protein 4;\Eukaryota; Metazoa; Chordata; Craniata; Vertebrata; Euteleostomi; Mammalia; Eutheria; Euarchontoglires; Glires; Rodentia; Myomorpha; Muroidea; Muridae; Murinae; Rattus|||\UBXN4_BOVIN\UBXN4_BOVIN\Q:1-114,H:1-113\48.25%ID\E:4e-35\RecName: Full=UBX domain-containing protein 4;\Eukaryota; Metazoa; Chordata; Craniata; Vertebrata; Euteleostomi; Mammalia; Eutheria; Laurasiatheria; Cetartiodactyla; Ruminantia; Pecora; Bovidae; Bovinae; Bos	
Mcavernosa00795	BMS1_HUMAN\BMS1_HUMAN\Q:1-302,H:140-433\65.35%ID\E:3e-124\RecName: Full=Ribosome biogenesis protein BMS1 homolog;\Eukaryota; Metazoa; Chordata; Craniata; Vertebrata; Euteleostomi; Mammalia; Eutheria; Euarchontoglires; Primates; Haplorrhini; Catarrhini; Hominidae; Homo|||\BMS1_SCHPO\BMS1_SCHPO\Q:1-337,H:132-477\47.11%ID\E:7e-85\RecName:	GO:0030686\cellular_component\90S preribosome|||\GO:0005730\cellular_component\nucleolus|||\GO:0005654\cellular_component\nucleoplasm|||\GO:0005634\cellular_component\nucleus|||\GO:0005524\molecular_function\ATP binding|||\GO:0005525\molecular_function\GTP binding|||\GO:0003924\molecular_function\GTPase activity|||\GO:0003723\molecular_function\RNA binding|||\GO:0034511\molecular_function\U3 snoRNA

gene	sprot_Top_BLASTP_hit	gene_ontology_blast
	Full=Ribosome biogenesis protein bms1;\Eukaryota; Fungi; Dikarya; Ascomycota; Taphrinomycotina; Schizosaccharomycetes; Schizosaccharomycetales; Schizosaccharomycetaceae; Schizosaccharomyces|||\BMS1_YEAST\BMS1_YEAST\Q:1-326,H:128-485\45.97%ID\E:1e-83\RecName: Full=Ribosome biogenesis protein BMS1;\Eukaryota; Fungi; Dikarya; Ascomycota; Saccharomycotina; Saccharomycetes; Saccharomycetales; Saccharomycetaceae; Saccharomyces|||\BMS1_HUMAN\BMS1_HUMAN\Q:838-1082,H:992-1257\54.31%ID\E:1e-75\RecName: Full=Ribosome biogenesis protein BMS1 homolog;\Eukaryota; Metazoa; Chordata; Craniata; Vertebrata; Euteleostomi; Mammalia; Eutheria; Euarchontoglires; Primates; Haplorrhini; Catarrhini; Hominidae; Homo|||\BMS1_HUMAN\BMS1_HUMAN\Q:564-854,H:647-927\45.42%ID\E:5e-63\RecName: Full=Ribosome biogenesis protein BMS1 homolog;\Eukaryota; Metazoa; Chordata; Craniata; Vertebrata; Euteleostomi; Mammalia; Eutheria; Euarchontoglires; Primates; Haplorrhini; Catarrhini; Hominidae; Homo|||\BMS1_YEAST\BMS1_YEAST\Q:853-1059,H:911-1135\53.3%ID\E:4e-61\RecName:	binding|||\GO:0000479\biological_process\endonucleolytic cleavage of tricistronic rRNA transcript (SSU-rRNA, 5.8S rRNA, LSU-rRNA)|||\GO:0000462\biological_process\maturation of SSU-rRNA from tricistronic rRNA transcript (SSU-rRNA, 5.8S rRNA, LSU-rRNA)|||\GO:0006364\biological_process\rRNA processing

gene	sprot_Top_BLASTP_hit	gene_ontology_blast
	Full=Ribosome biogenesis protein BMS1;\Eukaryota; Fungi; Dikarya; Ascomycota; Saccharomycotina; Saccharomycetes; Saccharomycetales; Saccharomycetaceae; Saccharomyces|||BMS1_SCHPO\BMS1_SCHPO\Q:853-1042,H:849-1056\52.86%ID\E:4e-56\RecName: Full=Ribosome biogenesis protein bms1;\Eukaryota; Fungi; Dikarya; Ascomycota; Taphrinomycotina; Schizosaccharomycetes; Schizosaccharomycetales; Schizosaccharomycetaceae; Schizosaccharomyces|||BMS1_SCHPO\BMS1_SCHPO\Q:550-851,H:458-764\31.89%ID\E:3e-31\RecName: Full=Ribosome biogenesis protein bms1;\Eukaryota; Fungi; Dikarya; Ascomycota; Taphrinomycotina; Schizosaccharomycetes; Schizosaccharomycetales; Schizosaccharomycetaceae; Schizosaccharomyces|||BMS1_YEAST\BMS1_YEAST\Q:624-854,H:580-830\32.71%ID\E:5e-20\RecName: Full=Ribosome biogenesis protein BMS1;\Eukaryota; Fungi; Dikarya; Ascomycota; Saccharomycotina; Saccharomycetes; Saccharomycetales; Saccharomycetaceae; Saccharomyces	

gene	sprot_Top_BLASTP_hit	gene_ontology_blast
Mcavernosa01653	GALM_HUMAN\GALM_HUMAN\Q:14-228,H:127-341\51.38%ID\E:4e-68\RecName: Full=Aldose 1-epimerase;\Eukaryota; Metazoa; Chordata; Craniata; Vertebrata; Euteleostomi; Mammalia; Eutheria; Euarchontoglires; Primates; Haplorrhini; Catarrhini; Hominidae; Homo|||GALM_BOVIN\GALM_BOVIN\Q:14-228,H:127-341\51.38%ID\E:4e-67\RecName: Full=Aldose 1-epimerase;\Eukaryota; Metazoa; Chordata; Craniata; Vertebrata; Euteleostomi; Mammalia; Eutheria; Laurasiatheria; Cetartiodactyla; Ruminantia; Pecora; Bovidae; Bovinae; Bos|||GALM_PONAB\GALM_PONAB\Q:14-228,H:127-341\50.46%ID\E:5e-67\RecName: Full=Aldose 1-epimerase;\Eukaryota; Metazoa; Chordata; Craniata; Vertebrata; Euteleostomi; Mammalia; Eutheria; Euarchontoglires; Primates; Haplorrhini; Catarrhini; Hominidae; Pongo	GO:0005737\cellular_component\cytoplasm|||GO:0070062\cellular_component\extracellular exosome|||GO:0004034\molecular_function\aldose 1-epimerase activity|||GO:0030246\molecular_function\carbohydrate binding|||GO:0033499\biological_process\galactose catabolic process via UDP-galactose|||GO:0006012\biological_process\galactose metabolic process|||GO:0006006\biological_process\glucose metabolic process
Mcavernosa03432	.	.
Mcavernosa03637	WIPI3_XENTR\WIPI3_XENTR\Q:4-238,H:1-341\54.09%ID\E:4e-114\RecName: Full=WD repeat domain phosphoinositide-interacting protein 3;\Eukaryota; Metazoa; Chordata;	GO:0005829\cellular_component\cytosol|||GO:0019898\cellular_component\extrinsic component of membrane|||GO:0034045\cellular_component\phagophore assembly site

gene	sprot_Top_BLASTP_hit	gene_ontology_blast
	Craniata; Vertebrata; Euteleostomi; Amphibia; Batrachia; Anura; Pipoidea; Pipidae; Xenopodinae; Xenopus; Silurana||||WIPI3_CHICK\WIPI3_CHICK\Q:4-238,H:1-341\54.09%ID\E:5e-114\RecName: Full=WD repeat domain phosphoinositide-interacting protein 3;\Eukaryota; Metazoa; Chordata; Craniata; Vertebrata; Euteleostomi; Archelosauria; Archosauria; Dinosauria; Saurischia; Theropoda; Coelurosauria; Aves; Neognathae; Galloanserae; Galliformes; Phasianidae; Phasianinae; Gallus||||WIPI3_DANRE\WIPI3_DANRE\Q:4-238,H:1-341\54.09%ID\E:7e-114\RecName: Full=WD repeat domain phosphoinositide-interacting protein 3;\Eukaryota; Metazoa; Chordata; Craniata; Vertebrata; Euteleostomi; Actinopterygii; Neopterygii; Teleostei; Ostariophysi; Cypriniformes; Cyprinidae; Danio	membrane||||GO:0080025\molecular_function\phosphatidylinositol-3,5-bisphosphate binding||||GO:0032266\molecular_function\phosphatidylinositol-3-phosphate binding||||GO:0000422\biological_process\autophagy of mitochondrion||||GO:0044804\biological_process\autophagy of nucleus||||GO:0006497\biological_process\protein lipidation||||GO:0034497\biological_process\protein localization to phagophore assembly site
Mcavernosa03638	.	.
Mcavernosa04452	.	.
Mcavernosa04512	TTC29_XENLA\TTC29_XENLA\Q:52-186,H:67-201\45.93%ID\E:2e-34\RecName: Full=Tetratricopeptide repeat protein	.

gene	sprot_Top_BLASTP_hit	gene_ontology_blast
	29;\Eukaryota; Metazoa; Chordata; Craniata; Vertebrata; Euteleostomi; Amphibia; Batrachia; Anura; Pipoidea; Pipidae; Xenopodinae; Xenopus; Xenopus|||\TTC29_MOUSE\TTC29_MOUSE\Q:52-180,H:60-188\45.74%ID\E:7e-33\RecName: Full=Tetratricopeptide repeat protein 29;\Eukaryota; Metazoa; Chordata; Craniata; Vertebrata; Euteleostomi; Mammalia; Eutheria; Euarchontoglires; Glires; Rodentia; Myomorpha; Muroidea; Muridae; Murinae; Mus; Mus|||\TTC29_RAT\TTC29_RAT\Q:52-180,H:60-188\46.51%ID\E:7e-33\RecName: Full=Tetratricopeptide repeat protein 29;\Eukaryota; Metazoa; Chordata; Craniata; Vertebrata; Euteleostomi; Mammalia; Eutheria; Euarchontoglires; Glires; Rodentia; Myomorpha; Muroidea; Muridae; Murinae; Rattus	
Mcavernosa05323	.	.
Mcavernosa05655	TXND3_HELCR\TXND3_HELCR\Q:2-538,H:80-634\40.92%ID\E:2e-135\RecName: Full=Thioredoxin domain-containing protein 3 homolog;\Eukaryota; Metazoa; Echinodermata; Eleutherozoa; Echinozoa; Echinoidea; Euechinoidea; Echinacea; Echinoida;	GO:0005623\cellular_component\cell|||GO:0004550\molecular_function\nucleoside diphosphate kinase activity|||GO:0030154\biological_process\cell differentiation|||GO:0045454\biological_process\cell redox homeostasis|||GO:0006241\biological_process\CTP biosynthetic process|||GO:0006183\biological_process\GTP

gene	sprot_Top_BLASTP_hit	gene_ontology_blast
	Echinometridae; Heliocidaris|||\TXND3_CIOIN\TXND3_CIOIN\Q:2-526,H:79-590\41.51%ID\E:2e-124\RecName: Full=Thioredoxin domain-containing protein 3 homolog;\Eukaryota; Metazoa; Chordata; Tunicata; Ascidiacea; Enterogona; Phlebobranchia; Cionidae; Ciona|||\TXND3_MOUSE\TXND3_MOUSE\Q:2-528,H:81-581\28.5%ID\E:5e-62\RecName: Full=Thioredoxin domain-containing protein 3;\Eukaryota; Metazoa; Chordata; Craniata; Vertebrata; Euteleostomi; Mammalia; Eutheria; Euarchontoglires; Glires; Rodentia; Myomorpha; Muroidea; Muridae; Murinae; Mus; Mus|||\TXND3_CIOIN\TXND3_CIOIN\Q:237-550,H:175-485\31.92%ID\E:3e-40\RecName: Full=Thioredoxin domain-containing protein 3 homolog;\Eukaryota; Metazoa; Chordata; Tunicata; Ascidiacea; Enterogona; Phlebobranchia; Cionidae; Ciona|||\TXND3_CIOIN\TXND3_CIOIN\Q:366-528,H:156-294\36.31%ID\E:1e-19\RecName: Full=Thioredoxin domain-containing protein 3 homolog;\Eukaryota; Metazoa; Chordata; Tunicata; Ascidiacea; Enterogona; Phlebobranchia; Cionidae; Ciona	biosynthetic process|||\GO:0007275\biological_process\multicellular organism development|||\GO:0007283\biological_process\spermatogenesis|||\GO:0006228\biological_process\UTP biosynthetic process

gene	sprot_Top_BLASTP_hit	gene_ontology_blast
Mcavernosa05804	.	.
Mcavernosa06970	.	.
Mcavernosa07334	.	.
Mcavernosa07482	GCN1_HUMAN\GCN1_HUMAN\Q:12-331,H:1-348\36.68%ID\E:5e-62\RecName: Full=eIF-2-alpha kinase activator GCN1 {ECO:0000250|UniProtKB:E9PVA8};\Eukaryota; Metazoa; Chordata; Craniata; Vertebrata; Euteleostomi; Mammalia; Eutheria; Euarchontoglires; Primates; Haplorrhini; Catarrhini; Hominidae; Homo||||GCN1_MOUSE\GCN1_MOUSE\Q:12-331,H:1-348\38.4%ID\E:6e-62\RecName: Full=eIF-2-alpha kinase activator GCN1 {ECO:0000305};\Eukaryota; Metazoa; Chordata; Craniata; Vertebrata; Euteleostomi; Mammalia; Eutheria; Euarchontoglires; Glires; Rodentia; Myomorpha; Muroidea; Muridae; Murinae; Mus; Mus||||ILA_ARATH\ILA_ARATH\Q:36-331,H:147-455\25.31%ID\E:1e-16\RecName: Full=Protein ILITYHIA {ECO:0000312|EMBL:AEE34290.1};\Eukaryota; Viridiplantae; Streptophyta; Embryophyta; Tracheophyta; Spermatophyta; Magnoliophyta;	GO:0005737\cellular_component\cytoplasm||||GO:0005829\cellular_component\cytosol||||GO:0016020\cellular_component\membrane||||GO:0005844\cellular_component\polysome||||GO:0005840\cellular_component\ribosome||||GO:0045296\molecular_function\cadherin binding||||GO:0019901\molecular_function\protein kinase binding||||GO:0019887\molecular_function\protein kinase regulator activity||||GO:0043022\molecular_function\ribosome binding||||GO:0003723\molecular_function\RNA binding||||GO:0008135\molecular_function\translation factor activity, RNA binding||||GO:0034198\biological_process\cellular response to amino acid starvation||||GO:1990253\biological_process\cellular response to leucine starvation||||GO:0033674\biological_process\positive regulation of kinase activity||||GO:0036003\biological_process\positive regulation of transcription from RNA polymerase II promoter in response to

gene	sprot_Top_BLASTP_hit	gene_ontology_blast
	eudicotyledons; Gunneridae; Pentapetalae; rosids; malvids; Brassicales; Brassicaceae; Camelineae; Arabidopsis	stress||||GO:0006417\biological_process\regulation of translation
Mcavernosa07546	NUP85_DANRE\NUP85_DANRE\Q:6-378,H:27-463\38.65%ID\E:2e-90\RecName: Full=Nuclear pore complex protein Nup85;\Eukaryota; Metazoa; Chordata; Craniata; Vertebrata; Euteleostomi; Actinopterygii; Neopterygii; Teleostei; Ostariophysi; Cypriniformes; Cyprinidae; Danio||||NUP85_RAT\NUP85_RAT\Q:6-378,H:27-465\35.96%ID\E:1e-86\RecName: Full=Nuclear pore complex protein Nup85;\Eukaryota; Metazoa; Chordata; Craniata; Vertebrata; Euteleostomi; Mammalia; Eutheria; Euarchontoglires; Glires; Rodentia; Myomorpha; Muroidea; Muridae; Murinae; Rattus||||NUP85_MOUSE\NUP85_MOUSE\Q:6-378,H:27-465\35.96%ID\E:6e-86\RecName: Full=Nuclear pore complex protein Nup85;\Eukaryota; Metazoa; Chordata; Craniata; Vertebrata; Euteleostomi; Mammalia; Eutheria; Euarchontoglires; Glires; Rodentia; Myomorpha; Muroidea; Muridae; Murinae; Mus; Mus	GO:0031965\cellular_component\nuclear membrane||||GO:0031080\cellular_component\nuclear pore outer ring||||GO:0017056\molecular_function\structural constituent of nuclear pore||||GO:0006406\biological_process\mRNA export from nucleus||||GO:0045893\biological_process\positive regulation of transcription, DNA-templated||||GO:0006606\biological_process\protein import into nucleus

gene	sprot_Top_BLASTP_hit	gene_ontology_blast
Mcavernosa09311	.	.
Mcavernosa09675	BAZ1A_MOUSE\BAZ1A_MOUSE\Q:392-1225,H:198-1043\30.99%ID\E:1e-70\RecName: Full=Bromodomain adjacent to zinc finger domain protein 1A;\Eukaryota; Metazoa; Chordata; Craniata; Vertebrata; Euteleostomi; Mammalia; Eutheria; Euarchontoglires; Glires; Rodentia; Myomorpha; Muroidea; Muridae; Murinae; Mus; Mus|||BAZ1A_HUMAN\BAZ1A_HUMAN\Q:596-1225,H:392-1041\32.72%ID\E:7e-67\RecName: Full=Bromodomain adjacent to zinc finger domain protein 1A;\Eukaryota; Metazoa; Chordata; Craniata; Vertebrata; Euteleostomi; Mammalia; Eutheria; Euarchontoglires; Primates; Haplorrhini; Catarrhini; Hominidae; Homo|||BAZ1A_MOUSE\BAZ1A_MOUSE\Q:1-154,H:1-155\51.59%ID\E:4e-39\RecName: Full=Bromodomain adjacent to zinc finger domain protein 1A;\Eukaryota; Metazoa; Chordata; Craniata; Vertebrata; Euteleostomi; Mammalia; Eutheria; Euarchontoglires; Glires; Rodentia; Myomorpha; Muroidea; Muridae; Murinae; Mus; Mus|||BAZ1A_HUMAN\BAZ1A_HUMAN\Q:1-149,H:1-150\51.32%ID\E:2e-38\RecName:	GO:0008623\cellular_component\CHRAC|||GO:0000228\cellular_component\nuclear chromosome|||GO:0046872\molecular_function\metal ion binding|||GO:0006338\biological_process\chromatin remodeling|||GO:0006261\biological_process\DNA-dependent DNA replication|||GO:0006355\biological_process\regulation of transcription, DNA-templated|||GO:0006351\biological_process\transcription, DNA-templated

gene	sprot_Top_BLASTP_hit	gene_ontology_blast
	Full=Bromodomain adjacent to zinc finger domain protein 1A;\Eukaryota; Metazoa; Chordata; Craniata; Vertebrata; Euteleostomi; Mammalia; Eutheria; Euarchontoglires; Primates; Haplorrhini; Catarrhini; Hominidae; Homo|||\BAZ1A_XENLA\BAZ1A_XENLA\Q:1438-1534,H:183-277\56.7%ID\E:4e-33\RecName: Full=Bromodomain adjacent to zinc finger domain protein 1A;\Eukaryota; Metazoa; Chordata; Craniata; Vertebrata; Euteleostomi; Amphibia; Batrachia; Anura; Pipoidea; Pipidae; Xenopodinae; Xenopus; Xenopus|||\BAZ1A_MOUSE\BAZ1A_MOUSE\Q:1432-1527,H:1104-1199\62.5%ID\E:2e-32\RecName: Full=Bromodomain adjacent to zinc finger domain protein 1A;\Eukaryota; Metazoa; Chordata; Craniata; Vertebrata; Euteleostomi; Mammalia; Eutheria; Euarchontoglires; Glires; Rodentia; Myomorpha; Muroidea; Muridae; Murinae; Mus; Mus|||\BAZ1A_HUMAN\BAZ1A_HUMAN\Q:1439-1527,H:1110-1198\66.29%ID\E:2e-32\RecName: Full=Bromodomain adjacent to zinc finger domain protein 1A;\Eukaryota; Metazoa; Chordata; Craniata; Vertebrata; Euteleostomi; Mammalia; Eutheria; Euarchontoglires; Primates; Haplorrhini; Catarrhini; Hominidae;	

gene	sprot_Top_BLASTP_hit	gene_ontology_blast
	Homo||||BAZ1A_XENLA\BAZ1A_XENLA\Q:1792-1895,H:507-610\34.62%ID\E:1e-17\RecName: Full=Bromodomain adjacent to zinc finger domain protein 1A;\Eukaryota; Metazoa; Chordata; Craniata; Vertebrata; Euteleostomi; Amphibia; Batrachia; Anura; Pipoidea; Pipidae; Xenopodinae; Xenopus; Xenopus||||BAZ1A_MOUSE\BAZ1A_MOUSE\Q:1665-1895,H:1298-1537\28.23%ID\E:2e-17\RecName: Full=Bromodomain adjacent to zinc finger domain protein 1A;\Eukaryota; Metazoa; Chordata; Craniata; Vertebrata; Euteleostomi; Mammalia; Eutheria; Euarchontoglires; Glires; Rodentia; Myomorpha; Muroidea; Muridae; Murinae; Mus; Mus||||BAZ1A_XENLA\BAZ1A_XENLA\Q:1146-1265,H:45-151\34.43%ID\E:2e-06\RecName: Full=Bromodomain adjacent to zinc finger domain protein 1A;\Eukaryota; Metazoa; Chordata; Craniata; Vertebrata; Euteleostomi; Amphibia; Batrachia; Anura; Pipoidea; Pipidae; Xenopodinae; Xenopus; Xenopus	
Mcavernosa10323	PO21_NASVI\PO21_NASVI\Q:162-467,H:418-757\30.9%ID\E:3e-34\RecName: Full=Retrovirus-related Pol polyprotein from type-1 retrotransposable element	GO:0004519\molecular_function\endonuclease activity||||GO:0046872\molecular_function\metal ion binding||||GO:0003676\molecular_function\nucleic acid

gene	sprot_Top_BLASTP_hit	gene_ontology_blast
	R2;\Eukaryota; Metazoa; Ecdysozoa; Arthropoda; Hexapoda; Insecta; Pterygota; Neoptera; Holometabola; Hymenoptera; Apocrita; Terebrantes; Chalcidoidea; Pteromalidae; Pteromalinae; Nasonia|||\POLR_DROME\POLR_DROME\Q:168-450,H:450-767\28.57%ID\E:9e-25\RecName: Full=Retrovirus-related Pol polyprotein from type-2 retrotransposable element R2DM;\Eukaryota; Metazoa; Ecdysozoa; Arthropoda; Hexapoda; Insecta; Pterygota; Neoptera; Holometabola; Diptera; Brachycera; Muscomorpha; Ephydroidea; Drosophilidae; Drosophila; Sophophora|||\PO21_BRACO\PO21_BRACO\Q:171-475,H:268-605\27.78%ID\E:2e-22\RecName: Full=Retrovirus-related Pol polyprotein from type-1 retrotransposable element R2;\Eukaryota; Metazoa; Ecdysozoa; Arthropoda; Hexapoda; Insecta; Pterygota; Neoptera; Holometabola; Diptera; Nematocera; Sciaroidea; Sciaridae; Bradysia|||\POLR_DROME\POLR_DROME\Q:9-153,H:63-228\28.74%ID\E:9e-07\RecName: Full=Retrovirus-related Pol polyprotein from type-2 retrotransposable element R2DM;\Eukaryota; Metazoa; Ecdysozoa;	binding|||\GO:0003964\molecular_function\RNA-directed DNA polymerase activity

gene	sprot_Top_BLASTP_hit	gene_ontology_blast
	Arthropoda; Hexapoda; Insecta; Pterygota; Neoptera; Holometabola; Diptera; Brachycera; Muscomorpha; Ephydroidea; Drosophilidae; Drosophila; Sophophora	
Mcavernosa10778	TS101_MOUSE\TS101_MOUSE\Q:33-111,H:253-391\30.94%ID\E:1e-08\RecName: Full=Tumor susceptibility gene 101 protein;\Eukaryota; Metazoa; Chordata; Craniata; Vertebrata; Euteleostomi; Mammalia; Eutheria; Euarchontoglires; Glires; Rodentia; Myomorpha; Muroidea; Muridae; Murinae; Mus; Mus|||TS101_HUMAN\TS101_HUMAN\Q:33-111,H:252-390\30.94%ID\E:1e-08\RecName: Full=Tumor susceptibility gene 101 protein;\Eukaryota; Metazoa; Chordata; Craniata; Vertebrata; Euteleostomi; Mammalia; Eutheria; Euarchontoglires; Primates; Haplorrhini; Catarrhini; Hominidae; Homo|||TS101_RAT\TS101_RAT\Q:33-111,H:253-391\30.94%ID\E:1e-08\RecName: Full=Tumor susceptibility gene 101 protein;\Eukaryota; Metazoa; Chordata; Craniata; Vertebrata; Euteleostomi; Mammalia; Eutheria; Euarchontoglires; Glires; Rodentia; Myomorpha; Muroidea; Muridae; Murinae; Rattus	GO:0005737\cellular_component\cytoplasm|||GO:0005829\cellular_component\cytosol|||GO:0005769\cellular_component\early endosome|||GO:0031901\cellular_component\early endosome membrane|||GO:0005768\cellular_component\endosome|||GO:0010008\cellular_component\endosome membrane|||GO:0000813\cellular_component\ESCRT I complex|||GO:0070062\cellular_component\extracellular exosome|||GO:0090543\cellular_component\Flemming body|||GO:0005770\cellular_component\late endosome|||GO:0031902\cellular_component\late endosome membrane|||GO:0005815\cellular_component\microtubule organizing center|||GO:0005730\cellular_component\nucleolus|||GO:0005634\cellular_component\nucleus|||GO:0005886\cellular_component\plasma membrane|||GO:0048306\molecular_function\calcium-dependent protein binding|||GO:0030374\molecular_function\nuclear receptor transcription coactivator

gene	sprot_Top_BLASTP_hit	gene_ontology_blast
		activity||||GO:0042803\molecular_function\protein homodimerization activity||||GO:0044877\molecular_function\protein-containing complex binding||||GO:0003714\molecular_function\transcription corepressor activity||||GO:0043130\molecular_function\ubiquitin binding||||GO:0031625\molecular_function\ubiquitin protein ligase binding||||GO:0046790\molecular_function\virion binding||||GO:0007050\biological_process\cell cycle arrest||||GO:0030154\biological_process\cell differentiation||||GO:0051301\biological_process\cell division||||GO:0008333\biological_process\endosome to lysosome transport||||GO:1990182\biological_process\exosomal secretion||||GO:0006858\biological_process\extracellular transport||||GO:0030216\biological_process\keratinocyte differentiation||||GO:0008285\biological_process\negative regulation of cell proliferation||||GO:0042059\biological_process\negative regulation of epidermal growth factor receptor signaling pathway||||GO:0007175\biological_process\negative regulation of epidermal growth factor-activated receptor activity||||GO:0045892\biological_process\negative regulation of transcription, DNA-templated||||GO:1903543\biological_process\positive

gene	sprot_Top_BLASTP_hit	gene_ontology_blast
		regulation of exosomal secretion||||GO:2000397\biological_process\positive regulation of ubiquitin-dependent endocytosis||||GO:1903774\biological_process\positive regulation of viral budding via host ESCRT complex||||GO:0048524\biological_process\positive regulation of viral process||||GO:1902188\biological_process\positive regulation of viral release from host cell||||GO:0006513\biological_process\protein monoubiquitination||||GO:0015031\biological_process\protein transport||||GO:0001558\biological_process\regulation of cell growth||||GO:1903551\biological_process\regulation of extracellular exosome assembly||||GO:0043405\biological_process\regulation of MAP kinase activity||||GO:1903772\biological_process\regulation of viral budding via host ESCRT complex||||GO:0043162\biological_process\ubiquitin-dependent protein catabolic process via the multivesicular body sorting pathway||||GO:0046755\biological_process\viral budding
Mcavernosa10779	TBC15_MOUSE\TBC15_MOUSE\Q:14-589,H:2-634\39.5%ID\E:2e-148\RecName: Full=TBC1 domain family member 15;\Eukaryota; Metazoa; Chordata; Craniata; Vertebrata; Euteleostomi;	GO:0005737\cellular_component\cytoplasm||||GO:0012505\cellular_component\endomembrane system||||GO:0005576\cellular_component\extracellular region||||GO:0005739\cellular_component\mitochondrion|||

gene	sprot_Top_BLASTP_hit	gene_ontology_blast
	Mammalia; Eutheria; Euarchontoglires; Glires; Rodentia; Myomorpha; Muroidea; Muridae; Murinae; Mus; Mus||||TBC15_HUMAN\TBC15_HUMAN\Q:14-622,H:2-685\37.46%ID\E:1e-143\RecName: Full=TBC1 domain family member 15;\Eukaryota; Metazoa; Chordata; Craniata; Vertebrata; Euteleostomi; Mammalia; Eutheria; Euarchontoglires; Primates; Haplorrhini; Catarrhini; Hominidae; Homo||||TBC17_MOUSE\TBC17_MOUSE\Q:22-572,H:7-592\37.9%ID\E:2e-129\RecName: Full=TBC1 domain family member 17;\Eukaryota; Metazoa; Chordata; Craniata; Vertebrata; Euteleostomi; Mammalia; Eutheria; Euarchontoglires; Glires; Rodentia; Myomorpha; Muroidea; Muridae; Murinae; Mus; Mus	|GO:0005096\molecular_function\GTPase activator activity||||GO:0017137\molecular_function\Rab GTPase binding||||GO:0090630\biological_process\activation of GTPase activity||||GO:0006886\biological_process\intracellular protein transport||||GO:0043087\biological_process\regulation of GTPase activity||||GO:0031338\biological_process\regulation of vesicle fusion
Mcavernosa10827	PRP4B_RAT\PRP4B_RAT\Q:378-645,H:502-772\53.74%ID\E:2e-70\RecName: Full=Serine/threonine-protein kinase PRP4 homolog;\Eukaryota; Metazoa; Chordata; Craniata; Vertebrata; Euteleostomi; Mammalia; Eutheria; Euarchontoglires; Glires; Rodentia; Myomorpha; Muroidea; Muridae; Murinae; Rattus||||PRP4B_MOUSE\PRP4B_MOUSE\Q:378-645,H:502-772\53.74%ID\E:3e-70\RecName:	GO:0071013\cellular_component\catalytic step 2 spliceosome||||GO:0005694\cellular_component\chromosome||||GO:0016607\cellular_component\nuclear speck||||GO:0005634\cellular_component\nucleus||||GO:0005524\molecular_function\ATP binding||||GO:0004674\molecular_function\protein serine/threonine kinase activity||||GO:0006397\biological_process\mRNA processing||||GO:0006468\biological_process\protein

gene	sprot_Top_BLASTP_hit	gene_ontology_blast
	Full=Serine/threonine-protein kinase PRP4 homolog;\Eukaryota; Metazoa; Chordata; Craniata; Vertebrata; Euteleostomi; Mammalia; Eutheria; Euarchontoglires; Glires; Rodentia; Myomorpha; Muroidea; Muridae; Murinae; Mus; Mus|||\PRP4_SCHPO\PRP4_SCHPO\Q:413-645,H:8-243\40.8%ID\E:2e-36\RecName: Full=Serine/threonine-protein kinase prp4;\Eukaryota; Fungi; Dikarya; Ascomycota; Taphrinomycotina; Schizosaccharomycetes; Schizosaccharomycetales; Schizosaccharomycetaceae; Schizosaccharomyces	phosphorylation|||\GO:0008380\biological_process\RNA splicing
Mcavernosa11156	.	.
Mcavernosa11924	GOLI4_XENTR\GOLI4_XENTR\Q:1-260,H:5-275\31.87%ID\E:3e-28\RecName: Full=Golgi integral membrane protein 4;\Eukaryota; Metazoa; Chordata; Craniata; Vertebrata; Euteleostomi; Amphibia; Batrachia; Anura; Pipoidea; Pipidae; Xenopodinae; Xenopus; Silurana|||\GOLI4_HUMAN\GOLI4_HUMAN\Q:1-182,H:5-186\35.16%ID\E:7e-27\RecName: Full=Golgi integral membrane protein 4;\Eukaryota; Metazoa; Chordata; Craniata; Vertebrata; Euteleostomi; Mammalia; Eutheria;	GO:0010008\cellular_component\endosome membrane|||\GO:0032580\cellular_component\Golgi cisterna membrane|||\GO:0016021\cellular_component\integral component of membrane

gene	sprot_Top_BLASTP_hit	gene_ontology_blast
	Euarchontoglires; Primates; Haplorrhini; Catarrhini; Hominidae; Homo||||GOLI4_RAT\GOLI4_RAT\Q:1-196,H:5-207\33.5%ID\E:2e-26\RecName: Full=Golgi integral membrane protein 4;\Eukaryota; Metazoa; Chordata; Craniata;Vertebrata; Euteleostomi; Mammalia; Eutheria; Euarchontoglires; Glires; Rodentia; Myomorpha; Muroidea; Muridae; Murinae; Rattus	
Mcavernosa12387	RBP2A_PLAF7\RBP2A_PLAF7\Q:228-388,H:2740-2870\22.98%ID\E:2e-06\RecName: Full=Reticulocyte-binding protein 2 homolog a {ECO:0000312|EMBL:CAD52492.1};\Eukaryota; Alveolata; Apicomplexa; Aconoidasida; Haemosporida; Plasmodiidae; Plasmodium; Plasmodium (Laverania)||||RBP2A_PLAF7\RBP2A_PLAF7\Q:225-378,H:2757-2882\25.32%ID\E:3e-06\RecName: Full=Reticulocyte-binding protein 2 homolog a {ECO:0000312|EMBL:CAD52492.1};\Eukaryota; Alveolata; Apicomplexa; Aconoidasida; Haemosporida; Plasmodiidae; Plasmodium; Plasmodium (Laverania)	GO:0016021\cellular_component\integral component of membrane|||GO:0016020\cellular_component\membrane|||GO:0005886\cellular_component\plasma membrane|||GO:0008201\molecular_function\heparin binding|||GO:0098609\biological_process\cell-cell adhesion
Mcavernosa12418	NSF_PONAB\NSF_PONAB\Q:4-370,H:6-358\53.68%ID\E:7e-126\RecName: Full=Vesicle-	GO:0005737\cellular_component\cytoplasm|||GO:0005524\molecular_function\ATP

gene	sprot_Top_BLASTP_hit	gene_ontology_blast
	fusing ATPase;\Eukaryota; Metazoa; Chordata; Craniata; Vertebrata; Euteleostomi; Mammalia; Eutheria; Euarchontoglires; Primates; Haplorrhini; Catarrhini; Hominidae; Pongo|||\NSF_HUMAN\NSF_HUMAN\Q:4-370,H:6-358\53.68%ID\E:8e-126\RecName: Full=Vesicle-fusing ATPase;\Eukaryota; Metazoa; Chordata; Craniata; Vertebrata; Euteleostomi; Mammalia; Eutheria; Euarchontoglires; Primates; Haplorrhini; Catarrhini; Hominidae; Homo|||\NSF_MOUSE\NSF_MOUSE\Q:4-370,H:6-358\53.16%ID\E:9e-126\RecName: Full=Vesicle-fusing ATPase;\Eukaryota; Metazoa; Chordata; Craniata; Vertebrata; Euteleostomi; Mammalia; Eutheria; Euarchontoglires; Glires; Rodentia; Myomorpha; Muroidea; Muridae; Murinae; Mus; Mus	binding|||\GO:0016787\molecular_function\hydrolase activity|||\GO:0046872\molecular_function\metal ion binding|||\GO:0015031\biological_process\protein transport
Mcavernosa12633	STML2_MOUSE\STML2_MOUSE\Q:35-237,H:27-243\70.05%ID\E:4e-103\RecName: Full=Stomatin-like protein 2, mitochondrial;\Eukaryota; Metazoa; Chordata; Craniata; Vertebrata; Euteleostomi; Mammalia; Eutheria; Euarchontoglires; Glires; Rodentia; Myomorpha; Muroidea; Muridae; Murinae; Mus; Mus|||\STML2_RAT\STML2_RAT\Q:35-237,H:27-	GO:0015629\cellular_component\actin cytoskeleton|||\GO:0008180\cellular_component\COP9 signalosome|||\GO:0019897\cellular_component\extrinsic component of plasma membrane|||\GO:0001772\cellular_component\immunological synapse|||\GO:0045121\cellular_component\membrane raft|||\GO:0005743\cellular_component\mitochondrial inner membrane|||\GO:0005758\cellular_component\mitochondri

gene	sprot_Top_BLASTP_hit	gene_ontology_blast
	243\70.05%ID\E:6e-103\RecName: Full=Stomatin-like protein 2, mitochondrial;\Eukaryota; Metazoa; Chordata; Craniata; Vertebrata; Euteleostomi; Mammalia; Eutheria; Euarchontoglires; Glires; Rodentia; Myomorpha; Muroidea; Muridae; Murinae; Rattus|||STML2_HUMAN\STML2_HUMAN\Q:35-262,H:27-268\67.77%ID\E:3e-102\RecName: Full=Stomatin-like protein 2, mitochondrial;\Eukaryota; Metazoa; Chordata; Craniata; Vertebrata; Euteleostomi; Mammalia; Eutheria; Euarchontoglires; Primates; Haplorrhini; Catarrhini; Hominidae; Homo	al intermembrane space|||GO:0005739\cellular_component\mitochondrion|||GO:0042101\cellular_component\T cell receptor complex|||GO:1901612\molecular_function\cardiolipin binding|||GO:0051020\molecular_function\GTPase binding|||GO:0035710\biological_process\CD4-positive, alpha-beta T cell activation|||GO:0006874\biological_process\cellular calcium ion homeostasis|||GO:0032623\biological_process\interleukin-2 production|||GO:0010876\biological_process\lipid localization|||GO:0042776\biological_process\mitochondrial ATP synthesis coupled proton transport|||GO:0006851\biological_process\mitochondrial calcium ion transmembrane transport|||GO:0034982\biological_process\mitochondrial protein processing|||GO:0007005\biological_process\mitochondrion organization|||GO:1900210\biological_process\positive regulation of cardiolipin metabolic process|||GO:0090297\biological_process\positive regulation of mitochondrial DNA replication|||GO:0010918\biological_process\positive regulation of mitochondrial membrane potential|||GO:0051259\biological_process\protein complex oligomerization|||GO:1990046\biological_process\stress-

gene	sprot_Top_BLASTP_hit	gene_ontology_blast
		induced mitochondrial fusion||||GO:0050852\biological_process\T cell receptor signaling pathway
Mcavernosa13288	.	.
Mcavernosa14493	PEAM1_ARATH\PEAM1_ARATH\Q:3-225,H:229-491\45.63%ID\E:7e-70\RecName: Full=Phosphoethanolamine N-methyltransferase 1;\Eukaryota; Viridiplantae; Streptophyta; Embryophyta; Tracheophyta; Spermatophyta; Magnoliophyta; eudicotyledons; Gunneridae; Pentapetalae; rosids; malvids; Brassicales; Brassicaceae; Camelineae; Arabidopsis||||PEAMT_SPIOL\PEAMT_SPIOL\Q:11-224,H:240-493\49.21%ID\E:5e-68\RecName: Full=Phosphoethanolamine N-methyltransferase;\Eukaryota; Viridiplantae; Streptophyta; Embryophyta; Tracheophyta; Spermatophyta; Magnoliophyta; eudicotyledons; Gunneridae; Pentapetalae; Caryophyllales; Chenopodiaceae; Chenopodioideae; Anserineae; Spinacia||||PEAM3_ARATH\PEAM3_ARATH\Q:11-225,H:236-490\47.06%ID\E:5e-68\RecName: Full=Phosphoethanolamine N-	GO:0005737\cellular_component\cytoplasm||||GO:0005829\cellular_component\cytosol||||GO:0008168\molecular_function\methyltransferase activity||||GO:0000234\molecular_function\phosphoethanolamine N-methyltransferase activity||||GO:0042425\biological_process\choline biosynthetic process||||GO:0006656\biological_process\phosphatidylcholine biosynthetic process||||GO:0009555\biological_process\pollen development||||GO:0009860\biological_process\pollen tube growth||||GO:0010183\biological_process\pollen tube guidance||||GO:0048528\biological_process\post-embryonic root development||||GO:0009826\biological_process\unidimensional cell growth

gene	sprot_Top_BLASTP_hit	gene_ontology_blast
	methyltransferase 3;\Eukaryota; Viridiplantae; Streptophyta; Embryophyta; Tracheophyta; Spermatophyta; Magnoliophyta; eudicotyledons; Gunneridae; Pentapetalae; rosids; malvids; Brassicales; Brassicaceae; Camelineae; Arabidopsis	
Mcavernosa15231	.	.
Mcavernosa15309	PNO1_NEMVE\PNO1_NEMVE\Q:17-293,H:4-238\67.51%ID\E:3e-130\RecName: Full=RNA-binding protein pno1;\Eukaryota; Metazoa; Cnidaria; Anthozoa; Hexacorallia; Actiniaria; Edwardsiidae; Nematostella|||PNO1_XENLA\PNO1_XENLA\Q:20-293,H:2-236\62.82%ID\E:4e-116\RecName: Full=RNA-binding protein PNO1;\Eukaryota; Metazoa; Chordata; Craniata; Vertebrata; Euteleostomi; Amphibia; Batrachia; Anura; Pipoidea; Pipidae; Xenopodinae; Xenopus; Xenopus|||PNO1_XENTR\PNO1_XENTR\Q:23-293,H:5-236\62.77%ID\E:2e-114\RecName: Full=RNA-binding protein PNO1;\Eukaryota; Metazoa; Chordata; Craniata; Vertebrata; Euteleostomi; Amphibia; Batrachia; Anura; Pipoidea; Pipidae; Xenopodinae; Xenopus; Silurana	GO:0005730\cellular_component\nucleolus|||GO:0003723\molecular_function\RNA binding

gene	sprot_Top_BLASTP_hit	gene_ontology_blast
Mcavernosa15943	.	.
Mcavernosa17684	DHRS7_MOUSE\DHRS7_MOUSE\Q:1-208,H:103-308\49.28%ID\E:5e-59\RecName: Full=Dehydrogenase/reductase SDR family member 7;\Eukaryota; Metazoa; Chordata; Craniata; Vertebrata; Euteleostomi; Mammalia; Eutheria; Euarchontoglires; Glires; Rodentia; Myomorpha; Muroidea; Muridae; Murinae; Mus; Mus|||\DHRS7_HUMAN\DHRS7_HUMAN\Q:1-201,H:103-301\50%ID\E:2e-57\RecName: Full=Dehydrogenase/reductase SDR family member 7;\Eukaryota; Metazoa; Chordata; Craniata; Vertebrata; Euteleostomi; Mammalia; Eutheria; Euarchontoglires; Primates; Haplorrhini; Catarrhini; Hominidae; Homo|||\DRS7C_XENTR\DRS7C_XENTR\Q:8-137,H:98-226\42.31%ID\E:1e-30\RecName: Full=Dehydrogenase/reductase SDR family member 7C;\Eukaryota; Metazoa; Chordata; Craniata; Vertebrata; Euteleostomi; Amphibia; Batrachia; Anura; Pipoidea; Pipidae; Xenopodinae; Xenopus; Silurana	GO:0016491\molecular_function\oxidoreductase activity
Mcavernosa17728	SHKD_DICDI\SHKD_DICDI\Q:320-557,H:283-522\31.1%ID\E:3e-17\RecName: Full=Dual specificity protein kinase shkD;\Eukaryota;	GO:0005622\cellular_component\intracellular|||GO:0016020\cellular_component\membrane|||GO:0005524\molecular_function\ATP

gene	sprot_Top_BLASTP_hit	gene_ontology_blast
	Amoebozoa; Mycetozoa; Dictyostelids; Dictyosteliales; Dictyosteliaceae; Dictyostelium||||SHKA_DICDI\SHKA_DICDI\Q:317-557,H:48-292\29.66%ID\E:7e-17\RecName: Full=Dual specificity protein kinase shkA;\Eukaryota; Amoebozoa; Mycetozoa; Dictyostelids; Dictyosteliales; Dictyosteliaceae; Dictyostelium||||FPS_FUJSV\FPS_FUJSV\Q:320-557,H:618-857\28.19%ID\E:2e-15\RecName: Full=Tyrosine-protein kinase transforming protein Fps;\Viruses; Ortervirales; Retroviridae; Orthoretrovirinae; Alpharetrovirus	binding||||GO:0004674\molecular_function\protein serine/threonine kinase activity||||GO:0004713\molecular_function\protein tyrosine kinase activity||||GO:0035556\biological_process\intracellular signal transduction
Mcavernosa17728	SHKD_DICDI\SHKD_DICDI\Q:320-557,H:283-522\31.1%ID\E:3e-17\RecName: Full=Dual specificity protein kinase shkD;\Eukaryota; Amoebozoa; Mycetozoa; Dictyostelids; Dictyosteliales; Dictyosteliaceae; Dictyostelium||||SHKA_DICDI\SHKA_DICDI\Q:317-557,H:48-292\29.66%ID\E:7e-17\RecName: Full=Dual specificity protein kinase shkA;\Eukaryota; Amoebozoa; Mycetozoa; Dictyostelids; Dictyosteliales; Dictyosteliaceae; Dictyostelium||||FPS_FUJSV\FPS_FUJSV\Q:320-557,H:618-857\28.19%ID\E:2e-15\RecName: Full=Tyrosine-protein kinase transforming	GO:0005622\cellular_component\intracellular||||GO:0016020\cellular_component\membrane||||GO:0005524\molecular_function\ATP binding||||GO:0004674\molecular_function\protein serine/threonine kinase activity||||GO:0004713\molecular_function\protein tyrosine kinase activity||||GO:0035556\biological_process\intracellular signal transduction

gene	sprot_Top_BLASTP_hit	gene_ontology_blast
	protein Fps;\Viruses; Ortervirales; Retroviridae; Orthoretrovirinae; Alpharetrovirus	
Mcavernosa17732	K0100_HUMAN\K0100_HUMAN\Q:1-1249,H:574-1883\33.41%ID\E:0\RecName: Full=Protein KIAA0100;\Eukaryota; Metazoa; Chordata; Craniata; Vertebrata; Euteleostomi; Mammalia; Eutheria; Euarchontoglires; Primates; Haplorrhini; Catarrhini; Hominidae; Homo|||K0100_MOUSE\K0100_MOUSE\Q:1-1249,H:574-1883\32.74%ID\E:0\RecName: Full=Protein KIAA0100;\Eukaryota; Metazoa; Chordata; Craniata; Vertebrata; Euteleostomi; Mammalia; Eutheria; Euarchontoglires; Glires; Rodentia; Myomorpha; Muroidea; Muridae; Murinae; Mus; Mus|||KIP_ARATH\KIP_ARATH\Q:327-668,H:1082-1456\23.16%ID\E:1e-12\RecName: Full=Protein KINKY POLLEN {ECO:0000303|PubMed:14675453};\Eukaryota; Viridiplantae; Streptophyta; Embryophyta; Tracheophyta; Spermatophyta; Magnoliophyta; eudicotyledons; Gunneridae; Pentapetalae; rosids; malvids; Brassicales; Brassicaceae; Camelineae; Arabidopsis	GO:0005576\cellular_component\extracellular region

gene	sprot_Top_BLASTP_hit	gene_ontology_blast
Mcavernosa17932	PB1_HUMAN\PB1_HUMAN\Q:3-1153,H:5-1184\35.74%ID\E:0\RecName: Full=Protein polybromo-1;\Eukaryota; Metazoa; Chordata; Craniata; Vertebrata; Euteleostomi; Mammalia; Eutheria; Euarchontoglires; Primates; Haplorrhini; Catarrhini; Hominidae; Homo||||PB1_MOUSE\PB1_MOUSE\Q:3-1153,H:5-1184\34.73%ID\E:0\RecName: Full=Protein polybromo-1;\Eukaryota; Metazoa; Chordata; Craniata; Vertebrata; Euteleostomi; Mammalia; Eutheria; Euarchontoglires; Glires; Rodentia; Myomorpha; Muroidea; Muridae; Murinae; Mus; Mus||||PB1_CHICK\PB1_CHICK\Q:229-1166,H:169-1196\35.39%ID\E:9e-161\RecName: Full=Protein polybromo-1;\Eukaryota; Metazoa; Chordata; Craniata; Vertebrata; Euteleostomi; Archelosauria; Archosauria; Dinosauria; Saurischia; Theropoda; Coelurosauria; Aves; Neognathae; Galloanserae; Galliformes; Phasianidae; Phasianinae; Gallus||||PB1_CHICK\PB1_CHICK\Q:46-799,H:181-877\25.76%ID\E:4e-56\RecName: Full=Protein polybromo-1;\Eukaryota; Metazoa; Chordata; Craniata; Vertebrata; Euteleostomi; Archelosauria; Archosauria; Dinosauria; Saurischia; Theropoda; Coelurosauria; Aves;	GO:0000228\cellular_component\nuclear chromosome||||GO:0005654\cellular_component\nucleoplasm||||GO:0016586\cellular_component\RSC-type complex||||GO:0003682\molecular_function\chromatin binding||||GO:0003677\molecular_function\DNA binding||||GO:0006338\biological_process\chromatin remodeling||||GO:0000278\biological_process\mitotic cell cycle||||GO:0008285\biological_process\negative regulation of cell proliferation||||GO:0006355\biological_process\regulation of transcription, DNA-templated||||GO:0006351\biological_process\transcription, DNA-templated

gene	sprot_Top_BLASTP_hit	gene_ontology_blast
	Neognathae; Galloanserae; Galliformes; Phasianidae; Phasianinae; Gallus|||\PB1_CHICK\PB1_CHICK\Q:37-632,H:373-861\24.14%ID\E:4e-39\RecName: Full=Protein polybromo-1;\Eukaryota; Metazoa; Chordata; Craniata; Vertebrata; Euteleostomi; Archelosauria; Archosauria; Dinosauria; Saurischia; Theropoda; Coelurosauria; Aves; Neognathae; Galloanserae; Galliformes; Phasianidae; Phasianinae; Gallus|||\PB1_CHICK\PB1_CHICK\Q:419-800,H:54-486\28.77%ID\E:5e-36\RecName: Full=Protein polybromo-1;\Eukaryota; Metazoa; Chordata; Craniata; Vertebrata; Euteleostomi; Archelosauria; Archosauria; Dinosauria; Saurischia; Theropoda; Coelurosauria; Aves; Neognathae; Galloanserae; Galliformes; Phasianidae; Phasianinae; Gallus|||\PB1_CHICK\PB1_CHICK\Q:3-142,H:5-145\49.65%ID\E:7e-36\RecName: Full=Protein polybromo-1;\Eukaryota; Metazoa; Chordata; Craniata; Vertebrata; Euteleostomi; Archelosauria; Archosauria; Dinosauria; Saurischia; Theropoda; Coelurosauria; Aves; Neognathae; Galloanserae; Galliformes; Phasianidae; Phasianinae; Gallus|||\PB1_CHICK\PB1_CHICK\Q:527-	

gene	sprot_Top_BLASTP_hit	gene_ontology_blast
	799,H:34-284\32.6%ID\E:2e-34\RecName: Full=Protein polybromo-1;\Eukaryota; Metazoa; Chordata; Craniata;Vertebrata; Euteleostomi; Archelosauria; Archosauria; Dinosauria; Saurischia; Theropoda; Coelurosauria; Aves; Neognathae; Galloanserae; Galliformes; Phasianidae; Phasianinae; Gallus|||PB1_CHICK\PB1_CHICK\Q:678-800,H:30-153\39.52%ID\E:2e-18\RecName: Full=Protein polybromo-1;\Eukaryota; Metazoa; Chordata; Craniata;Vertebrata; Euteleostomi; Archelosauria; Archosauria; Dinosauria; Saurischia; Theropoda; Coelurosauria; Aves; Neognathae; Galloanserae; Galliformes; Phasianidae; Phasianinae; Gallus|||PB1_CHICK\PB1_CHICK\Q:222-333,H:12-141\31.54%ID\E:1e-10\RecName: Full=Protein polybromo-1;\Eukaryota; Metazoa; Chordata; Craniata;Vertebrata; Euteleostomi; Archelosauria; Archosauria; Dinosauria; Saurischia; Theropoda; Coelurosauria; Aves; Neognathae; Galloanserae; Galliformes; Phasianidae; Phasianinae; Gallus|||PB1_CHICK\PB1_CHICK\Q:964-1054,H:1149-1261\29.82%ID\E:7e-07\RecName: Full=Protein polybromo-1;\Eukaryota; Metazoa; Chordata; Craniata;Vertebrata; Euteleostomi;	

gene	sprot_Top_BLASTP_hit	gene_ontology_blast
	Archelosauria; Archosauria; Dinosauria; Saurischia; Theropoda; Coelurosauria; Aves; Neognathae; Galloanserae; Galliformes; Phasianidae; Phasianinae; Gallus||||PB1_CHICK\PB1_CHICK\Q:2-149,H:480-623\23.49%ID\E:2e-06\RecName: Full=Protein polybromo-1;\Eukaryota; Metazoa; Chordata; Craniata; Vertebrata; Euteleostomi; Archelosauria; Archosauria; Dinosauria; Saurischia; Theropoda; Coelurosauria; Aves; Neognathae; Galloanserae; Galliformes; Phasianidae; Phasianinae; Gallus||||PB1_HUMAN\PB1_HUMAN\Q:964-1054,H:1150-1262\28.07%ID\E:5e-06\RecName: Full=Protein polybromo-1;\Eukaryota; Metazoa; Chordata; Craniata; Vertebrata; Euteleostomi; Mammalia; Eutheria; Euarchontoglires; Primates; Haplorrhini; Catarrhini; Hominidae; Homo||||PB1_MOUSE\PB1_MOUSE\Q:964-1054,H:1150-1262\28.07%ID\E:6e-06\RecName: Full=Protein polybromo-1;\Eukaryota; Metazoa; Chordata; Craniata; Vertebrata; Euteleostomi; Mammalia; Eutheria; Euarchontoglires; Glires; Rodentia; Myomorpha; Muroidea; Muridae; Murinae; Mus; Mus	

gene	sprot_Top_BLASTP_hit	gene_ontology_blast
Mcavernosa18050	SYAC_CAEEL\SYAC_CAEEL\Q:38-291,H:3-272\68.52%ID\E:1e-133\RecName: Full=Alanine--tRNA ligase, cytoplasmic {ECO:0000255|HAMAP-Rule:MF_03133};\Eukaryota; Metazoa; Ecdysozoa; Nematoda; Chromadorea; Rhabditida; Rhabditoidea; Rhabditidae; Peloderinae; Caenorhabditis|||SYAC_MOUSE\SYAC_MOUSE\Q:35-291,H:1-272\68.5%ID\E:3e-132\RecName: Full=Alanine--tRNA ligase, cytoplasmic {ECO:0000255|HAMAP-Rule:MF_03133};\Eukaryota; Metazoa; Chordata; Craniata; Vertebrata; Euteleostomi; Mammalia; Eutheria; Euarchontoglires; Glires; Rodentia; Myomorpha; Muroidea; Muridae; Murinae; Mus; Mus|||SYAC_HUMAN\SYAC_HUMAN\Q:35-291,H:1-272\68.13%ID\E:2e-131\RecName: Full=Alanine--tRNA ligase, cytoplasmic {ECO:0000255|HAMAP-Rule:MF_03133};\Eukaryota; Metazoa; Chordata; Craniata; Vertebrata; Euteleostomi; Mammalia; Eutheria; Euarchontoglires; Primates; Haplorrhini; Catarrhini; Hominidae; Homo	GO:0005737\cellular_component\cytoplasm|||GO:0004813\molecular_function\alanine-tRNA ligase activity|||GO:0016597\molecular_function\amino acid binding|||GO:0005524\molecular_function\ATP binding|||GO:0046872\molecular_function\metal ion binding|||GO:0000049\molecular_function\tRNA binding|||GO:0006419\biological_process\alanyl-tRNA aminoacylation|||GO:0006400\biological_process\tRNA modification
Mcavernosa18988	MYH9_HUMAN\MYH9_HUMAN\Q:5299-6165,H:882-1733\22.86%ID\E:2e-32\RecName:	GO:0015629\cellular_component\actin cytoskeleton|||GO:0042641\cellular_component\actomyosi

gene	sprot_Top_BLASTP_hit	gene_ontology_blast
	Full=Myosin-9;\Eukaryota; Metazoa; Chordata; Craniata; Vertebrata; Euteleostomi; Mammalia; Eutheria; Euarchontoglires; Primates; Haplorrhini; Catarrhini; Hominidae; Homo|||\MYH10_HUMAN\MYH10_HUMAN\Q:5318-6165,H:868-1740\23.03%ID\E:2e-31\RecName: Full=Myosin-10;\Eukaryota; Metazoa; Chordata; Craniata; Vertebrata; Euteleostomi; Mammalia; Eutheria; Euarchontoglires; Primates; Haplorrhini; Catarrhini; Hominidae; Homo|||\MYH9_CANLF\MYH9_CANLF\Q:5299-6165,H:882-1733\22.49%ID\E:5e-31\RecName: Full=Myosin-9;\Eukaryota; Metazoa; Chordata; Craniata; Vertebrata; Euteleostomi; Mammalia; Eutheria; Laurasiatheria; Carnivora; Caniformia; Canidae; Canis|||\MYH9_HUMAN\MYH9_HUMAN\Q:5316-6173,H:1001-1895\22.29%ID\E:4e-26\RecName: Full=Myosin-9;\Eukaryota; Metazoa; Chordata; Craniata; Vertebrata; Euteleostomi; Mammalia; Eutheria; Euarchontoglires; Primates; Haplorrhini; Catarrhini; Hominidae; Homo|||\MYH9_CANLF\MYH9_CANLF\Q:5316-6159,H:1001-1913\21.52%ID\E:3e-25\RecName: Full=Myosin-9;\Eukaryota; Metazoa; Chordata; Craniata; Vertebrata; Euteleostomi; Mammalia; Eutheria; Laurasiatheria; Carnivora; Caniformia;	n|||\GO:0005826\cellular_component\actomyosin contractile ring|||\GO:0005903\cellular_component\brush border|||\GO:0031252\cellular_component\cell leading edge|||\GO:0005913\cellular_component\cell-cell adherens junction|||\GO:0032154\cellular_component\cleavage furrow|||\GO:0005737\cellular_component\cytoplasm|||\GO:0005829\cellular_component\cytosol|||\GO:0070062\cellular_component\extracellular exosome|||\GO:0005925\cellular_component\focal adhesion|||\GO:0001772\cellular_component\immunological synapse|||\GO:0016020\cellular_component\membrane|||\GO:0016460\cellular_component\myosin II complex|||\GO:0097513\cellular_component\myosin II filament|||\GO:0031594\cellular_component\neuromuscular junction|||\GO:0005634\cellular_component\nucleus|||\GO:0005886\cellular_component\plasma membrane|||\GO:0032991\cellular_component\protein-containing complex|||\GO:0001726\cellular_component\ruffle|||\GO:0005819\cellular_component\spindle|||\GO:0001725\cellular_component\stress fiber|||\GO:0001931\cellular_component\uropod|||\GO:0003779\molecular_function\actin binding|||\GO:0051015\molecular_function\actin filament binding|||\GO:0030898\molecular_function\actin-dependent ATPase

gene	sprot_Top_BLASTP_hit	gene_ontology_blast
	Canidae; Canis||||MYH10_HUMAN\MYH10_HUMAN\Q:4967-6049,H:843-1930\22.26%ID\E:8e-25\RecName: Full=Myosin-10;\Eukaryota; Metazoa; Chordata; Craniata; Vertebrata; Euteleostomi; Mammalia; Eutheria; Euarchontoglires; Primates; Haplorrhini; Catarrhini; Hominidae; Homo||||MYH9_HUMAN\MYH9_HUMAN\Q:5299-6049,H:1184-1923\22.25%ID\E:1e-21\RecName: Full=Myosin-9;\Eukaryota; Metazoa; Chordata; Craniata; Vertebrata; Euteleostomi; Mammalia; Eutheria; Euarchontoglires; Primates; Haplorrhini; Catarrhini; Hominidae; Homo||||MYH9_CANLF\MYH9_CANLF\Q:5299-6049,H:1184-1923\22.35%ID\E:5e-21\RecName: Full=Myosin-9;\Eukaryota; Metazoa; Chordata; Craniata; Vertebrata; Euteleostomi; Mammalia; Eutheria; Laurasiatheria; Carnivora; Caniformia; Canidae; Canis||||MYH9_CANLF\MYH9_CANLF\Q:5454-6174,H:884-1677\21.25%ID\E:5e-20\RecName: Full=Myosin-9;\Eukaryota; Metazoa; Chordata; Craniata; Vertebrata; Euteleostomi; Mammalia; Eutheria; Laurasiatheria; Carnivora; Caniformia; Canidae; Canis||||MYH10_HUMAN\MYH10_HUMAN\Q:5598-6200,H:840-1390\23.41%ID\E:1e-18\RecName:	activity||||GO:0043531\molecular_function\ADP binding||||GO:0005524\molecular_function\ATP binding||||GO:0016887\molecular_function\ATPase activity||||GO:0045296\molecular_function\cadherin binding||||GO:0005516\molecular_function\calmodulin binding||||GO:0000146\molecular_function\microfilament motor activity||||GO:0008017\molecular_function\microtubule binding||||GO:0003777\molecular_function\microtubule motor activity||||GO:0003774\molecular_function\motor activity||||GO:0019904\molecular_function\protein domain specific binding||||GO:0042803\molecular_function\protein homodimerization activity||||GO:0043495\molecular_function\protein membrane anchor||||GO:0003723\molecular_function\RNA binding||||GO:0031532\biological_process\actin cytoskeleton reorganization||||GO:0030048\biological_process\actin filament-based movement||||GO:0031032\biological_process\actomyosin structure organization||||GO:0001525\biological_process\angiogenesis||||GO:0043534\biological_process\blood vessel endothelial cell migration||||GO:0032506\biological_process\cytokinetic process||||GO:0051295\biological_process\establishment of meiotic spindle

gene	sprot_Top_BLASTP_hit	gene_ontology_blast
	Full=Myosin-10;\Eukaryota; Metazoa; Chordata; Craniata; Vertebrata; Euteleostomi; Mammalia; Eutheria; Euarchontoglires; Primates; Haplorrhini; Catarrhini; Hominidae; Homo|||\MYH9_HUMAN\MYH9_HUMAN\Q:5571-6175,H:842-1512\24.75%ID\E:1e-16\RecName: Full=Myosin-9;\Eukaryota; Metazoa; Chordata; Craniata; Vertebrata; Euteleostomi; Mammalia; Eutheria; Euarchontoglires; Primates; Haplorrhini; Catarrhini; Hominidae; Homo|||\MYH9_CANLF\MYH9_CANLF\Q:5571-6175,H:842-1512\25.43%ID\E:6e-16\RecName: Full=Myosin-9;\Eukaryota; Metazoa; Chordata; Craniata; Vertebrata; Euteleostomi; Mammalia; Eutheria; Laurasiatheria; Carnivora; Caniformia; Canidae; Canis	localization|||\GO:0001768\biological_process\establishment of T cell polarity|||\GO:0001701\biological_process\in utero embryonic development|||\GO:0007229\biological_process\integrin-mediated signaling pathway|||\GO:0050900\biological_process\leukocyte migration|||\GO:0000212\biological_process\meiotic spindle organization|||\GO:0006509\biological_process\membrane protein ectodomain proteolysis|||\GO:0007018\biological_process\microtubule-based movement|||\GO:0030224\biological_process\monocyte differentiation|||\GO:0007520\biological_process\myoblast fusion|||\GO:1903919\biological_process\negative regulation of actin filament severing|||\GO:0006911\biological_process\phagocytosis, engulfment|||\GO:0070527\biological_process\platelet aggregation|||\GO:0030220\biological_process\platelet formation|||\GO:1903923\biological_process\positive regulation of protein processing in phagocytic vesicle|||\GO:0015031\biological_process\protein transport|||\GO:0008360\biological_process\regulation of cell shape|||\GO:0032796\biological_process\uropod organization
Mcavernosa19071	.	.

gene	sprot_Top_BLASTP_hit	gene_ontology_blast
Mcavernosa21397	.	.
Mcavernosa21398	RPA1_HUMAN\RPA1_HUMAN\Q:5-228,H:548-767\63.84%ID\E:3e-95\RecName: Full=DNA-directed RNA polymerase I subunit RPA1;\Eukaryota; Metazoa; Chordata; Craniata; Vertebrata; Euteleostomi; Mammalia; Eutheria; Euarchontoglires; Primates; Haplorrhini; Catarrhini; Hominidae; Homo|||\RPA1_MOUSE\RPA1_MOUSE\Q:5-228,H:555-774\62.95%ID\E:9e-95\RecName: Full=DNA-directed RNA polymerase I subunit RPA1;\Eukaryota; Metazoa; Chordata; Craniata; Vertebrata; Euteleostomi; Mammalia; Eutheria; Euarchontoglires; Glires; Rodentia; Myomorpha; Muroidea; Muridae; Murinae; Mus; Mus|||\RPA1_RAT\RPA1_RAT\Q:5-228,H:555-774\62.5%ID\E:1e-93\RecName: Full=DNA-directed RNA polymerase I subunit RPA1;\Eukaryota; Metazoa; Chordata; Craniata; Vertebrata; Euteleostomi; Mammalia; Eutheria; Euarchontoglires; Glires; Rodentia; Myomorpha; Muroidea; Muridae; Murinae; Rattus	GO:0005736\cellular_component\DNA-directed RNA polymerase I complex|||GO:0005654\cellular_component\nucleoplasm|||GO:0003682\molecular_function\chromatin binding|||GO:0003677\molecular_function\DNA binding|||GO:0001054\molecular_function\RNA polymerase I activity|||GO:0008270\molecular_function\zinc ion binding|||GO:1904750\biological_process\negative regulation of protein localization to nucleolus|||GO:0045815\biological_process\positive regulation of gene expression, epigenetic|||GO:0006363\biological_process\termination of RNA polymerase I transcription|||GO:0006361\biological_process\transcription initiation from RNA polymerase I promoter
Mcavernosa21581	CASP2_CHICK\CASP2_CHICK\Q:1-411,H:7-418\30.05%ID\E:4e-62\RecName: Full=Caspase-2;\Eukaryota; Metazoa; Chordata; Craniata;	GO:0005737\cellular_component\cytoplasm|||GO:0097200\molecular_function\cysteine-type endopeptidase activity involved in execution phase of

gene	sprot_Top_BLASTP_hit	gene_ontology_blast
	Vertebrata; Euteleostomi; Archelosauria; Archosauria; Dinosauria; Saurischia; Theropoda; Coelurosauria; Aves; Neognathae; Galloanserae; Galliformes; Phasianidae; Phasianinae; Gallus||||CASP2_HUMAN\CASP2_HUMAN\Q:1-411,H:32-447\32.95%ID\E:7e-60\RecName: Full=Caspase-2;\Eukaryota; Metazoa; Chordata; Craniata; Vertebrata; Euteleostomi; Mammalia; Eutheria; Euarchontoglires; Primates; Haplorrhini; Catarrhini; Hominidae; Homo||||CASP2_MOUSE\CASP2_MOUSE\Q:6-411,H:37-447\32.57%ID\E:1e-59\RecName: Full=Caspase-2;\Eukaryota; Metazoa; Chordata; Craniata; Vertebrata; Euteleostomi; Mammalia; Eutheria; Euarchontoglires; Glires; Rodentia; Myomorpha; Muroidea; Muridae; Murinae; Mus; Mus	apoptosis||||GO:0097194\biological_process\execution phase of apoptosis||||GO:0042981\biological_process\regulation of apoptotic process
Mcavernosa22143	ANM5_HUMAN\ANM5_HUMAN\Q:26-327,H:182-483\65.56%ID\E:9e-140\RecName: Full=Protein arginine N-methyltransferase 5;\Eukaryota; Metazoa; Chordata; Craniata; Vertebrata; Euteleostomi; Mammalia; Eutheria; Euarchontoglires; Primates; Haplorrhini; Catarrhini; Hominidae; Homo||||ANM5_PONAB\ANM5_PONAB\Q:26-327,H:182-483\65.56%ID\E:2e-139\RecName:	GO:0005737\cellular_component\cytoplasm||||GO:0005829\cellular_component\cytosol||||GO:0005794\cellular_component\Golgi apparatus||||GO:0035097\cellular_component\histone methyltransferase complex||||GO:0034709\cellular_component\methylosome||||GO:0005654\cellular_component\nucleoplasm||||GO:0005634\cellular_component\nucleus||||GO:0001046\molecular_function\core promoter sequence-specific DNA

gene	sprot_Top_BLASTP_hit	gene_ontology_blast
	Full=Protein arginine N-methyltransferase 5;\Eukaryota; Metazoa; Chordata; Craniata; Vertebrata; Euteleostomi; Mammalia; Eutheria; Euarchontoglires; Primates; Haplorrhini; Catarrhini; Hominidae; Pongo|||ANM5_MACFA\ANM5_MACFA\Q:26-327,H:182-483\65.23%ID\E:7e-139\RecName: Full=Protein arginine N-methyltransferase 5;\Eukaryota; Metazoa; Chordata; Craniata; Vertebrata; Euteleostomi; Mammalia; Eutheria; Euarchontoglires; Primates; Haplorrhini; Catarrhini; Cercopithecidae; Cercopithecinae; Macaca|||ANM5_HUMAN\ANM5_HUMAN\Q:327-377,H:587-637\47.06%ID\E:3e-08\RecName: Full=Protein arginine N-methyltransferase 5;\Eukaryota; Metazoa; Chordata; Craniata; Vertebrata; Euteleostomi; Mammalia; Eutheria; Euarchontoglires; Primates; Haplorrhini; Catarrhini; Hominidae; Homo|||ANM5_PONAB\ANM5_PONAB\Q:327-377,H:587-637\47.06%ID\E:3e-08\RecName: Full=Protein arginine N-methyltransferase 5;\Eukaryota; Metazoa; Chordata; Craniata; Vertebrata; Euteleostomi; Mammalia; Eutheria; Euarchontoglires; Primates; Haplorrhini; Catarrhini; Hominidae; Pongo|||ANM5_MACFA\ANM5_MACFA\Q:327-	binding|||GO:0044020\molecular_function\histone methyltransferase activity (H4-R3 specific)|||GO:0008469\molecular_function\histone-arginine N-methyltransferase activity|||GO:0042802\molecular_function\identical protein binding|||GO:0008327\molecular_function\methyl-CpG binding|||GO:0008168\molecular_function\methyltransferase activity|||GO:0046982\molecular_function\protein heterodimerization activity|||GO:0016274\molecular_function\protein-arginine N-methyltransferase activity|||GO:0035243\molecular_function\protein-arginine omega-N symmetric methyltransferase activity|||GO:0043021\molecular_function\ribonucleoprotein complex binding|||GO:0003714\molecular_function\transcription corepressor activity|||GO:0008283\biological_process\cell proliferation|||GO:0032922\biological_process\circadian regulation of gene expression|||GO:0006353\biological_process\DNA-templated transcription, termination|||GO:0042118\biological_process\endothelial cell activation|||GO:0090161\biological_process\Golgi ribbon formation|||GO:0043985\biological_process\histone H4-R3 methylation|||GO:0097421\biological_process\liver regeneration|||GO:0045596\biological_process\negative regulation of cell

gene	sprot_Top_BLASTP_hit	gene_ontology_blast
	377,H:587-637\47.06%ID\E:3e-08\RecName: Full=Protein arginine N-methyltransferase 5;\Eukaryota; Metazoa; Chordata; Craniata; Vertebrata; Euteleostomi; Mammalia; Eutheria; Euarchontoglires; Primates; Haplorrhini; Catarrhini; Cercopithecidae; Cercopithecinae; Macaca	differentiation|||\GO:0018216\biological_process\peptidyl-arginine methylation|||\GO:0035246\biological_process\peptidyl-arginine N-methylation|||\GO:1904992\biological_process\positive regulation of adenylate cyclase-inhibiting dopamine receptor signaling pathway|||\GO:0048714\biological_process\positive regulation of oligodendrocyte differentiation|||\GO:0044030\biological_process\regulation of DNA methylation|||\GO:0070372\biological_process\regulation of ERK1 and ERK2 cascade|||\GO:0007088\biological_process\regulation of mitotic nuclear division|||\GO:1901796\biological_process\regulation of signal transduction by p53 class mediator|||\GO:0006355\biological_process\regulation of transcription, DNA-templated|||\GO:0000387\biological_process\spliceosomal snRNP assembly
Mcavernosa22765	NEO1_MOUSE\NEO1_MOUSE\Q:31-714,H:65-727\31.07%ID\E:4e-78\RecName: Full=Neogenin;\Eukaryota; Metazoa; Chordata; Craniata; Vertebrata; Euteleostomi; Mammalia; Eutheria; Euarchontoglires; Glires; Rodentia;	GO:0009986\cellular_component\cell surface|||\GO:0005794\cellular_component\Golgi apparatus|||\GO:0005887\cellular_component\integral component of plasma membrane|||\GO:0097708\cellular_component\intracellular

gene	sprot_Top_BLASTP_hit	gene_ontology_blast
	Myomorpha; Muroidea; Muridae; Murinae; Mus; Mus||||NEO1_CHICK\NEO1_CHICK\Q:17-685,H:6-659\30.14%ID\E:1e-76\RecName: Full=Neogenin;\Eukaryota; Metazoa; Chordata; Craniata; Vertebrata; Euteleostomi; Archelosauria; Archosauria; Dinosauria; Saurischia; Theropoda; Coelurosauria; Aves; Neognathae; Galloanserae; Galliformes; Phasianidae; Phasianinae; Gallus||||NEO1_RAT\NEO1_RAT\Q:31-714,H:23-665\29.6%ID\E:5e-74\RecName: Full=Neogenin;\Eukaryota; Metazoa; Chordata; Craniata; Vertebrata; Euteleostomi; Mammalia; Eutheria; Euarchontoglires; Glires; Rodentia; Myomorpha; Muroidea; Muridae; Murinae; Rattus||||NEO1_MOUSE\NEO1_MOUSE\Q:429-720,H:563-843\26.94%ID\E:2e-18\RecName: Full=Neogenin;\Eukaryota; Metazoa; Chordata; Craniata; Vertebrata; Euteleostomi; Mammalia; Eutheria; Euarchontoglires; Glires; Rodentia; Myomorpha; Muroidea; Muridae; Murinae; Mus; Mus||||NEO1_RAT\NEO1_RAT\Q:429-720,H:501-781\26.6%ID\E:4e-18\RecName: Full=Neogenin;\Eukaryota; Metazoa; Chordata; Craniata; Vertebrata; Euteleostomi; Mammalia; Eutheria; Euarchontoglires; Glires; Rodentia; Myomorpha; Muroidea; Muridae; Murinae;	vesicle||||GO:0016020\cellular_component\membrane||||GO:0043025\cellular_component\neuronal cell body||||GO:0005654\cellular_component\nucleoplasm||||GO:0005886\cellular_component\plasma membrane||||GO:0098797\cellular_component\plasma membrane protein complex||||GO:0070700\molecular_function\BMP receptor binding||||GO:0045296\molecular_function\cadherin binding||||GO:0039706\molecular_function\co-receptor binding||||GO:0038023\molecular_function\signaling receptor activity||||GO:0007411\biological_process\axon guidance||||GO:0007155\biological_process\cell adhesion||||GO:0055072\biological_process\iron ion homeostasis||||GO:0007520\biological_process\myoblast fusion||||GO:0048681\biological_process\negative regulation of axon regeneration||||GO:1901215\biological_process\negative regulation of neuron death||||GO:0050709\biological_process\negative regulation of protein secretion||||GO:0001764\biological_process\neuron migration||||GO:0030513\biological_process\positive regulation of BMP signaling pathway||||GO:0048679\biological_process\regulation of axon regeneration||||GO:2001222\biological_process\regulation of neuron

gene	sprot_Top_BLASTP_hit	gene_ontology_blast
	Rattus||||NEO1_CHICK\NEO1_CHICK\Q:428-720,H:517-797\26.51%ID\E:3e-15\RecName: Full=Neogenin;\Eukaryota; Metazoa; Chordata; Craniata; Vertebrata; Euteleostomi; Archelosauria; Archosauria; Dinosauria; Saurischia; Theropoda; Coelurosauria; Aves; Neognathae; Galloanserae; Galliformes; Phasianidae; Phasianinae; Gallus	migration||||GO:0006355\biological_process\regulation of transcription, DNA-templated
Mcavernosa22932	HNRL1_MOUSE\HNRL1_MOUSE\Q:42-427,H:212-601\53.33%ID\E:3e-139\RecName: Full=Heterogeneous nuclear ribonucleoprotein U-like protein 1;\Eukaryota; Metazoa; Chordata; Craniata; Vertebrata; Euteleostomi; Mammalia; Eutheria; Euarchontoglires; Glires; Rodentia; Myomorpha; Muroidea; Muridae; Murinae; Mus; Mus||||HNRL1_HUMAN\HNRL1_HUMAN\Q:42-427,H:211-600\53.08%ID\E:3e-139\RecName: Full=Heterogeneous nuclear ribonucleoprotein U-like protein 1;\Eukaryota; Metazoa; Chordata; Craniata; Vertebrata; Euteleostomi; Mammalia; Eutheria; Euarchontoglires; Primates; Haplorrhini; Catarrhini; Hominidae; Homo||||HNRPU_HUMAN\HNRPU_HUMAN\Q:42-434,H:288-675\45.2%ID\E:2e-107\RecName: Full=Heterogeneous nuclear ribonucleoprotein U {ECO:0000303|PubMed:1628625};\Eukaryota;	GO:0005654\cellular_component\nucleoplasm||||GO:0005634\cellular_component\nucleus||||GO:0019899\molecular_function\enzyme binding||||GO:0003723\molecular_function\RNA binding||||GO:0006355\biological_process\regulation of transcription, DNA-templated||||GO:0009615\biological_process\response to virus||||GO:0006396\biological_process\RNA processing||||GO:0006351\biological_process\transcription, DNA-templated

gene	sprot_Top_BLASTP_hit	gene_ontology_blast
	Metazoa; Chordata; Craniata;Vertebrata; Euteleostomi; Mammalia; Eutheria; Euarchontoglires; Primates; Haplorrhini; Catarrhini; Hominidae; Homo	
Mcavernosa23092	.	.
Mcavernosa23639	.	.
Mcavernosa23645	LDHD_HUMAN\LDHD_HUMAN\Q:37-381,H:20-414\53.42%ID\E:1e-141\RecName: Full=Probable D-lactate dehydrogenase, mitochondrial;\Eukaryota; Metazoa; Chordata; Craniata; Vertebrata; Euteleostomi; Mammalia; Eutheria; Euarchontoglires; Primates; Haplorrhini; Catarrhini; Hominidae; Homo|||\LDHD_MOUSE\LDHD_MOUSE\Q:44-381,H:27-391\56.44%ID\E:3e-136\RecName: Full=Probable D-lactate dehydrogenase, mitochondrial;\Eukaryota; Metazoa; Chordata; Craniata; Vertebrata; Euteleostomi; Mammalia; Eutheria; Euarchontoglires; Glires; Rodentia; Myomorpha; Muroidea; Muridae; Murinae; Mus; Mus|||\DLD_ARATH\DLD_ARATH\Q:41-382,H:103-469\38.27%ID\E:2e-80\RecName: Full=D-lactate dehydrogenase [cytochrome], mitochondrial;\Eukaryota; Viridiplantae;	GO:0005743\cellular_component\mitochondrial inner membrane|||\GO:0005739\cellular_component\mitochondrion|||\GO:0004458\molecular_function\D-lactate dehydrogenase (cytochrome) activity|||\GO:0050660\molecular_function\flavin adenine dinucleotide binding

gene	sprot_Top_BLASTP_hit	gene_ontology_blast
	Streptophyta; Embryophyta; Tracheophyta; Spermatophyta; Magnoliophyta; eudicotyledons; Gunneridae; Pentapetalae; rosids; malvids; Brassicales; Brassicaceae; Camelineae; Arabidopsis	
Mcavernosa24360	HMCN1_HUMAN\HMCN1_HUMAN\Q:66-360,H:3114-3384\22.88%ID\E:5e-08\RecName: Full=Hemicentin-1;\Eukaryota; Metazoa; Chordata; Craniata; Vertebrata; Euteleostomi; Mammalia; Eutheria; Euarchontoglires; Primates; Haplorrhini; Catarrhini; Hominidae; Homo|||HMCN2_MOUSE\HMCN2_MOUSE\Q:61-367,H:745-1021\24.85%ID\E:9e-08\RecName: Full=Hemicentin-2;\Eukaryota; Metazoa; Chordata; Craniata; Vertebrata; Euteleostomi; Mammalia; Eutheria; Euarchontoglires; Glires; Rodentia; Myomorpha; Muroidea; Muridae; Murinae; Mus; Mus|||HMCN1_HUMAN\HMCN1_HUMAN\Q:66-359,H:3490-3844\22.31%ID\E:2e-07\RecName: Full=Hemicentin-1;\Eukaryota; Metazoa; Chordata; Craniata; Vertebrata; Euteleostomi; Mammalia; Eutheria; Euarchontoglires; Primates; Haplorrhini; Catarrhini; Hominidae; Homo|||HMCN1_MOUSE\HMCN1_MOUSE\Q:40-354,H:3493-3747\21.77%ID\E:2e-07\RecName:	GO:0005604\cellular_component\basement membrane|||GO:0005938\cellular_component\cell cortex|||GO:0030054\cellular_component\cell junction|||GO:0032154\cellular_component\cleavage furrow|||GO:0070062\cellular_component\extracellular exosome|||GO:0005509\molecular_function\calcium ion binding|||GO:0007049\biological_process\cell cycle|||GO:0051301\biological_process\cell division|||GO:0050896\biological_process\response to stimulus|||GO:0007601\biological_process\visual perception

gene	sprot_Top_BLASTP_hit	gene_ontology_blast
	Full=Hemicentin-1 {ECO:0000312|MGI:MGI:2685047};\Eukaryota; Metazoa; Chordata; Craniata;Vertebrata; Euteleostomi; Mammalia; Eutheria; Euarchontoglires; Glires; Rodentia; Myomorpha; Muroidea; Muridae; Murinae; Mus; Mus|||HMCN1_MOUSE\HMCN1_MOUSE\Q:55-359,H:2718-3004\23.05%ID\E:4e-07\RecName: Full=Hemicentin-1 {ECO:0000312|MGI:MGI:2685047};\Eukaryota; Metazoa; Chordata; Craniata;Vertebrata; Euteleostomi; Mammalia; Eutheria; Euarchontoglires; Glires; Rodentia; Myomorpha; Muroidea; Muridae; Murinae; Mus; Mus|||HMCN1_HUMAN\HMCN1_HUMAN\Q:67-359,H:2730-3005\21.79%ID\E:6e-07\RecName: Full=Hemicentin-1;\Eukaryota; Metazoa; Chordata; Craniata;Vertebrata; Euteleostomi; Mammalia; Eutheria; Euarchontoglires; Primates; Haplorrhini; Catarrhini; Hominidae; Homo|||HMCN1_HUMAN\HMCN1_HUMAN\Q:62-367,H:3393-3670\22.89%ID\E:1e-05\RecName: Full=Hemicentin-1;\Eukaryota; Metazoa; Chordata; Craniata;Vertebrata; Euteleostomi; Mammalia; Eutheria; Euarchontoglires; Primates; Haplorrhini; Catarrhini; Hominidae; Homo	

gene	sprot_Top_BLASTP_hit	gene_ontology_blast
Mcavernosa25195	FBP1_STRPU\FBP1_STRPU\Q:220-791,H:227-823\39.97%ID\E:3e-115\RecName: Full=Fibropellin-1;\Eukaryota; Metazoa; Echinodermata; Eleutherozoa; Echinozoa; Echinoidea; Euechinoidea; Echinacea; Echinoida; Strongylocentrotidae; Strongylocentrotus|||FBP1_STRPU\FBP1_STRPU\Q:221-791,H:173-785\38.66%ID\E:6e-111\RecName: Full=Fibropellin-1;\Eukaryota; Metazoa; Echinodermata; Eleutherozoa; Echinozoa; Echinoidea; Euechinoidea; Echinacea; Echinoida; Strongylocentrotidae; Strongylocentrotus|||FBP1_STRPU\FBP1_STRPU\Q:205-791,H:304-899\38.94%ID\E:2e-110\RecName: Full=Fibropellin-1;\Eukaryota; Metazoa; Echinodermata; Eleutherozoa; Echinozoa; Echinoidea; Euechinoidea; Echinacea; Echinoida; Strongylocentrotidae; Strongylocentrotus|||FBP1_STRPU\FBP1_STRPU\Q:205-751,H:353-936\39.66%ID\E:6e-106\RecName: Full=Fibropellin-1;\Eukaryota; Metazoa; Echinodermata; Eleutherozoa; Echinozoa; Echinoidea; Euechinoidea; Echinacea; Echinoida; Strongylocentrotidae; Strongylocentrotus|||NOTC1_XENTR\NOTC1_XENTR\Q:228-791,H:397-983\38.94%ID\E:4e-104\RecName: Full=Neurogenic locus notch	GO:0032579\cellular_component\apical lamina of hyaline layer|||GO:0031410\cellular_component\cytoplasmic vesicle|||GO:0005615\cellular_component\extracellular space|||GO:0005509\molecular_function\calcium ion binding

gene	sprot_Top_BLASTP_hit	gene_ontology_blast
	homolog protein 1;\Eukaryota; Metazoa; Chordata; Craniata; Vertebrata; Euteleostomi; Amphibia; Batrachia; Anura; Pipoidea; Pipidae; Xenopodinae; Xenopus; Silurana|||\NOTC1_MOUSE\NOTC1_MOUSE\Q:228-791,H:398-984\38.67%ID\E:2e-102\RecName: Full=Neurogenic locus notch homolog protein 1;\Eukaryota; Metazoa; Chordata; Craniata; Vertebrata; Euteleostomi; Mammalia; Eutheria; Euarchontoglires; Glires; Rodentia; Myomorpha; Muroidea; Muridae; Murinae; Mus; Mus|||\FBP1_STRPU\FBP1_STRPU\Q:263-791,H:172-709\39.45%ID\E:4e-99\RecName: Full=Fibropellin-1;\Eukaryota; Metazoa; Echinodermata; Eleutherozoa; Echinozoa; Echinoidea; Euechinoidea; Echinacea; Echinoida; Strongylocentrotidae; Strongylocentrotus|||\NOTC1_XENTR\NOTC1_XENTR\Q:223-788,H:658-1345\33.57%ID\E:3e-94\RecName: Full=Neurogenic locus notch homolog protein 1;\Eukaryota; Metazoa; Chordata; Craniata; Vertebrata; Euteleostomi; Amphibia; Batrachia; Anura; Pipoidea; Pipidae; Xenopodinae; Xenopus; Silurana|||\NOTC1_MOUSE\NOTC1_MOUSE\Q:205-791,H:628-1349\33.33%ID\E:2e-93\RecName: Full=Neurogenic locus notch homolog protein	

gene	sprot_Top_BLASTP_hit	gene_ontology_blast
	1;\Eukaryota; Metazoa; Chordata; Craniata; Vertebrata; Euteleostomi; Mammalia; Eutheria; Euarchontoglires; Glires; Rodentia; Myomorpha; Muroidea; Muridae; Murinae; Mus; Mus|||\NOTC1_XENTR\NOTC1_XENTR\Q:228-787,H:128-712\38.06%ID\E:1e-91\RecName: Full=Neurogenic locus notch homolog protein 1;\Eukaryota; Metazoa; Chordata; Craniata; Vertebrata; Euteleostomi; Amphibia; Batrachia; Anura; Pipoidea; Pipidae; Xenopodinae; Xenopus; Silurana|||\FBP1_STRPU\FBP1_STRPU\Q:172-670,H:392-935\38.83%ID\E:1e-90\RecName: Full=Fibropellin-1;\Eukaryota; Metazoa; Echinodermata; Eleutherozoa; Echinozoa; Echinoidea; Euechinoidea; Echinacea; Echinoida; Strongylocentrotidae; Strongylocentrotus|||\NOTC1_XENTR\NOTC1_XENTR\Q:227-790,H:241-790\35.64%ID\E:1e-87\RecName: Full=Neurogenic locus notch homolog protein 1;\Eukaryota; Metazoa; Chordata; Craniata; Vertebrata; Euteleostomi; Amphibia; Batrachia; Anura; Pipoidea; Pipidae; Xenopodinae; Xenopus; Silurana|||\NOTC1_XENTR\NOTC1_XENTR\Q:222-791,H:542-1221\33.67%ID\E:5e-87\RecName: Full=Neurogenic locus notch homolog protein	

gene	sprot_Top_BLASTP_hit	gene_ontology_blast
	1;\Eukaryota; Metazoa; Chordata; Craniata; Vertebrata; Euteleostomi; Amphibia; Batrachia; Anura; Pipoidea; Pipidae; Xenopodinae; Xenopus; Silurana|||\NOTC1_MOUSE\NOTC1_MOUSE\Q:205-787,H:553-1180\35.03%ID\E:5e-87\RecName: Full=Neurogenic locus notch homolog protein 1;\Eukaryota; Metazoa; Chordata; Craniata; Vertebrata; Euteleostomi; Mammalia; Eutheria; Euarchontoglires; Glires; Rodentia; Myomorpha; Muroidea; Muridae; Murinae; Mus; Mus|||\NOTC1_XENTR\NOTC1_XENTR\Q:172-788,H:665-1383\32.38%ID\E:7e-87\RecName: Full=Neurogenic locus notch homolog protein 1;\Eukaryota; Metazoa; Chordata; Craniata; Vertebrata; Euteleostomi; Amphibia; Batrachia; Anura; Pipoidea; Pipidae; Xenopodinae; Xenopus; Silurana|||\NOTC1_XENTR\NOTC1_XENTR\Q:211-790,H:18-640\34.93%ID\E:2e-86\RecName: Full=Neurogenic locus notch homolog protein 1;\Eukaryota; Metazoa; Chordata; Craniata; Vertebrata; Euteleostomi; Amphibia; Batrachia; Anura; Pipoidea; Pipidae; Xenopodinae; Xenopus; Silurana|||\NOTC1_MOUSE\NOTC1_MOUSE\Q:206-748,H:89-675\35.74%ID\E:1e-85\RecName:	

gene	sprot_Top_BLASTP_hit	gene_ontology_blast
	Full=Neurogenic locus notch homolog protein 1;\Eukaryota; Metazoa; Chordata; Craniata; Vertebrata; Euteleostomi; Mammalia; Eutheria; Euarchontoglires; Glires; Rodentia; Myomorpha; Muroidea; Muridae; Murinae; Mus; Mus|||\NOTC1_MOUSE\NOTC1_MOUSE\Q:212-790,H:21-641\33.54%ID\E:2e-83\RecName: Full=Neurogenic locus notch homolog protein 1;\Eukaryota; Metazoa; Chordata; Craniata; Vertebrata; Euteleostomi; Mammalia; Eutheria; Euarchontoglires; Glires; Rodentia; Myomorpha; Muroidea; Muridae; Murinae; Mus; Mus|||\NOTC1_MOUSE\NOTC1_MOUSE\Q:205-710,H:856-1425\34.59%ID\E:3e-78\RecName: Full=Neurogenic locus notch homolog protein 1;\Eukaryota; Metazoa; Chordata; Craniata; Vertebrata; Euteleostomi; Mammalia; Eutheria; Euarchontoglires; Glires; Rodentia; Myomorpha; Muroidea; Muridae; Murinae; Mus; Mus|||\FBP1_STRPU\FBP1_STRPU\Q:270-791,H:22-557\33.93%ID\E:1e-67\RecName: Full=Fibropellin-1;\Eukaryota; Metazoa; Echinodermata; Eleutherozoa; Echinozoa; Echinoidea; Euechinoidea; Echinacea; Echinoida; Strongylocentrotidae; Strongylocentrotus|||\NOTC1_XENTR\NOTC1_XENTR\Q:222-631,H:962-1424\33.84%ID\E:7e-	

gene	sprot_Top_BLASTP_hit	gene_ontology_blast
	58\RecName: Full=Neurogenic locus notch homolog protein 1;\Eukaryota; Metazoa; Chordata; Craniata; Vertebrata; Euteleostomi; Amphibia; Batrachia; Anura; Pipoidea; Pipidae; Xenopodinae; Xenopus; Silurana|||\NOTC1_MOUSE\NOTC1_MOUSE\Q:222-678,H:963-1555\30.32%ID\E:1e-47\RecName: Full=Neurogenic locus notch homolog protein 1;\Eukaryota; Metazoa; Chordata; Craniata; Vertebrata; Euteleostomi; Mammalia; Eutheria; Euarchontoglires; Glires; Rodentia; Myomorpha; Muroidea; Muridae; Murinae; Mus; Mus|||\NOTC1_MOUSE\NOTC1_MOUSE\Q:172-485,H:1171-1562\28.39%ID\E:2e-18\RecName: Full=Neurogenic locus notch homolog protein 1;\Eukaryota; Metazoa; Chordata; Craniata; Vertebrata; Euteleostomi; Mammalia; Eutheria; Euarchontoglires; Glires; Rodentia; Myomorpha; Muroidea; Muridae; Murinae; Mus; Mus|||\NOTC1_XENTR\NOTC1_XENTR\Q:172-488,H:1170-1563\26.93%ID\E:2e-12\RecName: Full=Neurogenic locus notch homolog protein 1;\Eukaryota; Metazoa; Chordata; Craniata; Vertebrata; Euteleostomi; Amphibia; Batrachia; Anura; Pipoidea; Pipidae; Xenopodinae; Xenopus; Silurana	

gene	sprot_Top_BLASTP_hit	gene_ontology_blast
Mcavernosa25451	TF3C3_HUMAN\TF3C3_HUMAN\Q:152-960,H:117-886\38.52%ID\E:1e-178\RecName: Full=General transcription factor 3C polypeptide 3;\Eukaryota; Metazoa; Chordata; Craniata; Vertebrata; Euteleostomi; Mammalia; Eutheria; Euarchontoglires; Primates; Haplorrhini; Catarrhini; Hominidae; Homo|||\SFC4_SCHPO\SFC4_SCHPO\Q:802-953,H:843-999\40.51%ID\E:5e-22\RecName: Full=Transcription factor tau subunit sfc4;\Eukaryota; Fungi; Dikarya; Ascomycota; Taphrinomycotina; Schizosaccharomycetes; Schizosaccharomycetales; Schizosaccharomycetaceae; Schizosaccharomyces|||TFC4_YEAST\TFC4_YEAST\Q:800-960,H:881-1025\32.93%ID\E:8e-17\RecName: Full=Transcription factor tau 131 kDa subunit;\Eukaryota; Fungi; Dikarya; Ascomycota; Saccharomycotina; Saccharomycetes; Saccharomycetales; Saccharomycetaceae; Saccharomyces|||TFC4_YEAST\TFC4_YEAST\Q:164-614,H:118-606\20.28%ID\E:3e-11\RecName: Full=Transcription factor tau 131 kDa subunit;\Eukaryota; Fungi; Dikarya; Ascomycota; Saccharomycotina;	GO:0031965\cellular_component\nuclear membrane|||GO:0005730\cellular_component\nucleolus|||GO:0005654\cellular_component\nucleoplasm|||GO:0005634\cellular_component\nucleus|||GO:0000127\cellular_component\transcription factor TFIIIC complex|||GO:0003677\molecular_function\DNA binding|||GO:0042791\biological_process\5S class rRNA transcription by RNA polymerase III|||GO:0006359\biological_process\regulation of transcription by RNA polymerase III|||GO:0006383\biological_process\transcription by RNA polymerase III|||GO:0006351\biological_process\transcription, DNA-templated|||GO:0042797\biological_process\tRNA transcription by RNA polymerase III

gene	sprot_Top_BLASTP_hit	gene_ontology_blast
	Saccharomycetes; Saccharomycetales; Saccharomycetaceae; Saccharomyces	
Mcavernosa25785	.	.
Mcavernosa26601	.	.
Mcavernosa27173	SGS1_YEAST\SGS1_YEAST\Q:82-207,H:683-803\40%ID\E:5e-16\RecName: Full=ATP-dependent helicase SGS1 {ECO:0000303|PubMed:7969174};\Eukaryota; Fungi; Dikarya; Ascomycota; Saccharomycotina; Saccharomycetes; Saccharomycetales; Saccharomycetaceae; Saccharomyces||||RQL4A_ARATH\RQL4A_ARATH\Q:82-190,H:458-560\40%ID\E:2e-13\RecName: Full=ATP-dependent DNA helicase Q-like 4A;\Eukaryota; Viridiplantae; Streptophyta; Embryophyta; Tracheophyta; Spermatophyta; Magnoliophyta; eudicotyledons; Gunneridae; Pentapetalae; rosids; malvids; Brassicales; Brassicaceae; Camelineae; Arabidopsis||||RECQ_HAEIN\RECQ_HAEIN\Q:90-200,H:41-143\35.65%ID\E:4e-13\RecName: Full=ATP-dependent DNA helicase RecQ;\Bacteria; Proteobacteria;	GO:0005737\cellular_component\cytoplasm||||GO:0005730\cellular_component\nucleolus||||GO:0031422\cellular_component\RecQ helicase-Topo III complex||||GO:0005524\molecular_function\ATP binding||||GO:0043140\molecular_function\ATP-dependent 3'-5' DNA helicase activity||||GO:0004003\molecular_function\ATP-dependent DNA helicase activity||||GO:0003677\molecular_function\DNA binding||||GO:0009378\molecular_function\four-way junction helicase activity||||GO:0051276\biological_process\chromosome organization||||GO:0000729\biological_process\DNA double-strand break processing||||GO:0032508\biological_process\DNA duplex unwinding||||GO:0006265\biological_process\DNA topological change||||GO:0006268\biological_process\DNA unwinding involved in DNA replication||||GO:0000724\biological_process\double-strand break repair via homologous

gene	sprot_Top_BLASTP_hit	gene_ontology_blast
	Gammaproteobacteria; Pasteurellales; Pasteurellaceae; Haemophilus	recombination||||GO:0031292\biological_process\gene conversion at mating-type locus, DNA double-strand break processing||||GO:0031573\biological_process\intra-S DNA damage checkpoint||||GO:0045132\biological_process\meiotic chromosome segregation||||GO:0000706\biological_process\meiotic DNA double-strand break processing||||GO:0000070\biological_process\mitotic sister chromatid segregation||||GO:0010947\biological_process\negative regulation of meiotic joint molecule formation||||GO:0010520\biological_process\regulation of reciprocal meiotic recombination||||GO:0001302\biological_process\replicative cell aging||||GO:0000723\biological_process\telomere maintenance||||GO:0000722\biological_process\telomere maintenance via recombination||||GO:0031860\biological_process\telomeric 3' overhang formation
Mcavernosa27529	.	.
Mcavernosa28002	DEGS1_BOVIN\DEGS1_BOVIN\Q:1-324,H:1-323\57.41%ID\E:7e-141\RecName: Full=Sphingolipid delta(4)-desaturase DES1;\Eukaryota; Metazoa; Chordata; Craniata;	GO:0005789\cellular_component\endoplasmic reticulum membrane||||GO:0016021\cellular_component\integral component of membrane||||GO:0005739\cellular_component\mitochondri

gene	sprot_Top_BLASTP_hit	gene_ontology_blast
	Vertebrata; Euteleostomi; Mammalia; Eutheria; Laurasiatheria; Cetartiodactyla; Ruminantia; Pecora; Bovidae; Bovinae; Bos||||DEGS1_XENTR\DEGS1_XENTR\Q:1-315,H:1-315\57.14%ID\E:8e-138\RecName: Full=Sphingolipid delta(4)-desaturase DES1;\Eukaryota; Metazoa; Chordata; Craniata; Vertebrata; Euteleostomi; Amphibia; Batrachia; Anura; Pipoidea; Pipidae; Xenopodinae; Xenopus; Silurana||||DEGS1_CHICK\DEGS1_CHICK\Q:1-315,H:1-315\57.14%ID\E:3e-137\RecName: Full=Sphingolipid delta(4)-desaturase DES1;\Eukaryota; Metazoa; Chordata; Craniata; Vertebrata; Euteleostomi; Archelosauria; Archosauria; Dinosauria; Saurischia; Theropoda; Coelurosauria; Aves; Neognathae; Galloanserae; Galliformes; Phasianidae; Phasianinae; Gallus	on||||GO:0042284\molecular_function\sphingolipid delta-4 desaturase activity||||GO:0046513\biological_process\ceramide biosynthetic process||||GO:0006633\biological_process\fatty acid biosynthetic process
Mcavernosa28270	.	.
Mcavernosa29278	.	.
Mcavernosa29636	LRC34_MOUSE\LRC34_MOUSE\Q:8-317,H:5-338\37.28%ID\E:7e-63\RecName: Full=Leucine-rich repeat-containing protein 34;\Eukaryota; Metazoa; Chordata; Craniata; Vertebrata;	GO:0005737\cellular_component\cytoplasm||||GO:0005730\cellular_component\nucleolus||||GO:0030154\biological_process\cell differentiation

gene	sprot_Top_BLASTP_hit	gene_ontology_blast
	Euteleostomi; Mammalia; Eutheria; Euarchontoglires; Glires; Rodentia; Myomorpha; Muroidea; Muridae; Murinae; Mus; Mus||||LRC34_HUMAN\LRC34_HUMAN\Q:2-308,H:48-378\38.39%ID\E:2e-62\RecName: Full=Leucine-rich repeat-containing protein 34;\Eukaryota; Metazoa; Chordata; Craniata; Vertebrata; Euteleostomi; Mammalia; Eutheria; Euarchontoglires; Primates; Haplorrhini; Catarrhini; Hominidae; Homo||||LRC34_RAT\LRC34_RAT\Q:8-317,H:5-338\36.98%ID\E:8e-62\RecName: Full=Leucine-rich repeat-containing protein 34;\Eukaryota; Metazoa; Chordata; Craniata; Vertebrata; Euteleostomi; Mammalia; Eutheria; Euarchontoglires; Glires; Rodentia; Myomorpha; Muroidea; Muridae; Murinae; Rattus	
Mcavernosa29916	CAAP1_MOUSE\CAAP1_MOUSE\Q:63-137,H:110-184\41.33%ID\E:5e-12\RecName: Full=Caspase activity and apoptosis inhibitor 1;\Eukaryota; Metazoa; Chordata; Craniata; Vertebrata; Euteleostomi; Mammalia; Eutheria; Euarchontoglires; Glires; Rodentia; Myomorpha; Muroidea; Muridae; Murinae; Mus; Mus||||CAAP1_HUMAN\CAAP1_HUMAN\Q:65-139,H:132-206\41.33%ID\E:3e-11\RecName:	GO:0006915\biological_process\apoptotic process||||GO:0042981\biological_process\regulation of apoptotic process

gene	sprot_Top_BLASTP_hit	gene_ontology_blast
	Full=Caspase activity and apoptosis inhibitor 1;\Eukaryota; Metazoa; Chordata; Craniata; Vertebrata; Euteleostomi; Mammalia; Eutheria; Euarchontoglires; Primates; Haplorrhini; Catarrhini; Hominidae; Homo|||\CAAP1_BOVIN\CAAP1_BOVIN\Q:65-250,H:133-355\26.03%ID\E:5e-11\RecName: Full=Caspase activity and apoptosis inhibitor 1;\Eukaryota; Metazoa; Chordata; Craniata; Vertebrata; Euteleostomi; Mammalia; Eutheria; Laurasiatheria; Cetartiodactyla; Ruminantia; Pecora; Bovidae; Bovinae; Bos	
Mcavernosa30125	DPYD_MOUSE\DPYD_MOUSE\Q:4-113,H:729-828\59.29%ID\E:3e-26\RecName: Full=Dihydropyrimidine dehydrogenase [NADP(+)];\Eukaryota; Metazoa; Chordata; Craniata; Vertebrata; Euteleostomi; Mammalia; Eutheria; Euarchontoglires; Glires; Rodentia; Myomorpha; Muroidea; Muridae; Murinae; Mus; Mus|||DPYD_RAT\DPYD_RAT\Q:4-113,H:729-828\57.52%ID\E:9e-26\RecName: Full=Dihydropyrimidine dehydrogenase [NADP(+)];\Eukaryota; Metazoa; Chordata; Craniata; Vertebrata; Euteleostomi; Mammalia; Eutheria; Euarchontoglires; Glires; Rodentia; Myomorpha; Muroidea; Muridae; Murinae;	GO:0005737\cellular_component\cytoplasm|||GO:0005829\cellular_component\cytosol|||GO:0051539\molecular_function\4 iron, 4 sulfur cluster binding|||GO:0017113\molecular_function\dihydropyrimidine dehydrogenase (NADP+) activity|||GO:0004159\molecular_function\dihydrouracil dehydrogenase (NAD+) activity|||GO:0071949\molecular_function\FAD binding|||GO:0005506\molecular_function\iron ion binding|||GO:0050661\molecular_function\NADP binding|||GO:0042803\molecular_function\protein homodimerization activity|||GO:0002058\molecular_function\uracil binding|||GO:0019483\biological_process\beta-alanine

gene	sprot_Top_BLASTP_hit	gene_ontology_blast
	Rattus||||DPYD_PIG\DPYD_PIG\Q:4-104,H:729-831\59.05%ID\E:1e-25\RecName: Full=Dihydropyrimidine dehydrogenase [NADP(+)];\Eukaryota; Metazoa; Chordata; Craniata; Vertebrata; Euteleostomi; Mammalia; Eutheria; Laurasiatheria; Cetartiodactyla; Suina; Suidae; Sus	biosynthetic process||||GO:0007623\biological_process\circadian rhythm||||GO:0006145\biological_process\purine nucleobase catabolic process||||GO:0006208\biological_process\pyrimidine nucleobase catabolic process||||GO:0042493\biological_process\response to drug||||GO:0007584\biological_process\response to nutrient||||GO:0014070\biological_process\response to organic cyclic compound||||GO:0006214\biological_process\thymidine catabolic process||||GO:0006210\biological_process\thymine catabolic process||||GO:0006212\biological_process\uracil catabolic process||||GO:0019860\biological_process\uracil metabolic process
Mcavernosa30509	CEBPZ_MOUSE\CEBPZ_MOUSE\Q:59-364,H:40-381\32.39%ID\E:6e-39\RecName: Full=CCAAT/enhancer-binding protein zeta;\Eukaryota; Metazoa; Chordata; Craniata; Vertebrata; Euteleostomi; Mammalia; Eutheria; Euarchontoglires; Glires; Rodentia; Myomorpha; Muroidea; Muridae; Murinae; Mus; Mus||||CEBPZ_HUMAN\CEBPZ_HUMAN\Q:53-364,H:34-381\31.46%ID\E:1e-38\RecName: Full=CCAAT/enhancer-binding protein	GO:0005634\cellular_component\nucleus||||GO:0000978\molecular_function\RNA polymerase II proximal promoter sequence-specific DNA binding||||GO:0001077\molecular_function\transcriptional activator activity, RNA polymerase II proximal promoter sequence-specific DNA binding||||GO:0045944\biological_process\positive regulation of transcription by RNA polymerase II

gene	sprot_Top_BLASTP_hit	gene_ontology_blast
	zeta;\Eukaryota; Metazoa; Chordata; Craniata; Vertebrata; Euteleostomi; Mammalia; Eutheria; Euarchontoglires; Primates; Haplorrhini; Catarrhini; Hominidae; Homo|||\YEK9_SCHPO\YEK9_SCHPO\Q:219-364,H:84-228\37.42%ID\E:4e-23\RecName: Full=Uncharacterized protein C4F10.09c;\Eukaryota; Fungi; Dikarya; Ascomycota; Taphrinomycotina; Schizosaccharomycetes; Schizosaccharomycetales; Schizosaccharomycetaceae; Schizosaccharomyces	
Mcavernosa31208	ANKF1_HUMAN\ANKF1_HUMAN\Q:302-849,H:139-650\36.27%ID\E:1e-97\RecName: Full=Ankyrin repeat and fibronectin type-III domain-containing protein 1;\Eukaryota; Metazoa; Chordata; Craniata;Vertebrata; Euteleostomi; Mammalia; Eutheria; Euarchontoglires; Primates; Haplorrhini; Catarrhini; Hominidae; Homo	.
Mcavernosa31439	ANR54_HUMAN\ANR54_HUMAN\Q:56-265,H:85-292\42.38%ID\E:2e-52\RecName: Full=Ankyrin repeat domain-containing protein 54;\Eukaryota; Metazoa; Chordata; Craniata;	GO:0005737\cellular_component\cytoplasm|||GO:0030496\cellular_component\midbody|||GO:0005634\cellular_component\nucleus|||GO:0019887\molecular_function\protein kinase regulator

gene	sprot_Top_BLASTP_hit	gene_ontology_blast
	Vertebrata; Euteleostomi; Mammalia; Eutheria; Euarchontoglires; Primates; Haplorrhini; Catarrhini; Hominidae; Homo||||ANR54_BOVIN\ANR54_BOVIN\Q:56-265,H:84-291\42.65%ID\E:2e-52\RecName: Full=Ankyrin repeat domain-containing protein 54;\Eukaryota; Metazoa; Chordata; Craniata; Vertebrata; Euteleostomi; Mammalia; Eutheria; Laurasiatheria; Cetartiodactyla; Ruminantia; Pecora; Bovidae; Bovinae; Bos||||ANR54_RAT\ANR54_RAT\Q:34-265,H:63-291\41.2%ID\E:5e-52\RecName: Full=Ankyrin repeat domain-containing protein 54;\Eukaryota; Metazoa; Chordata; Craniata; Vertebrata; Euteleostomi; Mammalia; Eutheria; Euarchontoglires; Glires; Rodentia; Myomorpha; Muroidea; Muridae; Murinae; Rattus	activity||||GO:0044877\molecular_function\protein-containing complex binding||||GO:0006913\biological_process\nucleocytoplasmic transport||||GO:0045648\biological_process\positive regulation of erythrocyte differentiation||||GO:1902531\biological_process\regulation of intracellular signal transduction
Mcavernosa31888	.	.
Mcavernosa32022	.	.
Mcavernosa32023	DCAF4_BOVIN\DCAF4_BOVIN\Q:128-508,H:63-493\26.97%ID\E:1e-40\RecName: Full=DDB1- and CUL4-associated factor 4;\Eukaryota; Metazoa; Chordata; Craniata;Vertebrata; Euteleostomi; Mammalia; Eutheria;	GO:0071013\cellular_component\catalytic step 2 spliceosome||||GO:0080008\cellular_component\Cul4-RING E3 ubiquitin ligase complex||||GO:0071011\cellular_component\precatalytic spliceosome||||GO:0005682\cellular_component\U5

gene	sprot_Top_BLASTP_hit	gene_ontology_blast
	Laurasiatheria; Cetartiodactyla; Ruminantia; Pecora; Bovidae; Bovinae; Bos|||\DCAF4_HUMAN\DCAF4_HUMAN\Q:297-508,H:278-494\35.59%ID\E:5e-35\RecName: Full=DDB1- and CUL4-associated factor 4;\Eukaryota; Metazoa; Chordata; Craniata; Vertebrata; Euteleostomi; Mammalia; Eutheria; Euarchontoglires; Primates; Haplorrhini; Catarrhini; Hominidae; Homo|||\DC4L2_HUMAN\DC4L2_HUMAN\Q:336-508,H:225-394\39.43%ID\E:2e-32\RecName: Full=DDB1- and CUL4-associated factor 4-like protein 2;\Eukaryota; Metazoa; Chordata; Craniata; Vertebrata; Euteleostomi; Mammalia; Eutheria; Euarchontoglires; Primates; Haplorrhini; Catarrhini; Hominidae; Homo	snRNP|||\GO:0003723\molecular_function\RNA binding|||\GO:0016567\biological_process\protein ubiquitination|||\GO:0008380\biological_process\RNA splicing
Mcavernosa32260	.	.
Mcavernosa32533	PAR14_HUMAN\PAR14_HUMAN\Q:5-316,H:1495-1799\43.81%ID\E:4e-72\RecName: Full=Poly [ADP-ribose] polymerase 14;\Eukaryota; Metazoa; Chordata; Craniata; Vertebrata; Euteleostomi; Mammalia; Eutheria; Euarchontoglires; Primates; Haplorrhini; Catarrhini; Hominidae; Homo|||\PAR14_MOUSE\PAR14_MOUSE\Q:5-	GO:0005737\cellular_component\cytoplasm|||\GO:0005829\ cellular_component\cytosol|||\GO:0016020\cellular_component\membrane|||\GO:0005634\cellular_component\nucleus|||\GO:0019899\molecular_function\enzyme binding|||\GO:0003950\molecular_function\NAD+ ADP-ribosyltransferase activity|||\GO:0070403\molecular_function\NAD+ binding|||\GO:0045087\biological_process\innate immune

gene	sprot_Top_BLASTP_hit	gene_ontology_blast
	316,H:1511-1815\41.59%ID\E:5e-67\RecName: Full=Poly [ADP-ribose] polymerase 14;\Eukaryota; Metazoa; Chordata; Craniata; Vertebrata; Euteleostomi; Mammalia; Eutheria; Euarchontoglires; Glires; Rodentia; Myomorpha; Muroidea; Muridae; Murinae; Mus; Mus|||PAR15_HUMAN\PAR15_HUMAN\Q:117-316,H:482-676\48.77%ID\E:1e-57\RecName: Full=Poly [ADP-ribose] polymerase 15;\Eukaryota; Metazoa; Chordata; Craniata; Vertebrata; Euteleostomi; Mammalia; Eutheria; Euarchontoglires; Primates; Haplorrhini; Catarrhini; Hominidae; Homo	response|||GO:0010629\biological_process\negative regulation of gene expression|||GO:0060336\biological_process\negative regulation of interferon-gamma-mediated signaling pathway|||GO:0042532\biological_process\negative regulation of tyrosine phosphorylation of STAT protein|||GO:1902216\biological_process\positive regulation of interleukin-4-mediated signaling pathway|||GO:0042531\biological_process\positive regulation of tyrosine phosphorylation of STAT protein|||GO:0006471\biological_process\protein ADP-ribosylation|||GO:0070212\biological_process\protein poly-ADP-ribosylation|||GO:0006355\biological_process\regulation of transcription, DNA-templated|||GO:0006351\biological_process\transcription, DNA-templated

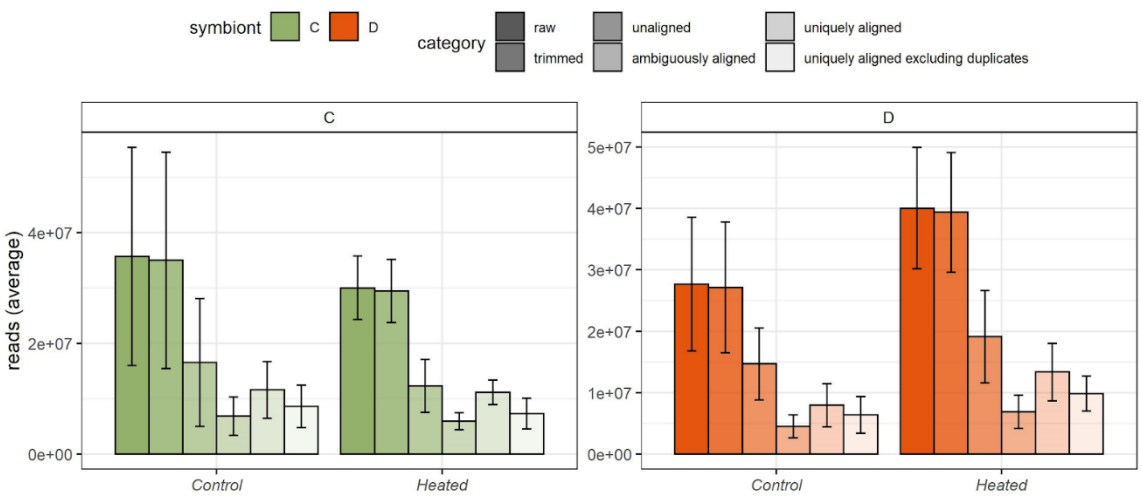

Supplementary Fig. S1. Summary of trimming and alignment statistics resulting from the processing of 24 *M. cavernosa* MBD-BS libraries aligned to the genome assembly generated by the laboratory of Dr. M. Matz (https://matzlab.weebly.com/data--code.html) using the *bismark pipeline*. Bars represent read averages and standard errors between 6 libraries for each of the four symbiont/treatment combinations. ***C*** refers to *Cladocopium* spp. Symbionts and ***D*** refers to symbionts of the genera *Durusdinium*.

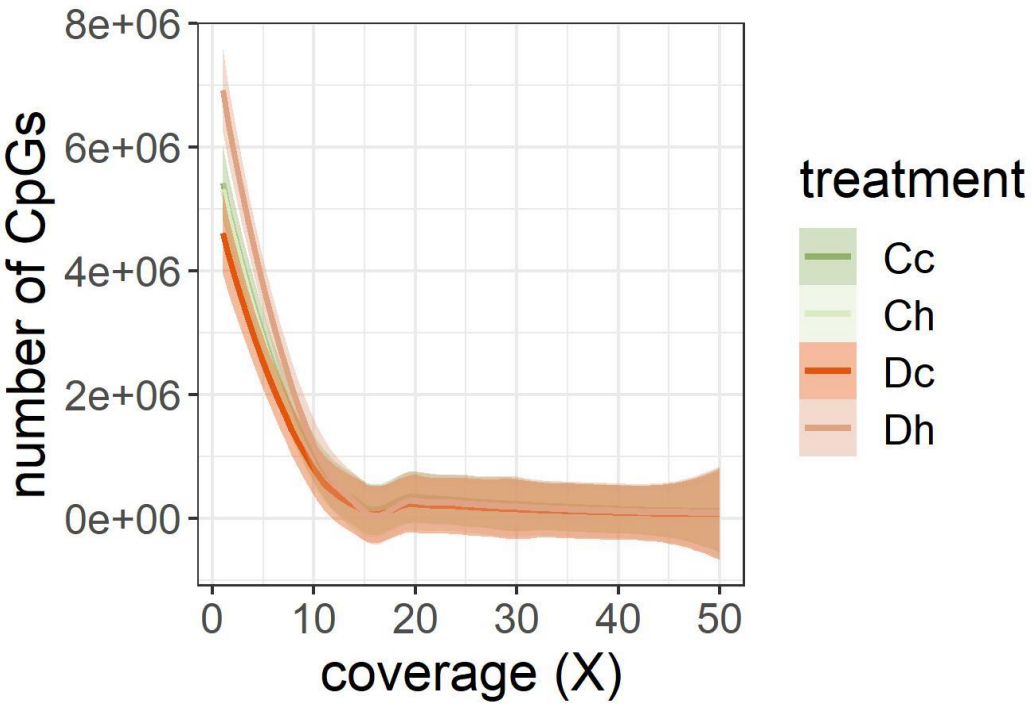

Supplementary Fig. S2. CpG sites coverage distribution by treatment combination of uniquely aligned and duplicated reads resulting from 24 MBD-BS libraries aligned to the *M. cavernosa* genome. Treatment combinations represent corals hosting either symbionts of the genera *Cladocopium* (**C**) or *Durusdinium* (**D**) maintained in control temperature (**c**) or exposed to a short-term heat stress (**h**).

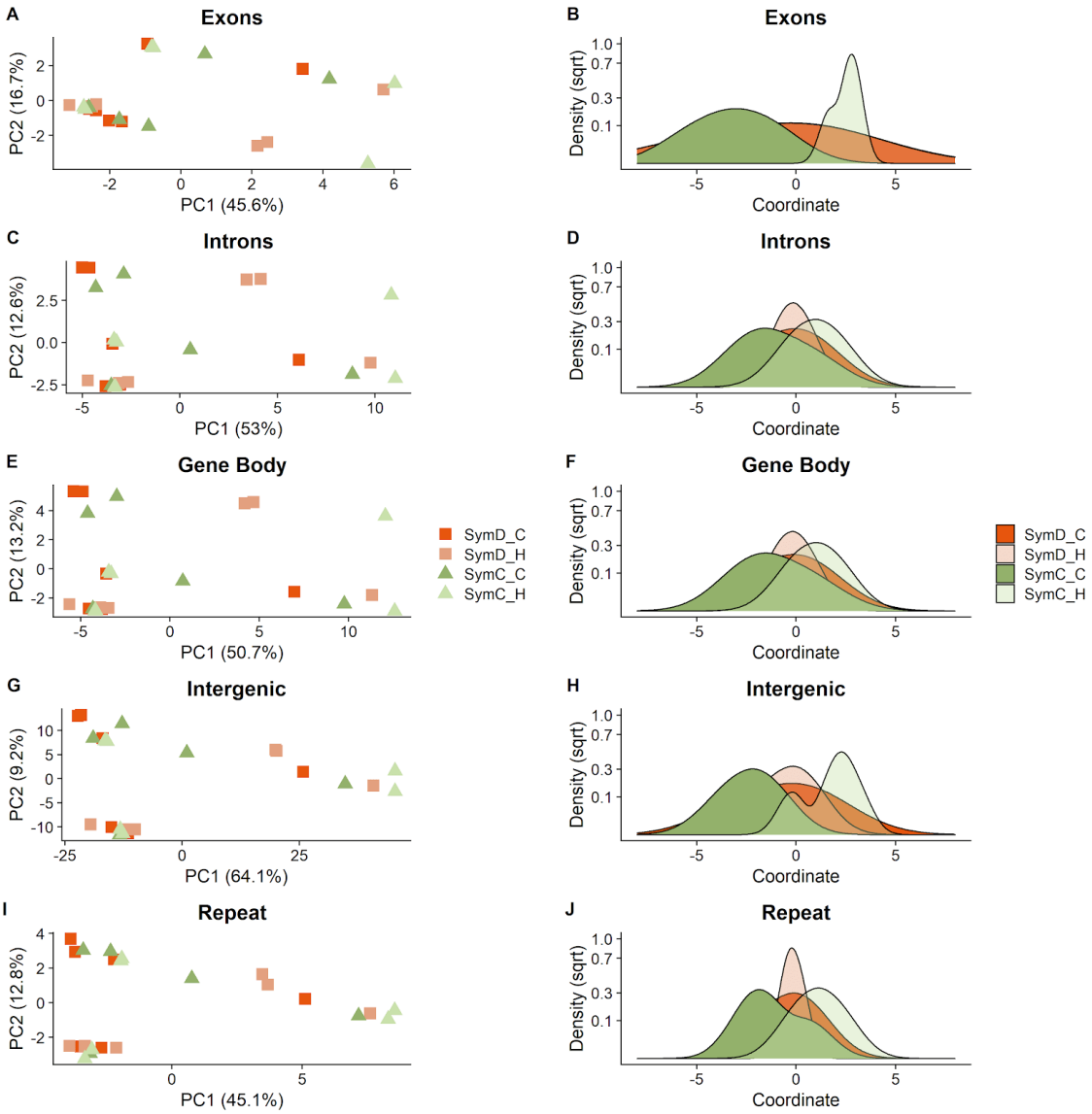

Supplementary Fig. S3. Principal component analysis (left) and Discriminant Analysis of principal components (right) ordinations of DNA methylation response to symbiont shuffling and thermal stress. Analyses were separated by genomic features overlapping with methylated CpG loci. [exons (A & B), introns (C & D), gene body (E & F, includes introns, exons and UTRs), intergenic (G & H) and repeat (i.e. transposable elements, I & J)]. Treatment combinations (as colors) represent corals hosting either symbionts of the genera *Cladocopium* (**SymC**) or *Durusdinium* (**SymD**) maintained in control temperature (**C**) or exposed to a short-term heat stress (**H**)

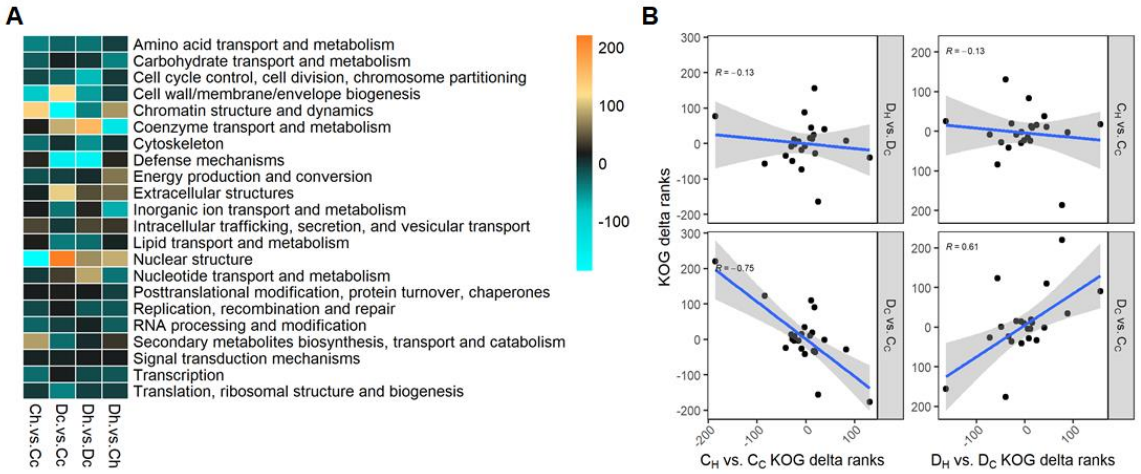

Supplementary Fig.S4. Eukaryotic ortholog group (KOG) enrichment analysis results. **(A)** KOG functional categories hyper- hypomethylated (indicated by color) for contrasts of experimental groups (Ch = *Cladocopium*/heated, Cc = *Cladocopium*/control, Dh = *Durusdinium*/heated, Dc = *Durusdinium*/control). **(B)** Correlation plots of KOG changes between the responses of both dominant symbiont types to thermal stress (Ch versus Cc; left and Dh versus Dc; right) with symbiont shift in control corals (DC versus CC; below), and to each other (top panels).

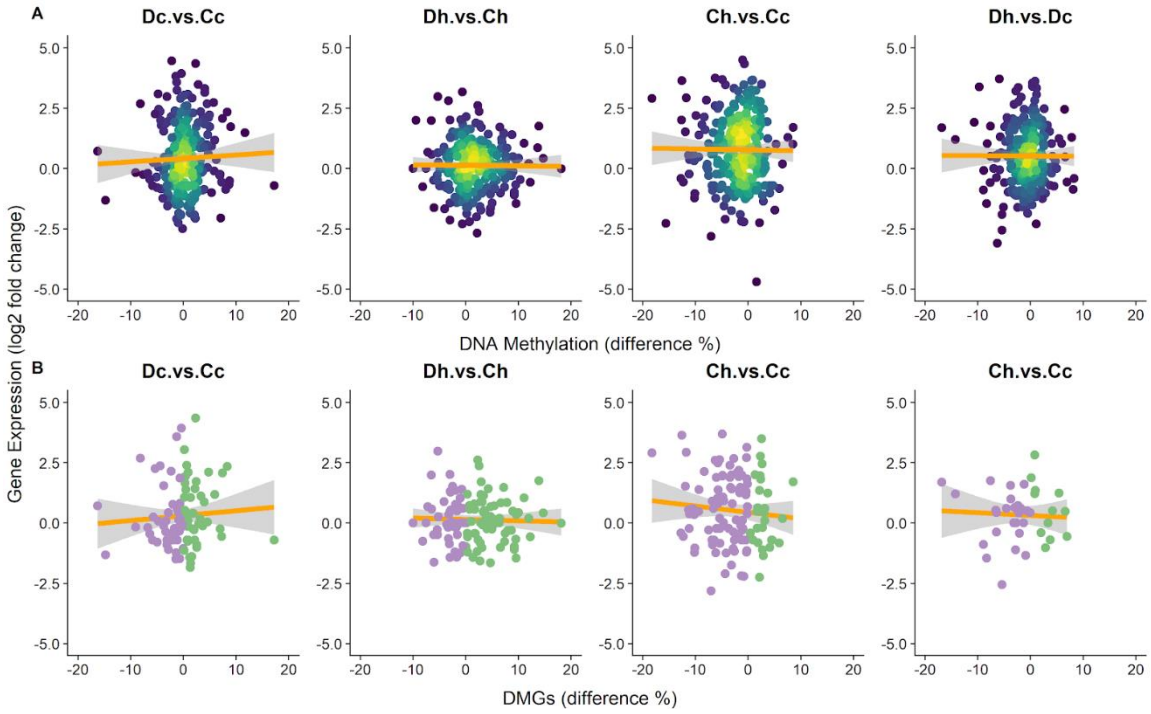

Supplementary Fig. S5 Relationship between average gene methylation difference (%) and changes in gene expression (log2-fold) for contrasts of experimental groups (Ch = *Cladocopium*/heated, Cc = *Cladocopium*/control, Dh = *Durusdinium*/heated, Dc = *Durusdinium*/control). **(A)** Experimental group average for each gene covered. **(B)** Only significant Differentially methylated genes (DMGs).

Appendix D: Supplementary materials for Chapter V

Supplementary Table S1. PERMANOVA results of lipid compound numbers in *A. cervicornis* fragments by site, class and their interaction.

	df	Sum of Sqs.	Mean Sqs	F. Model	R^2	p-value
site	1	0.1487	0.14866	5.973	0.0057	**0.0054**
class	7	20.8127	2.97324	119.453	0.7972	**0.0001**
site:class	7	0.3670	0.05242	2.106	0.0141	**0.0142**
Residuals	192	4.7789	0.02489		0.1831	
Total	207	26.1072			1.0000	

Supplementary Table S2. Results of chi-square analysis comparing proportions of each lipid class.

Class	Estimate 1	Estimate 2	statistic	P.adj (FDR)
ChE	0.002954824	0.004641770	3144940	< **0.0001**
FA	0.009378445	0.008007381	931593	< **0.0001**
MG	0.258805196	0.228595074	21092503	< **0.0001**
MGDG	0.041926616	0.068187624	55418486	< **0.0001**
PC	0.046957393	0.059219600	12606000	< **0.0001**
PE	0.123915736	0.063869320	183717098	< **0.0001**
TG	0.400967793	0.463937250	68529306	< **0.0001**
WE	0.115093997	0.103541980	5839907	< **0.0001**

ChE cholesterol ester, **FA** Fatty acid, **MG** mono-acyl glycerol, **MGDG** Monogalactosyldiacylgylcerol, **PC** Phosphatidylcholine, **PE** Phosphatidylethanolamine, **TG** Triglyceride and **WE** Wax ester. *p-values* were adjusted using the Benjamini-Hochberg correction.

Supplementary Table S3. TagSeq read counts per sample at different processing stages (raw, post-quality filtering and mapped)

stage	Min.	Max.	Median	Total
raw	7,248,899	18,067,458	11,497,504	309,224,452
post_trim	3,210,092	8,793,512	5,313,577	140,773,629
mapped	2,170,526	6,305,585	3,757,251	98,918,140

Supplementary Table S4. Gene ontology (GO) enrichment analysis results for Biological Processes (BP), Cellular Components (CC), and Molecular Functions (MF). Negative delta rank values indicate up-regulation in corals outplanted to the deep reef. Only terms with adjusted p-values (FDR) < 0.01 are shown.

Ontology	Genes	GO term	delta.rank	P.adj
BP	34/279	ribosome biogenesis	-1887	7.24E-45
BP	5/23	one-carbon metabolic process	-1761	0.002937
BP	3/39	nucleoside diphosphate metabolic process	-1253	0.00724
BP	8/110	purine-containing compound metabolic process	-959	1.78E-04
BP	57/670	cellular component organization or biogenesis	-920	3.84E-24
BP	7/75	ATP metabolic process	-903	0.00724
BP	77/999	macromolecule biosynthetic process	-631	4.24E-16
BP	23/306	amide transport	-528	0.001157
BP	15/234	cellular localization	-521	0.00724
BP	31/444	small molecule metabolic process	-423	0.002232
BP	31/409	organic substance transport	-388	0.008739
BP	30/361	G protein-coupled receptor signaling pathway	621	5.48E-06
CC	28/246	ribosomal subunit	-528	1.47E-26
CC	10/63	polymeric cytoskeletal fiber	-520	1.69E-07
CC	16/145	large ribosomal subunit	-518	7.03E-16
CC	12/89	small ribosomal subunit	-514	4.62E-10
CC	6/38	microtubule	-494	3.16E-04
CC	47/494	ribonucleoprotein complex	-296	3.35E-15

CC	21/327	transferase complex	146	0.004909
CC	4/115	extracellular region	275	6.53E-04
CC	1/74	synapse part	298	0.003804
CC	1/14	DNA replication factor C complex	683	0.003804
MF	32/345	structural constituent of ribosome	-1869	1.81E-29
MF	45/497	structural molecule activity	-1569	1.81E-29
MF	14/111	cytoskeletal protein binding	-1106	0.005394
MF	27/208	isomerase activity	-815	0.005394
MF	24/299	purine nucleoside binding	-769	0.00101
MF	31/440	ATPase activity	629	0.00101
MF	23/263	obsolete rhodopsin-like receptor activity	804	0.00101
MF	12/234	helicase activity	899	6.23E-04

Supplementary Table S5. Eukaryotic orthologous groups (KOG) enrichment analysis results. Negative delta rank values indicate up-regulation in corals outplanted to the deep reef. Only terms with FDR < 10% are shown.

Genes	KOG term	delta.rank	P.adj
45/645	Translation, ribosomal structure and biogenesis	-1422	2.87E-23
26/411	Replication, recombination and repair	906	1.63E-06
27/598	RNA processing and modification	519	0.00234
208/3032	Signal transduction mechanisms	252	0.00279
6/156	Nucleotide transport and metabolism	-795	0.0185
50/375	Energy production and conversion	-501	0.0204
135/1657	Post-translational modification, protein turnover, chaperones	-232	0.0347
52/833	Transcription	278	0.0691

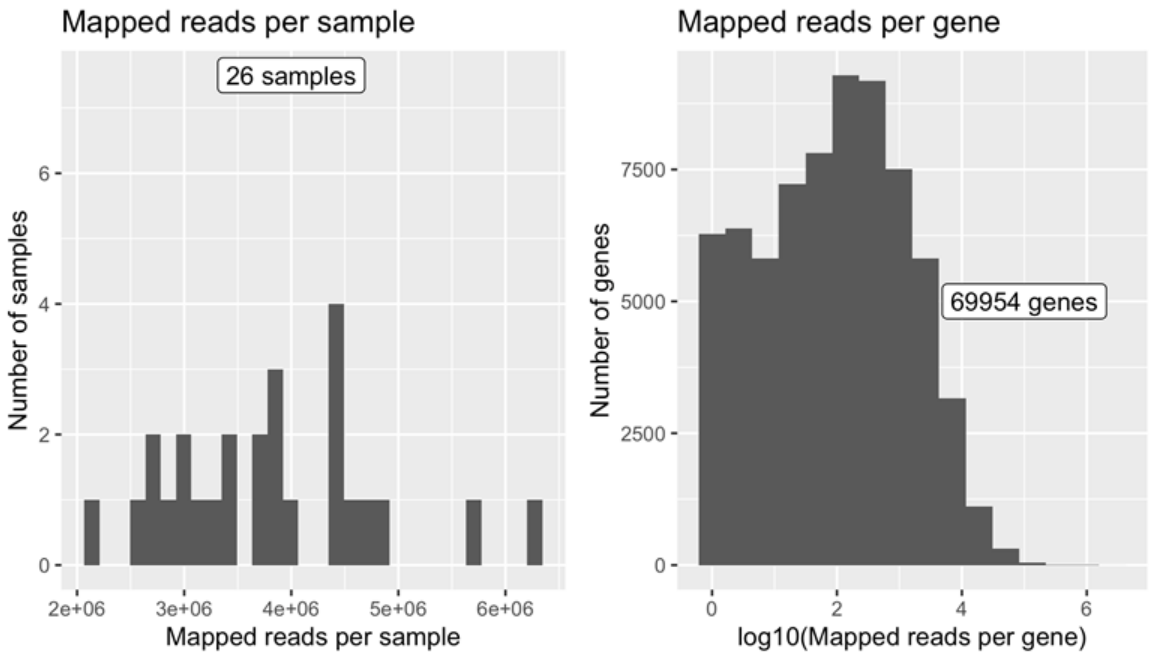

Supplementary Fig. S1. Tag-Seq mapping statistics. Number of mapped reads per sample (left) and number of mapped reads per gene.

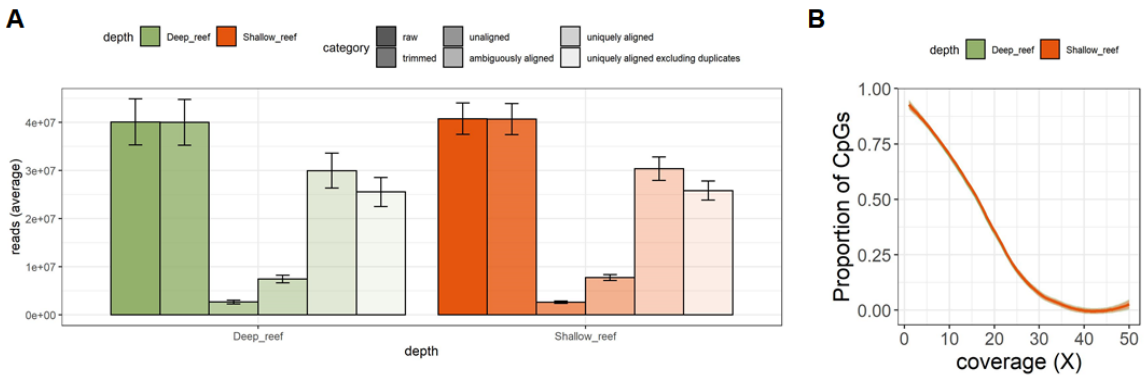

Supplementary Fig. S2. (A) Summary of trimming and alignment statistics resulting from the processing of 26 WGBS libraries aligned to the *A. cervicornis* genome assembly generated by the laboratory of Dr. Iliana B. Baums using the bismark pipeline. **(B)** CpG sites coverage distribution by treatment combination of uniquely aligned and de-duplicated reads.

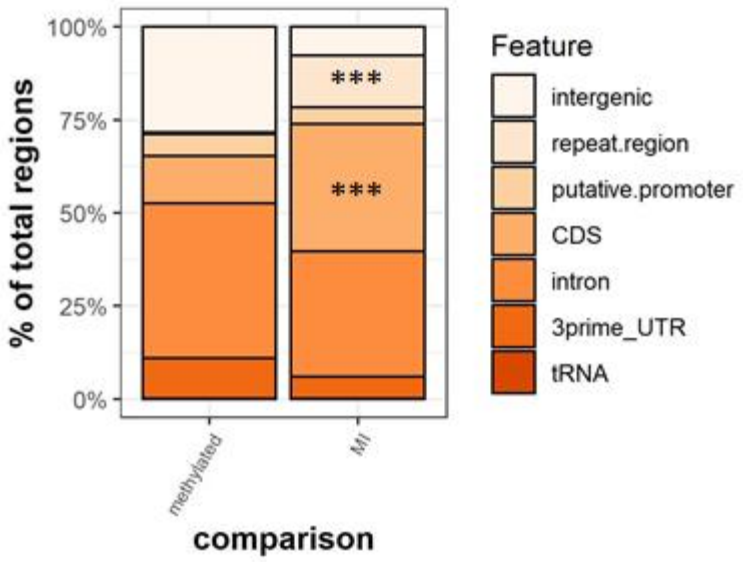

Supplementary Fig. S3. Proportion of methylated CpGs and methylation islands (MI) overlapping genomic features. Asterisks indicate significant enrichment (FDR adjusted p-values < 0.0001).

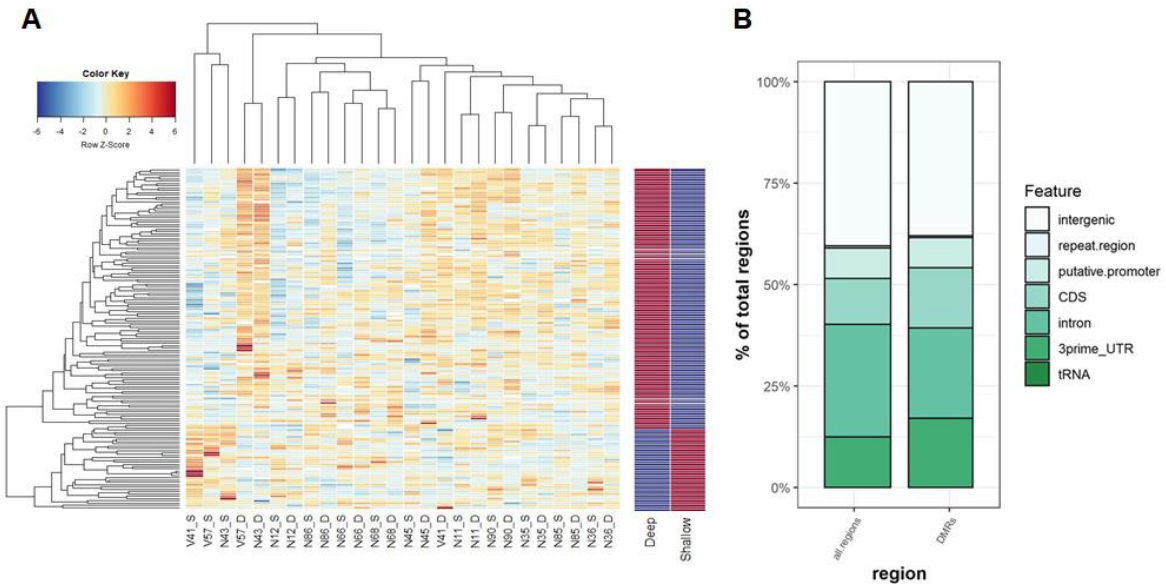

Supplementary Fig. S4 (A) Heatmap illustrating methylation level variability across 142 differentially methylated regions (DMRs) between all samples (left) and grouped by outplanting sites (right). **(B)** Proportion of covered CpGs and DMRs overlapping genomic features.

VITA

JAVIER A. RODRIGUEZ CASARIEGO

	Born, Havana, Cuba
2003 - 2008	B.S., Biology University of Havana Havana, Cuba
2008 - 2012	Junior Research Scientist/Teaching Graduate Instructor, Center for Marine Research, University of Havana Havana, Cuba
2008 - 2012	M.S., Marine Biology University of Havana Havana, Cuba
2014 - 2016	Sr. Laboratory Technician Florida International University Miami, Florida
2016 - 2021	Doctoral Student Florida International University Miami, Florida
	NSF-CREST Fellow Center for Aquatic Chemistry and Environment (CAChE) Florida International University Miami, Florida

PUBLICATIONS AND RELEVANT PRESENTATIONS

2021 Rodriguez-Casariego J. A., R. Cunning, A. C. Baker, J. M. Eirin-Lopez, Symbiont shuffling induces differential DNA methylation responses to thermal stress in the coral *Montastraea cavernosa*. *Molecular Ecology* (Accepted)

2021 Lugo Charriez K., L. Soledade Lemos, Y. Carrazana, JA. Rodríguez-Casariego, JM. Eirin-Lopez, RA. Hauser-Davis, P. Gardinali, N. Soares Quinete, Application of an improved chloroform-free lipid extraction method to staghorn coral (*Acropora cervicornis*) lipidomics assessments. *Bull Environ Contam Toxicol*. PMID: 33392686.

2020 Rodríguez-Casariego JA, AE Mercado-Molina, D Garcia-Souto, I Ortiz, C Lopes, IB Baums, AM Sabat and JM Eirin-Lopez, Genome-wide DNA methylation analysis reveals a conserved epigenetic response to seasonal environmental variation in the staghorn coral *Acropora cervicornis*. *Front. Mar. Sci.* 7: 822

2020 Rodriguez-Casariego J. A., I. Ortiz, A. Mercado-Molina, D. Garcia-Souto, A. Sabat, I. B. Baums, J. M. Eirin-Lopez, Seasonal variation on DNA methylation patterns in the staghorn coral *Acropora cervicornis* in Culebra Island, PR. Ocean Science Meeting, San Diego, CA. Type of contribution: Poster

2020 Rodriguez-Casariego J. A., A. Mercado-Molina, D. Garcia-Souto, I. B. Baums, A. Sabat and J. M. Eirin-Lopez, Epigenetic and demographic responses of stony corals to

hurricanes Irma and Maria in Puerto Rico. HurriCon, Greenville, NC. Type of contribution: Oral communication

2019 Rodriguez-Casariego J. A., A. Mercado-Molina, I. B. Baums, A. Sabat and J. M. Eirin-Lopez Non-genetic mechanisms of coral response to global change: preliminary epigenetic analyses in corals impacted by hurricanes Irma and Maria in Puerto Rico. ASLO 2019, San Juan, PR. Type of contribution: Oral communication

2018 Rodriguez-Casariego JA, M Ladd, A Shantz, C Lopez, MS Cheema, CB Kim, S Roberts, JW Fourqurean, J Ausio, D Burkepile, JM Eirin-Lopez, Coral epigenetic responses to nutrient stress: Histone H2A.X phosphorylation dynamics and DNA methylation in the staghorn coral *Acropora cervicornis. Ecology and Evolution* 8 (23), 12193-12207

2018 Beal, A., Rodriguez-Casariego, J., Rivera-Casas, C., Suarez-Ulloa, V., & Eirin-Lopez, J. M., Environmental Epigenomics and Its Applications in Marine Organisms, *in Population Genomics: Marine Organisms*, M. Oleksiak and O.Rajora, ed. Springer Nature.

2018 Rodriguez-Casariego J. A., M. Ladd, A. Shantz, C. Lopez, M. S. Cheema, B. Kim, S. Roberts, J. Fourqurean, J. Ausio, D. Burkepile, J. M. Eirin-Lopez, Nutrient loading hinders mechanisms involved in the epigenetic maintenance of genome integrity in the stony coral *Acropora cervicornis*. 9th International Symbiosis Society Congress, Corvallis OR. Type of contribution: Oral communication.

2017 Rodrigo Gonzalez-Romero, Suarez-Ulloa V., Rodriguez-Casariego, J, Daniel Garcia-Souto, Gabriel Diaz, Abraham Smith, Juan Jose Pasantes, Gary Rand, Jose M. Eirin-Lopez. Effects of Florida Red Tides on histone variant expression and DNA methylation in the Eastern oyster *Crassostrea virginica. Aquatic Toxicology* 186: 196–204

2017 Jose M. Eirin-Lopez* and Javier A. Rodriguez-Casariego*, Coral responses to global change: an epigenetic perspective. Coral Reef Conservation Program (CRCP) Learning Exchange. Type of contribution: Oral communication. (*Equal contribution)

2017 Rodriguez-Casariego J. A., S. Campbell, M. Ladd, A. Shantz, S. Roberts, D. Burkepile, J. M. Eirin-Lopez, Nutrient loading hinders mechanisms involved in the epigenetic maintenance of genome integrity in the stony coral *Acropora cervicornis*. 38th AMLC Conference. Merida, Yucatan, Mexico. Type of contribution: Oral communication.

2012 Rodríguez-Casariego J, E Perera, Perdomo- Morales R. Purificación de isoformas de proteasas tipo tripsina de crustáceos. *Rev. Invest. Mar.* 32(1): 1-8.

2012 Perera E, Rodríguez-Casariego J, L Rodríguez-Viera, J Calero, R Perdomo-Morales, J M Mancera, Lobster (*Panulirus argus*) hepatopancreatic trypsin isoforms and their digestion efficiency. *Biol. Bull.* 222(2): 158-70.

2011 Perera E, L Rodríguez-Viera, J Rodríguez-Casariego, I Fraga, O Carrillo, G Martínez-Rodríguez, JM Mancera, Dietary protein quality differentially regulates trypsin enzymes at the secretion and transcription level in *Panulirus argus* by distinct signaling pathways. *Journal of Experimental Biology*; 215 (Pt 5):853-62.